AN EXTREME-VALUE MODEL OF SURFACE-POINT RAIN-RATE DISTRIBUTION FOR THE PREDICTION OF MICROWAVE RAIN ATTENUATION IN SOUTHERN AFRICA

by

Ronald Jarvie Seeber

Submitted in partial fulfilment of the requirements

for the degree of

Master of Electronic Engineering

in the Faculty of Engineering,

University of Pretoria,

Pretoria

October, 1985

Opgedra aan Lenie, Anton, Werner en Konrad

en

my ouers

AN EXTREME-VALUE MODEL OF SURFACE-POINT RAIN-RATE DISTRIBUTION FOR THE PREDICTION OF MICROWAVE RAIN ATTENUATION IN SOUTHERN AFRICA

by

Ronald Jarvie Seeber

Leader: Prof D.C. Baker

Co-leader: Prof W.J.R. Alexander

Department of Electronic Engineering

Master of Electronic Engineering

SYNOPSIS

A semi-empirical model for the probability distribution of point rainfall rate is presented. The model was developed for predicting the probability distribution of rain attenuation on microwave links on the Southern African subcontinent. The attenuation distribution is required for obtaining the average annual outage of terrestrial and earth-to-satellite communication links. The model is an extension of the extreme-value method presented by Lin. As in Lin's method the distribution of randomly varying rain rate is approximated by the lognormal distribution and the distribution of annual rain-rate maxima by the log-Gumbel distribution. The extension of the extreme-value method comprises new, generalized relationships for the scale parameter α and the position parameter U of the log-Gumbel distribution. The expressions developed for U are a function of mean annual rainfall (MAR), climatic region and rain-gauge integration time, while α has a constant value. The relationships were obtained from an analysis of the depth-duration-frequency diagram for Southern Africa, by Midgley and Pitman. The resulting rain-rate model gives distributions which are a function of only MAR and climatic region ('coastal' or 'inland'). Integration time is variable, ranging from 5 to 1440 minutes. Curves of the cumulative rain-rate distribution are given for various integration times, for various mean annual rainfalls and for the two climatic regions concerned. By using the curves the rain-rate distribution and -- by means of existing attenuation models -- also the rain-attenuation distribution, may be obtained for locations for which no rain-rate data are available. The 15-minute rain-rate predictions for locations on the Southern African subcontinent agree well with observed distributions. However, for two islands in the South Indian and South Atlantic oceans, respectively, the results were poor. However, this does not necessarily invalidate the extreme-value theory used in the model. The model gives rain-rate estimates for the Southern African subcontinent which are equivalent to a two-year measurement programme. Although the model was developed to provide distributions of primarily a 5-min integration time, a lack

of data precluded testing the model at this integration time for Southern Africa. However, the model was extensively tested at 5-min integration time for USA locations, with satisfactory results. The model was also tested for predicting the rain-attenuation distribution on earth-to-satellite microwave links in the USA, using a well-known attenuation model. These results were very satisfactory. It is concluded that the model should be suitable for predicting rain attenuation on the Southern African subcontinent, not only for earth-to-satellite links, but also for terrestrial links. The model obviates geographical interpolation of rain-rate and rain-attenuation distributions. The results for Southern Africa and the USA support the log-Gumbel and lognormal approximations, as well as Lin's extreme-value theory. That MAR is an important determinant of the rain-rate distribution is in agreement with the Rice-Holmberg model. The results are furthermore in agreement with the hypothesis that the spatial and temporal characteristics of rain are relatively invariant within large geographical regions, while the frequency of rain occurrences varies from location to location. The approach followed in developing the model could be used for establishing models of greater geographical resolution and extent.

Keywords:

Rain-rate distribution, rain-rate model, rain-attenuation distribution, microwave links, rain attenuation, extreme-value theory, log-Gumbel distribution, lognormal distribution.

SINOPSIS

'N EKSTREEMWAARDEMODEL VIR DIE OPPERVLAK-PUNTREëNINTENSITEIT-VERDELING VIR DIE VOORSPELLING VAN MIKROGOLF-REëNVERSWAKKING IN SUIDELIKE AFRIKA

'n Semiëmpiriese model vir die waarskynlikheidsverdeling van puntreënintensiteit word aangebied. Die model is ontwikkel vir die voorspelling van die waarskynlikheidsverdeling van reënverswakking van mikrogolfverbindings op die Suider-Afrikaanse subkontinent. Die verswakkingverdeling is nodig om die gemiddelde jaarlikse faling van aardse en aarde-na-satelliet-kommunikasieverbindings te bepaal. Die model is 'n uitbreiding van die ekstreemwaardemetode van Lin. Soos in Lin se metode word die verdeling van willekeurig variërende reënintensiteit met die lognormaalverdeling benader en die verdeling van jaarlikse reënintensiteitmaksima met die log-Gumbel-verdeling. Die uitbreiding van die ekstreemwaardemetode behels nuwe, veralgemeende verwantskappe vir die skaalparameter α en die posisieparameter U van die log-Gumbel-verdeling. Die uitdrukkings wat vir U ontwikkel is, is 'n funksie van gemiddelde jaarreënval (GJR), klimaatstreek en reënmeter-integrasietyd, terwyl α 'n konstante waarde het. Die verwantskappe is verkry uit 'n ontleding van Midgley en Pitman se diepte/duur/frekwensie-diagram vir Suidelike Afrika. Die resulterende reënintensiteitmodel gee verdelings wat 'n funksie is van slegs GJR en klimaatstreek ('kus' of 'binneland'). Integrasietyd is veranderlik en strek van 5 tot 1440 minute. Krommes van die kumulatiewe reënintensiteitverdeling word verskaf vir verskeie integrasietye, vir verskeie jaarreënvalle en vir die twee klimaatstreke gebruik. Met die krommes kan die reënintensiteitverdeling en -- deur middel van bestaande verswakkingsmodelle -- ook die reënverswakkingverdeling, verkry word vir plekke waarvoor geen intensiteitdata beskikbaar is nie. Die 15-minuut-reënintensiteitvoorspellings vir plekke op die Suider-Afrikaanse subkontinent stem goed ooreen met waargenome verdelings. Vir twee eilande in die Suid-Indiese en Suid-Atlantiese oseane, onderskeidelik, is die resultate egter swak. Die ekstreemwaardeteorie word egter nie daardeur ongeldig gemaak nie. Die model lewer reënintensiteit-voorspellings vir die Suider-Afrikaanse subkontinent wat gelykstaande is aan 'n meetprogram van twee jaar. Alhoewel die model ontwikkel is om verdelings van 'n integrasietyd van hoofsaaklik 5 min te lewer, kon, weens 'n gebrek aan data, geen toetse by hierdie integrasietyd vir Suider-Afrika uitgevoer word nie. Die model is egter uitvoerig by 'n integrasietyd van 5 min vir VSA-plekke getoets, met bevredigende resultate. Dit is ook beproef vir die voorspelling van die reënverswakkingverdeling vir aarde-na-satelliet-mikrogolfverbindings in die VSA, deur middel van 'n welbekende verswakkingsmodel. Die resultate was baie bevredigend. Daar word gekonkludeer dat die model geskik behoort te wees vir die voorspelling van reënverswakking op die Suider-Afrikaanse subkontinent, nie net vir aarde-na-satelliet-verbindings nie, maar ook vir aardverbindings. Die model skakel geografiese interpolasie van reënintensiteit- en reënverswakkingverdelings uit. Die resultate vir Suider-Afrika en die VSA

ondersteun die log-Gumbel- en lognormaal-benadering, asook Lin se ekstreemwaardeteorie. Dat die GJR 'n belangrike bepaler van die reënintensiteitverdeling is, is in ooreenstemming met die Rice-Holmberg-model. Die resultate is verder in ooreenstemming met die hipotese dat die ruimtelike en temporele eienskappe van reën betreklik invariant binne groot geografiese gebiede is, maar dat die voorkomsfrekwensie van reën van plek tot plek wissel. Die benadering wat by die ontwikkeling van die model gevolg is kan gebruik word om modelle van groter geografiese resolusie en omvang daar te stel.

Sleutelwoorde:

Reënintensiteitverdeling, reënintensiteitmodel, reënverswakkingverdeling, mikrogolfverbindings, reënverswakking, ekstreemwaardeteorie, log-Gumbel-verdeling, lognormaalverdeling.

ACKNOWLEDGEMENTS

The contributions of the following are gratefully acknowledged:

- Mmes A Botha and J F Jansen for typing the manuscript.
- The National Institute for Telecommunications Research of the CSIR for making available all necessary facilities.
- The leader, prof D.C. Baker, the co-leader, prof W.J.R. Alexander and the external examiner, prof W. James, for their valuable suggestions.
- S.H. Lin and D.C. Midgley & W.V. Pitman, without whose published work this thesis would not have been possible.
- The South African Weather Bureau of the Dept. of Transport for their kind assistance in providing rain data.

TABLE OF CONTENTS

(continued on next page)

(continued on next page)

Chapter 1

INTRODUCTION

The use of radio communication systems operating at microwave and millimetre-wave frequencies has been growing rapidly in recent years. This has been the case for both terrestrial and earth-to-satellite communication systems. The growth has been brought about by increasing demands for radio channel capacity for the transmission of electrical signals for telephony, television and data communication. The increase in the number of terrestrial and earth-to-satellite microwave communication systems is causing congestion of the radio frequency spectrum. Spectrum congestion necessitates the use of higher frequencies in order to cope with the demand for channel capacity.

At the higher microwave frequencies and especially millimetre-wave frequencies, radio communication systems suffer from adverse propagation phenomena caused by the troposphere. Apart from certain unwanted effects under clear-air conditions there are propagation phenomena caused by more visible atmospheric constituents. Precipitation such as hail, snow, rain, cloud, fog, dust and sand could all have an effect on propagation [Hall, 1979]. These so-called hydrometeors may have a profound influence on the performance and availability of both analog and digital radio communication systems [CCIR, 1982b and 1982c].

The hydrometeors, when their linear dimensions are greater than about one-tenth of the radio wavelength, impede the free propagation of the radiowave. For

instance, by absorbing and scattering the transmitted electromagnetic power along the propagation path, the raindrops cause the received signal in the link to be attenuated. Attenuation may in turn cause the performance of the link to deteriorate and could, in the worst case, cause a communication outage [CCIR, 1982d]. The propagation effects depend mainly on the size and shape of the hydrometeors, their dielectric properties, their abundance in the troposphere, as well as the parameters of the radio system used.

Frequencies above 10 GHz are now coming into use all over the world. In this frequency range rain, of the various forms of precipitation mentioned, is a matter of great concern. It causes severe attenuation of the radiowaves and is furthermore responsible for the phenomena of radio-frequency interference and depolarization of the radiowaves.

Of the above three propagation phenomena rain attenuation is the most important, being an aspect that has to be considered in the design of all communication links operating above 10 GHz. The magnitude of the attenuation by rain at a particular instant in time is a complicated function of the number, size, shape, orientation and dielectric properties of the drops in each elemental part of the radio path. In general, the more intense the precipitation, the greater the attenuation. The attenuation is also a function of the frequency (or wavelength) and, to some extent, the polarization used. The attenuation in dB increases approximately with the square of the frequency above about 8 GHz. Above 10 GHz rain attenuation is usually the single most critical determinant of system performance and availability, in some cases causing outages amounting to many hours per year.

The second phenomenon, radio-frequency interference caused by rain, is also a function of the microphysical

properties of the rain and, as a consequence, the rainfall rate. It is also a function of the frequency and polarization of the system. The magnitude of the interference is furthermore very much a function of geometry [CCIR, 1982e]. A volume of rain coinciding with the intersection of radiation lobes of antennas of transmitting and receiving stations, possibly well separated and belonging to different radio systems, but operating at the same frequency, presents a mechanism of coupling the two systems. Due to scattering by the raindrops a fraction of the transmitted power of the one system will couple into the receiver of the other system, interfering with the wanted signal. In the worst case the interference will cause a system outage. Rain interference has presented itself as a formidable problem with the advent of earth-to-satellite communication systems. As frequency allocations for the latter overlap with those of terrestrial systems, the relatively high equivalent isotropically radiated power (EIRP) of the earth stations in the earth-to-satellite links is a potential source of interference to terrestrial systems. Rain interference may be a problem at frequencies as low as 4 GHz.

The third phenomenon, depolarization caused by rain, is a matter of concern in the case of dual-polarization radio links operating at microwave and millimetre-wave frequencies [CCIR, 1982f]. An additional, orthogonal polarization is presently being introduced on single-polarization radio systems all over the world. This is happening because the addition of the orthogonal polarization enables frequency re-use and effectively doubles the channel capacity without increasing the bandwidth. Rain, however, has the effect of depolarizing the electromagnetic wave. Consequently, a fraction of the power transmitted on one polarization state will be cross-polarized and will be received in the polarization port of the orthogonal polarization at the receive antenna.

This cross-polarized signal acts as a source of interference to the signal of the wanted polarization and may, during periods of heavy rainfall, cause system outages. The magnitude of rain depolarization depends on rainfall rate to a large extent and also increases with frequency. It may be a problem at frequencies as low as 4 GHz.

When designing a microwave or millimetre-wave radio link it is imperative to have a reasonable estimate of the expected average annual outage, be it caused by rain attenuation, rain interference or rain depolarization. Of prime importance in any attempt to predict or estimate the average outage by any of these mechanisms is a knowledge of the statistics of nearly instantaneous rainfall rate at the location in question. In particular, the average annual cumulative probability distribution of rain rate (or rain intensity) is required.

In Southern Africa there is a need for the prediction of rain attenuation, rain interference and rain depolarization on both terrestrial and earth-satellite links. The need to establish a capability to predict rain attenuation, especially, is a matter of great urgency. In this part of the world, as in the majority of developed countries, there is a paucity of reliable long-term nearly instantaneous rain-rate data from which the average annual rain-rate distribution may be compiled. This thesis has therefore been aimed at devising a method for obtaining the required rain-rate distribution at arbitrary locations on the subcontinent from other widely available climatological parameters. It describes the development of a semi-empirical mathematical model that provides the rain-rate distribution from only the mean annual rainfall figure and the climate designation ('coastal' or 'inland') of the location in question. The thesis furthermore discusses the application of rain-rate distributions from the model in

existing attenuation models for obtaining the rain-attenuation distribution.

The rain-rate model has been developed mainly for the more urgent requirement of predicting the annual average cumulative distribution of rain attenuation on radio links -- and is presented as a model for that purpose. It has the potential, however, also to be applied to the fields of rain interference and rain depolarization. Moreover, the information is presented in a manner which also allows the model to be of use outside of the field of electrical engineering, should that be necessary.

In the following chapter the reader is introduced to the problem of rain-attenuation prediction as it is manifested in Southern Africa. It is shown that the main problem is obtaining the rain-rate distribution. Chapter 3 deals with an investigation into a theoretical extreme-value method, published elsewhere, for obtaining the rain-rate distribution. The method has been found valid, but also has limitations. In Chapter 4 it is shown that the general validity of the extreme-value method leads to the hypothesis that a rain-rate model may be developed. The development of the model is then described in Chapter 5, followed by a summary of the model and an analysis of its characteristics in Chapter 6.

Results from the application of the model to Southern African locations are given in Chapter 7. The Southern African observed distributions, against which the theoretical distributions for this subcontinent are evaluated, are given in Chapter 8. This chapter also gives the details of the Southern African locations and describes some of the features of the observed distributions.

Results of rain-rate prediction by the model for North American locations are given in Chapter 9. The

model was tested for North American locations as a precursor for testing it for actual attenuation prediction on that subcontinent. The attenuation predictions on that subcontinent were necessary because of a lack of attenuation data in Southern Africa with which the method could be tested. Chapter 10 gives the results, for North America, of the prediction of rain attenuation on earth-satellite paths, using the rain-rate model.

A summary of results is given in Chapter 11, followed by General Discussion, Conclusion and Recommendations in Chapters 12, 13 and 14, respectively.

Chapter 2

THE PROBLEM

In this chapter the requirements for rain-attenuation prediction as formulated by the international radio engineering community is first given. The most important facets of the problem of prediction, as they relate to Southern Africa, are then discussed. It is shown that the main problem for Southern Africa is obtaining the rain-rate distribution and that the problem is aggravated by a paucity of suitable rain statistics. It is further shown that of the many existing models for predicting the rain-rate distribution, not one will meet the requirement in Southern Africa.

2.1 The primary requirement: The attenuation distribution

For the engineering of terrestrial and earth-satellite radio links operating at frequencies above 10 GHz, the average annual cumulative probability distribution of rain attenuation for the total path, at the given frequency and polarization, is required [Fedi, 1981b and Brussaard, 1981]. The average cumulative distribution of attenuation allows one to find the necessary rain fade margin to be included in the power budget of the link in order to meet one's availability objective. The specified availability is usually in the range of 99,9 to 99,999% over the long-term. Fig. 1 shows examples of the cumulative distribution at 11,7 GHz for earth-satellite paths at various locations in the USA, which were obtained by measurement over a period of one year [Ippolito et al., 1983]. The measurements for the paths were done at

different antenna elevation angles, but they have been scaled by Ippolito et al. to the same angle so as to enable comparisons to be made. The percentage of time that the abscissa is exceeded is given on a logarithmic scale. The attenuation value on the abscissa is equal to the rain margin required when the vertical axis is taken to represent the annual outage percentage (which is 100% minus the availability percentage). The distributions have been obtained over too short a period to be regarded as annual averages, but they nevertheless show the large variation from one location to another. The graphs illustrate that significantly different fade margins would have been required for the different paths, if an annual outage of, say, 0,01% had been the maximum outage allowed during the year of measurement.

The rain-attenuation distribution is a statistical quantity which is difficult to obtain by attenuation measurement over periods of less than two or three years, because of large year-to-year variability in the rainfall of a location [Crane, 1980 and Dutton and Dougherty, 1979]. Also, because of large location-to-location variability in rainfall [Lin et al., 1980 and Watson et al., 1982, p 1], attenuation measurements made at one location may not be representative of the situation on a similar path at another location. Even when a 2- or 3-year measured attenuation distribution is available for a link at a particular location, it is not always easy to scale this distribution to that of the annual average distribution of another path at the same location, but which may have a different frequency, polarization or path length [URSI, 1981].

2.2 A secondary requirement: The rain-rate distribution

The fact that obtaining the annual average attenuation distribution by attenuation measurement is hampered by large inter-annual and geographic variability has in

recent years led to the development of methods whereby the distribution for a path may be predicted from rain statistics [URSI, 1981]. The majority of these prediction methods, such as those of Fedi [1981a], CCIR [1982b and 1982c], Misme & Fimbel [1975] and Lin [1977 and 1979], utilize the average annual cumulative distribution of point rainfall rate. It is required that the rain-rate distribution be compiled from rain rates which have been measured continuously and nearly instantaneously. The measurements should also be made over a long period (many years) and should be made at a representative point on the surface, in the area where the link is to operate. The requirement that the rain-rate data should be nearly instantaneous implies that the rain-rate measurements be based on a rain-gauge integration time (or collecting period) of 5 minutes or less[1]. Fig. 2 gives examples of nearly instantaneous rain-rate distributions obtained by measurement over a period of 3 years [Goldhirsh, 1980]. The vertical axis gives the percentage of time (on a logarithmic scale) that the rain rate on the abscissa was exceeded. The distribution labeled 'combined' is the average for the 3 years. Also shown are the distributions of the best and the worst years of the 3-year period. Not one of the distributions is necessarily representative of the average over the long-term.

2.3 Difficulty in obtaining the rain-rate distribution in Southern Africa

The above-mentioned rain-attenuation prediction methods would probably have sufficed for Southern Africa, had it not been for a problem with the availability of

---

1. There is some variation in the literature as to what is meant by the term 'nearly instantaneous'. We will adhere to the given definition throughout the thesis.

rain-rate statistics. In Southern Africa, as is the case in many other developed regions of the world, there is a paucity of nearly instantaneous rain-rate data. Rainfall is continuously recorded by autographic rain-gauges of the South African Weather Bureau at about 100 locations throughout the subcontinent. However, the rainfall quantities reflected in the statistics available are integrated over 15 minutes. This is significantly higher than the integration time required by any of the known rain-attenuation prediction methods. The probability values of distributions are very integration-time dependent, as may be seen from Lin [1979], Bodtmann and Ruthroff [1974] and Damosso et al. [1981].

Empirical relationships have been established for other continents by which the distribution of nearly instantaneous integration time may be derived from distributions at higher integration times [Damosso et al., 1981]. We could possibly use these relationships to obtain distributions of an integration time of 5 minutes or less from 15-minute distributions, the latter being compiled[2] from the Weather Bureau data available. However, it is uncertain as to whether these integration-time relationships hold in Southern Africa.

If the 15-min statistics are nevertheless used for obtaining distributions at low integration time, there is furthermore the problem of an inadequate density of gauging points. Suitable 15-min statistics are available for only about 20 of the 100 measuring stations on the subcontinent. For the remainder the data is in the form of daily strip charts. To obtain the cumulative distributions from these is a very tedious process. Therefore, with only 20 observed 15-min rain-rate distributions available geographic interpolation for other locations has to be considered. However,

---

2. Compiled 15-min distributions are discussed in Chapter 8.

interpolation presents a problem when large distances or more than one rainfall regime are involved, as will be the case when using data of only 20 locations for the whole of the subcontinent. This is an aspect well illustrated by Dutton [1977]. It is shown that interpolation only becomes feasible after the rain rate has been characterized by a number of independent parameters -- which happens to be available for the USA, but not for Southern Africa.

The two problems, therefore, i.e. the uncertainty in the integration-time dependence of the rain-rate distributions of this subcontinent and the difficulty of interpolating geographically, stand in the way of obtaining nearly instantaneous rain-rate statistics for use in the attenuation prediction methods mentioned in Section 2.2. The methods will not be attractive for application on this subcontinent, unless a reliable way can be found of obtaining estimates of the nearly instantaneous rain-rate distributions.

Another possibility is to use one of the many existing rain-rate models.

2.4 Inadequacy of existing rain-rate models

Continuing efforts in many countries during the past years to overcome the problem of the lack of nearly instantaneous rain-rate data have led to the development of models -- regional and global -- for the estimation of the nearly instantaneous point rain-rate distribution. For Southern Africa, seemingly viable models[3] for the estimation of the rain-rate distribution are those of Rice and Holmberg [1973], CCIR [1978, 1982a], as well as

---

3. There are many models found in the literature. The majority, however, utilize rain parameters not generally available in Southern Africa.

the model inherent to the procedure used in the global rain attenuation model by Crane [1980]. These models employ parameters that are mapped on a global scale and will give rain-rate distributions for integration times ranging from 1 to 5 minutes. These distributions are suitable for application in one or another of the attenuation prediction methods of Section 2.2.

The problem with the above-mentioned models, however, is that their geographical maps, which delineate the rain climate zones, do not have sufficient resolution for the Southern African region. What may easily be recognised as different rainfall regimes have occasionally been grouped together in the same climatic region -- possibly inadvertently, but more likely because of a lack of rainfall data when the maps were devised. A lack of data is also seen as a problem by Fedi [1981b] in characterizing, in sufficient detail, the rain-rate climates of many countries.

Fig. 3, more fully discussed in Appendix G, illustrates the point in regard to the method of CCIR [1982a]. It shows the standard CCIR curves for all the rain-climate regions covering the lower part of the Southern African subcontinent. Also shown are the observed 15-minute distributions of two Southern African locations, JBM Hertzog Airport (Bloemfontein) and Alexander Bay, which are both well within region E of the rain-rate estimation method of CCIR. Although, because of different integration times, the CCIR curves can not be directly compared with the observed curves, it is clear that neither curve E, nor any single one of the other CCIR curves, will adequately provide for both locations. That the CCIR curve cannot possibly be representative of both locations is also illustrated by differences in the climate type of the two locations. JBM Hertzog is situated in a continental climate with predominantly summer rainfall and has a mean annual rainfall of 561 mm. Alexander Bay is situated in a

desert climate and receives only 44 mm, mostly in winter. (See Table 1 and map of Fig. 30 for particulars about the locations). The average number of days per year with thunder is 65 for Bloemfontein (a few kilometers from JBM Hertzog Airport), while for Alexander Bay it is a meagre 0,9 [S A Weather Bureau, 1954].

The CCIR [1982a] method therefore obviously does not adequately resolve the differences in rainfall climate in the Southern African region. The same applies to the earlier method of CCIR [1978] as well as the methods of, Crane [1980] and Rice and Holmberg [1973]. The latter method is possibly better from the point of view of utilizing two parameters, one of which is widely available (mean annual rainfall). However, the other parameter is a continentality factor which, according to the map given, also does not resolve the difference in rain-rate distribution between, for instance, Bloemfontein and Alexander Bay. Another approach is therefore required to obtain the nearly instantaneous rain-rate distribution.

2.5 Summary

The attenuation-prediction methods developed elsewhere could have been used, had the cumulative distribution of nearly instantaneous point rainfall rate been widely available. Obtaining the nearly instantaneous rain-rate distributions from the relatively coarse 15-min observed distributions is considered inadvisable, however, as empirical relationships from other continents would have to be used. The number of observed 15-min distributions available for the subcontinental region is also not large enough to make interpolation for other locations feasible. The existing models for predicting the rain-rate distribution do not give accurate distributions for the region. Another approach is required.

Chapter 3

AN EXTREME-VALUE INVESTIGATION

On the basis of the fairly widespread availability of 15-minute rain-rate data in Southern Africa a decision was made to investigate the approach offered by Lin [1976, 1977, 1978 and 1979]. Lin [1977] demonstrated a successful method for the prediction of the rain-attenuation distribution on a terrestrial link, using a rain-rate distribution of 5-minute integration time. In a later paper Lin [1979] showed that 5-minute rain rates may also be used for attenuation estimation on earth-satellite links using an adaptation of the original method. Furthermore, Lin [1976] showed that 5-min rain-rate distributions at the higher rain rates (above about 50 mm/h) may be obtained from the series of annual maximum rain rates, by a theory of extreme-value statistics. An extension to this extreme-value method was later made by Lin [1978] whereby, by including the mean annual rainfall of the location, the complete 5-min rain-rate distribution (i.e. including the region below 50 mm/h) could be obtained.

As this latter method of Lin theoretically applies to rain rates of any integration time, it is in principle possible to obtain 15-min rain-rate distributions for 56 locations in Southern Africa. The locations are those for which 15-min annual rain-rate maxima are available from the South African Weather Bureau. They are given in Table 5. Obtaining 15-min distributions for 36 more locations in the region (For 20 of the 56 locations the observed 15-min distributions may be obtained directly from the Weather Bureau statistics) would be a significant

improvement in terms of the problem of geographical interpolation. It was to alleviate the interpolation problem that it was initially decided to test Lin's method for Southern Africa (although, as said before, there is a risk involved in interpolation). This was done with the view to converting the 15-min distributions resulting from the application of the extreme-value method to 5-min distributions, using the relationships of Damosso et al. [1981]. The 5-min distributions would then be used in the two above-mentioned attenuation models. For those locations without data interpolation could then be attempted. The favourable results with the extreme-value method, however, provided new perspectives, as is illustrated in Chapter 4.

It is to be noted that Lin's extreme-value theory has been used with success by Kanellopoulos et al. [1981] and Watson et al. [1982]. In the latter reference the extreme-value theory of Lin [1976] was used, amongst others, to devise rain attenuation maps for Europe. It is further to be noted that in the process of devising the maps for Europe it was decided to standardize on a rain-rate database of 5-min integration time. Support for an integration time of 5 min for rain attenuation prediction is also given by Ippolito [1984], who claims that rain rates of shorter integration times are susceptible to error of measurement. The extreme-value theory and rain rates of an integration time of 5 minutes for rain attenuation prediction therefore seem to be in order.

In order to test the extreme-value method of Lin [1978] rain-rate distributions of an integration time of 15 minutes were calculated for a number of locations. These included 17 locations from the Southern African subcontinental region, as well as two island locations from the South Indian and South Atlantic oceans. The data used were the 15-min annual maxima obtained from the South African Weather Bureau. The calculated

distributions are compared with the observed distributions described in Chapter 8. Before giving the results, however, Lin's method is briefly described. This is done in the section to follow, the application of the method being given in Section 3.2.

3.1 Lin's extreme-value theory

Lin [1976] showed that the rain-rate distribution of a location may be obtained from the series of annual maximum rain rates of the location, by using a theory of extreme-value statistics. However, the distribution obtained by this method does not include the region below about 50 mm/h. An extension to the method was later made [Lin, 1978] whereby, by using mean annual rainfall[1] (MAR) in addition to the annual-maximum series, the complete rain-rate distribution is obtained. The theory assumes a log-Gumbel distribution[2] for the series of annual maximum rain rates of a specified integration time, with cumulative probability given by

$$P(r) \equiv P(R_1 \geq r) = 1 - e^{-e^{-y}} \qquad (3.1)$$

and return period given by

---

1. The term 'mean annual rainfall' and its abreviation MAR is used, rather than 'mean annual precipitation' (MAP). The latter has a more general meaning, including forms of precipitation other than rain.

2. See Appendix D for a description of the Gumbel and log-Gumbel distributions. Lin does not use the term log-Gumbel distribution. However, the distribution he uses is commonly referred to by that name amongst hydrologists.

$$Q(r) \equiv Q(R_1 > r) = \frac{1}{P(r)} = \frac{1}{1 - e^{-e^{-y}}} \qquad (3.2)$$

where the reduced variate y is given by

$$y = \alpha[\ln(r) - U] \qquad (3.3)$$

R_1 is the annual maximum rain rate (in mm/h), r is the variate rain rate (in mm/h) and ln[~] is the natural logarithm. U and α are two extreme-value parameters, α being a parameter of scale and U a parameter of location (or position, also called 'the mode'). They are obtained by an analytical procedure (given by Eqs. D4 to D12 of Appendix D) whereby the theoretical distribution is fitted to the observed distribution. The latter is obtained from the annual series of rain rates $R_1(j)$ of as many consecutive years as are available for a location; the years given by j = 1, 2, 3, ...M. In Eqs. D4 to D12 the parameter X(j) is therefore substituted by $R_1(j)$.

Lin's theory furthermore assumes a lognormal distribution for the parent distribution of rain rate, the cumulative distribution function of which is given by

$$P(R > r) \simeq P_0 \cdot \frac{1}{2} \operatorname{erfc}\left[\frac{\ln(r) - \ln(R_m)}{\sqrt{2}\, S_R}\right] \qquad (3.4)$$

where R is the randomly varying rain rate, P_0 (or P(R>0)) is the probability that rain will fall at the respective location, erfc[~] is the complementary error function [Schwartz, 1980] and r is as defined before. R_m is the

median of R during the raining time and S_R is the standard deviation of ln(R) during the raining time.

Using relationships derived by Gumbel [1954 and 1958], Lin [1978] set up three equations which relate the mean annual rainfall and the extreme-value parameters α and U, to the parameters of the parent distribution of Eq. 3.4.

The equations are:

$$S_R = \frac{P_0\ N}{\alpha} \cdot \phi \left[\Phi^{-1} \left[1 - \frac{1}{P_0\ N} \right] \right] \qquad (3.5)$$

$$R_m = \exp \left[U - S_R \cdot \Phi^{-1} \left[1 - \frac{1}{P_0\ N} \right] \right] \qquad (3.6)$$

$$W = R_m \cdot e^{\frac{S_R^2}{2}} \cdot P_0 \cdot 8760 \qquad (3.7)$$

where $\phi[\sim]$ denotes the normal probability density function and $\Phi^{-1}[\sim]$ the inverse of the standard unit normal probability function. N is the number of rain-gauge integration-time intervals per year, given by

$$N = \frac{8760}{D} \qquad (3.8)$$

where D is the integration time in hours. W is the mean annual rainfall (MAR) in mm.

3.2 The extreme-value theory applied to Southern Africa

Rain-rate distributions for 15-min integration time were calculated for a total of 19 locations, using the 15-min annual maxima and the mean annual rainfall of the locations, as described in Section 3.1. The locations, given in Table 1, include all those for which long-term observed 15-min distributions could be compiled from readily available statistics, obtained from autographic rain-gauges. The South Indian and South Atlantic islands of Marion and Gough are also included. The locations are from widely differing climatic regions, as may be seen from the map of Fig. 30 (the climatic designations being defined in Table 8).

Subsection 3.2.1 deals with the data used, while the results are given in Subsection 3.2.2. A discussion and evaluation is given in Subsection 3.2.3.

3.2.1 Data of annual maximum rain rate and mean annual rainfall

A series of annual maximum 15-min rainfall depths (amounts) $H_1(j)$ was obtained from the South African Weather Bureau for each of the 19 locations of Table 1. An example of the annual series is given in Table 2 -- for Port Elizabeth -- where the 15-min rainfall depths are given in mm. The period of the annual-maximum series for each location is given in Table 3. The depth series was converted to a rain-rate series $R_1(j)$ in mm/h, using the relationship $R_1(j) = H_1(j)/D$ where D is the integration time in hours (D = 0,25 h).

The mean annual rainfall W, given in Table 1, was also obtained from the South African Weather Bureau.

3.2.2 Results

The parameters U and α were obtained as described by Lin [1976 or 1978], which is the same as using Eqs. D4 to D12 of Appendix D. In the equations $X_1(j)$ was substituted by $R_1(j)$, the latter being the series for which the parameters U and α are required. The values of U, α and W were then used in the simultaneous solution of Eqs. 3.5 to 3.7 of Section 3.1 (the equations are transcendental and were solved by computer iteration). The values of P_0, S_R and R_m thus obtained for each location are given in Table 3, together with the values of α and U. Utilizing these values in Eq. 3.4 the distributions of Figs. 4 to 22 were obtained (the dot-dash lines). The dotted lines in the figures give the observed distributions, obtained as described in Chapter 8.

Results on comparing a calculated distribution with an observed distribution may be presented in various ways. It has been decided to put the emphasis on the deviation in the exceedance probability at a particular value of rain rate, rather than the rain-rate deviation at a particular level of probability. The probability deviation is slightly more useful for visualizing the attenuation prediction error. That is because in most rain attenuation prediction methods any error (or deviation) in rain-rate probability (at a particular value of rain rate) is equivalent to the error in attenuation probability. The alternative -- to obtain the error in attenuation for a particular error in rain rate -- entails a mathematical exercise, involving a particular model for the attenuation distribution. It is therefore not recommended.

Referring to Figs. 4 to 22 the following observations are made. Deviations of less than a factor of 2 occur over the larger part of the probability range for all locations. Table 4, which gives the greatest overall deviation for each location, shows that it occurs mostly in the tail regions, i.e. at very high or very low rain rates (rain rate is given in brackets in Table 4). There are only 4 exceptions: Alexander Bay, DF Malan, George and Gough Island. At these locations the greatest deviation occurs at moderate rain rates. In the case of the former two locations the observed probability is over-estimated, while in the case of the latter two it is under-estimated. The maximum greatest overall deviation in probability occurs at Keetmanshoop, South West Africa, where the calculated curve over-estimates the observed by a factor[3] of about 10 at a variate rain rate level of r=0 mm/h[4]. The next two greatest deviations occur at Marion Island and Port Elizabeth where, at r=0 mm/h, the observed distributions are over-estimated by a factor of about 7. In the case of Marion Island the calculated probability even exceeds 100% -- a theoretical impossibility. The next greatest deviations are over-estimations of about 4 for both Grootfontein (Cape Province) and Upington; the former also at a rain-rate level of r=0 mm/h, but the latter in the low-probability (high-rain-rate) tail region. Of the 19 locations 12 exhibit a deviation ratio of less than 4 over the whole

---

3. In the tables of this thesis a positive deviation ratio indicates an over-estimation, while a negative ratio indicates an under-estimation.

4. A probability at a rain rate of r=0 mm/h is the same as the probability that it rains, P_0, or P(R>0). A further point to note is that, as for the observed distributions, we have assumed that P(R>0) is approximately the same as P(R>0,4). The statistics obtained from the Weather Bureau did not go below R=0,4 mm/h.

of the probability range. Eight have a deviation of less than 3, while only one (George, Fig. 7) has a deviation of less than 2.

At a rain-rate level of r=0 mm/h it may be seen from Table 4 that there are under-estimations for about as many locations as there are over-estimations. However, the under-estimations in general are not as severe as some over-estimations. The under-estimations do not exceed a factor of 3,6 where, as has been pointed out, the over-estimation at this rain-rate level is 10 for Keetmanshoop. At 14 locations the deviation at r=0 mm/h is less than 4, while for 12 it is less than 3. For 6 locations it is less than 2.

The agreement between calculated and observed curves improves dramatically advancing from the variate rain-rate level of r=0 mm/h to r=2 mm/h. Also, as can be seen from the curves, there is a marked improvement with decreasing rain rates in the right-hand tail region. To enable comparisons with results given later, the distributions at rain-rate values greater than 2 mm/h and at probability values greater than 0,001% are considered in greater depth than the tails lying below these values. For this purpose a column is provided in Table 4 which gives the greatest deviation in the region concerned for every location. The location which here provides the greatest deviation is again Keetmanshoop, where as can be seen from Fig. 14, over-estimation occurs over the whole region below about 15 mm/h. The maximum over-estimation for Keetmanshoop above 2 mm/h and above 0,001% is a factor of about 8, occuring at 2 mm/h and increasing with decreasing rain rate to the absolute maximum of 10,2 at r=0 mm/h. Of the 19 locations 18 have a probability deviation of ratio 4 or less over the whole of the range of values above 2 mm/h and above 0,001%, while 13 have a deviation of less than 3. For 9 locations the deviation is less than 2.

For reasons of comparison with the work of another author [Segal, 1979] the probability deviation is considered at the probability level of 0,003% (probability of the observed distribution). Here all locations exhibit a deviation which is less than 2. In about three-quarters of the cases under-estimations occur, while the remainder are over-estimations.

On the whole the shape of the calculated curves are concave and are therefore similar to those of the observed distributions. For those locations where the probability at 0 mm/h is excessively over-estimated there is a larger under-estimation at moderate rain rates than for most of the other locations. Figs. 6, 9, 14, 17 and 19 are examples of locations where this is the case. Regarding the low-probability tail region: there is sometimes under-estimation and sometimes over-estimation, but over-estimation is predominant. There seems to be no systematic deviation anywhere in the probability range.

3.2.3 Discussion and evaluation

A deviation of less than 3 in probability at a specific level of rain rate is regarded as acceptable while a deviation of less than 2 is regarded as good. A deviation greater than a factor of 4 is regarded as excessive. These criteria have been formulated after considering the performance of many other models found in the literature. The fact that all locations display a deviation of less than 2 over the larger part of the probability range is similar to the results obtained by Lin [1978] for North America and is encouraging. However, the excessive deviations (above a factor of 4) in the tail regions of very high and very low rain rates for a substantial proportion of stations (about one third) is disturbing and needs further investigation.

As far as the region of very low rain rate is concerned, it can be shown that the probability in the region below a rain-rate level of about 2 mm/h is very dependent on the value of P_0 used in Eq. 3.4 to obtain the calculated distribution. This is also intuitively felt as P_0 (the probability that it rains, given by the intercept on the vertical axis) must be closely related to the values of the probability of rain rates close to 0 mm/h. It can also be shown that the value of P_0 as obtained by Eqs. 3.5 to 3.7 is very sensitive to the value of α. The parameter α in turn is a function of the log-Gumbel standard deviation as per equation D4 of Appendix D. Any small error in the standard deviation will therefore be reflected as a relatively large error in P_0. The situation is that one sometimes has difficulty in establishing the log-Gumbel standard deviation accurately with an annual series of a limited number of years, because of sampling error [Midgley and Pitman, 1978]. A finite time base is also seen as a problem by Chu and Schecker [1985]. In the case of Keetmanshoop, for instance, the excessively high value of P_0 may have been due to too high a value of standard deviation (too low a value of α). The unnecessarily high value of standard deviation would nevertheless not have caused the distribution to differ seriously in the moderate rain-rate range. To illustrate: Raising the value of α for Keetmanshoop by 20% from the value given in Table 3 alters it to 2,25. This causes an equivalent change in U to 3,40 according to Eq. D14 of Appendix D[5]. With these values of α and U the following values of P_0, R_m and S_R are obtained:

---

5. Although strictly speaking Eq D5 rather than Eq D14 applies, it is more convenient to use Eq D14. The error, however, will be negligible.

P_0 = 1,17%
R_m = 0,61
S_R = 1,39

It is noted that while P_0 has decreased by a factor of about 4, R_m has increased by a factor of 10 (see Table 3). The above values produce the distribution of Fig. 23, on the axes of which the observed distribution for Keetmanshoop has been repeated. As can be seen much better agreement is now obtained, especially at low rain rates. The calculated P(R>0) now over-estimates the observed by a factor of only 2,1. At 2 mm/h the over-estimation is now less than 2, as opposed to the previous value of 8. The agreement in the high-rain-rate tail region is now also much better. There has also been an improvement in the region of moderate rain rate, although this is not very pronounced. In general, therefore, a better fit is obtained. It is therefore very likely that the value of α calculated from the annual series is too low. The cause is that the log-Gumbel standard deviation is too high, probably because of too limited a data sample -- although the 28-year sample is not the smallest of the 19 locations.

Similar improvements in agreement between the predicted and the observed distribution, by increasing the value of α, may likewise be demonstrated for the other locations displaying too high a probability at r=0 mm/h -- i.e. East London, Grootfontein (CP), Marion Island and Port Elizabeth. Comparing the value of α for East London, Grootfontein (CP), Keetmanshoop and Port Elizabeth with the average value of α for the remaining 13 locations on the subcontinent, one finds that they are all significantly lower. The average is 3,2 while the highest among the 4 locations is for East London, with a value of 2,42 (see Table 3). This, plus the fact that higher values of α for these locations will give better

fits to the observed distributions, indicate that the values of α for these locations are too low. Overall improvement by the downward adjustment of α may likewise be demonstrated for those locations where P_0 has been appreciably under-estimated, viz. J G Strydom and Pretoria.

Fortunately, however, a value of α which is not very accurate and the consequent values of P_0, R_m and S_R do not significantly affect the lognormal distribution, except in the tail regions of very high or very low rain rates. The insensitivity of the lognormal distribution to P_0, at moderate rain rates, is supported by Chu and Schecker [1985]. These authors have demonstrated that extrapolating an observed point rain-rate distribution at moderate rain rates to higher and lower rates using a lognormal approximation is insensitive to the observed raining time P_0 -- except at very low rain rates. It has been found that errors of even an order of magnitude in P_0 will not significantly affect the distribution at most levels of rain rate. Moreover, the change obtained in probability in the high-rain-rate tail region by changing the value of α is not as great as for P_0, at least not in the range of interest. It is therefore only the very low rain-rate region which is seriously affected. A mitigating factor, however, is the fact that the very low rain rates are seldom used for rain attenuation prediction on communication links.

As far as the region of very high rain rates is concerned, the excessive deviations here are caused by statistical instability in the observed distribution. The effect is evident at probability levels below 0,001%, where the deviations are relatively large. Statistical non-stationarity in the region below 0,001% has been the main reason for concentrating on the region above that when giving results in the previous subsection. Lin [1978] also shows that statistical instability is very

likely at these levels of probability. At Newark, New Jersey, for instance, the addition of the data of two more years to the data from 19 previous years altered the 5-min observed probability by a factor of 4 at a rain-rate level of 170 mm/h.

Excluding the probability region below 0,001% because of statistical instability and the region below 2 mm/h because of its over-sensitivity to the value of α, the following conclusions are drawn: Generally speaking the agreement being below a factor of 2 over the whole range, for 9 out of 19 locations (i.e. about 50%), is good. The results represent a confidence level of about 50% and is especially significant when considering that the locations are from widely differing climates. Although the deviation is excessive for one of the 19 locations (Keetmanshoop), being a factor of about 8 at 2 mm/h, it is not seen as a serious matter. It only confirms the fact that due to a limited time base in the annual-maximum series it may in some cases be difficult to obtain the value of α accurately.

Of particular significance is the performance of the method at a probability level of 0,003%. Here the deviations all are below a factor of 2 (see Table 4). Although this represents a confidence level of 100% the sample of locations may not have been large enough for this value to be regarded as the true confidence level of the method. Let it be assumed that the true confidence level at an accuracy of 2, at the probability level of 0,003%, is 90%. Segal [1979] has shown that in order to obtain the probability at the level of 0,003% to an accuracy of a factor of 2 (100%) and to a confidence level of 90%, at least two years of observation is required. It can therefore be said that the estimation method produces results which are equivalent to a measurement programme of more than two years. It is therefore a method worth considering, the results

pointing to the general validity of Lin's extreme-value method. The lognormal approximation for the distribution of randomly varying rain rate, as well as the validity of the log-Gumbel approximation for the distribution of annual maxima are therefore supported. The theoretical distributions seem to be valid, not only for locations on different subcontinents, but also for various integration times -- keeping in mind that in Lin [1978] results were obtained for North America at 5-min integration time. A large degree of commonality in the statistical characteristics of the rain on different continents is indicated. The method therefore commands a high degree of confidence as a technique for obtaining rain-rate distributions at various integration times and for various localities.

3.3 Summary and conclusion

Satisfactory results have been obtained with Lin's extreme-value method for estimating the rain-rate distribution at 15-min integration time in Southern Africa. It seems to be valid for the subcontinental region as a whole, and also for the climates of the South Indian and South Atlantic oceans. There is some difficulty in obtaining the correct value of α in a few cases, but this does not invalidate the theory. The theory points to commonality in the statistical behaviour of rain rates on various continents. The method as it stands, however, presents two problems in regard to a subcontinent-wide capability for rain-attenuation prediction. Firstly, the 5-minute rain-rate distributions that the two preferred[6] attenuation prediction methods require [Lin, 1977 and 1979] cannot be obtained directly by the extreme-value method, because 5-min annual maxima are not readily available in the region.

---

6. These methods are preferred to other methods for various reasons, as discussed in Chapter 10.

A possiblity is to use maxima of either 15, 30, 45, 60 or 1440 minutes to obtain distributions of the corresponding integration time. These could then be converted to 5-min distributions. As was discussed in Section 2.3, there is a risk involved in doing such conversions. Secondly, although somewhat alleviated by the number of stations for which maxima are available, there is still the problem of geographic interpolation. There are only 56 stations for which annual maxima are available, representing an average of approximately 40000 km^2 per station. Any attempt to interpolate the calculated distributions for other locations will, because of the large distances spanning different rainfall regimes between stations, prove to be futile.

Chapter 4

HYPOTHESIS FOR EXTENDING THE EXTREME-VALUE APPROACH

Of prime concern is the ability to obtain 5-minute rain-rate distributions for application in the rain-attenuation models of Lin [1977 and 1979]. Had rain-rate maxima at this integration time been freely available in Southern Africa, it would have been possible to obtain the necessary distributions using Lin's extreme-value method described in the previous section. However, maxima of only 15, 30, 45, 60 and 1440 minutes are available for only the 56 autographic rainfall stations of Table 5. Even if the 5-minute distributions could be derived from distributions at the above integration times -- the latter as obtained by the extreme-value method -- the sparse population of stations militates against geographic interpolation for other locations.

These problems raise the question whether it is not perhaps feasible to model the extreme-value parameters α and U, used in Lin's method, on other more widely available rain-related parameters. Four aspects point to the feasibility of modelling.

Firstly, there are the results from the previous chapter that indicate that the log-Gumbel approximation for annual maximum rain rates and the lognormal approximation for the parent distribution of rain rate are valid over large geographic regions and at various integration times. Especially the lognormal distribution has found wide acceptability as an approximation to the parent distribution of rain rate, as may be seen from Chu and

Schecker [1985], Macchiarella [1985], Kanellopoulos [1983a], Kanellopoulos and Clarke [1981a and 1981b], Kanellopoulos et al. [1981] and Segal [1980]. Already having at one's disposal two well-behaved distributions seems to be a good starting point in any modelling effort. Furthermore, Lin's extreme-value method has also given satisfactory results in Greece [Kanellopoulos et al., 1981] and has been used in the development of a climatic map of rain attenuation for Europe [Watson et al., 1982]. Apart from the favourable results obtained in Lin [1976 and 1978] and in Chapter 3, there is therefore relatively substantial support for the utility of the extreme-value method. It seems logical to exploit the method to the full.

The second aspect that points to the feasibility of modelling is that it intuitively seems possible to extrapolate from the values of the extreme-value parameters α and U at higher integration times, to those at lower integration time. The values of the parameters at 5 minutes may thus possibly be obtained from their values at 15, 30, 45, 60 and 1440 minutes -- all of which may be calculated from the annual maxima available for the 56 locations of Table 5.

Thirdly, considering the observed 15-min distributions of Chapter 8, a noticeable trend is that of higher cumulative probabilities with higher mean annual rainfall, in general (see Figs. 4 to 22). This creates the suspicion that there may be relationships between the parameters of the lognormal distribution -- which has been shown to approximate the observed distributions satisfactorily -- and mean annual rainfall. Such relationships would imply relationships between either or both of the parameters α and U of the log-Gumbel distribution and mean annual rainfall, as α and U are related to the lognormal parameters P_0, S_R and R_m by Eqs. 3.5 to 3.7.

The fourth aspect supporting a modelling approach is the work done by Midgley and Pitman [1978]. These authors devised a depth-duration-frequency diagram for the hydrological community in Southern Africa (shown in Fig. 24), which is based on certain extreme-value relationships. Although at this stage it is not clear exactly how the diagram may relate to the problem of finding a rain-rate model, the following points are noted from the work (see Appendix C):

- Use was made of the observed annual-maximum series of many locations, of rainfall amounts of various integration times, including 15, 30, 45, 60 and 1440 minutes.

- Log-Gumbel distributions were successfully fitted to the annual-maximum series of rainfall amounts of all integration times.

- For a particular climatic region and for a particular integration time an empirical relationship was established between the mean of a log-Gumbel distribution and mean annual rainfall. This was done for two climatic regions and various integration times.

- The variate rainfall depth, i.e. the value of rainfall depth exceeded by an annual maximum depth of a specified return period (or probability), given by h in quadrant C of Fig. 24, is a function of integration time (or duration, as it is called in the report). It is also a function of mean annual rainfall and climatic region. Furthermore, according to Fig. 24, the quantity h bears some relation to a log-Gumbel distribution.

- The quantity h is necessarily related to the variate rain rate r by $h=rD$, where D is the integration time.

The above observations about the work of Midgley and Pitman suggest that relationships exist amongst the parameters of certain log-Gumbel distributions, mean annual rainfall, climatic region and integration time. The log-Gumbel distributions are all associated with rainfall depths, which are equal to rain rates when multiplied by the integration time. As Lin's extreme-value theory uses the log-Gumbel distribution it is therefore very likely that an investigation into the Midgley-and-Pitman depth-duration-frequency diagram will provide something of use.

On the basis of the above considerations the following hypothesis is presented: The general paucity of rain-rate data on the subcontinent may be overcome. Lin's extreme-value method could possibly be extended by developing generalized model expressions for α and U, rather than using values derived from the annual maximum rain-rate series of one location only. It should be possible to relate α and U at a particular integration time to other more widely available rain-related parameters. Furthermore, it should be possible to extrapolate from the values of α and U at higher integration times in order to find the values at 5 minutes. It is proposed, therefore, that a rain-rate model for Southern Africa, based on the log-Gumbel distribution of annual-maximum rain rates and the lognormal distribution of time-varying rain rate be developed. It is furthermore proposed that the relationships for α and U may possibly be established from relationships in the Midgley-and-Pitman [1978] depth-duration-frequency diagram.

Chapter 5

DEVELOPMENT OF THE RAIN-RATE MODEL

Based on the hypothesis of Chapter 4, an investigation was made into the utilization of the depth-duration-frequency diagram by Midgley and Pitman [1978]. The investigation resulted in a rain-rate model for the Southern African subcontinent. Some of the extreme-value relationships embodied in the diagram were utilized to obtain generalized expressions for the extreme-value parameters α and U, for use in Lin's extreme-value method. The model expressions for the parameters α and U are semi-empirical and are based on the extreme rain-rate data of various integration times of the 56 locations of Table 5. The resulting model may be classed as a mathematical semi-empirical extreme-value-based model for surface point rain-rate distribution. It may be used for obtaining an estimate of the cumulative surface point rain-rate distribution, at integration times ranging from 5 to 1440 minutes, for arbitrary locations on the Southern African subcontinent. The only input parameters required are those of climatic region (one of two regions) and the mean annual rainfall of the location. The 5-minute distributions which the model provides have the potential of being utilized in the two preferred rain-attenuation prediction methods, one being for terrestrial paths [Lin, 1977], the other being for earth-to-satellite paths [Lin, 1979 or Lin et al., 1980].

The main purpose of this chapter is to define the rain-rate model and to describe its development. The theory of Lin's extreme-value method is so fundamental to the model that the reader is advised to refer once again

to Section 3.1. Section 5.1 gives the relationships from the Midgley-and-Pitman report which are relevant to the development of the model. In Section 5.2 it is shown how these relationships were utilized in order to obtain the expressions for the extreme-value parameters α and U. The section leans heavily on the detailed discussion of the Midgley-and-Pitman relationships in Appendix C. The various aspects of the Midgley-and-Pitman diagram is extensively treated in the appendix as all theoretical and empirical aspects of the model will not be appreciated unless the diagram is fully understood.

5.1 Analytical relationships of the Midgley-and-Pitman DDF diagram

The depth-duration-frequency diagram (DDF diagram) of Midgley and Pitman [1978], shown in Fig. 24, is based on an analysis of the parameters of the log-Gumbel[1] distributions of rainfall depths, at various integration times, of 56 locations spread throughout the subcontinent. The positions of the locations are shown on the map of Fig. 25 and are listed in Table 5. The DDF diagram had been designed for the hydrological community in Southern Africa with the aim of providing, at arbitrary locations, the return period (or probability) of exceeding certain amounts of rainfall in time intervals of a specified length.

The only input parameters that the DDF diagram uses, apart from the length of the collecting interval (or duration or integration time), are the mean annual rainfall figure and a designation as to whether the location is climatically 'coastal' or 'inland'. A full description of the development of the diagram and the relevant analytical relationships are presented in Appendix C. Figs. 26 and 27 give some relationships used in the

1. See Appendix D for the log-Gumbel distribution.

design of the diagram. They are extensively discussed in Appendix C. Fig. 28 shows the method of construction, also discussed in Appendix C.

We note from Appendix C that the relationships of the three quadrants of the DDF diagram may be expressed mathematically. The remainder of this section is devoted to a summary of these relationships.

Quadrant A of the DDF diagram (see Fig. 24) gives h_a, the rainfall depth (in mm) in a certain time interval D (the duration), which is exceeded with a return period of 20 years, at a location with a mean annual rainfall (MAR) of 500 mm. The expression for h_a is given by Eq. C24, to be

$$h_a = \frac{r_0 \cdot D}{(1+BD)^n} \qquad (5.1)$$

where r_0, B and n are constants associated with either of the two climatic regions, 'inland' or 'coastal'. D is given in hours.

Quadrant B transforms the 20-year, 500-mm/a value h_a to h_b, which is the 500-mm/a value for a return period of $Q(h_b)$ years. It does so by utilizing a log-Gumbel distribution which, according to Eq. C27 of Appendix C, is given by

$$P(h_b) = 1 - e^{-e^{-y''}} = \frac{1}{Q(h_b)} \qquad (5.2)$$

where the reduced variate y" is given by

$$y'' = \alpha''[\ln(h_b) - U'']$$

$$= 3{,}5726[\ln(h_b) - U''] \qquad (5.3)$$

and where the 20-year value of h_b, according to Eq. C30, is given by

$$(h_b)_{20} = h_a$$

Eq. 5.3 is the reduced variate given by Eq. C28 of Appendix C and as can be seen α'' is a constant and therefore invariant with any parameter such as integration time, MAR or climatic region. U" is undefined, but as can be seen from combining Eqs. C31 and C33 the ratio h_a/h_b can be obtained without knowing the value of U", as it is a function of only the return period $Q(h_b)$.

Finally, to conclude the description of the relevant relationships of the diagram and according to Eq. C34, the $Q(h_b)$-year, 500-mm/a value h_b is, in quadrant C, converted to h, the actual Q(h)-year depth value to be exceeded at a location receiving W millimetres per year. It is given by

$$h = h_b F \qquad (5.4)$$

where F is an empirical multiplication factor of which an approximation is given by Eq. C35. The approximation is shown in Fig. 29 and is given by

$$F = 0,25 + 1,61 \cdot 10^{-3} \cdot W \qquad (5.5)$$

where W is the mean annual rainfall in mm.

5.2 Mathematical procedure to find expressions for α and U

The aim is to find expressions for the extreme-value parameters α and U (of Eq. 3.3 in Section 3.1) in terms of mean annual rainfall, climatic region and integration time.

It is noted from the theory of the DDF diagram, as explained in Appendix C, that the rainfall depth h (in mm), given on the vertical axis of quadrant C of the diagram, is the actual rainfall depth of duration D exceeded at a given return period Q(h). It is also noted that h represents an approximation to the variate of a log-Gumbel distribution. This distribution is given by Eq. C11 of Appendix C, to be

$$P(h) \equiv P(H_1 > h) = \frac{1}{Q(h)} = 1 - e^{-e^{-y'}} \qquad (5.6)$$

where the reduced variate y' is given by Eq. C12, to be

$$y' = \alpha'[\ln(h) - U'] \qquad (5.7)$$

H_1 is the annual maximum rainfall depth that exceeds the variate h with probability P(h). Q(h) is the return period in years. The parameter of scale α' was found to be invariant with integration time, MAR and climatic

region and, from Eq. C13, is given by

$$\alpha' = 3,5726 \qquad (5.8)$$

The parameter of location U' is seen to be a function of integration time, MAR and climatic region. It is given by Eq. C14 of Appendix C and is defined at integration times of 15, 60 and 1440 minutes (according to Eqs. C6 to C10).

It is realized that the distribution of Eq. 5.6 is similar to the distribution of which the parameters are needed, i.e. the distribution of Eq. 3.1. It is suspected that α' and U' may be related to α and U of Eq. 3.3, but the relationship is not clear. It is therefore necessary to investigate.

Per definition the rain rate R (in mm/h) is given by

$$R \equiv \frac{H}{D} \qquad (5.9)$$

where H is the collected depth of rain in time interval D. From this relationship follows that the annual maximum rain rate R_1 of Eq. 3.1, is given by

$$R_1 \equiv \frac{H_1}{D} \qquad (5.10)$$

where H_1 is the maximum rainfall depth. Similarly, the variate r (in mm/h) of Eq. 3.1, is given by

$$r = \frac{h}{D} \tag{5.11}$$

where h is the variate rainfall depth in mm.

Substituting for R_1 and r from Eqs. 5.10 and 5.11 in the condition for the probability of Eq. 3.1, we have

$$P(R_1 \geq r) = P\{\frac{H_1}{D} \geq \frac{h}{D}\} \tag{5.12}$$

It logically follows that

$$P\{\frac{H_1}{D} \geq \frac{h}{D}\} = P\{H_1 \geq h\} \tag{5.13}$$

Therefore, from Eqs. 5.12 and 5.13

$$P\{R_1 \geq r\} = P\{H_1 \geq h\} \tag{5.14}$$

From Eqs. 3.1, 5.6 and 5.14, we may then write

$$1 - e^{-e^{-y}} = 1 - e^{-e^{-y'}} \tag{5.15}$$

from which follows

$$y = y' \tag{5.16}$$

The expression of Eq. 5.11 may be substituted for r in

Eq. 3.3, to give

$$y = \alpha\{\ln(\frac{h}{D}) - U\} \tag{5.17}$$

Eq. 5.17 may be rewritten to give

$$y = \alpha\left[\ln(h) - \{U + \ln(D)\}\right] \tag{5.18}$$

It then follows from Eqs. 5.18, 5.7 and 5.16 that

$$\alpha = \alpha' \tag{5.19}$$

and

$$U = U' + \ln(D) \tag{5.20}$$

From Eqs. 5.8 and 5.19, then

$$\alpha = 3,5726 \tag{5.21}$$

which defines one of the required extreme-value parameters, so that Eq. 3.3 may be rewritten to give

$$y = 3,5726\ \{\ln(r) - U\} \tag{5.22}$$

According to Eq. 5.20 an expression for U' is needed in order to define U. However, U' is only defined at 15, 60 and 1440 minutes, which does not meet the requirement of 5 minutes (see Eqs. C14 and C6 to C10). In order to overcome this difficulty the following approach is used:

It has been shown by Eq. C33 of Appendix C that

$$h_b = h_a \cdot e^{\left\{\frac{y'' - 2,9702}{3,5726}\right\}} \tag{5.23}$$

Combining Eqs. 5.4 and 5.23 gives

$$h = h_aF \cdot e^{\left\{\frac{y'' - 2,9702}{3,5726}\right\}} \tag{5.24}$$

Substituting this expression for h in Eq. 5.11 the expression for r becomes

$$r = \frac{h_aF}{D} \cdot e^{\left\{\frac{y'' - 2,9702}{3,5726}\right\}} \tag{5.25}$$

In turn substituting this expression for r in Eq. 5.22, the following is obtained:

$$y = 3,5726\left[\ln\left[\frac{h_aF}{D} \cdot e^{\left\{\frac{y'' - 2,9702}{3,5726}\right\}}\right] - U\right] \tag{5.26}$$

$$= 3,5726\left[\ln\{\frac{h_aF}{D}\} + \{\frac{y" - 2,9702}{3,5726}\} - U\right] \qquad (5.27)$$

Eq. 5.27 may be rewritten to give

$$U = \ln\{\frac{h_aF}{D}\} + \{\frac{y" - y - 2,9702}{3,5726}\} \qquad (5.28)$$

The parameters h and h_b are related by the simple relationship of Eq. 5.4, which involves no probability relationship. Their return periods, other variables being constant, are therefore the same. Therefore

$$Q(h) = Q(h_b) \qquad (5.29)$$

From Eqs. 5.2, 5.6 and 5.29 it follows that

$$\frac{1}{1 - e^{-e^{-y'}}} = \frac{1}{1 - e^{-e^{-y"}}} \qquad (5.30)$$

which implies that

$$y' = y" \qquad (5.31)$$

From Eqs. 5.16 and 5.31 it follows that

$$y = y" \qquad (5.32)$$

In Eq. 5.28 y may now substituted by y", to give

$$U = \ln\{\frac{h_a F}{D}\} - \frac{2,9702}{3,5726} \qquad (5.33)$$

$$= \ln\{\frac{h_a F}{D}\} - 0,8314 \qquad (5.34)$$

Substituting the expression of Eq. 5.1 for h_a, Eq. 5.34 becomes

$$U = \ln\left[\{\frac{r_0}{(1+BD)^n}\} \cdot F\right] - 0,8314 \qquad (5.35)$$

Substituting now for the values of r_0, B and n for the two climatic regions, respectively, from Appendix C (see table following Eq. C24), the following is obtained:

$$U = \ln\left[\{\frac{217,8}{(1 + 4,164D)^{0,8832}}\} \cdot F\right] - 0,8314 \qquad (5.36)$$

for the 'inland' region, and

$$U = \ln\left[\{\frac{122,8}{(1 + 4,779D)^{0,7372}}\} \cdot F\right] - 0,8314 \qquad (5.37)$$

for the 'coastal' region.

In Eqs. 5.36 and 5.37 the parameter U is defined at any integration time D. If an extrapolation is made to a slightly lower value of D than is catered for on the DDF diagram (6 min), which should be in order, the requirement of a 5-min integration time is met. Although the upper limit of integration time on the DDF diagram is 100h there is no need to go beyond 1440 minutes. Other than the integration time the parameter U is only a function of climatic region and MAR, considering that F is a function of MAR only, according to Eq. 5.5. The value of U is therefore easily found by evaluating either of Eqs. 5.36 or 5.37, whichever is appropriate, once the climatic region and MAR is known and after the integration time has been decided upon. Eq. 5.5 is, of course, first used to obtain the value of F from the MAR. The value of U obtained is then used in Eq. 3.6 and the value of α from Eq. 5.21 is used in Eq. 3.5. The value of mean annual rainfall is used once again, in Eq. 3.7. The values of the parameters P_0, S_R and R_m, obtained by solving Eqs. 3.5 to 3.7 simultaneously, is, as a consequence, a function of MAR, climatic region and integration time. The rain-rate distribution of Eq. 3.4 is therefore implicitly a function of these parameters. A semi-empirical mathematical model of rain-rate distribution has thus been established, requiring as inputs only mean annual rainfall and climatic region and in which integration time is a variable.

The 'inland' region, according to Midgley and Pitman [1978], is associated with areas in which convective thunderstorm rain predominates, while the 'coastal' region is associated with areas in which maritime stratiform rain predominates. As a rule of thumb the 'coastal' region may be regarded as the region within about 100 km from the coastline, while the 'inland' region is more than 100 km away. A more accurate representation, however, may be the delineation of the climatic regions

on the map of Fig. 25, obtained from Op ten Noort and Stephenson [1982]. These authors employ the Midgley and Pitman DDF diagram for flood peak calculation in Southern Africa and has found it necessary to delineate the two regions. However, they warn that the map should be used only as a guide. As far as mean annual rainfall is concerned, it ranges from 50 to 2000 mm in the DDF diagram. However, as there are no fundamental limitations in the theory or otherwise, the use of the model below 50 mm should be in order. For rainfalls above 2000 mm/a, however, a certain amount of caution should be exercised. This is discussed in Section 6.5.

The model is summarized in Chapter 6. A specimen calculation showing how the distribution is obtained is given in Appendix E. The model expressions for α and U are verified by comparing calculated rainfall depth values to readings from the DDF diagram, in Appendix F.

5.3 Summary and conclusion

A semi-empirical mathematical rain-rate model has been established. Generalized expressions have been obtained for α and U from relationships in the Midgley and Pitman [1978] DDF diagram for use in Lin's extreme-value method. The cumulative distribution of rain rate may now be calculated from only the mean annual rainfall figure and the climatic designation of the location in question. Only a 'coastal' and an 'inland' climate designation are used. Integration time is variable, ranging from 5 to 1440 minutes. The 5-min distributions from the model are potentially suitable for use in two well-established rain-attenuation prediction methods. The model, however, needs to be tested. Before the testing is described the model is summarized and characterized in the chapter to follow.

Chapter 6

THE MODEL

The purpose of this chapter is to summarize and characterize the rain-rate model developed in Chapter 5. A summary of its mathematical relationships is given in Section 6.1. Some characteristic curves of rain-rate distribution from the model are given in Section 6.2. Section 6.3 is devoted to the sensitivity of the model to its input parameters, while Section 6.4 discusses some other significant characteristics. Section 6.5 deals with extrapolation to mean annual rainfalls beyond 2000 mm.

6.1 Summary of model

The model of rain-rate distribution is an extreme-value-based model consisting of two main parts. The first part is given by generalized expressions for the extreme-value parameters α and U in the reduced variate $y = \alpha(\ln r - U)$. The parameter α is invariant with mean annual rainfall, climatic region or integration time and is given by

$$\alpha = 3,5726 \qquad (6.1)$$

For the parameter U there is a separate expression for each of the two climatic regions. They are

$$U = \ln\left[\frac{217,8 \cdot F}{(1+4,164\ D)^{0,8832}}\right] - 0,8314 \qquad (6.2)$$

for the 'inland' region, which is associated with areas dominated by convective thunderstorm rain, and

$$U = \ln\left[\frac{122,8 \cdot F}{(1+4,779\ D)^{0,7372}}\right] - 0,8314 \qquad (6.3)$$

for the 'coastal' region, which is associated with areas dominated by widespread frontal rain. In the expressions for U, the parameter F is given by

$$F = 0,25 + 1,61 \cdot 10^{-3} \cdot W \qquad (6.4)$$

where W is the mean annual rainfall in mm. W is variable in the range 0 to 2000 mm. D is the the rain-gauge integration time in hours, ranging from 5 to 1440 minutes. The map of Fig. 25 may be used as a guide in obtaining the climatic-region designation. However, as a rule of thumb in Southern Africa, an 'inland' location is one which is farther than 100 km from the nearest coastline, while a 'coastal' location is within 100 km from the coastline.

The second part of the model consists of a log-normal cumulative distribution function as an approximation to the parent distribution of rain rate. It is given by

$$P(R>r) \simeq P_0 \cdot \frac{1}{2} \operatorname{erfc}\left[\frac{\ln(r) - \ln(R_m)}{\sqrt{2}\, S_R}\right] \tag{6.5}$$

where P_0, R_m and S_R are determined by solving the following three transcendental equations simultaneously by computer :

$$S_R = \frac{P_0\, N}{\alpha} \cdot \phi\left[\Phi^{-1}\left[1 - \frac{1}{P_0\, N}\right]\right] \tag{6.6}$$

$$R_m = \exp\left[U - S_R \cdot \Phi^{-1}\left[1 - \frac{1}{P_0\, N}\right]\right] \tag{6.7}$$

$$W = R_m \cdot e^{\frac{S_R^2}{2}} \cdot P_0 \cdot 8760 \tag{6.8}$$

In the above three equations α is obtained from Eq. 6.1 and U from either of Eq. 6.2 or 6.3, whichever is appropriate.

6.2 Model standard curves

Figs. 31 to 46 give some standard curves which result from employing the model at integration times of 5, 15, 30 and 60 minutes, in each climatic region and at various mean annual rainfalls up to 2000 mm.

Figs. 31 and 32 give the standard 5-minute model distributions for the 'inland' region, for various mean annual rainfalls. Figs. 33 and 34 give the distributions for the 'coastal' region.

Figs. 35 to 38 give the distributions for the two regions for a 15-minute integration time, followed by Figs. 39 to 42 which are for 30 minutes. Lastly a set of curves for a 60-minute integration time is given in . Figs. 43 to 46.

6.3 Sensitivity to input parameters

Mean annual rainfall

It is to be noted from the model distributions of Figs. 31 to 46 that there is about an order of magnitude difference in probability per octave of MAR at the higher rain rates, at all four integration times given and in both climatic regions. At lower rain rates the differences become smaller.

Climatic region

Using a mean annual rainfall of 1000 mm and an integration time of 5 minutes for the 'inland' and 'coastal' regions one obtains the curves of Fig. 47. This illustrates that the equiprobable rain rate for

the 'inland' region is about 70% higher than for the 'coastal' region at about the 0,001% level. On the probability axis the difference approaches about one order of magnitude at the higher rain rates.

Rain-gauge integration time

Taking a location which is in the 'inland' region and which has a mean annual rainfall of 1000 mm, and changing the integration time from 5 to 30 to 60 minutes, the set of curves of Fig. 48 is obtained. The fact that the lower integration times give higher probabilities at high rain rates is understandable as some high short-interval rates will not be reflected in longer-interval averages. This has also been found in practice by Bodtmann and Ruthroff [1974] and Lin [1979]. The 5-minute rates are approximately 50% to 80% higher than the 60-minute rates at the same level of probability.

6.4 Other model characteristics

Some other characteristics of the curves deserve attention. Firstly, it is noticeable that the higher the integration time, the higher the intercept on the vertical axis, in general (see Fig. 48). This is perfectly normal as the intercept (the probability of R>0) is obtained from the annual number of clock-duration integration-time intervals in which any rain is received. As the actual time of the rain event may be less than the clock interval during which it occurred, the time so obtained will of necessity be greater than the true raining time. The difference between true raining time and the intercept on the vertical axis becomes less as the integration time is decreased. However, as explained in Chapter 3 the accuracy of the extreme-value-based curves below 2 mm/h is limited, due to the sensi-

tivity of the derived value of P_0 to the value of α. Not too much significance should therefore be attached to the actual value of the intercept on the vertical axis.

A second interesting characteristic is that the distributions for the 'inland' and 'coastal' regions are identical at the 1440-minute (24h) level (curves for this integration time are not shown, however). At lower integration times the 'inland' distributions at high rain rates (higher than about 10 mm/h) have higher probability values than the 'coastal' distributions (See Fig. 47). The reason for this is that over short periods there is a greater likelihood of high rain rates for convective thunderstorm rain (the 'inland' region) than for widespread frontal rain (the 'coastal region), while at the 1440-minute level the production from widespread frontal rain matches that from thunderstorms. Similarly, as may be seen in Fig. 47, low rain rates (below about 10 mm/h) are more likely in the 'coastal' region over short periods, while at 1440 minutes the rain production from thunderstorms is able to match that from widespread frontal rain.

6.5 Extrapolation to beyond 2000 mm/a

Although the mathematical relationships of the model will provide rain-rate distributions at any mean annual rainfall, the distributions cannot be obtained with a large degree of confidence at very high mean annual rainfalls. The model was developed from data of stations with mean annual rainfalls not exceeding 1100 mm. Application to rainfalls beyond this level therefore necessarily involves extrapolation. Although it is felt that extrapolations are in order, 2000 mm is considered to be the upper limit that one could safely extrapolate to. In part this figure is obtained from the suggestion

by Midgley and Pitman [1978] that the extreme-value relationships may be extrapolated to 2000 mm. Another reason for not extrapolating to beyond 2000 mm/a is that few locations in Southern Africa, which is to be the prime area of application of the model, receive more than this amount.

Chapter 7

RAIN-RATE PREDICTIONS FOR SOUTHERN AFRICA

Having developed a model of rain-rate distribution for Southern Africa, a necessary next step would be to make an evaluation. The only database available which geographically extends over a fair proportion of the Southern African subcontinent, is the set of 15-min observed distributions discussed in Chapter 8. The model shall be tested against these distributions. Chapter 8 also describes the relevant features of the locations and their distributions. The results obtained when comparing these distributions with predictions from the model are given in Section 7.1. A discussion of the results follows in Section 7.2, including an evaluation at 5-minute integration time. Section 7.3 gives a summary and conclusion.

7.1 Results of 15-min predictions for Southern Africa

Distributions of an integration time of 15 min were predicted for the 19 locations of Table 1. The annual rainfall normals (or means) of the locations used in the model, were as provided by the South African Weather Bureau. The appropriate climatic designation was determined by a simple criterion: Locations less than 100 km from the nearest coastline were taken to be 'coastal', further away they were taken to be 'inland'. For the subcontinental locations concerned the climatic classification according to this criterion happened to agree with the climatic-region delineation on the map of Fig. 25. The climate designations used for the various locations are listed in Table 1. The resultant

distributions are illustrated by the solid curves of Figs. 49 to 67. Deviations from the observed distributions, at points which are of concern, are given as ratios in Table 9.

As the results for the continental and island locations differ widely they are considered separately.

7.1.1 Continental locations

The majority of the continental locations have their largest deviation of the predicted distribution from the observed distribution in the tail region of either very high or very low probability. The maximum greatest overall deviation in probability occurs at Port Elizabeth (Fig. 64) where in the tail region at 80 mm/h the predicted distribution under-estimates the observed value by a factor of 10. This is followed by JBM Hertzog, George, East London and Jan Smuts, all of which have deviation ratios of approximately ±5 in the high-rain-rate tail region (see Table 9). Of the 17 continental locations 10 exhibit a probability deviation of ratio[1] 3 or less over the whole of the probability range.

In the region of very low probability (or high rain rates) the model over-estimates for some locations while it under-estimates for others. At r=0 mm/h and up to about 2 mm/h, however, there is consistent under-estimation of the probability, as is illustrated by the deviations at r=0 mm/h given in Table 9. This under-estimation decreases very rapidly with increasing rain rate so that at about 5 mm/h there is a reversal to an over-estimation for all locations. The trend to over-estimate is, for some locations, only sustained over

---

1. In this thesis, unless otherwise specified, the modulus value of the ratio is indicated.

a small range of rain rates before reverting back to a moderate under-estimation.

As is discussed in detail later (Subsection 7.2.3.), the distribution below 2 mm/h is not very important. Also, below a probability of 0,001%, the observed distribution is not stable statistically. Considering, therefore, the region above 2 mm/h and above 0,001%, the following may be noted for continental locations: The maximum deviation in probability between the predicted and the observed distribution for any location is a ratio of 5,0 (see Table 9). This is at Keetmanshoop, South West Africa (Fig. 59), where an under-estimation occurs at about 30 mm/h in the region 0,01% to 0,001%. Keetmanshoop is the only location with a probability deviation higher than a ratio of 3. The maximum deviation in rain rate, expressed as a percentage of the observed, is 70%. This occurs at a probability level of 0,1% at George (Fig. 52), where the observed rain rate of 8 mm/h is over-estimated.

Still considering the region above 2 mm/h and above 0,001%, the following may be noted: The largest absolute deviation in rain rate is 40 mm/h which is at 0,001%, at Port Elizabeth (Fig. 64). That represents a 44% under-estimation. It may also be noted from Table 9 that 10 out of the 17 continental locations do not exhibit deviations of more than a ratio of 2 in probability anywhere in the region of concern. For 8 locations the greatest deviations are well below a ratio of 2. That is a slightly larger proportion than obtained by Lin's method in Chapter 3.

Also shown in Table 9 is the probability deviation experienced at an observed probability of 0,003% (included for comparison purposes). It can be seen that 16 of the 17 locations display a deviation ratio of less than 4. The same number obtains when the deviation

threshold is decreased to 3. For 13 out of the 17 continental locations the estimated distributions deviate from the observed distributions by no more than a factor of 2. That is not quite as good as with Lin's method, where for all stations the deviation was never more than 2.

Other features to note in the region above 2 mm/h and above 0,001% are the following: At the 0,01% level the maximum deviation in rain rate, expressed as a percentage, occurs at George (Fig. 52). Here the observed rain rate of 20 mm/h is over-estimated by 50%, the large over-estimation being similar to the condition found for this location at the 0,1% level. The maximum deviation in absolute rain rate at the level of 0,01% is 11 mm/h, which is at Jan Smuts (Fig. 56).

On the whole the shape of observed and predicted curves are alike, the predicted curves following the concave shape of the observed curves in general. Only in the regions of very high and very low probabilities are there any tendencies that may be regarded as a positive divergence of the two curves.

7.1.2 Island locations

The predictions for the two islands Marion and Gough (Figs. 62 and 53) differ vastly from the observed distributions, except in the vicinity of about 5 mm/h. Above 5 mm/h an over-estimation results, with the predicted and observed distributions diverging rapidly with increasing rain rate. For both Marion and Gough the difference in probability between predicted and observed distributions becomes more than two orders of magnitude in the tail region of low probability.

At below 5 mm/h the predictions present under-esti-

mations. The under-estimations are also larger than those for the continental locations at 0 mm/h, reaching a ratio of about 6 in both cases, as can be seen from Table 9.

7.2 Discussion of results

In Section 7.1 the results were considered separately for continental and island locations. This was done because of the vast differences in quality of agreement between observed and predicted distributions for the two groups, which are henceforth treated separately.

7.2.1 Fifteen-minute predictions at island locations

The results for the two islands, Marion and Gough, undoubtedly point to a failure of the model in those maritime regions, as over-estimations of two orders of magnitude occur at higher rain rates. It is clear that either of the model expressions for the extreme-value parameters α or U, or both, are not appropriate for these locations. In Chapter 3 the values of the extreme-value parameters for Gough Island were obtained using Lin's method directly, i.e. obtaining the values from the observed rain-rate annual maxima over 25 years. The value for U thus obtained was 3,57 and therefore markedly different from the value that the model expression gives, i.e. 5,14. It provided a distribution with a maximum deviation of ratio 2,4, which was acceptable.

For Marion Island the value of U by Lin's method was 3,16, while the model produced a value of 4,87 -- also the markedly different. The deviation between the observed distribution and the distribution calculated by Lin's method, in the range above 2 mm/h and above 0,001%, was 3,2 at most. That was acceptable. The inability of

the model to predict reliably at these locations is therefore not due to Lin's extreme-value theory being invalid here. It seems that the 'coastal' model expression for U is unsuitable for the region (the expression for U for the 'inland' region being equally unsuitable). The values of α in both cases do not differ significantly from the values as obtained by Lin's method and, as is explained in Subsection 3.2.3, would not significantly affect the greater part of the distribution anyway. That the expression for U may be in error is not surprising. The model is based on data from the continent alone and on rainfall stations of which the mean annual rainfall does not exceed 1100 mm/a. The mean annual rainfalls for Gough and Marion are approximately 3400 mm/a and 2500 mm/a, respectively. These figures suggest rainfall regimes vastly different from those of the continent and imply that extrapolation of the relationships of the model would be very unreliable.

7.2.2 Fifteen-minute predictions at continental locations

The results for the continental locations are for the larger part of the probability range within the limits of acceptability -- using the criterion that deviation ratios below 3 represent acceptable predictions. However, the deviations in the tail regions at high and low probability tend to become large, with probability deviations larger than a ratio of 3 for some locations. The consistent under-estimation in the region of very low rain rates (below 2 mm/h), such as in the case of Durban (Fig. 61), may be due to too high a value of α. As has been shown in Subsection 3.2.3 the decrease of α has the effect of increasing the intercept P_0 on the ordinate and the probability at very low rates. A lower value of α will also have the effect of raising the right-hand tail of the distribution, while slightly lowering the probability at moderate rain-rate levels. With the possible exception of three locations -- George,

JBM Hertzog and Pretoria -- better overall agreement should in general be obtained by lowering the value of α.

However, the tendency to under-estimate at low rain rates decreases very rapidly with an increase in rain rate. At 2 mm/h it has almost disappeared, so that the region which is most important in terms of the radio engineering requirements is not affected.

The relatively large deviations at probability levels lower than 0,001% seem to be due to statistical instability in the observed distribution, as is illustrated for Port Elizabeth in Fig 64. When, for instance, the observed distributions for Port Elizabeth are considered on a year-by-year basis, some interesting features are revealed at the higher rain rates. At this location, where the largest overall deviation for the continental locations occurs, large inter-annual variation is manifest. The effect is so large that at the 60-mm/h level the contribution in probability from one storm only (on 1st September 1968) outweighed the contribution from all remaining storms of the 25-year period, by as much as a factor of 2. At the 88 mm/h level there is no contribution to the 25-year distribution other than from the said storm. Table 7 shows these events. As can be seen from the table all events beyond 22 mm (88 mm/h) are contributed by the month of September. That they all came from the particular storm was established from daily records of the S A Weather Bureau.

The question is whether this type of storm does not perhaps occur so seldom as to unnecessarily have biased the observed distribution obtained from 25 years of data (shown in Fig 64). For instance, if another 25 years passes without a similar storm occurring, the observed distribution could be very different from the one of Fig 64. It is interesting that applying Lin's extreme-value method -- as described in Chapter 3 -- to

the series of annual maximum rain rates for Port Elizabeth, a distribution is obtained which is indeed closer to the model distribution (see Fig. 19). A close look at the situation shows that in calculating the distribution of Fig. 19 the extreme-value method implicitly considered the return period of this storm by virtue of the annual maximum for 1968. As may be seen from Table 2 the maximum for 1968 was 34,7 mm per 15 minutes (or 138,8 mm/h). It has been established from Weather Bureau records that this maximum was contributed by the referenced storm. It was also the highest value for the period of record as can be seen from Table 2. In the extreme-value method the said storm was therefore considered, as its annual maximum was used in the calculation of α and U. In effect therefore its contribution to the average rain-rate distribution was appropriately weighted according to its return period (or probability). Provided then that the extreme-value theory holds for Port Elizabeth -- and we have no reason to believe that it does not -- the calculated distribution[2] of Fig. 19 should not be biased and could be more representative of the very long-term than the 25-year observed distribution. On the basis of a comparison with this calculated distribution the model gives an acceptable prediction, although still under-estimating to some extent.

The other locations for which divergence of the predicted and the observed curves occurs below about 0,001% may also be due to statistical instability. However, the only other location where the model distribution deviates seriously from the observed distribution below 0,001% is East London. The same argument as for Port Elizabeth may be applied here, although no single

---

2. As we have discussed in Subsection 3.2.3 the value of α obtained by the extreme-value method may be slightly low. Its adjustment to a more appropriate value, however, will make very little difference to that part of the distribution we are concerned with.

storm was responsible for the relatively high values of probability. However, even if the distribution by the extreme-value method is taken to be the more correct long-term distribution (see Fig. 6) there nevertheless seems to be a tendency for the predicted distribution to under-estimate at high rain rates. This result and that for Port Elizabeth may point to characteristically high probabilities at high rain rates for the southern and southeastern coastal regions. The slight under-estimation which occurs at Louis Botha (Durban) (Fig. 61) at high rain rates reinforces this suspicion.

7.2.3 Evaluation of model at 15-min integration time

It has already been stated that the model is not suitable for application in the South Atlantic and South Indian Ocean regions. However, in Section 7.1.1 the model seemed to be promising for the Southern African subcontinental region. A more thorough evaluation of its potential for predicting in this region will be attempted.

For the purpose of evaluating the model, it would seem reasonable to exclude that part of the observed distribution which is obviously not stable statistically. For the majority of locations this instability becomes visible in the region below 0,001% probability, so that the model will only be evaluated above this level. Statistical instability in the observed distribution obtained over a period as long as 20 years has also been identified by Lin [1978]. Furthermore, because of the excessive deviation at very low rain rate it seems reasonable to exclude the region below 2 mm/h as well. For the present engineering requirement, this region is not very significant. These have been the main reasons for concentrating on the region above 2 mm/h and above 0,001%, when the main features of the results were given in Section 7.1, as well as in previous chapters.

Considering the region above 2 mm/h and above 0,001%, then, the maximum deviation in probability for the 17 continental locations is a ratio of 5,0. The station at which this deviation occurs (Keetmanshoop) is the only one at which the deviation is more than a ratio of 3. For 10 locations of the 17 the probability prediction deviates from the observed probability by a ratio of 2 or less, over the whole region. There is no systematic deviation, other than consistent, but slight, overestimation at a probability level of about 0,1% -- corresponding to moderate rain rates. This may be due to too high a value of α.

At present there is a lack of an objective standardized method of evaluating and comparing prediction procedures. Most authors follow rudimentary approaches. We will try to evaluate the results in terms of the alternative of making measurements to obtain the required distribution. A useful approach offered is that by Segal [1979]. This author developed a semi-empirical method for Canada for establishing the period of measurement that, in view of the year-to-year variability, would be required to obtain the rain-rate probability to a specified accuracy at a specified level of confidence. In order to make comparisons we consider the confidence level we have obtained with the model at a probability of 0,003%. This value of probability is representative of the high-rain-rate tail region of the distributions. Usually it is difficult to obtain the distribution at these levels [URSI, 1981], although it is often required for link design. We will therefore consider the confidence level at a probability of 0,003% and an accuracy of ratio 2.

Table 9 gives the deviation ratio for the various locations at a level of 0,003%. The number of continental locations exhibiting a deviation ratio of 2 or less is 13. As they constitute 17 fairly randomly selected continental locations, the confidence level achieved by

the model for continental locations at an accuracy of a factor of 2 is 13 out of 17, or approximately 75%. According to Segal, for the probability in the vicinity of 0,003% to be established with an accuracy of a factor of 2 with respect to the long-term mean and with a confidence limit of 75%, more than a year's observation is required. This is the minimum time that would therefore be required to match that which is available from the model. Effectively, the minimum observation period is two years, as measurements over fractions of a year will result in distorted averages. For lower probabilities even longer observation periods are required - 11 years in the case of 0,0001%. Likewise, if better accuracy is required, the observation period also becomes longer. To improve the accuracy from a ratio of 2 to a ratio of 1,5 the minimum observation period has to increase from slightly more than a year to 5 years at a probability level of 0,003%. The rate of increase in accuracy with an increase in observation period is indeed very low. At an accuracy ratio of 1,3 (30%), for example, a 12-year observation period is required, at a probability level of 0,003% and a confidence limit of 75%.

The continental locations tested provided for a range of climates according to the classification system of Köppen and Geiger [1936] (see map of Fig. 30 and Table 8). Included were mean annual rainfalls from 44 to 1050 mm, altitudes from 0 to 1800 m and a latitude and longitude range of 14° each, as can be seen from Table 1. The locations can therefore be regarded as a fairly representative and random sample of all Southern African locations. On this basis and in view of the above analysis we may state that the model should, at the majority of locations and especially in the region of high rain rates, provide 15-minute distributions as accurately as can be established with a two-year measurement programme. The model can therefore be regarded as having general validity and utility for 15-minute predic-

tions anywhere in the Southern African subcontinental region. Also, the general accuracy of a factor of 2 or less in probability over a total range of probabilities of three orders of magnitude (1% to 0,001%) seems to provide distributions at arbitrary locations unattainable by other means.

7.2.4 Evaluation at 5-min integration time

A question which arises is whether the model is suitable for estimating 5-minute distributions reasonably accurately. The prime objective has been to be able to obtain distributions at this integration time, which then may be used in a terrestrial attenuation model [Lin, 1977] and an earth-satellite attenuation model [Lin, 1979]. Since data has not been available to test the rain-rate model at 5-min integration time in Southern Africa, it will be shown heuristically that predictions at this integration should be in order. Firstly, it is a fact that the extreme-value theory incorporated into the rain-rate model applies at any integration time, including 5 minutes. Furthermore, satisfactory results from the theory have already been obtained in the USA at 5 minutes [Lin, 1976 and 1978]. Secondly, there is no evidence that the value of α at 5 minutes should be significantly different from the constant value which in the DDF diagram has been found to apply at 15, 60 and 1440 minutes. A constant value of α over a large range of integration times is also supported by Watson et al. [1981 p 44-45], who has found α to be invariant over a range of 1 to 1440 minutes in Belgium and Italy[3]. Thirdly, we have no reason to believe that the model expressions for U can not be used for a reasonably accurate extrapolation down to 5 minutes, after having

3. It should, however, be noted that α in the rain-rate model has a generalised value which applies to all locations, while Watson has found location-to-location variability.

implicitly been proven to hold in the DDF diagram at 15, 60 and 1440 minutes.

Confidence in the model's capability at 5-min integration time also stems from the fact that the integration-time dependence in U is derived from an integration-time relationship in annual maxima exceeded, given by $r = r_0/(1+BD)^n$ (see Eq. 5.35), and the fact that this relationship has the same functional form as that which has been empirically established for the United Kingdom [NERC, 1975 and Watson et al., 1981, p 44-45][4].

Lastly, comparing the ratio in probability between 5- and 60-minute rain rates as measured for Europe with that from the model, no great differences are found. For example, from the model and for an 'inland' location with 700 mm/a, the quotient of the 60-minute rate upon 5-min rate C_R, at a level of 0,001%, is found to be 0,57. This compares favourably with an empirical value of C_R of approximately 0,50 for Italy [Damosso et al., 1981]. Also, the ratio C_R of 0,45, given by Watson et al. [1982, p 29] as an average for Europe, is not significantly different. Similarly, for a 'coastal' location with an annual rainfall of 700 mm, the model gives a ratio of 0,65, while the corresponding values from Damosso et al. [1981] and Watson et al. [1982, p 29] are 0,56 and 0,45, respectively (Watson uses the same value for all locations, despite the climatic region). Assuming that in reality the ratios for the European and Southern African regions are not significantly different, the Southern African model may then on the basis of its slightly higher C_R values give a slight under-estimation of the 5-minute rain-rate probability.

---

4. It is to be noted that where the constants in the relationship of the model are specific to each climatic region, the constants of the UK relationship are specific to classes of magnitude of mean annual rainfall.

All indications therefore are that the model would be valid on the Southern African subcontinent at lower integration times, including 5 minutes. However, the model should not be used for integration times lower than 5 minutes, before tests have been made at these integration times.

Further proof of the capability of the model to predict at 5-min integration time is obtained later on in the thesis. This is in Chapter 9, where results from using the model to predict at 5-min integration time at North American locations, are given.

7.2.5 General

The predictions from the model are consistent with the hypothesis that statistically the spatial and temporal characteristics of rain are relatively invariant over large selections of geographic areas, while the frequency of rain occurrences varies from location to location [Goldhirsh, 1981]. As can be seen from the standard rain-rate curves of the model (Figs. 31 to 46) an increase in mean annual rainfall at any integration time is associated with an increase in rain-rate probability. Since mean annual rainfall varies from location to location, then in terms of the model, the cumulative probability also varies from location to location. It is shown by Lin [1976] that the frequency of annual rain-rate extremes of order one and higher (the frequency of rainfall occurrences, therefore) is directly related to the cumulative probability. It therefore follows that there is a relationship between mean annual rainfall and the frequency of rain occurrences -- according to the model. That is in agreement with the above hypothesis, the 'large selections of geographic areas' pertaining to the two climatic regions of the model.

Despite the relatively good results obtained with the model at 15-min integration time, it seems that the value of α could be slightly too high. The systematic over-estimation at moderate rain rates and the systematic under-estimation at r=0 mm/h indicates that this may be the case. It would therefore seem that the model could be improved by lowering the value of α. However, the value of α also affects U, so that new expressions for U would have to be obtained, by following the procedures of Appendix C.

Furthermore, although the results in general are acceptable, it would seem that the model slightly under-estimates at the higher rain rates in the eastern and southeastern coastal regions. This is a matter that should be investigated further.

7.3 Summary and conclusion

Very favourable results have been obtained with the model at 15-min integration time on the Southern African subcontinent. Results for two islands were un-acceptable. This was due to unsuitable model expressions, and did not invalidate the extreme-value theory. Data has not been available for testing the model at an integration time of 5 min in Southern Africa. However, various reasons are given why it should be valid at this integration time as well. The results are consistent with a hypothesis by Goldhirsh [1981], supporting the theory that the frequency of rain occurrences varies from location to location. Improve-ment should be possible for subcontinental locations, by adjusting the value of α in the model.

Chapter 8

SOUTHERN AFRICAN OBSERVED DISTRIBUTIONS

In order to have tested the validity of Lin's extreme-value method for Southern Africa in Chapter 3, a data base of observed distributions was required. Observed distributions were also required in Chapter 7 for testing the model developed in Chapter 5 and summarized in Chapter 6. This chapter describes the data base used.

It is described how the measurements were obtained and processed (Sections 8.1 and 8.2). In Section 8.3 the features of the locations are discussed, before giving the distributions in Section 8.4. In this latter section the essential features of the distributions are also described.

8.1 The statistics

The South African Weather Bureau provided long-term statistics obtained from continuously measured 15-minute rain rates for a number of stations. From these statistics the observed distributions of this integration time could be compiled. The data obtained consisted of the number of occurrences, for every month of the year, but as a total for a number of years, of 15-min rainfall depths in various depth intervals. The depth intervals are as given in Table 7, which gives the number of occurrences (or frequency) in every month, for Port Elizabeth. As can be seen the intervals range from 0,1 mm to 44 mm, which is equivalent to the range 0,4 to

176 mm/h. As there were no events beyond 36 mm for Port Elizabeth, the table is terminated at this value. The statistics had been compiled by the Weather Bureau from the charts of autographic rain gauges. The gauges were of the Cassella float-chamber type, which displays the accumulated rainfall as a trace on a 24-h clockwork-driven chart. The rainfall is accumulated up to 10 mm, at which point the float chamber is rapidly emptied by a syphoning process. The gauge is then ready for another accumulation. The 15-min quantities used in the frequency statistics are routinely obtained by the Weather Bureau by reading from the charts the increment in accumulated rainfall for every clock quarter-hour. The sum of all 15-min increments over a 24-h period is usually also checked against the total from a standard rain-gauge situated within metres of the Cassella gauge. Usually the differences are negligible.

8.2 The processing of the statistics

The 15-min cumulative frequency distribution for every month of the year was obtained by considering, at the upper bound of every interval, the frequency at which the bound was exceeded, i.e. the sum total of all frequencies to the right of the respective interval was obtained (see Table 7). This was then divided by the number of years of record to obtain the average annual 15-min cumulative frequency distribution for the respective month of the year. By then summing the frequency of exceedance for all the months of the year, at every level (upper bound) of rainfall depth, the average annual 15-min frequency distribution was obtained. Every figure was then transformed to cumulative probability by multiplying by the fraction that the interval (15 minutes) constitutes out of a total year. Simultaneously, the corresponding depth exceeded (the upper bound of the interval) was normalised to hourly based rain rate by multiplying by 4.

As an example, we see from Table 7 that the 14-mm level was exceeded in the months of January, September and October. For January the total frequency by which 14 mm was exceeded over the 25-year period is 1, giving an average of 0,07145 per year. For September the total frequency is 14, noting that this was for 24 years, and giving a yearly average of 0,58333. The average for October is 0,07145. The average for all months of the year at a level of 14 mm is therefore the sum of the averages for the 3 months, which is 0,72623. Fifteen minutes constitutes a fraction of 15/525600 of a total year which, when multiplied by the frequency, gives a probability of 0,00207%. This then is the probability to be associated with an hourly rain rate of 14 x 4 = 56 mm/h. This value is a point in the distributions of the dotted lines of Figs. 19 and 64. In all cases the curves were obtained by logarithmic interpolation of the probability between the points, spaced 8 mm/h apart at the higher rain rates and 4 mm/h apart below 8 mm/h. In effect, therefore, the interpolation on the logarithmic scale of the graph is by straight lines.

8.3 Features of the locations

Table 1 lists, in alphabetical order, the locations for which observed distributions were obtained, together with some relevant parameters. The locations were all those for which long-term 15-minute data could be obtained and came to a total of 17 continental locations plus two island locations.

The positions of the continental stations are indicated on the map of Fig. 30. The stations represent the major climatic regions of the subcontinent, as can be seen from the delineation of the climatic regions in Fig. 30 and the definitions given in Table 8. On the basis of their proximity to a coastline (i.e. less than

about 100 km) 6 of the continental locations may be regarded as 'coastal'. The islands included are the South Indian and South Atlantic islands of Marion and Gough, respectively. Mean annual rainfall for the stations on the continent ranges from 44 to 1050 mm but is as high as 3395 mm on one of the islands. The continental locations cover a range of altitudes above sea level of 0 to 1800 m and are spread over a range of 14° latitude and 14° longitude (see Table 1).

8.4 The distributions

For the 19 distributions obtained, the minimum period of record was 7 years and the maximum 25 years (see Table 1). The distributions are given as the dotted lines in the graphs of Figs. 4 to 22 where they are compared with distributions calculated by Lin's extreme-value method, as in Chapter 3. They have been repeated in Figs. 49 to 67 for the purpose of comparing them, in Chapter 7, to distributions from the rain-rate model developed. In both sets of figures they are given in alphabetical order according to location. All graphs were plotted on the same scale. The vertical axis gives, on a logarithmic scale and as a percentage of time, the annual average cumulative probability of exceeding the rain rate (in mm/h) on the horizontal axis.

As can be seen from the figures there are great differences between the observed distributions of the various locations. Excluding the distributions of the two islands, which will be treated separately, the following differences may be pointed out:

Comparing cumulative probabilities in the region of 0,001% to 0,1% and at varying levels of rain rate the largest probability difference is between Alexander Bay and Pretoria (see Figs. 4 and 20). Here, at a rain rate

of 15 mm/h, the probability at the former is 0,001%, while being almost 0,1% at the latter -- a difference of two orders of magnitude. At a cumulative probability level of 0,01% the greatest difference in rain-rate level is between Alexander Bay (Fig. 4) and Louis Botha (Durban) (Fig. 16) where the rain rates are 6 mm/h and 45 mm/h respectively (a ratio of about 8). At the 0,001% level the greatest difference is between Alexander Bay and East London (Fig. 6) where the respective rates are 15 mm/h and 96 mm/h (a ratio of about 6). It is interesting that, with the exception of Pretoria, the above extremes all occur at coastal locations.

Regarding inland locations only, and considering the probability region of 0,001% to 0,1%, the largest probability difference occurs between Pretoria and Upington. Here at 44 mm/h Pretoria has a probability of 0,01%, while Upington (Fig. 21) has 0,001%, i.e. one order of magnitude lower than that of Pretoria. The lowest rain rate at the 0,01% level is that of Keetmanshoop which is 19 mm/h (Fig. 14) and the highest that of Pretoria (Fig. 20), which is 44 mm/h (about 2,3 times higher). At the 0,001% level Upington has the lowest rain rate, which is 44 mm/h, while Pretoria again exhibits the highest value, i.e. 82 mm/h (almost twice as much).

Location-to-location differences also exist in total raining time percentage P(R>0). The highest of all continental locations is that of Louis Botha (Fig. 16), at 4,6% of the year. The lowest is that of Alexander Bay (Fig. 4), at 0,37% (a factor of about 12 lower than the figure for Louis Botha). Again these overall extremes occur at coastal locations. In the inland region alone Jan Smuts (Fig. 11) has the highest percentage of raining time, i.e. 2,6%, while Keetmanshoop (Fig. 14) has the lowest, i.e. 0,55% (almost 5 times lower than that for Jan Smuts). Jan Smuts is followed closely by Pretoria, with a raining time percentage of 2,4%.

Gough and Marion islands (Figs. 8 and 17, respectively) display characteristics somewhat different from those of the continental locations. They have a very high probability of very low rain rates (below 5 mm/h), while their tail regions of high rain rates are rather similar to those of coastal locations of the Southern and Western Cape, such as DF Malan (Fig. 5) and George (Fig. 7). The predominance of low rain rates is also demonstrated by their relatively high percentage of total raining time, which in both cases is approximately 15%, as compared to the continental maximum of 4,6%.

A similarity that exists amongst all the curves is that, broadly speaking, they have a concave shape. In the low-probability region, however, some curves deviate from this shape to some extent.

Chapter 9

RAIN-RATE PREDICTIONS FOR NORTH AMERICA

In Southern Africa suitable rain attenuation data is not yet available for testing the developed rain-rate model for attenuation prediction. An alternative approach has therefore to be followed. It was decided to investigate the outcome when applying the rain-rate distributions from the model to the prediction of rain attenuation for North American locations. This was decided in the hope that the North American rain-rate climate is sufficiently similar to that of Southern Africa for the rain-rate model to be valid there also. Support for possible similarities is found in a hypothesis by Goldhirsh [1981], which is based on a study of rain rates in the USA and which reads as follows: "The spatial and temporal characteristics of precipitation, especially the more convective types, are relatively invariant over large selections of geographic locations, while the frequency of rain occurrences are different from location to location". As was explained in Subsection 7.2.5 the theory of the rain-rate model operates exactly on the basis of location-to-location variation in the frequency of rain occurrences. Because of this and because the model may be regarded as a fair representation of the Southern African rain-rate climate, it seems that the South African rain-rate climate (at 15 min integration time, at least) is similar to that of North America.

A prerequisite for attenuation prediction in North America is that the model should be capable of predicting the 5-minute rain-rate distribution. To investigate this

aspect we applied the model to 20 locations in the USA for which observed 5-min distributions were available from the literature. The result of this exercise is the subject of this chapter.

9.1 Observed distributions

The locations tested were those of Table 10, which also gives the mean annual rainfall, the climatic region as by Köppen and Geiger [1936] and the distance from the nearest ocean.

The locations represent a large proportion of North American locations for which published 5-minute distributions are available and constitute all the locations from the contiguous United States for which Lin [1978] gives observed distributions. In that sense and because they are situated country-wide they represent a fairly random sample of locations from the USA. They are also of widely differing climatic regions, as may be seen from the Köppen and Geiger [1936] climatic designations in Table 10.

The observed distributions all are for the 20-year period of 1953 to 1972. They are given by the dotted lines of Figs. 68 to 87. As can be seen from the figures the distributions only cover the rain-rate region in excess of about 30 mm/h.

9.2 Prediction results

Distributions of an integration time of 5 minutes were obtained from the model for the 20 locations of Table 10. The mean annual rainfall used (given in Table 10) was obtained from NOAA [1971]. In applying the rain-rate model the 100-km-from-coast criterion, as was

used for Southern Africa in Chapter 7, was initially applied to obtain the climatic designation of either 'coastal' or 'inland'.

With the exception of 4 out of the 20 locations the initial results, by visual comparision, were acceptable. The four exceptions were Binghamton (New York), Harrisburg (Pennsylvania), Scranton (Pennsylvania) and Lynchburg (Virginia), all near the East Coast, but farther than 100 km from the coastline, as may be seen from Table 10. For these four locations the distribution was over-estimated by the 'inland' distribution over the whole of the rain-rate range, although not excessively so, as is shown by the curves marked 'Inland' in Figs. 78, 80, 82 and 84. The over-estimation raised the possibility that these locations may have a maritime type rain-rate climate. As a consequence, a prediction was attempted using the 'coastal' designation in the model. The result was that the 'coastal' curves consistently under-estimated the probability over the whole of the rain-rate range. The 'coastal' curves, however, gave slightly better agreement at the lower rain rates. On the basis of this result it may be argued that the 'coastal' region of the model is more representative of the climate in the eastern and northeastern United States, up to several hundred kilometers from the coast. A set of results of the deviations between predicted and observed distributions has been obtained on the basis of the 'coastal' region extending up to 400 km from the coast. The essential features of the results are given in Table 11, which also gives the preferred climatic region designation. The preferred region is also indicated in the figures.

The greatest overall deviation in probability (greatest over the whole probability region) occurs in the high-rain-rate tail region for the majority of locations. Unfortunately, the observed distributions in

the low-rain-rate tail region are incomplete, so that no comparisons can be made here. For the available portions of the distributions the absolute maximum deviation is a factor of 7,1. This is a rather excessive underestimation for Valentine, Nebraska, occurring at 190 mm/h.

It seems from the figures (Figs. 68 to 87) that statistical instability of the observed distribution prevails in the region of very high rain rate. This is especially evident for Scranton, Pennsylvania, where in the region below 0,0001% there is an abrubt change in the curvature of the observed distribution (see Fig. 82).

The deviation is therefore considered over two other ranges of probability of the observed distribution, to see whether there is any improvement. The region above 0,0001% excludes some of the statistical instability. In this region the maximum overall deviation for the 20 locations is again Valentine, with the value of 7,1 occurring at 190 mm/h as before. However, there have been improvement in the greatest deviation for 7 of the 20 locations. In this region 15 of the 20 locations display a greatest deviation ratio of 4 and below, while 11 are within a deviation ratio of 3. Two locations have a greatest deviation ratio of not more than 2. The region above 0,001% excludes more statistical instability and shows a further improvement: There are now 17 locations with a greatest deviation ratio of not more than 4, 14 have a greatest deviation ratio of not more than 3 and 7 have a greatest deviation ratio of not more than 2.

Analysing the deviations at the fixed level of 0,003% (of the observed distribution), as was done for comparison with the work of Segal [1979] in Chapters 3 and 7, we obtain the following: The deviation for 18 of the 20 locations is a factor of 4 or less. It is a

factor of 3 or less for 14 locations and a factor of 2 or less for 8 locations.

9.3 Discussion

Similar to what has been found when testing either Lin's method or the model at 15-min integration time in Southern Africa, there are large deviations between predicted and observed distributions in the tail regions of high rain rate. This is to be expected, because of statistical instability in the observed distribution at very high rain rates [Lin, 1978]. The effect is also illustrated by the improvement in agreement (in terms of the proportion of locations having their greatest deviation below a certain threshold) when the right-hand tail region is excluded. There is consistent improvement if, firstly, probabilities below 0,0001% and, secondly, probabilities below 0,001%, are excluded.

Table 12 illustrates that the 5-min predictions for North America over the range above 0,001% and above 2 mm/h, in general, are not as good as the predictions of 15-min distributions for Southern Africa. The table gives the number of locations (with the percentage of locations in brackets) for which the greatest deviation is equal to or less than the value indicated. The results from Chapter 3 and Chapter 7 have also been included. For the Southern African locations the model performed slightly better than Lin's extreme-value method. For 70% of the North American locations the model gave a greatest deviation which was a factor of 3 or less in the probability range above 0,001%. This is an acceptable prediction capability.

A comparison at the fixed probability level of 0,003% gives similar results, as can be seen from Table 13. The model did not perform as well in North America

as it did in Southern Africa, especially when predictions within a factor of 2 were required. In only 40% of the cases the requirement was met, as opposed to 76% in Southern Africa. However, acceptable predictions (with deviations a factor of 3 and below) were obtained for the majority of locations (70%) at this level of probability.

The less favourable performance of the model in North America may in part be attributed to the relatively coarse climatic classification of 'coastal' and 'inland'. The East Coast locations, viz. Binghamton, Harrisburg, Scranton, Pittsburgh, Lynchburg, Trenton and Newark all display observed distributions which lie between the two model distributions. It is therefore very likely that their distributions result from rainfall which is partly of the stratiform maritime type and partly of the convective thunderstorm type. The fact that the model does not provide for this kind of situation will inevitably lead to some error, although the error has been shown (in Section 9.2) not to be excessive. Improvement of the model in regard to this aspect should nevertheless be considered.

The acceptable results with the model in North America confirm Lin's method, as well as the hypothesis that the method may be extended by developing generalized expressions for α and U. However, as seen in the previous paragraph, improvement is required for the model to obtain better results in areas where a mixture of 'inland' and 'coastal' climates prevails. This may be achieved by further refining the expressions for U and α. Such a refinement would require the introduction of another independent climatological parameter. This parameter should also be widely available, for ease of use.

The results give further credibility to the hypothesis [Goldhirsh, 1981] that the frequency of rain

varies from location to location within large selections of geographic regions, while the temporal and spatial characteristics are relatively invariant (the same argument as in Subsection 7.2.5 applies). The favourable results obtained on two continents with the same set of relationships indicate that the 'large selections of geographic regions' transcend continental boundaries. The results point to the universality of the model and rain-rate climatology in general.

9.4 Summary and conclusion

The rain-rate model gave acceptable distributions in the USA, although it did not perform as well as in Southern Africa. Lin's method, as well as the viability of modelling the extreme-value parameters of α and U on mean annual rainfall and two climatic regions, are confirmed. The results also confirmed the hypothesis by Goldhirsh [1981]. Better agreement at locations with no strong predominance in either of the two climates of 'inland' and 'coastal' may, however, be possible with a further refinement in the expressions for U and α. In general the model provides rain-rate distributions in the contiguous USA of which the accuracy is better than a factor of 3. This suggests that it could be useful for predicting the rain-rate and rain attenuation distributions on that subcontinent.

Chapter 10

RAIN-ATTENUATION PREDICTIONS ON EARTH-SATELLITE PATHS

The rain-rate model described in Chapter 5 and summarized in Chapter 6 has been developed for the purpose of predicting rain attenuation on terrestrial and earth-to-satellite radio links, utilizing 5-min rain-rate distributions from the model in the two attenuation models of Lin [1977] and Lin [1979], respectively. Testing the application of the rain-rate distributions from the model in the two attenuation models in Southern Africa is hampered by a lack of (as yet) suitable rain-attenuation data. Observed attenuation distributions of at least a year or two are required in order to make quantitative comparisons of any sort. As a second best approach the rain-rate model is tested for rain-attenuation prediction in North America, where earth-satellite attenuation data are available from locations in several climatic regions.

The attenuation prediction model by Lin [1979] is utilized. Apart from its suitability from the point of view of using 5-min integration time, this model is recommended for various reasons. It has been proven to be a reliable model for the USA, as has been confirmed by Ippolito [1981 and 1984] and Ippolito et al. [1983]. The model has also been found suitable by Rustako [1982] and is considered a well-established model by Macchiarella [1985], with applicability to locations also outside the United States.

The choice of North America for attenuation prediction tests has also been prompted by the acceptable

agreement found between predicted and observed 5-min rain-rate distributions, as has been described in Chapter 9. Using North American data also makes sense from the point of view of the recommended earth-satellite attenuation model being semi-empirically derived from data obtained in that region.

The North American climatic regions involved are similar to those of Southern Africa, as can be seen from Tables 8 and 10. To a certain extent therefore the results in North America would be indicative of what could be expected in Southern Africa.

In the sections to follow the attenuation model used is first described before the observed distributions and the prediction results are given.

10.1 The rain-attenuation model

The model is defined by the following formulas:

$$A_T = aR^b \cdot L \cdot \left[\frac{1}{1 + \frac{L}{\overline{L}(R)}} \right] \qquad (10.1)$$

where A_T is the total path attenuation (in dB) exceeded at the same level of probability as the 5-min rain rate R (in mm/h). The expression aR^b gives the specific attenuation (in dB/km) where a and b are constants depending on temperature, drop-size distribution, frequency and polarization. Average values of these constants may be obtained from CCIR [1982d]. L is the length of the radio path (in km) and is given by

$$L = \frac{(h_R - G)}{\sin \theta} \qquad (10.2)$$

where h_R is the rain height, assumed to reach up to the freezing level, and taken to be 4 km above mean sea level. G is the altitude above sea level (in km) and θ is the elevation angle of the antenna. $\overline{L}(R)$ is an empirical quantity described as the characteristic path length and is given by

$$\overline{L}(R) = \frac{2636}{R - 6,2} \qquad (10.3)$$

10.2 Observed distributions

During recent years observed rain-attenuation distributions, obtained over one or more years on earth-space paths at various locations in the USA, have been published. Some of these, selected to cover different climates, have been duplicated in the graphs of Figs. 88 to 99 for comparison with the predicted distributions. The observed distributions are given by the circles in the figures and cover the frequency range of 11 to 29 GHz. The vertical axis of each graph gives, on a logarithmic scale, the percentage of time that the attenuation on the horizontal axis is exceeded. The publications from which the observed distributions were obtained are given in the captions to the figures. The locations involved are given in Table 14, which also shows that mean annual rainfall ranges from about 380 mm to 1300 mm.

10.3 Prediction results

As a first step, 5-minute rain-rate distributions were obtained for the locations of Table 14, using the rain-rate model. The mean annual rainfall and climatic designation for each location were as given in Table 14. For mean annual rainfall the 1931-1960 normal for the nearest gauging station, given in NOAA [1971], was used. In the cases of Crawford Hill and Wallops Island the average of the two nearest stations was used, as it seemed that a more representative figure would be obtained in this way. For Etam the MAR supplied by the author who published the observed attenuation was used [Rogers, 1981]. The snow component in the figures was neglected. Locations were regarded as 'coastal' if they were less than 100 km from an ocean. An exception was the eastern and northeastern states, where, based on the experience with the rain-rate model in Chapter 9, a criterion of 400 km was applied. Two more exceptions to this rule of thumb occurred. Tampa, Florida, situated virtually on the coast, is known to have a high degree of thunderstorm activity and was therefore taken as 'inland'. Grant Park, Illinois, was taken to be 'coastal', as the indications are that frontal rain predominates in Northern Illinois [Landsberg, 1974]. The choice of 'coastal' was made with some degree of hind-sight, as will be discussed further on.

As a second step, the 5-min rain-rate distributions from the rain-rate model were applied in the attenuation model described. Attenuation distributions were obtained for the various paths of the locations of Table 14. In the attenuation model the frequency and elevation angle that had been used in obtaining the observed distributions were used. The constants a and b of Eq. 10.1 were obtained from CCIR [1982d], for horizontal polarization and by using the recommended interpolation procedure for the frequency specified. The $0^{o}C$ isotherm, and there-

fore h_R, was in all cases taken as 4 km, as is recommended for the attenuation model. The ground elevation shown in Table 14 was either taken from NOAA [1971] or estimated from topographical maps. The solid lines of Figs. 88 to 99 give the predicted distributions.

Fig. 88 shows the observed distributions obtained concurrently at Clarksburg, MD, at 28,56 and 11,6 GHz, at an elevation angle of 43,5° [Kumar, 1982]. The predicted distributions, using the MAR for Washington National Airport and a 'coastal' designation, show satisfactory agreement. The probability deviation is a factor of 2 at most in both cases. This is of the same order as the difference in the probability, at 28,56 GHz, between the average 2-year observed distribution and the distribution of one of the observation years, as given by Kumar [1982].

In Fig. 89 distributions are given at 28,56 and 11,7 GHz and at elevation angles of 38,6° and 27°, respectively, for Crawford Hill, NJ. [Arnold et al., 1981]. The predicted distributions, using the average MAR for Trenton and Atlantic City, (both in New Jersey) give satisfactory approximations to the observed curves, the deviation ratio also not exceeding a factor of 2. The variation from one observation year to another during the period, as given by Arnold et al. [1981] for the 11,7 GHz observations, is, over most of the range, much larger than the deviation between the observed and predicted curves.

For Austin, TX, classed as 'inland', the distributions are given by Fig. 90 for 28,56 and 13,6 GHz. The two observed distributions have been obtained concurrently and at the same elevation angle, i.e. 52° [Vogel, 1982]. The agreement is once again good for both frequencies. At the point where the deviation is greatest, for the 28,56-GHz case, the probability of the predicted

curve is higher than that of the observed by a ratio of 1,8. For 13,6 GHz the maximum deviation ratio is 1,4.

The predictions at 28,56 and 13,6 GHz and at 27,3° elevation at Grant Park, Ill., shown in Fig. 91, presented a problem as this location is situated close to Lake Michigan, but is about 1300 km from the nearest ocean. It was only by plotting the attenuation-distribution curves for both the 'inland' and 'coastal' designations that it could be established that the 'coastal' curves give a better approximation to the observed curves from Lin [1979]. However, there is a tendency here for the slopes of the 'inland' curves in both cases (not shown) to follow those of the observed curves at the higher rain rates. This may point to a mixture of 'coastal' and 'inland' climates. With the relatively short time base of one year for the observed distribution, though, firm conclusions cannot be drawn. The agreement is nevertheless good, with the predicted curves at both 28,56 and 13,6 GHz over-estimating the observed curves by a ratio of 1,7 at most.

Palmetto, GA, and Blacksburg, VA, shown in Figs. 92 and 93, exhibit excellent agreement between predicted and observed distributions at 17,8 and 19,06 GHz, respectively [Lin et al., 1980], [Andrews et al., 1982]. For both locations the differences are less than a factor of 1,3. Of particular note is the good agreement for Blacksburg at low probabilities, when compared to a difference between best and worst years of as high as a ratio of 3,7 in the region 0,001% to 0,01% [Andrews et al., 1982].

Figs. 94 and 95 give the results for Wallops Island, VA, and Etam, WV at 28,56 and 11,6 GHz [Goldhirsh, 1982 and Rogers, 1981]. The agreement is good, but the rather close agreement at Etam may be fortuitous, in view of the short observation time of one year. Wallops Island has a

maximum deviation of a factor of only 1,6 and Etam has a maximum deviation of only about 1,3.

Longmont, CO, is the location with the lowest MAR for which results have been obtained (Fig. 96). It was taken to be 376 mm, which is the mean for Denver, the nearest gauging station given in NOAA [1971]. The predicted distribution at 17,8 GHz shows satisfactory agreement with the 2-year observed distribution obtained by radiometer [Lin et al., 1980]. The greatest deviation is in the low-probability tail region, where the predicted curve is a ratio of 2,9 higher than the observed. Over the whole range of probabilities above 0,003% the agreement for this path is within the variation from the first observation year to the second [Lin et al., 1980].

The results at 11,7 GHz for Greenbelt, MD and Waltham, MA, (Figs. 97 and 98) are not as good as the aforementioned results, but nevertheless reasonable. Greenbelt displays its greatest deviation at high probabilities, where the predicted curve attains a probability value 3,2 times higher than the observed value [Ippolito, 1981]. This is not excessive, though, when viewed against a difference of ratio 2,6 between the best and worst years during the observation period, as given by Ippolito et al. [1983]. For Waltham the predicted attenuation-distribution curve consistently lies at higher probability values than the observed distribution [Nackoney and Davidson, 1982], but nowhere deviates by a ratio of more than 3,7. This is acceptable in view of the variation of 4,7 from one observation year to the next, which was experienced at about the 0,001% level, as is illustrated by Nackoney and Davidson. [1982].

Tampa, FL, situated in a subtropical region, was the location with the highest MAR. Fig. 99 shows that at 19,04 GHz the 'inland' prediction curve gives good agreement in the region of high probability, but rather poor

agreement in the low-probability tail region. The ratio in probability by which the predicted curve under-estimates the observed distribution [Tang and Davidson, 1982] approaches a factor of 6.

10.4 Discussion

Of a total of 16 distributions predicted at locations in widely differing climates, 12 gave an agreement with the observed distribution which was within a factor of 2 over the whole of the probability range. Of the remaining 4 paths the deviation on only one path exceeded a factor of 3,7. This was in the subtropical climate of Florida where an under-estimation of a factor of 6 occurred in the region of high rain rates. We regard the results which are within a factor of 2 as very satisfactory, as the following comparison will show.

A recent analysis on the performance of various attenuation prediction methods was done by Crane [1985]. A large number of prediction methods were applied to a very large database of measurements made on earth-to-satellite paths. It was shown that of 20 methods of predicting the attenuation distribution from rain-rate climate models (i.e. not using a measured rain-rate distribution) only two gave a root-mean-square deviation[1] of less than a factor of 2 (less than 100%) [Crane, 1985, Table 6]. In one case the rms deviation was even as high as 2,44 (144%). Furthermore, when

---

1. The root mean square deviation (rms deviation) was calculated from the logarithms of the probability deviations for eight attenuation levels, logarithmically spaced from 1,8 to 13,3 dB. A single value was obtained by appropriately weighting all paths in the database.

measured rain-rate distributions were used, the best rms deviation obtained by any model was 1,85 (85%). Interestingly, the worst deviation obtained by a prediction from a measured rain-rate distribution was 2,91 (191%), which was a larger deviation than the worst deviation of 2,44 obtained by a rain climate model.

The rms deviation for the results of this chapter has not been calculated. However, in view of the above and having experienced no deviations of more than a factor of 2 for the majority of locations, it may be argued that the method may be comparable to the best available.

Concerning those four locations for which deviations exceeded a factor of 2: Deviations up to a factor of 4 may be regarded as acceptable in view of the year-to-year variation which, in the majority of cases, seemed to approach this level. In general, the deviation of the predicted distribution from the observed distribution was well within the range of year-to-year variation of the observed. This suggests that, with the exception of the subtropical region in the south, the prediction method gave better results than could have been obtained by one year of measurement. This is significant, in view of the various climates and the range of mean annual rainfalls of 380 mm to 1200 mm included. We therefore regard the method as very satisfactory for the USA.

The severe deviation for the path in subtropical Florida may be due to statistical instability in the observed distribution. According to Tang and Davidson [1982] some exceptional weather was experienced during the observation period. The observed distribution may therefore be atypical of the long term, similarly to what has been found for the rain-rate distribution of Port Elizabeth (discussed in Subsection 7.2.2 and illustrated in Fig 64). Observed distributions on a year-by-year basis are required to make a more thorough evaluation.

It therefore remains inconclusive as to whether the prediction method is totally unsatisfactory in this climatic region.

The favourable results tend to support the attenuation model employed. Considering also previous results obtained by Lin [1979] the model, with the possible exception of the southern subtropical region, seems to have general validity for the contiguous United States.

The good results generally tend to support the validity of the rain-rate model for the contiguous United States, as was the case when observed and predicted rain-rate distributions were compared in Chapter 9. The lognormal hypothesis for the distribution of randomly varying rain rate and the log-Gumbel hypothesis for the series of annual maximum rain rates, as well as the relationships between them [Lin, 1976 and Lin, 1978] are therefore given further support.

The satisfactory results for the North American continent is significant as only Southern African extreme rain-rate data were used in the development of the rain-rate model. The results therefore as in Chapter 9 suggest a high degree of commonality in the statistical characteristics of the rain-rate climate of the Southern African and North American subcontinents.

The results once again are consistent with the hypothesis that the spatial and temporal characteristics of rain are relatively invariant within large geographic regions, while the frequency of rain occurrences varies from location to location [Goldhirsh, 1981]. It has already been shown in Subsection 7.2.5 that the theory of the model supports that part of the hypothesis which says that the frequency of rain occurrences varies from location to location. Moreover, the results of this chapter are in agreement with that part of the hypothesis which

states that the spatial characteristics of rain, statistically speaking, are relatively invariant within large geographic regions. The results are from the application of an attenuation model which satisfactorily characterized storms spatially (albeit not over very large distances, due to the limited extent of the earth-to-satellite path) in many climatic regions by an expression, (Eq. 10.3), which is a function of only the rain rate. Such a degree of uniformity is in agreement with the 'spatial' aspect of the above hypothesis. As for the remaining part of the hypothesis, the results do not give any proof of geographical invariance of the temporal characteristics of rain. However, as the spatial and temporal characteristics of a volume process such as rain are not totally divorced from one another, and as the former displays geographical invariance, it would not be surprising to find the same for the latter.

On the basis of the support the prediction method gives to the above-mentioned hypothesis, and also on the basis of the applicability of the rain-rate model to both Southern Africa and the contiguous United States, there is a very good likelihood that the method will give similar results with rain-attenuation prediction on earth-satellite paths in Southern Africa.

Two factors that may influence the accuracy of a prediction in Southern Africa, however, are the vertical extent of rain and the drop-size distribution. As for the former, there are indications that storms extend to about the same height above sea level (i.e. about 4 km) in the midlatitude regions all over the world [CCIR, 1982a]. Southern African storms described by Carte [1979], Carte and Kidder [1977], Held [1980] and Proctor [1983] do not seem to deviate significantly in vertical extent from those in North America [Crane, 1980], for instance. The same rain height recommended for North America may therefore be used when applying the method to

Southern Africa. The probability distribution of raindrop size also does not vary greatly in the midlatitude regions of the world -- at least not significantly enough so as to create a problem with rain-attenuation prediction [CCIR, 1982d]. The reference listed for obtaining the values of a and b (which depend on drop-size distribution) may thus be safely used for predictions in Southern Africa.

In terms of its utility for both the United States and Southern Africa the following points should be noted about the method. The rain-rate model has a theoretical basis which allows extrapolations to very low levels of probability, should that be necessary. In terms of its input parameters it is very easy to apply. It uses only the two widely available parameters of mean annual rainfall and climatic region. As an alternative to calculating the rain-rate distribution himself the user may utilize the standard 5-min curves given in Section 6.2 (Figs. 31 to 34). In using mean annual rainfall the method provides an attenuation distribution which is specific to the location. It may at some locations therefore be more accurate than methods which utilize standard rain-rate distributions for large geographical regions, but which do not take account of local forcing of rainfall by, for instance, orographic effects. In making use of only two climatic regions, 'coastal' and 'inland', there may at a proportion of locations be some uncertainty as to which one applies. The user making predictions for the USA may, however, benefit from consulting NOAA [1971], which gives the number of thunderstorm days per year for some climatically representative locations. These statistics may give some indication of the type of rain-rate climate of a particular location. For Southern African locations a publication by the SA Weather Bureau [1954] may be consulted, giving the average annual number of thunderstorm days for about 140 locations situated country-wide. A map of

Southern Africa for this parameter may also be found in SA Weather Bureau (1957].

A major advantage of the prediction method of this chapter is that it obviates geographical interpolation of rain-rate and attenuation distributions. It also makes scaling of attenuation distributions in terms of frequency, polarization and path length redundant. Interpolation and scaling are problematical exercises, as has been pointed out in Chapter 2.

Lastly, it should be noted that as for terrestrial system design, the model of Lin [1977] is recommended. The model we have used for the earth-to-satellite predictions of this chapter is, in essence, an adaptation of the terrestrial model. The terrestrial model differs from the earth-to-satellite model only in terms of the path length. Instead of Eq. 10.2 the actual length of the terrestrial path is used for the value of L. All arguments in support of the earth-to-satellite prediction method described here apply to the terrestrial model as well. The terrestrial model has also found wide acceptance as a valid prediction model. Acampora [1981] regards it as acceptable for the USA and Garcia-Lopez and Casares-Giner [1981] and Kanellopoulos [1983b] support its use in various other parts of the world. It is expected that accuracies comparable to those found by Lin [1977] for the USA will be obtained for Southern Africa, when distributions from the rain-rate model is used in the terrestrial attenuation model. Also, similar accuracies should be obtained for the USA, using the rain-rate model.

The terrestrial attenuation model has already been used in conjunction with the rain rate model in Southern Africa for the prediction of rain attenuation on 11,7-GHz paths in a nation-wide digital radio relay system. Curves of rain-attenuation distribution, used for the

design of this radio relay system may be found in Seeber [1983]. The curves are for the two climatic regions of 'inland' and 'coastal' and for mean annual rainfalls ranging from 100 to 1500 mm.

10.5 Summary and conclusion

With the exception of the southern subtropical region, satisfactory estimates are obtained of the rain attenuation distribution on earth-satellite paths in the continental USA. The method obviates interpolation and scaling of attenuation or rain-rate distributions and provides attenuation distributions which are more site-specific than some other methods. It also allows extrapolations to be made to very low levels of probability. The results support the validity of the Southern African rain-rate model for the USA. They furthermore support the log-Gumbel hypothesis of annual maximum rain rates and the lognormal hypothesis of randomly varying rain rate. The Lin [1979] attenuation model is also supported. The hypothesis that the spatial and temporal characteristics of rain are statistically invariant over large geographic regions, while the frequency of rain occurrences varies from location to location, is for the larger part supported. The results indicate a large degree of commonality in the rain-rate characteristics of the Southern African and North American subcontinents. A good likelihood exists for the attenuation prediction method to give acceptable predictions in Southern Africa as well. The same applies to the terrestrial attenuation model by Lin [1977], in which the 5-min rain-rate distributions from the model may be applied.

Chapter 11

SUMMARY OF RESULTS

The results obtained thus far in this thesis may be summarized as follows:

An investigation was made into an extreme-value method by Lin [1978] for obtaining the rain-rate distribution from the series of annual maximum rain rates and mean annual rainfall. The results were favourable, pointing to the applicability of the method to the Southern African and North American subcontinents, as well as islands in the South Atlantic and South Indian oceans. The method is also applicable to various integration times. The log-Gumbel distribution for annual maximum rain rates and the lognormal distribution for time-varying rain rate were supported.

Using extreme-value relationships embodied in a report by Midgley and Pitman [1978], published for the hydrological community in Southern Africa, a semi-empirical rain-rate model was developed. The model is based on the above-mentioned extreme-value theory. The only data used were observed annual maximum rainfall rates and mean annual rainfall. The rain-rate maxima were of various integration times and included about 1000 station years of data. The model has the potential of predicting rain-rate distributions of any integration time from 5 to 1440 minutes from only the mean annual rainfall figure and the climate of the location in question. Only two climatic regions are used: 'coastal' and 'inland'. In determining the appropriate region the map of Fig. 25 may be used as a guide.

The model was applied to 17 locations on the Southern African subcontinent and two islands in the South Indian and South Atlantic oceans, to predict rain-rate distributions at 15-min integration time. Only in the case of the two islands were the predictions not acceptable. It was concluded that the model is valid for rain-rate prediction at 15-min integration time on the Southern African subcontinent and that there was a very good chance of it being acceptable at 5-min integration time as well.

Due to a lack of 5-min data in Southern Africa the rain-rate model was next applied to 20 widespread USA locations for rain-rate prediction at 5-min integration time. Favourable results were obtained. The theory of the model and the results were in agreement with the hypothesis [Goldhirsh, 1981] that the frequency of rain occurrences varies from location, while the temporal and spatial characteristics are invariant over large geographical regions. The combined results for Southern Africa and the USA as well as the validity of the Goldhirsh hypothesis pointed to the universality of the model, and indicated very strongly that 5-min predictions in Southern Africa should be feasible.

Lastly, the rain-rate model was applied to the prediction of attenuation on earth-satellite paths in the USA, using 5-min distributions from the model in a well-known attenuation model. The results were very encouraging and confirmed all previous conclusions, as well as the above-mentioned hypothesis. It also confirmed the belief that rain-attenuation prediction in Southern Africa will indeed be possible if the 5-min rain-rate distributions from the model are employed in existing methods of attenuation prediction -- for both earth-to-satellite and terrestrial links.

Chapter 12

GENERAL DISCUSSION

12.1 General aspects

When all the results obtained are viewed together it seems that there can be no further doubt as to the validity, in practice, of the extreme-value theory by Lin [1976 and 1978]. Not only has the theory been proven to hold at 15-min integration time in Southern Africa, but when incorporated into a model the latter also gave acceptable results. These results were of a three-fold nature: The prediction (or the estimation) of 15-min rain-rate distributions in Southern Africa, the prediction of 5-min rain-rate distributions in the United States, as well as the prediction of rain attenuation in the United States. By implication the log-Gumbel approximation for annual maximum rain rates and the lognormal approximation for time-varying rain rate are supported. Lin's relationships between the parameters of the two distributions are, of course, also supported. The unfavourable results for the islands of Marion and Gough are due to unsuitable expressions for α and U, but most likely for U, for these two locations. As has been demonstrated in Subsection 7.2.1 the results do not necessarily invalidate the extreme-value theory for these locations. The extreme-value theory gave satisfactory results at the island locations when appropriate values of α and U were used.

The fact that analytical expressions for U relating it to mean annual rainfall and climatic region has been found, in part supports the hypothesis that the log-

Gumbel extreme-value parameters may be related to other widely available climatological parameters. The hypothesis is, of course, not supported in regard to α, as no dependence has been found. The constant value of α of 3,5726 decided upon gives adequate results, although under-estimation of the cumulative rain rate probabilities below 2 mm/h and over-estimation at moderate rain rates (at 15-min integration time) indicate that this value of α may be too high.

Having also found an integration-time dependence in the two expressions for U, the hypothesis about the possibility of extrapolation down to 5 minutes is supported. The good results with the model when predicting rain-rate distributions at 15-minute integration time were possible only because the relationships of quadrants B and C of the DDF diagram (Fig. 24) of Midgley and Pitman [1978] were sound. Concerning quadrant A of the diagram, the results give proof of the validity of its relationships at an integration time of 5 and 15 minutes only. However, in view of the fact that the integration-time relationship seems sound, as discussed in Subsection 7.2.4, it seems that the relationships of quadrant A should not be seriously questioned. These conclusions in regard to the DDF diagram may be of concern to the hydrological community also.

On the whole, it is significant that the model has been developed without the use of any observed cumulative rain-rate distribution whatsoever. Only a pool of annual maxima of a large number of station years (about 1000) were considered. No adjustments to the parameters were made on the basis of comparisons with observed parent distributions of rain rate. These are aspects that should give a large degree of credibility to the approach. The pooling of the data has also overcome the problem of non-stationarity in α and U when their values are obtained from a limited time series of annual

maxima. For some locations this may give a cumulative distribution of greater accuracy than would be obtained by Lin's method.

Some other observations about the model are the following: It is similar to the rain-rate model of Rice and Holmberg [1973] in the sense of having only two input parameters. Both use mean annual rainfall as one of the input parameters. Like the Rice-and-Holmberg model, the model of this thesis displays a consistent increase in probability at any fixed level of rain rate with an increase in mean annual rainfall -- the other input parameter remaining constant. The new model's second input parameter, the climatic-region designation, is easily obtained for Southern Africa whereas the continentality factor of the Rice-and-Holmberg model is difficult to establish from the world map given.

The theoretical basis of the log-Gumbel and log-normal distributions allow extrapolations of the rain-rate distribution to be made to very low levels of probability. The problem of obtaining the rain-rate distribution at values of rain rate greater than 50 mm/h, seen by URSI [1981] to be a difficult task, appears to be solved. Also, having been based on a theory of extremes, it provides for those rain events which occur very rarely (once in a number of years), but which according to CCIR [1982d] produce the highest values of attenuation. In that sense it provides distributions of a truly long-term nature. Its use therefore obviates the need for a long-term measurement programme which would be required for establishing probabilities associated with rare events.

The two simple input parameters of MAR and climatic region make it easy to use the model, obviating geographical interpolation of rain-rate distributions and providing distributions at locations for which no rain-rate data are available. Also, in using mean annual

rainfall, rain-rate predictions may be made at locations for which little is known about the rainfall (such as in mountainous areas), but where the MAR may be obtained by sophisticated techniques such as 'trend surface analysis' [Schulze, 1976]. The relatively coarse climatic-region classification may be at the expense of accuracy for locations which have a mixture of 'inland' and 'coastal' climates. However, locations of this nature are few, compared to those which are well defined. In Southern Africa the 100-km criterion could therefore be applied without much difficulty. However, for locations with a mixture of the two climates, taking a value somewhere between the two respective probabilities would be justified. For this purpose the annual number of thunderstorm days, published in SA Weather Bureau [1954], could be useful.

The prediction methods we have proposed in Chapter 10 for obtaining the rain attenuation distribution on terrestrial and earth-to-satellite paths -- i.e. using the attenuation models of Lin [1977] and Lin [1979], respectively, in conjunction with the rain-rate model -- meet the four requirements as laid down by URSI [1981]. It is said that for a prediction method to be widely used it should (1) be easy to apply, (2) possibly have a physical significance, (3) give good agreement when tested with experimental results obtained in different regions, and (4) not be too critically dependent on the techniques used for obtaining the rainfall intensity data. The latter requirement, if measurement of the intensity (or rain rate) is implied, strictly speaking does not even apply, as the rain-rate model makes measurement unnecessary. The need for geographically mapping rain-rate zones -- seen by URSI [1981] as an asset in rain attenuation prediction -- also falls away.

12.2 Future work

An improved model may be possible by refining the expressions for α and U. As has been mentioned in Appendix C, the time bases of a large proportion of stations had been too short to obtain their log-Gumbel standard deviations with any degree of confidence. As a result the constant value of α decided upon may not be accurate enough. There is furthermore the indication that the value of α may be slightly too high. For some stations the annual data for a considerable number of additional years have recently become available at the South African Weather Bureau. The inclusion of this data should create more confidence in the values of the log-Gumbel standard deviation and may make it possible to utilize the standard deviations of more than the eight stations now used, in establishing trends with climatic region or other parameters. In the process some definite trend in α with MAR may also materialize. New attempts should also be made at finding relationships between α and other widely available climatic parameters. Parameters such as the average annual number of days with thunderstorms, the average number of days with rain (of various thresholds) and the frequency of lightning should be considered. The latter parameter is now well mapped for the whole of the lower part of the subcontinent, due to an extensive program of measurement [NEERI, 1982].

A re-analysis is also recommended in view of the rather coarse climatic classification presently used, which may not adequately provide for all locations. With more data it may be possible to establish new and better relationships for U. Ideally in the new expressions U should not only be a function of mean annual rainfall and integration time, but should also be a function of some other objective and easily obtainable climatic parameter. This parameter should indicate the degree of continentality of the location, but in a more sophisti-

cated way than simply by 'inland' and 'coastal'. The same parameters as suggested for α may be considered.

As a further refinement, clock-duration corrections should be made in the data as suggested by Hershfield [1961] and checks should be done for outliers as suggested by Watson et al. [1981, p 46]. Annual-maxima series that possibly consist of more than one distribution should be identified [Watson et al., 1981, p 47]. In calculating the log-Gumbel standard deviations and means the non-asymptotic, rather than the asymptotic, forms of the equations should be used [Lin, 1976].

In order to refine the integration-time relationships of the model a serious attempt should be made to obtain data at integration times lower than 15 minutes. Although it is not easy to obtain average annual observed distributions over a period of a few years the relationships could possibly be found by studying a representative number of storms. Also, the 30- and 45-minute data, which has been neglected in developing the integration-time relationships of the DDF diagram, should be applied, at least for checking the resultant relationships.

Consideration should be given to extending the model for application to other climatic regions of the world, by pooling together with the Southern African data, data at various integration times from various parts of the world. This of course, could also assist in improving the expressions for α and U for local use. A finer climatic-region classification and more accurate integration-time relationships could thus possibly be established. It may also be possible to extend the integration-time capability down to 1 minute or less, for use in other attenuation prediction methods.

It should be noted that future modelling procedures do not necessarily have to follow those of the present

model exactly. An approach of modelling the parent distribution of rain rate by modelling the parameters of the extreme-value distribution has been established (it seems that this has not been done before). Any form of modelling which results in sound relationships between α and U of the log-Gumbel extreme-value distribution and other widely available meteorological parameters, will suffice. Also, for those locations with long-term continuously observed rain-rate data, consideration could, for modelling purposes, be given to finding α and U from the complete rain-rate distribution. This may be done by first fitting a lognormal distribution to the observed distribution, in the process finding the parameters P_0, S_R and R_m. Of course, if any of these parameters are available by other means, the fitting process will be so much easier. As a second step α and U may then be found using these parameters in conjunction with mean annual rainfall and utilizing the relationships of Chapter 3. Eventually, following a variety of procedures, a unified database for the extreme-value parameters may be established for large parts of the globe. The availability of such a database could eventually lead to a global model. It is, of course, suggested that such a model be based on the fundamental assumptions of a log-Gumbel distribution of annual maxima and a lognormal distribution of time-varying rain-rate, as well as Lin's extreme-value theory linking the two distributions.

Lin's theory presents a unified view of looking at the parent distribution of rain rate and the distribution of annual maximum rain rates. If it is assumed that the theory is sound and is obeyed in practice, then it is implied that the parent distribution of rain rate is defined by the log-Gumbel distribution of annual maxima plus the mean annual rainfall. What perhaps is more important for the hydrologist is the converse -- the fact that the log-Gumbel distribution of annual maxima ensues

from a knowledge of the observed parent distribution and mean annual rainfall, as discussed in the preceding paragraph. This may be an extremely powerful tool for establishing the return period of short-duration rainfall depths of a location. A far greater degree of accuracy may be possible, as compared to fitting a log-Gumbel distribution to the series of annual maxima of a limited time base. This may be especially so if the lognormal distribution is fitted to moderate rain rates only, up to the point where non-stationarity becomes evident. The concept has been demonstrated for Keetmanshoop, for instance, where in Subsection 3.2.3 the calculated value of α and U were adjusted so that the lognormal distribution provided a better fit to the observed parent distribution. It can be shown that this adjustment changed the return period of 25 mm of rain per 15 minutes from 11 to 15 years -- a significant change. The question that has to be resolved is whether the lognormal distribution may be fitted to the observed distribution with a sufficient degree of accuracy so as to be of use to the hydrologist.

Chapter 13

CONCLUSION

- A rain rate model enabling the prediction of microwave and millimetre-wave rain attenuation on terrestrial and earth-to-satellite links has been developed for Southern Africa.

- The model provides what has been found to be the most critical determinant in rain attenuation prediction, namely the annual average cumulative distribution of point rainfall rate. The latter is not generally available on the Southern African subcontinent and also cannot be obtained by existing rain-rate models.

- The model will predict the rain-rate distribution at locations for which no rain-rate data are available. It provides the distribution from only the mean annual rainfall and a designation as to whether the location is climatically 'coastal' or 'inland'.

- Rain-rate distributions of any rain-gauge integration time between 5 and 1440 minutes can be provided.

- The model has been tried at an integration time of 15 minutes in Southern Africa and has been found valid, in general giving predictions of an accuracy of a factor of 2 in probability. There are indications that it may give slight under-estimations at high rain rates for southern and southeastern coastal locations.

- The model has also been found valid at 5-min integration time in the USA. The conclusion is that it has general validity on both the Southern African subcontinent and the contiguous United States.

- The 5-min rain-rate distributions from the model may be used in the rain attenuation models of Lin [1977] and Lin [1979], in order to provide attenuation predictions on terrestrial and earth-space radio links, respectively.

- The utilization of the model for the prediction of rain attenuation on earth-to-satellite paths in the USA has given satisfactory results, the accuracy being within a factor of 2 in probability, in general. Indications are that the same accuracy will be obtained in Southern Africa.

- It is envisaged that attenuation prediction by the model on terrestrial paths in Southern Africa will be approximately to the same accuracy as that obtained by Lin [1977] for the USA.

- The model is an extension of Lin's extreme-value theory. It involved finding generalized expressions for the extreme-value parameters α and U. That was done on the basis of the hypotheses, (a) that the values of the extreme-value parameters at low integration times may be extrapolated from their values at higher integration times and, (b) that the parameters may be modelled on widely available climatic parameters. The hypotheses have been confirmed in regard to U. Generalized expressions for U, in which it is a function of mean annual rainfall, climate region and integration time, have been obtained from algebraic and graphical relationships of the DDF diagram of Midgley and Pitman [1978]. The parameter α has been found to be a constant.

- Rain rates used in the development of the model were only of the annual-maximum type. No adjustments were made on the basis of observed parent distributions.

- The pooling of the annual-maximum data and the resulting expressions for the extreme-value parameters solve the problem of inaccuracies in the parameters which may result from too limited a time base in annual maxima.

- The theory of the model, as well as the results, support the larger part of the hypothesis by Goldhirsh [1981], i.e. that the frequency of rain occurrences varies from location to location, while the spatial and temporal characteristics are rather invariant over large geographic areas.

- In general the results from the model at 15-min integration time in Southern Africa and 5-min integration time in North America indicate that fairly universal climatic laws operate on the two continents.

- The results obtained using the model support the log-Gumbel approximation for the series of annual maximum rain rates and the lognormal approximation for the parent distribution of rain rate. Support is also given to some of the extreme-value relationships in the DDF diagram of Midgley & Pitman [1978].

- Lin's extreme-value theory, based on the above-mentioned distributions, has been confirmed for the Southern African subcontinent and for two islands in the South Atlantic and South Indian oceans. The subcontinent spans a range of climates from maritime to continental and includes annual rainfalls from 44 to 1050 mm. The rainfall on one of the islands is as high as 3400 mm/a.

- The model in general slightly under-estimates in the region of very low rain rates (below about 2 mm/h), while it slightly over-estimates at moderate rain rates. This indicates that the present value of α is slightly too high.

- The model enables extrapolation of the rain-rate distribution down to very low levels of probability (or high rain rate), which is difficult to do otherwise. The distribution at very low probabilty is sometimes required for link design. Provision is therefore made for events occurring only once in a number of years, but which give the highest values of attenuation. The need for a programme of long-term measurement is therefore obviated.

- The rain-rate model is easy to use from the point of view of using simple input parameters. However, the choice between the two climatic regions may be somewhat subjective, possibly requiring interpolation in borderline cases.

Chapter 14

RECOMMENDATIONS

- The log-Gumbel and lognormal distributions, as well as Lin's extreme-value theory, have proved to be viable for rain-rate modelling and should be considered in future modelling efforts.

- An improved model for Southern Africa should be attempted by making certain refinements and including additional data of annual maximum rain rate. Attempts should be made at modelling the rain-rate climate more finely than with 'coastal' and 'inland' regions, possibly using other widely available climatological parameters.

- A global model should be attempted by pooling together data of annual maximum rain rates from various parts of the globe.

- Observed rain-rate distributions can be a source of knowledge on the extreme-value parameters α and U and should be considered for extending the data base of extreme-value parameters for rain attenuation modelling. It should also be considered by hydrologists as a means of establishing return periods with greater certainty.

REFERENCES

Acampora, A.S. [1981], Rain margin improvement using resource sharing in 12 GHz satellite downlinks. The Bell System Tech. Journal, Vol 60, No 2, Feb 1981, pp 167-192.

Andrews, J.H., Ozbay, C., Pratt, T., Bostian, C.W., Manus, E.A., Gaines, J.M., Marshall, R.E., Stutzman, W.L. and Wiley, P.H. [1982], Results of the VPI and SU COMSTAR experiment. Radio Science, Vol 17, No 6, Nov-Dec 1982, pp 1349-1359.

Arnold, H.W., Cox, D.C. and Rustako, A.J. (Jr) [1981], Rain attenuation at 10-30 GHz along earth-space paths: elevation angle, frequency, seasonal and diurnal effects. IEEE Trans. on Communications, Vol 29, No 5, May 1981, pp 716-721.

Bodtmann, W.F. and Ruthroff, C.L. [1974], Rain attenuation on short radio paths : Theory, experiment and design. The Bell System Technical Journal, Vol 53, No 7, Sept 1974, pp 1329-1349.

Brussaard, G. [1981], Prediction of attenuation due to rainfall on earth-space links. Radio Science, Vol 16, No 5, Sept-Oct 1981, pp 745-760.

Carte, A.E. [1979], Sustained storms on the Transvaal Highveld. South African Geographical Journal, Vol 61, No 1, 1979, pp 39-56.

Carte, A.E. and Kidder, R.E. [1977], Lightning in relation to precipitation. Journal of Atmospheric and Terrestrial Physics, Vol 39, 1977, pp 139-148.

CCIR [1978], Radiometeorological data. Rep. 563-1 of Recommendations and Reports of the CCIR, Vol. V: Propagation in Non-Ionized Media, XIVth Plenary Assembly, Kyoto, 1978, pp 69-89.

CCIR [1982a], Radiometeorological data. Rep. 563-2 of Recommendations and Reports of the CCIR, Vol V: Propagation in Non-Ionized Media, XVth Plenary Assembly, Geneva, 1982, pp 96-123.

CCIR [1982b], Propagation data required for line-of-sight radio-relay systems. Ibid., Rep. 338-4, 36 pp, pp 291-314.

CCIR [1982c], Propagation data required for space telecommunication systems. Ibid., Rep. 564-2, pp 331-373.

CCIR [1982d], Attenuation by hydrometeors, in particular, and other atmospheric particles. Ibid., Report 721-1, pp 167-181.

CCIR [1982e], Scattering by precipitation. Ibid., Report 721-1, pp 167-181.

CCIR [1982f], Cross-polarization due to the atmosphere. Ibid., Report 722-1, pp 185-193.

Chu, T.S. and Schecker, J.A. [1985], Extrapolation of point rain rate distributions. Electronics Letters, Vol 21, No 17, 15th August 1985, pp 754-755.

Crane, R.K. [1980], Prediction of attenuation by rain. IEEE Transactions on Communications, Vol 28, No 9, Sept 1980, pp 1717-1733.

Crane, R.K. [1985], Comparative evaluation of several rain attenuation prediction models. Radio Science, Vol 20, No 4, July-Aug 1985, pp 843-863.

Damosso, E.; De Renzis, G.; Lingua, B. and Ossola, P. [1981], Influence of the integration time and the height of rain-gauge on rainfall rate statistics. IEE Second Intl. Conference on Antennas and Propagation, 13-16 April 1981, Heslington, York, UK. IEE Conference Publication No 195, Part 2, pp 283-287.

Dutton, E.J. [1977], Precipitation variability in the USA for microwave terrestrial system design. Report OT 77-134 of the Office of Telecommunications of the US Dept. of Commerce, Nov 1977, 126 pp, pp 20-24.

Dutton, E.J. and Dougherty, H.T. [1979], Year-to-year variability of rainfall for microwave applications in the USA. IEEE Trans. on Communications, Vol 27, No 5, May 1979, pp 829-832.

Fedi, F. [1981a], Rain attenuation on earth-satellite links: a prediction method based on point rainfall intensity. Ann. Télécommunic, Vol 36, No 1-2, Jan-Feb 1981, pp 73-77.

Fedi, F. [1981b], Prediction of attenuation due to rainfall on terrestrial links. Radio Science, Vol 16, No 5, Sept-Oct 1981, pp 731-743.

Garcia-Lopez, J.A. and Casares-Giner, V. [1981], Modified Lin's empirical formula for calculating rain attenuation on a terrestrial path. Electronics Letters, Vol 17, No 1, 8 Jan 1981, pp 34-36.

Goldhirsh, J. [1980], Cumulative slant path fade statistics associated with the COMSTAR beacon at 28.56 GHz for Wallops Island, Virginia over a three year period. Report APL/JHU SIR8OU-048, Applied Physics Laboratory, The John Hopkins University, Laurel, Maryland 20810, December 1980, 69 pp.

Goldhirsh, J. [1981], Prediction of absolute rain fade distributions for earth-satellite paths employing radar modelling techniques - general methods for extrapolation of fade statistics to other locations. Report APL/JHU S1R81U-034, Applied Physics Laboratory, The John Hopkins University, Laurel, Maryland 20810, October 1981, 42 pp, p 22.

Goldhirsh, J. [1982], Slant path fade and rain-rate statistics associated with the COMSTAR beacon at 28.56 GHz for Wallops Island, Virginia over a three-year period. IEEE Trans on Antennas and Propagation, Vol 30, No 2, March 1982, pp 191-198.

Gumbel, E.J. [1954], Statistical theory of extreme values and some practical applications. U.S. Department of Commerce, National Bureau of Standards; Applied Series No 33, Feb. 1954, 51 pp.

Gumbel, E.J. [1958], Statistics of extremes. Columbia University Press, New York, 1958, 375 pp.

Hall, M.P.M. [1979], Effects of the troposphere on radio communication. The Institution of Electrical Engineers, London, 1979, 206 pp, Chapter 3.

Held, G. [1980], Radar observations of an unusual cloud burst in South Africa. Meteorologische Rundschau, Vol 33, April 1980, pp 37-42.

Hershfield, D.M. [1961], Estimating the probable maximum precipitation. J. of the Hydraulics Division, Proc. of the Am. Soc. of Civil Eng., September 1961, pp 99-116.

Ippolito, L.J. [1981], Radio progagation for space communication systems. Proc of the IEEE, Vol 69, No 6, June 1981, pp 697-727.

Ippolito, L.J., Kaul, R.D. and Wallace, R.G. [1983], Propagation effects handbook for satellite systems design. Third Edition, NASA Reference Publication 1082(03), June 1983, 450 pp, p 179.

Ippolito, L.J. [1984], Rain attenuation prediction for communications satellite systems. Paper no AIAA-87-0718 of Collection of Technical Papers from AIAA 10th Communication Satellite Systems Conference, 19-22 March 1984. Paper published by AIAA (CP 842), New York, pp 319-326.

Jahnke, Emde and Lösch [1960], Tables of higher functions. Sixth Ed., McGraw Hill, 1960, 318 pp., p 31.

Kanellopoulos, J.D. [1983a], A rigorous analysis for the study of rain attenuation and depolarization statistics for terrestrial and earth-space links. Radio Science, Vol 18, No 5, Sept-Oct 1983, pp 709-719.

Kanellopoulos, J.D. [1983b], Extension of Lin empirical formula for the prediction of rain attenuation. Radio Science, Vol 18, No 2, March-April 1983, pp 237-240.

Kanellopoulos, J.D. and Clarke, R.H. [1981a], Prediction of cross-polarization discrimination statistics for propagation through spatially nonuniform rain. Radio Science, Vol 16, No 2, March-April 1981, pp 197-201.

Kanellopoulos, J.D. and Clarke, R.H. [1981b], A study of the joint statistics of rain depolarization and attenuation applied to the prediction of radio link performance. Radio Science, Vol 16, No 2, March-April 1981, pp 203-211.

Kanellopoulos, J.D., Kefalas, H. and Androulakakis, N.I. [1981], Analysis of long-term rain attenuation statistics. Radio Science, Vol 16, No 6, Nov-Dec 1981, pp 1361-1363.

Köppen, W. and Geiger, R. [1936], Handbuch der Klimatologie. Vol 1, C, Verlagsbuchhandlung, Gebrüder Borntraeger, Berlin, 1936.

Kumar, P.N. [1982], Precipitation fade statistics for 19/29-GHz COMSTAR beacon signals and 12-GHz radiometric measurements. Comsat Technical Review, Vol 12, No 1, Spring 1982, pp 1-27.

Landsberg, H.E. [1974], (Editor-in-chief), World Survey of climatology, Vol 11: Climates of North America, Amsterdam, The Netherlands: Elsevier, 1974, 420 pp, p 213.

Lin, S.H. [1976], Rain-rate distributions and extreme-value statistics. The Bell System Technical Journal, Vol 55, No 8, Oct. 1976, pp 1111-1124.

Lin, S.H. [1977], Nationwide long-term rain rate statistics and empirical calculation of 11-GHz microwave rain attenuation. The Bell System Technical Journal, Vol 56, No 9, Nov. 1977, pp 1581-1604.

Lin, S.H. [1978], More on rain rate distributions and extreme value statistics. The Bell System Technical Journal, Vol 57, No 5, May-June 1978, pp 1545-1568.

Lin, S.H. [1979], Empirical rain attenuation model for earth-satellite paths. IEEE Trans. on Communications, Vol 27, No 5, May 1979, pp 812-817.

Lin, S.H., Bergmann, H.J. and Pursley, M.V. [1980], Rain attenuation on earth-satellite paths - summary of 10-year experiments and studies. The Bell System Tech. Journal, Vol 59, No 2, Feb. 1980, pp 183-228.

Macchiarella, G. [1985], A comparative analysis of some prediction methods for rain attenuation statistics in earth-to-space links. Radio Science, Vol 20, No 1, Jan-Feb 1985, pp 35-49.

Midgley, D.C. & Pitman, W.V. [1978], A depth-duration-frequency diagram for point rainfall in Southern Africa. Report 2/78 of the Hydrological Research Unit, University of the Witwatersrand, Johannesburg, South Africa, Aug 1978, 62 pp.

Misme, P. and Fimbel, J. [1975], Détermination théoretique et expérimentale de l'affaiblissement par la pluie sur un trajet radioélectrique. Ann. Télécommunic., Vol 30, No 5-6, May 1975, pp 149-158.

Nackoney, O.G. and Davidson, D. [1982], Results of 11.7-GHz CTS rain attenuation measurements at Waltham, Massachusetts. Radio Science, Vol 17, No 6, Nov-Dec 1982, pp 1435-1442.

NEERI [1982], Lightning recording scheme. Leaflet published by the National Electrical Engineering Research Institute of the CSIR, P O Box 395, Pretoria, 0001, South Africa, 1982, 4 pp.

NERC [1975], Flood Studies Report, Vol II: Meteorological Studies. Natural Environment Research Council, 27 Charing Cross Road, London, UK, 1975, 81 pp, pp 24-28.

NOAA [1971], Climatological Data - Annual Summary for 1971, Vol 22, No 13, pp 726-733. Published by US Dept of Commerce, National Oceanic and Atmospheric Administration, National Climatic Center, Federal Building, Asheville, North Carolina 28801.

Op ten Noort, T.H. and Stephenson, D. [1982], Flood peak calculation in South Africa. Report No 2/1982 of the Water Systems Research Programme, Department of Civil Engineering, University of the Witwatersrand, Jan Smuts Ave, Johannesburg, South Africa, Nov. 1982, 89 pp, p 15.

Proctor, D.E. [1983], Lightning and precipitation in a small multicellular thunderstorm. Journal of Geophysical Research, Vol 88, No C9, 20 June 1983, pp 5421-5440.

Rice, P.L. and Holmberg, N.R. [1973], Cumulative time statistics of surface-point rainfall rates. IEEE Trans. on Communications, Vol 21, No 10, Oct. 1973, pp 1131-1136.

Rogers, D.V. [1981], Diversity- and single-site radiometric measurements of 12-GHz rain attenuation in different climates. Second International Conference on Antennas and Propagation, Heslington, York, England, 13-16 April 1981, IEE Conference Publication No 195, Part 2, pp 118-123.

Rustako, A.J. [1982], Rain attenuation and depolarization over an earth space path at 12 GHz: experimental results using the CTS beacon. IEEE Trans. on Antennas and Propagation (USA), Vol 30, No 4, July 1982, pp 720-725.

S.A. Weather Bureau [1954], Climate of South Africa. Part 1: Climate Statistics. Published by the Government Printer, Pretoria, as Weather Bureau publication No 19, 1954, 160 pp, pp 37 and 40.

S.A. Weather Bureau [1957], Climate of South Africa. Part 4: Rainfall Maps. Published by the Government Printer, Pretoria, as Weather Bureau publication No 22, 1957, 44 pp, map no 6.

Schulze, R.E. [1976], On the application of trend surfaces of precipitation to mountainous areas. Water SA, Vol 2, No 3, July 1976, pp 110-117.

Schwartz, M. [1970], Information transmission, modulation and noise. McGraw Hill Book Co., 1970, 672 pp, pp 326-330.

Seeber, R.J. [1983], Krommes vir die ontwerp van die reënverswakkingsmarge van aardverbindings by 11,7 GHz in Suidelike Afrika. Report No TEL-195 of the National Institute for Telecommunications Research of the CSIR, P O Box 3718, Johannesburg, South Africa, Nov 1983, 81 pp.

Segal, B. [1979], High-intensity rainfall statistics for Canada. Report No 1329-E, Communications Research Centre, Department of Communications, Ottawa, Canada, Nov. 1979, 124 pp, pp 15-17 and 56.

Segal, B. [1980], An analytical examination of mathematical models for the rainfall rate distribution function. Annales des Télécommunications, Vol 35, No 11-12, Nov-Dec 1980, pp 434-438.

Tang, D.D. and Davidson, D. [1982], Diversity reception of COMSTAR satellite 19/29-GHz beacons with the Tampa Triad, 1978-1981. Radio Science, Vol 17, No 6, Nov-Dec 1982, pp 1477-1488.

URSI Workshop Session Chairmen [1981], URSI workshop report: Effects of the lower atmosphere on radio propagation at frequencies above 1 GHz. Radio Science, Vol 16, No 5, Sept-Oct 1981, pp 813-824.

Vogel, W.J. [1982], Measurements of satellite beacon attenuation at 11.7, 19.04, and 28.56 GHz and radiometric site diversity at 13.6 GHz. Radio Science, Vol 17, No 6, Nov-Dec 1982, pp 1511-1520.

Watson, P.A., Sathiaseelan, V., and Potter, B. [1981], Development of a climatic map of rainfall attenuation for Europe. Interim Report, Report 300, University of Bradford Postgraduate School of Electrical and Electronic Engineering, Bradford, United Kingdom, March 1981, 134 pp.

Watson, P.A., Gunes, M., Potter, B.A., Sathiaseelan, V. and Leitao, J. [1982], Development of a climatic map of rainfall attenuation for Europe. Final Report, Report 327, University of Bradford Postgraduate School of Electrical and Electronic Engineering, Bradford, United Kingdom, June 1982, 153 pp.

APPENDICES

APPENDIX A : FIGURES

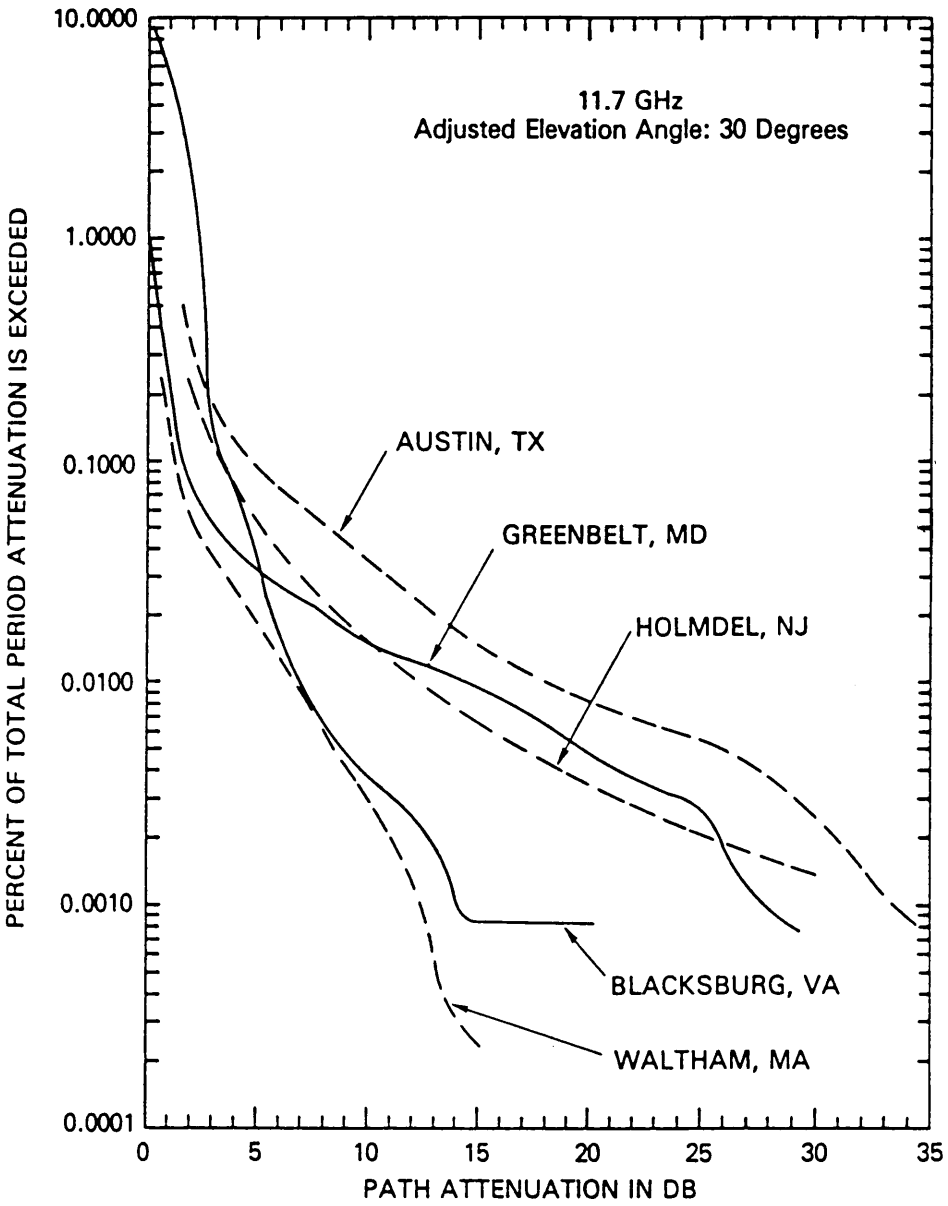

Fig. 1 Examples of the annual cumulative distribution of rain attenuation reproduced from Ippolito et al. [1983, p182]. The distributions are one-year observed distributions for earth-to-satellite paths at 11,7 GHz. They have been scaled to the same elevation angle of 30 degrees.

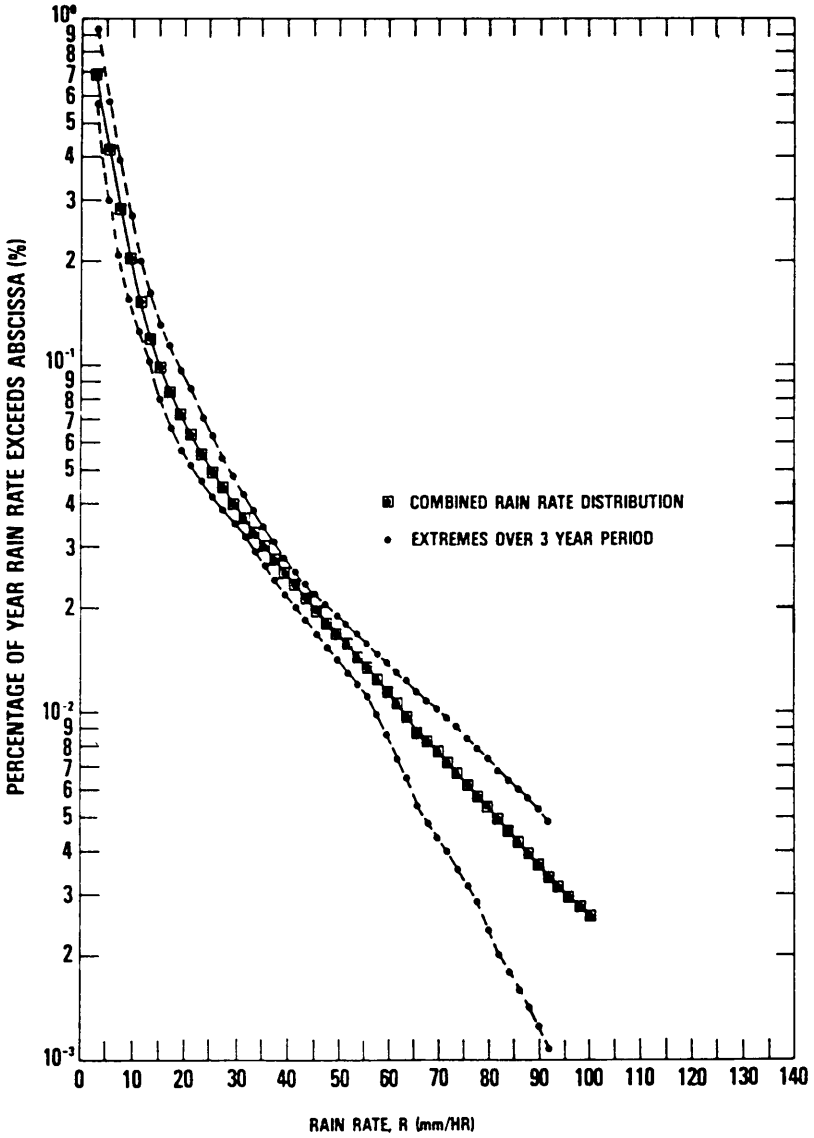

Fig. 2 Examples of the annual cumulative distribution of nearly instantaneous rainfall rate reproduced from Goldhirsh [1980, p26]. The distributions were obtained over a 3-year period, with the combined distribution showing the average for the 3 years.

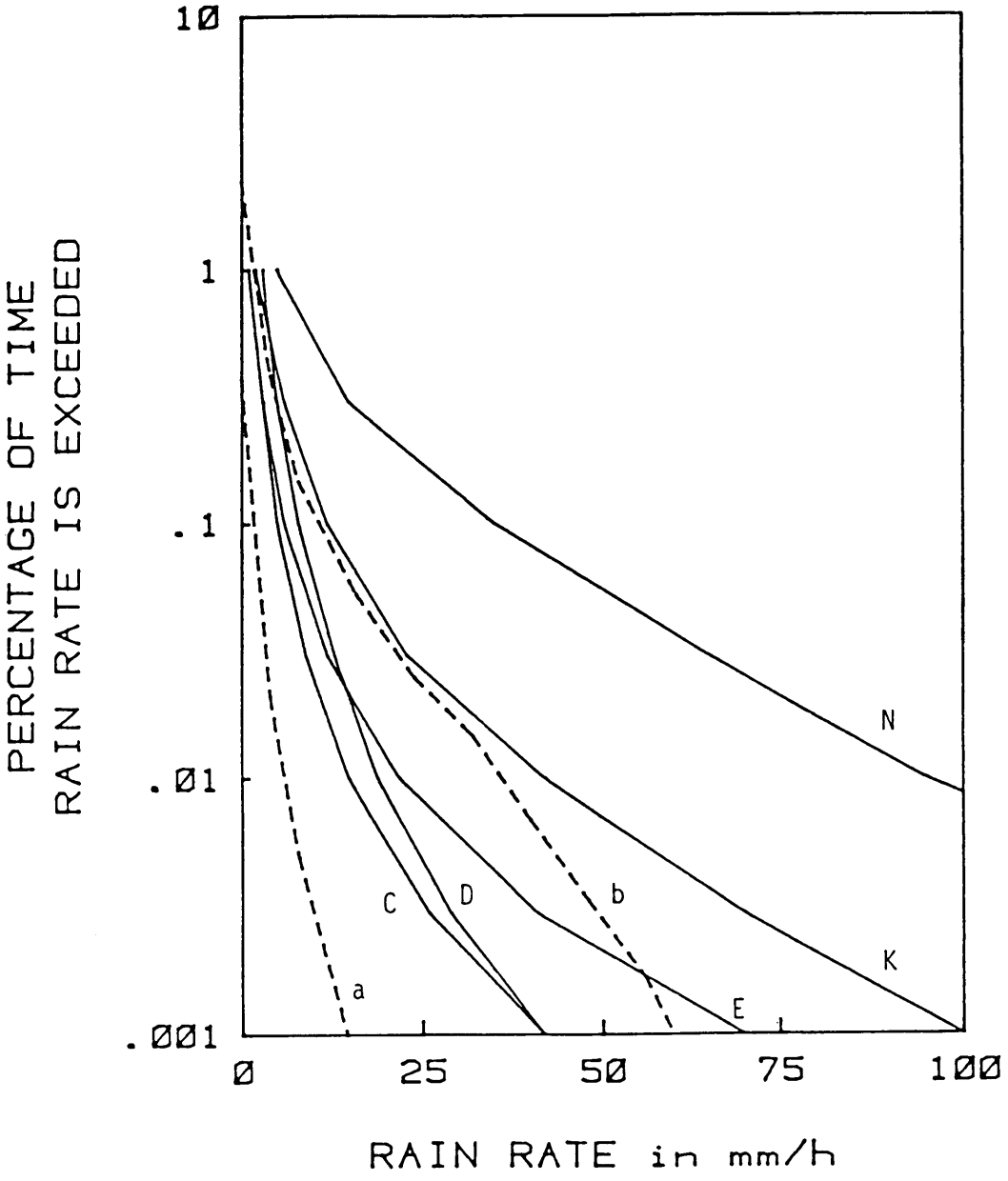

Fig. 3 Comparison of CCIR distributions with observed distributions in Southern Africa. Curves C, D, E, K and N represent the CCIR distributions. Curves a and b give long-term observed 15-min distributions for Alexander Bay and JBM Hertzog, respectively. Both locations are in CCIR region E.

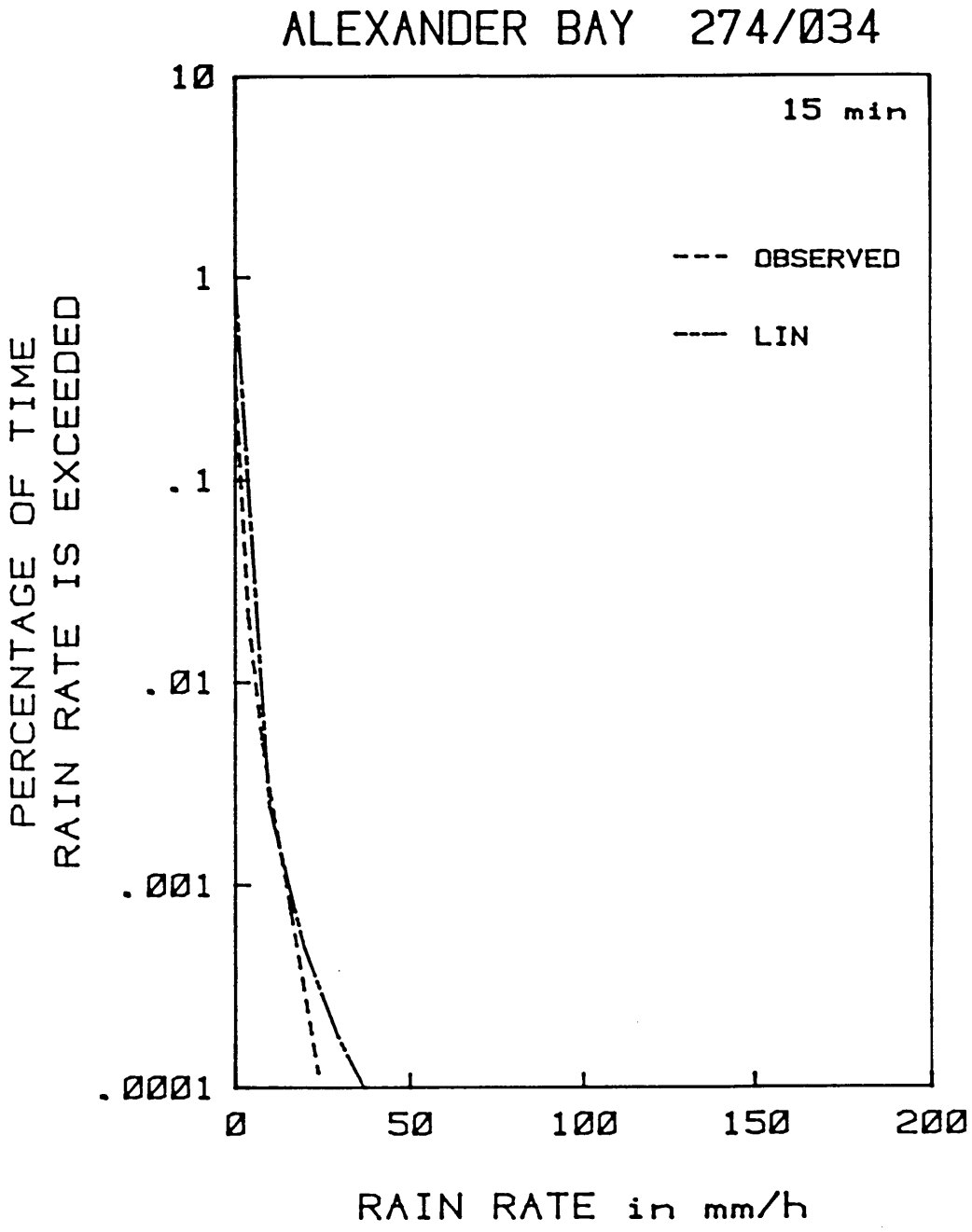

Fig. 4 Rain-rate distributions of 15-min integration time as observed and as calculated by Lin's method, for Alexander Bay.

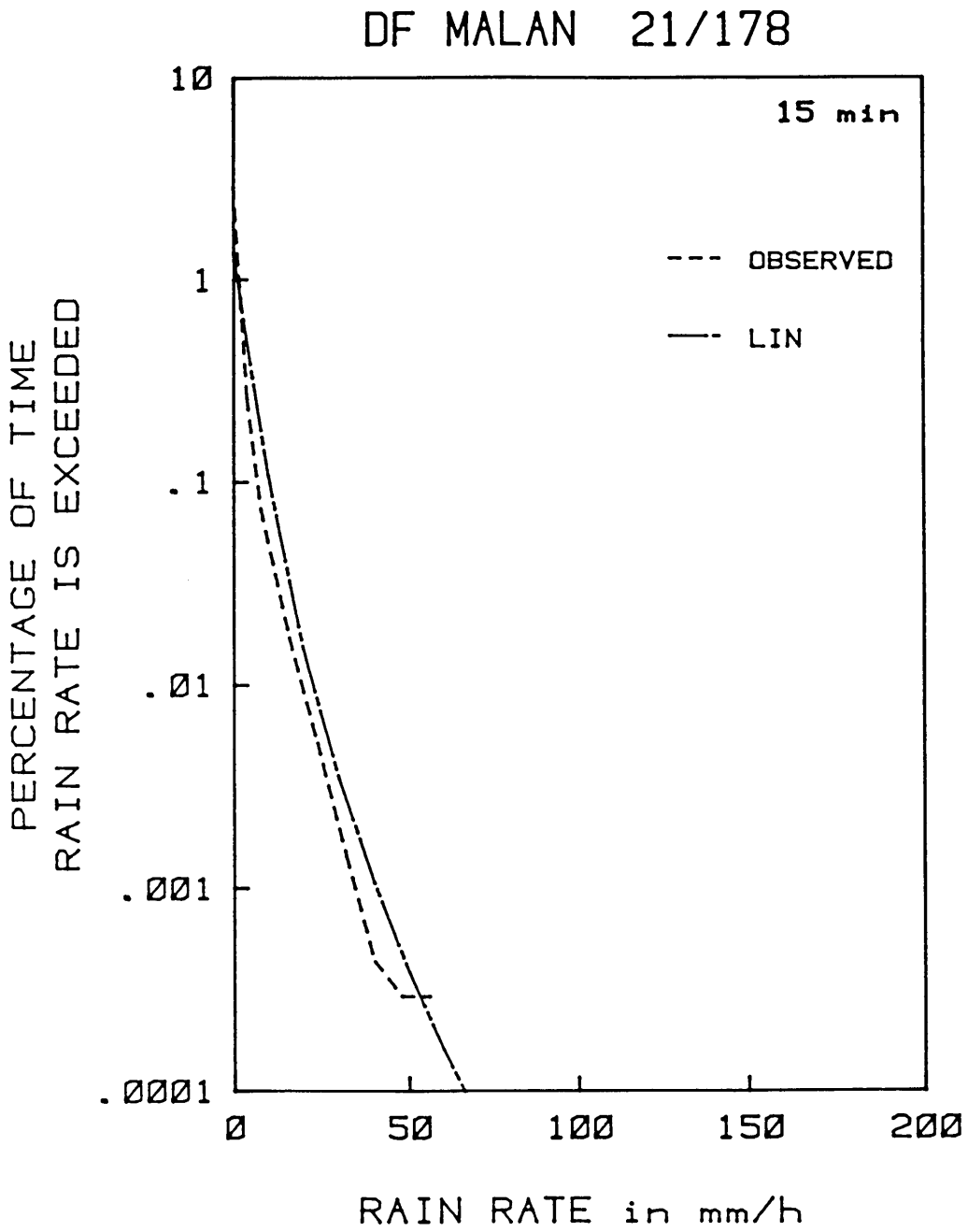

Fig. 5 Rain-rate distributions of 15-min integration time as observed and as calculated by Lin's method, for DF Malan Airport, Cape Town.

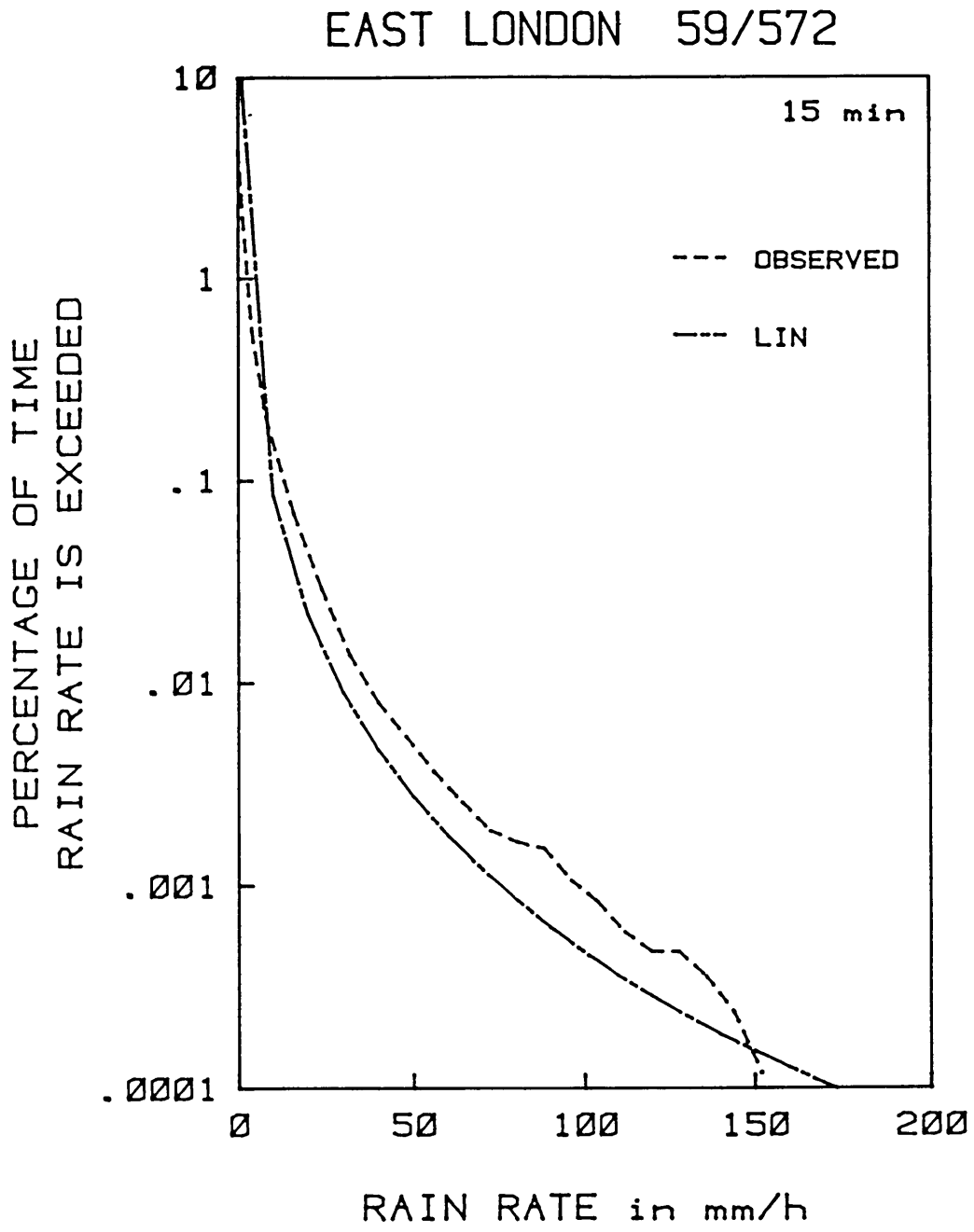

Fig. 6 Rain-rate distributions of 15-min integration time as observed and as calculated by Lin's method, for East London.

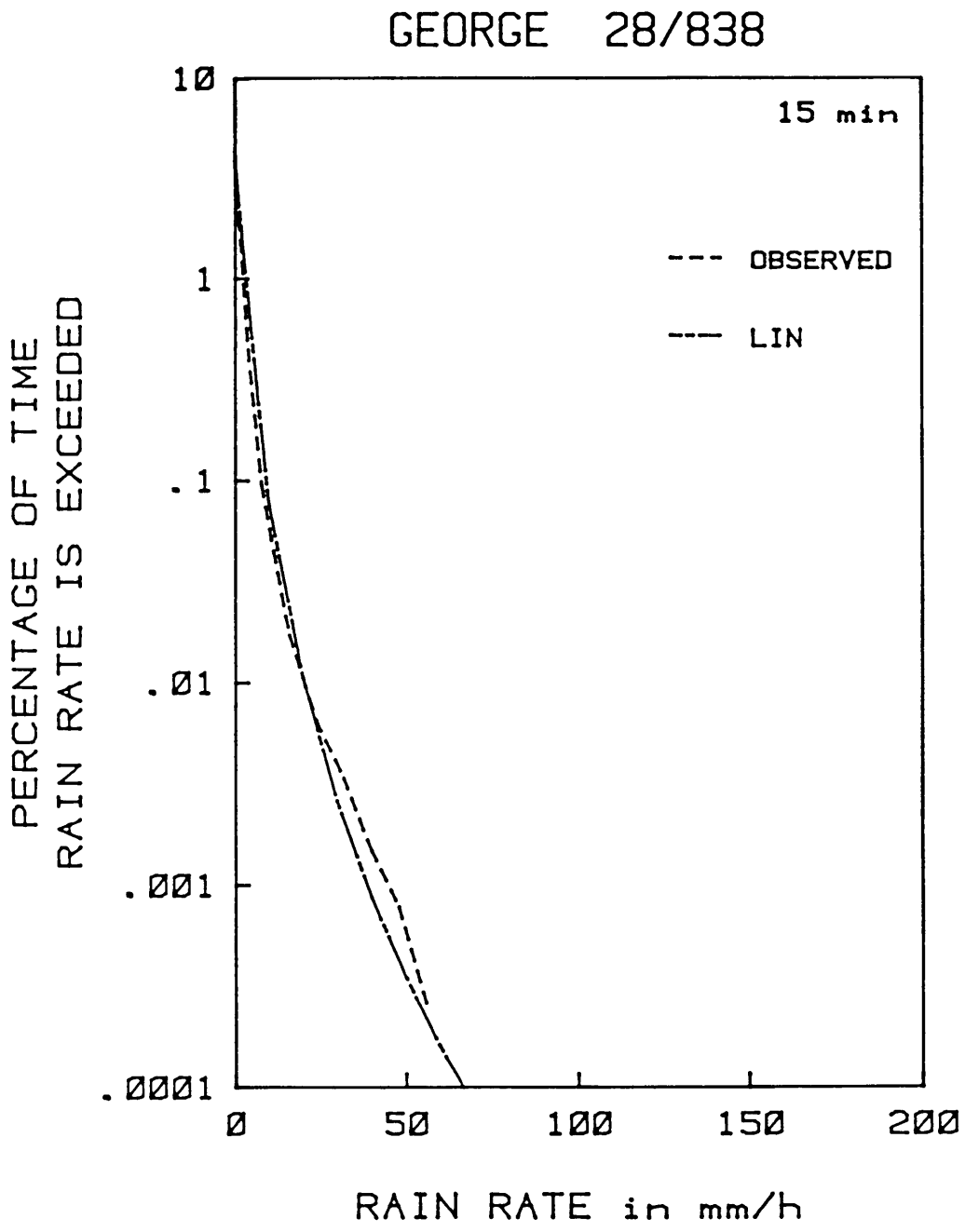

Fig. 7 Rain-rate distributions of 15-min integration time as observed and as calculated by Lin's method, for George.

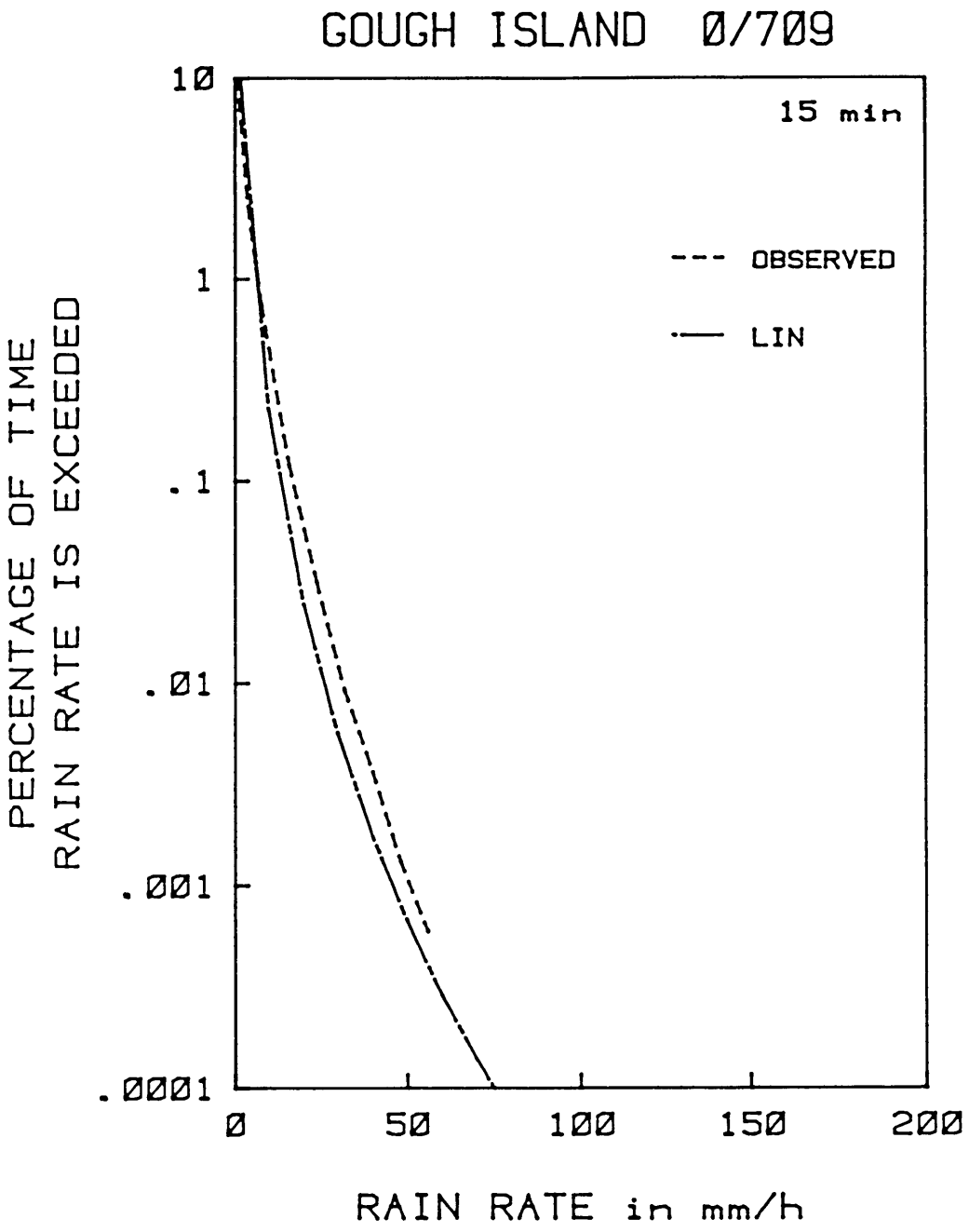

Fig. 8 Rain-rate distributions of 15-min integration time as observed and as calculated by Lin's method, for Gough Island, South Atlantic Ocean.

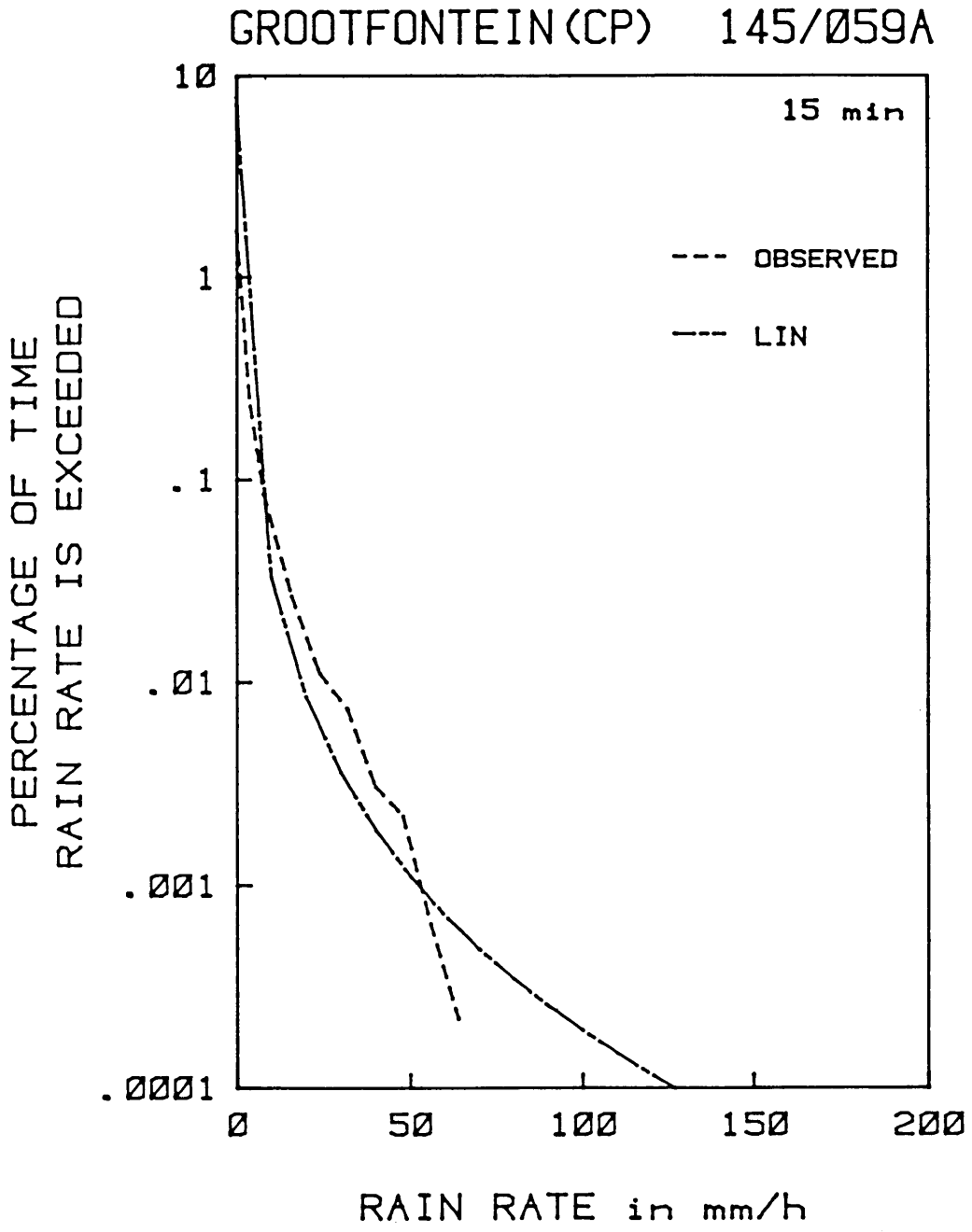

Fig. 9 Rain-rate distributions of 15-min integration time as observed and as calculated by Lin's method, for Grootfontein, Cape Province.

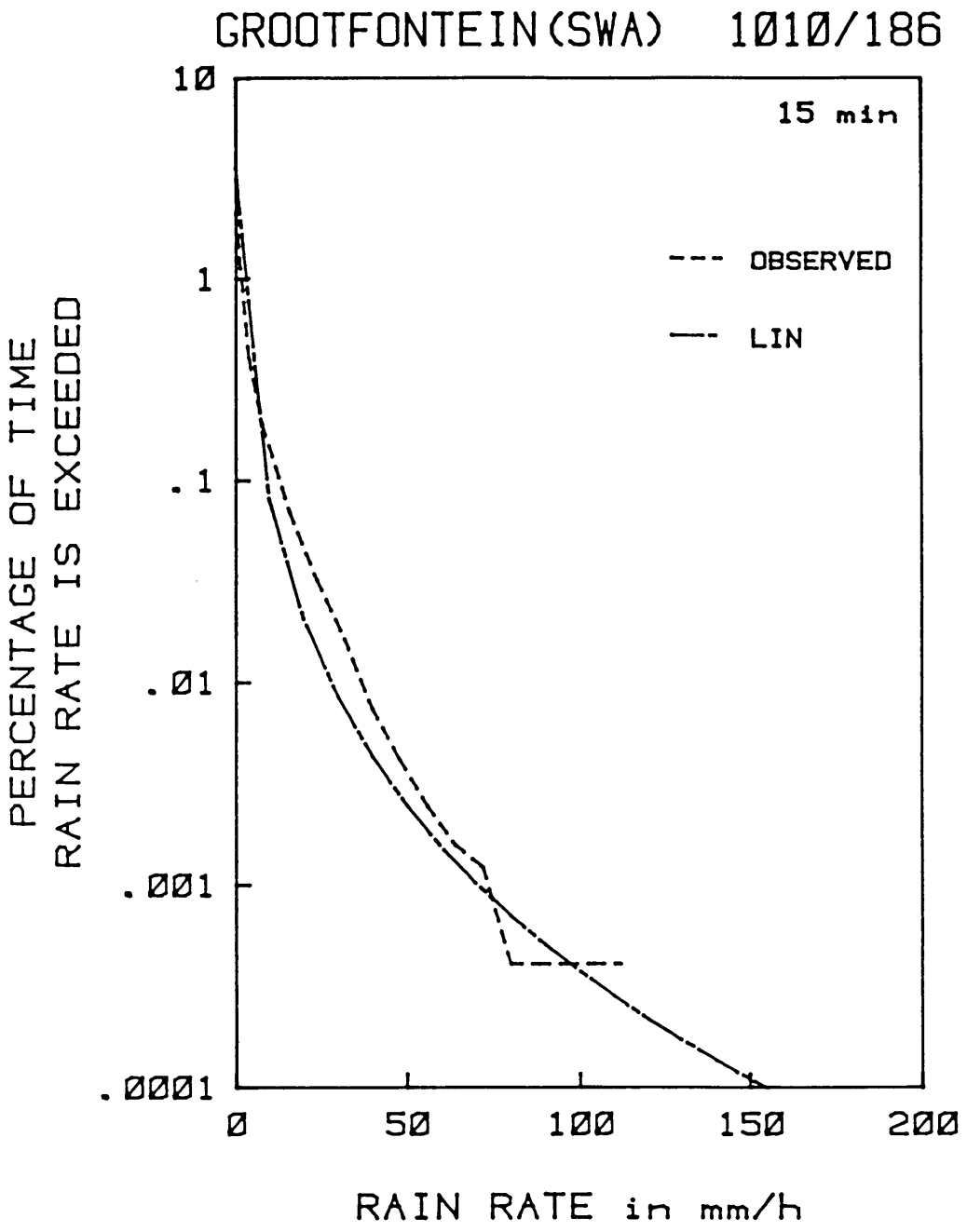

Fig. 10 Rain-rate distributions of 15-min integration time as observed and as calculated by Lin's method, for Grootfontein, South West Africa.

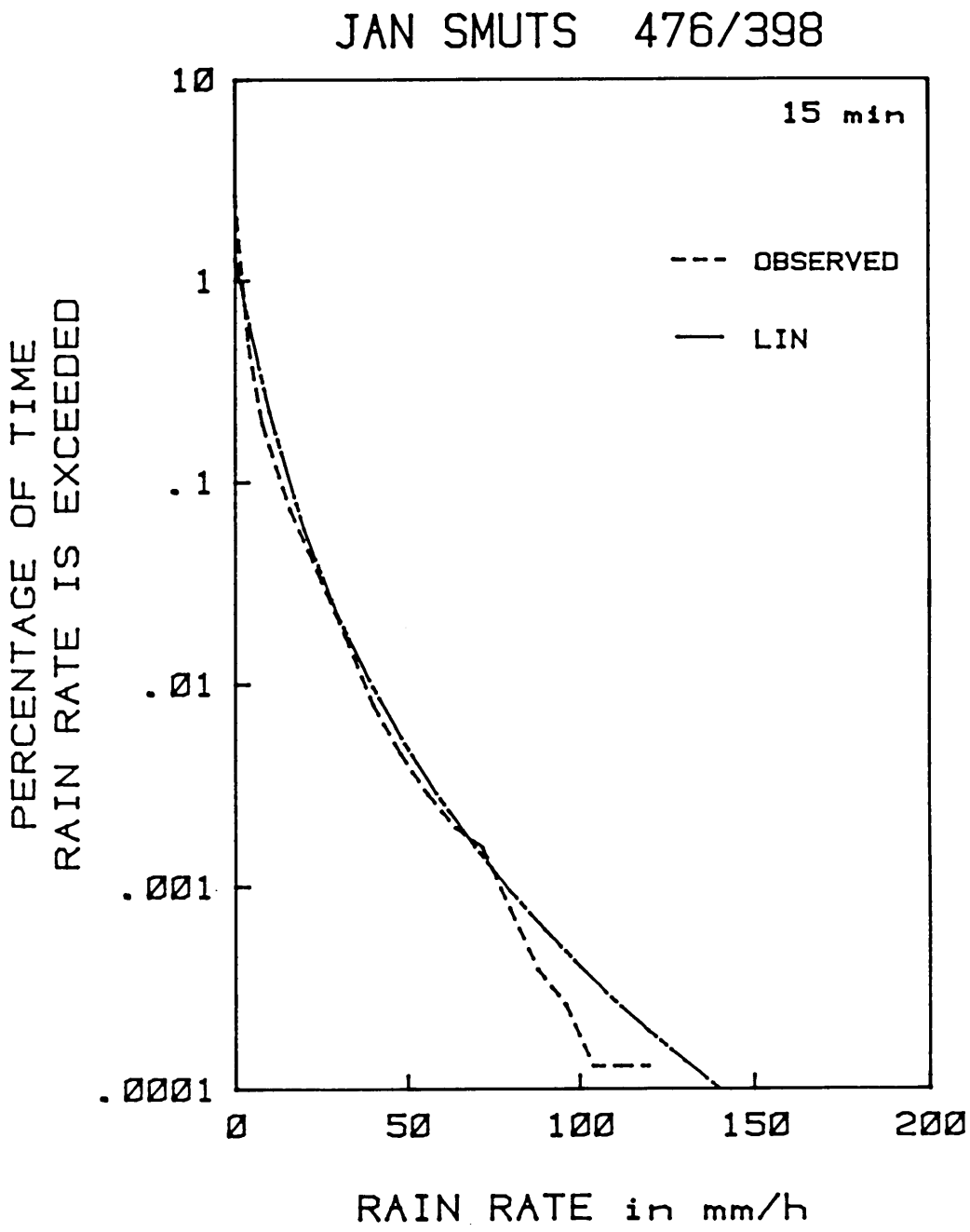

Fig. 11 Rain-rate distributions of 15-min integration time as observed and as calculated by Lin's method, for Jan Smuts Airport, Johannesburg.

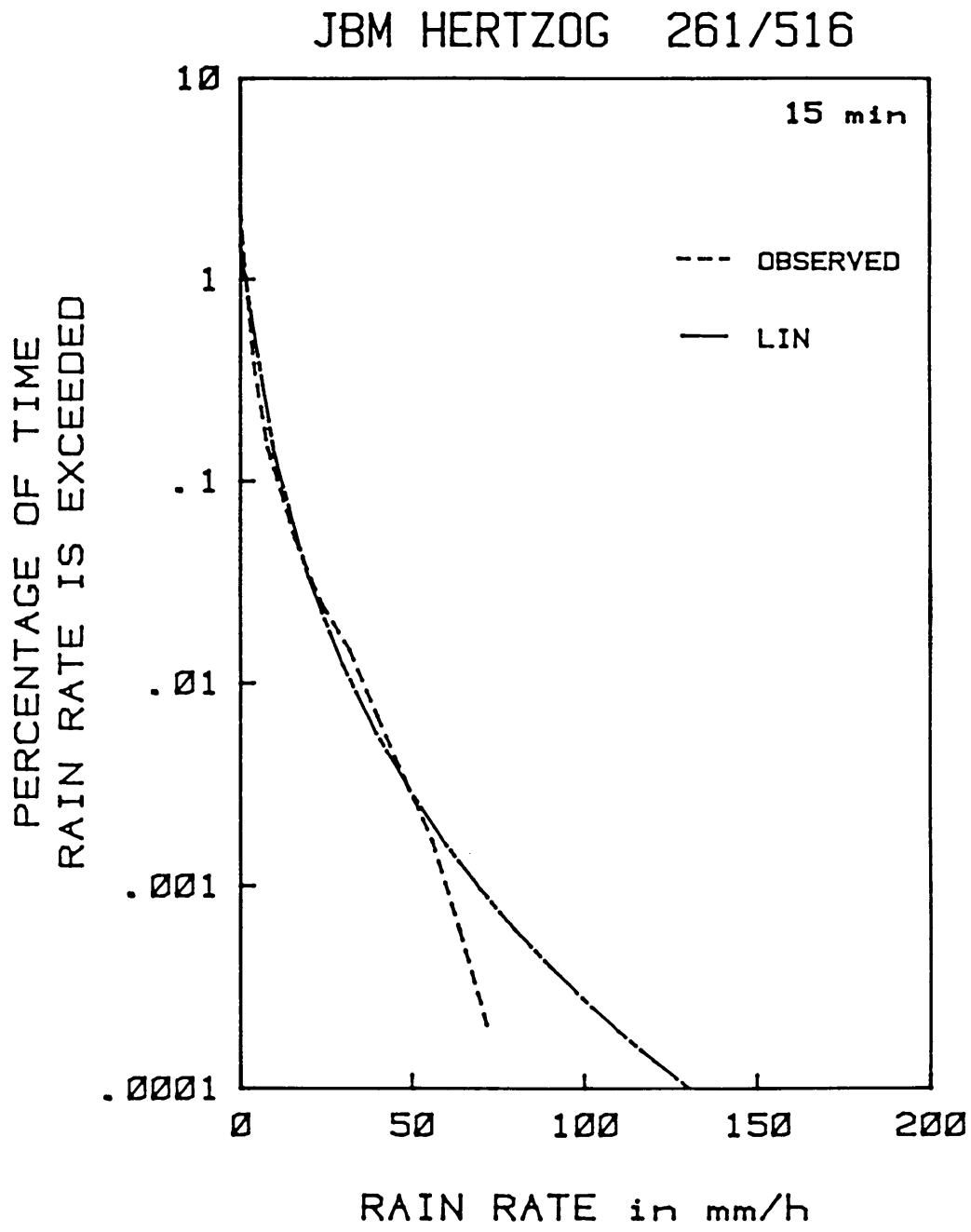

Fig. 12 Rain-rate distributions of 15-min integration time as observed and as calculated by Lin's method, for JBM Hertzog Airport, Bloemfontein.

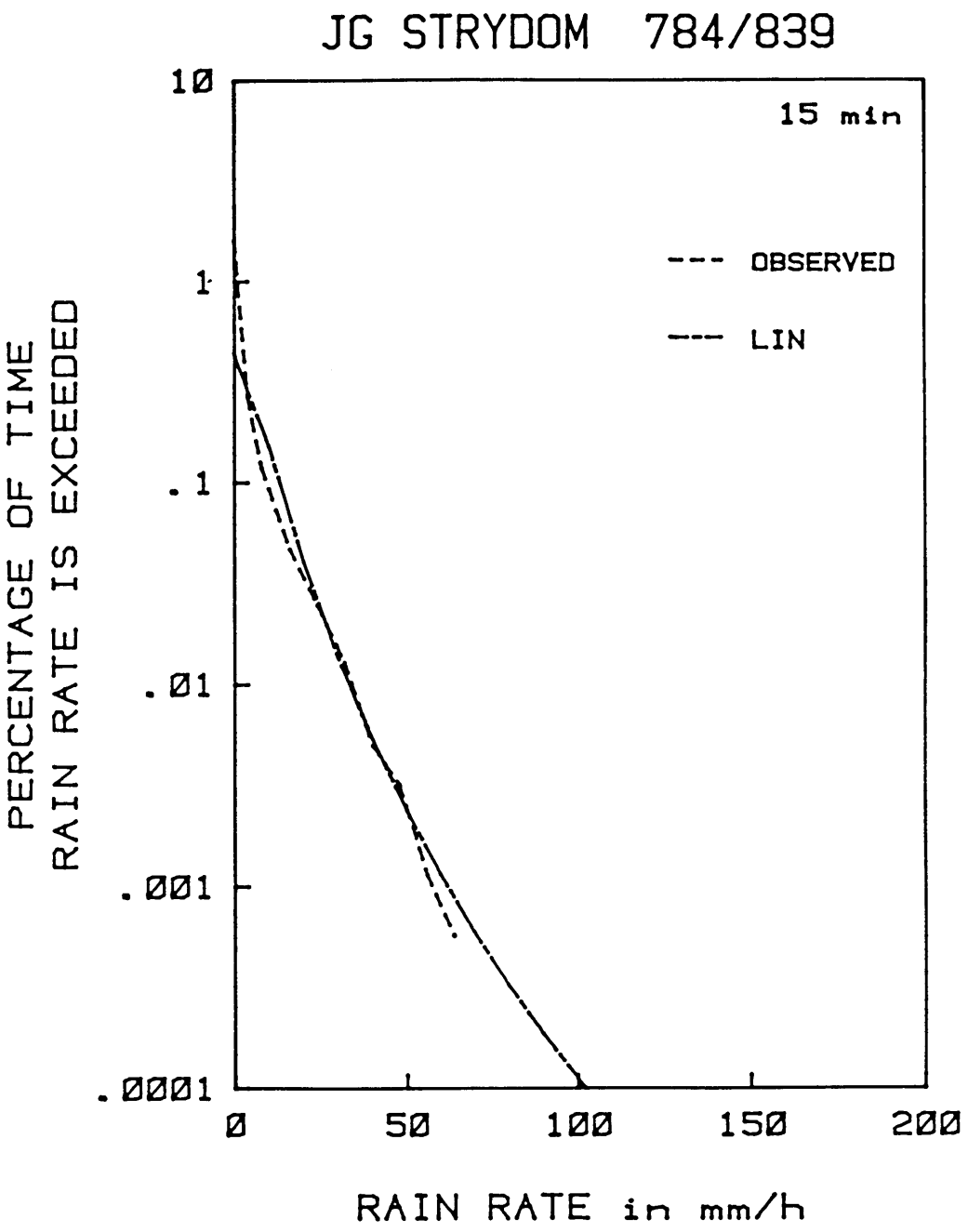

Fig. 13 Rain-rate distributions of 15-min integration time as observed and as calculated by Lin's method, for JG Strydom Airport, Windhoek, South West Africa.

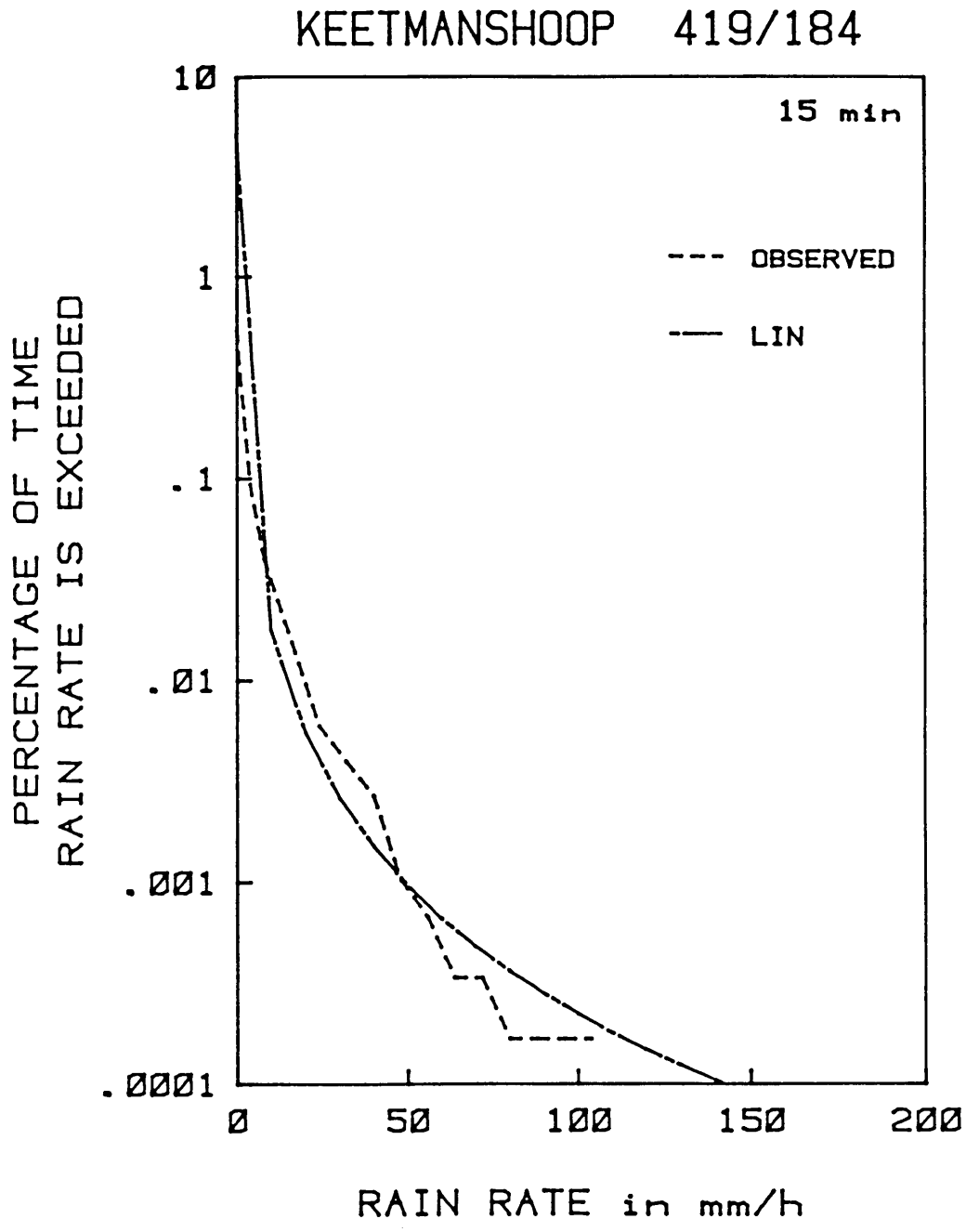

Fig. 14 Rain-rate distributions of 15-min integration time as observed and as calculated by Lin's method, for Keetmanshoop, South West Africa.

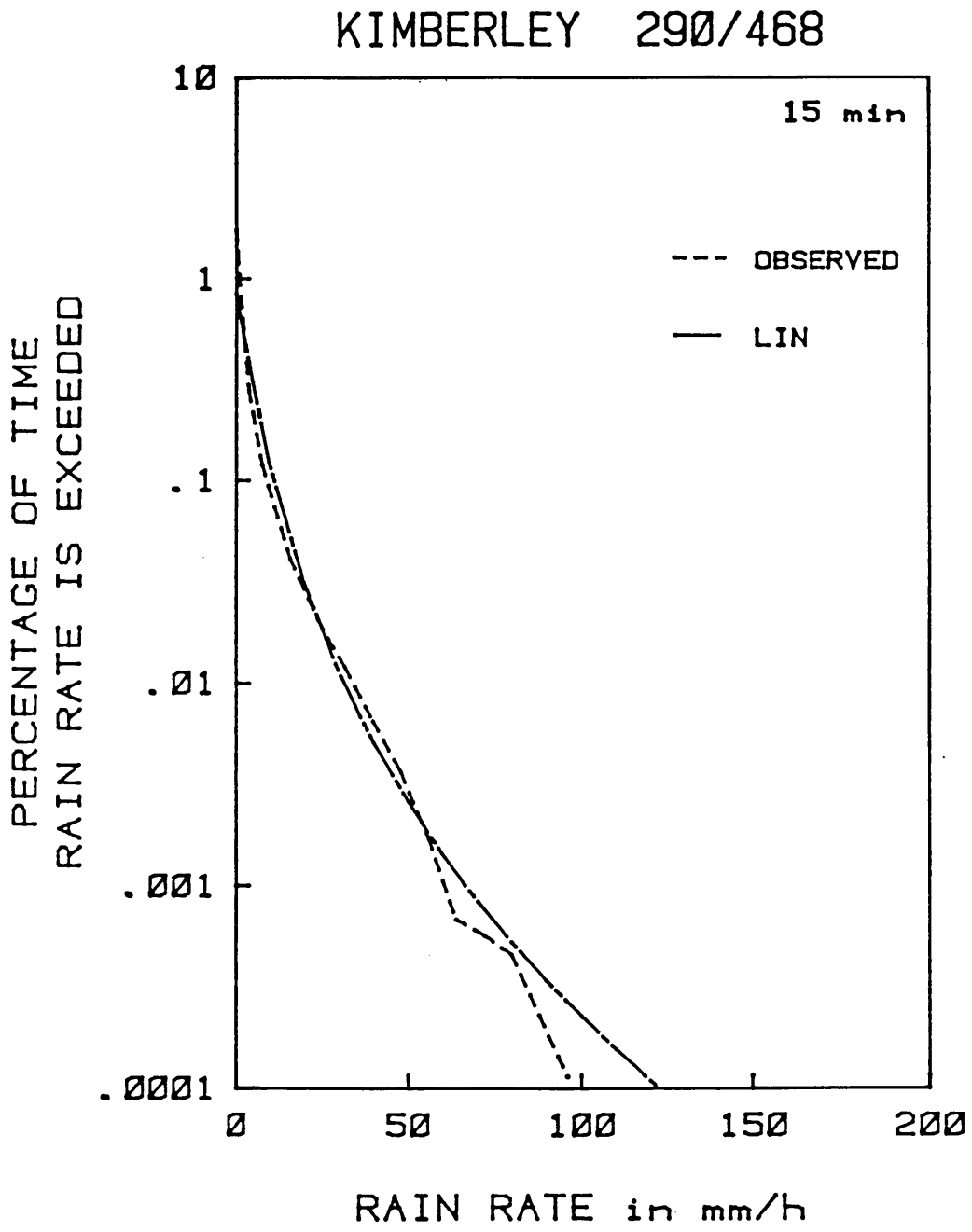

Fig. 15 Rain-rate distributions of 15-min integration time as observed and as calculated by Lin's method, for Kimberley.

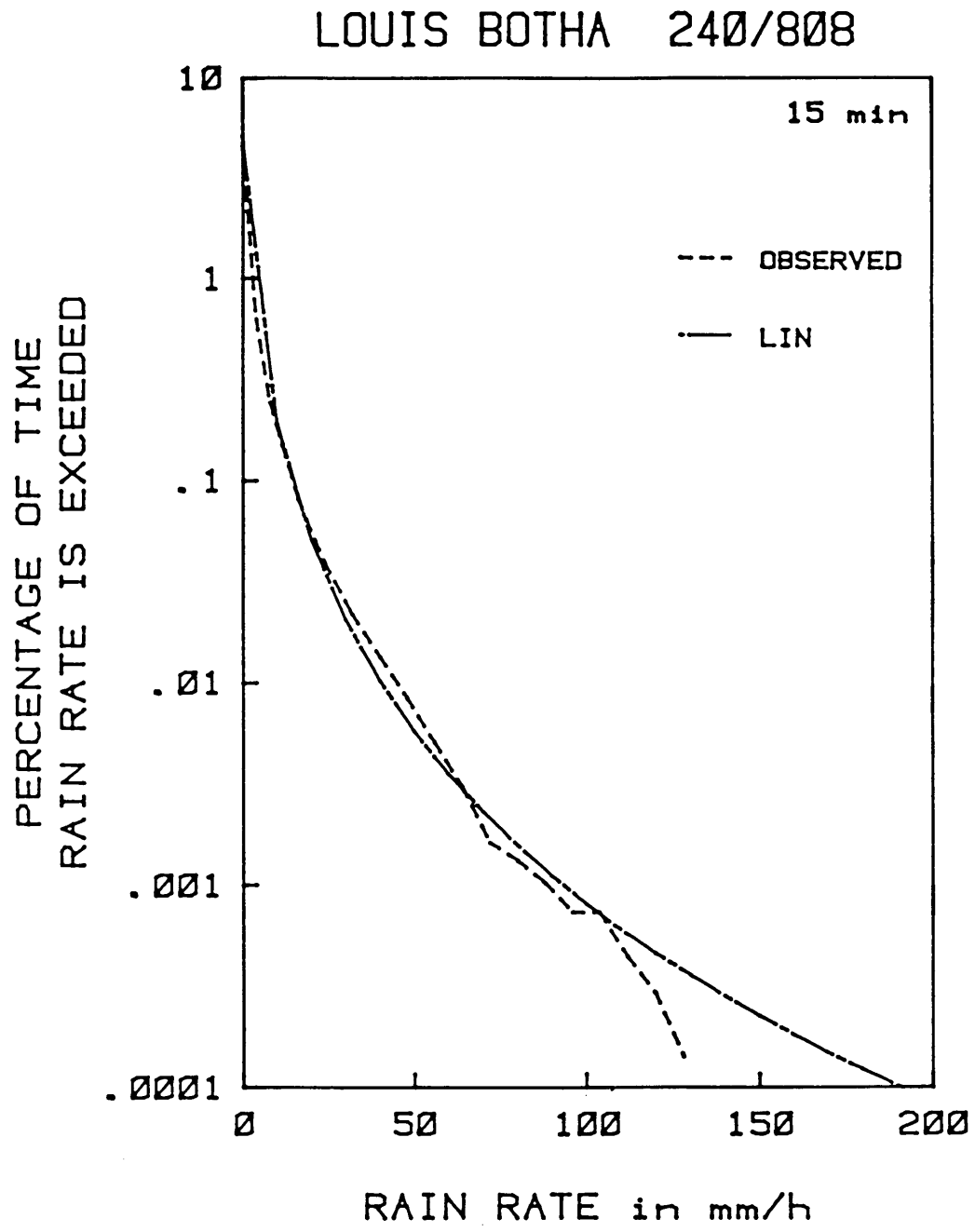

Fig. 16 Rain-rate distributions of 15-min integration time as observed and as calculated by Lin's method, for Louis Botha Airport, Durban.

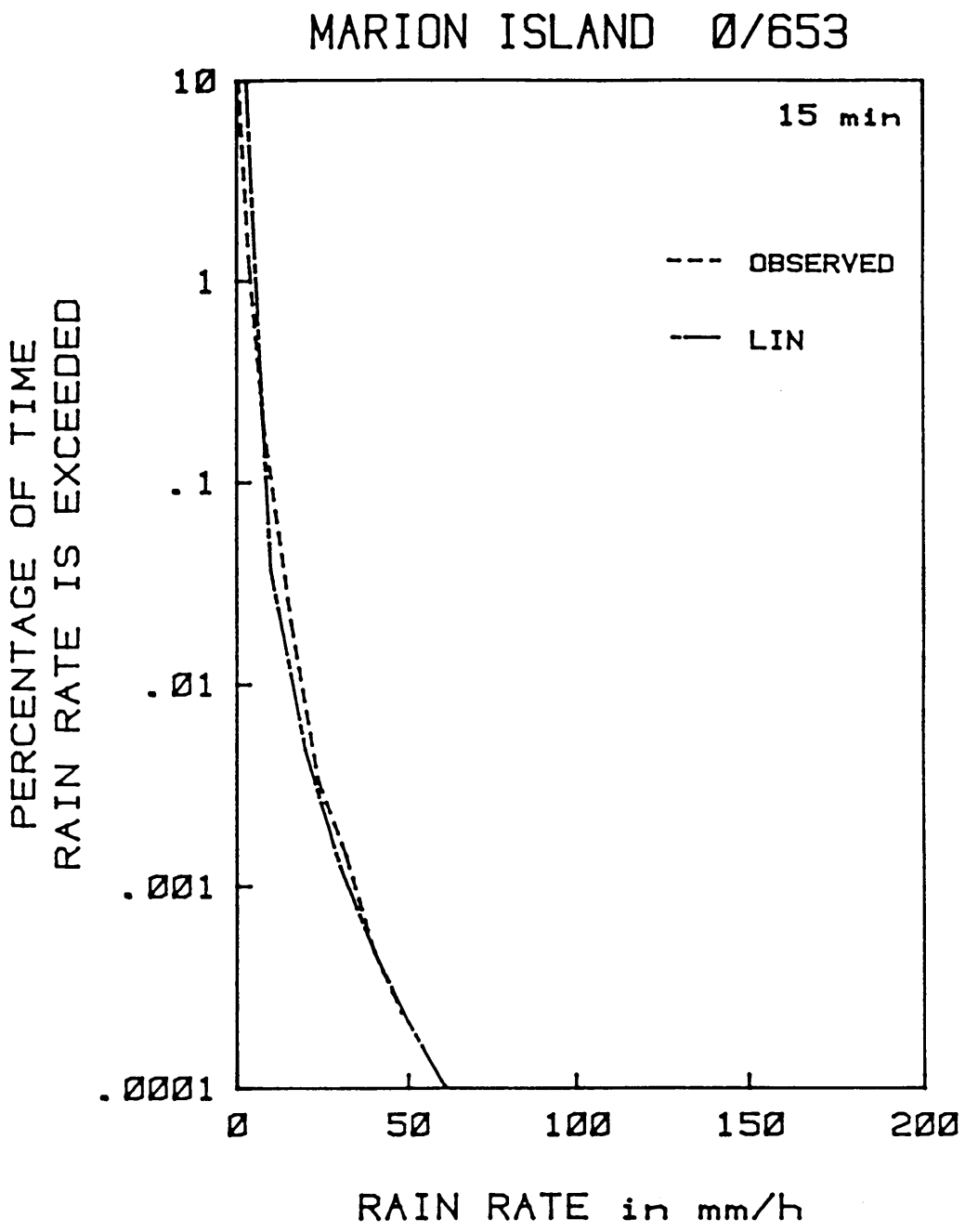

Fig. 17 Rain-rate distributions of 15-min integration time as observed and as calculated by Lin's method, for Marion Island, South Indian Ocean.

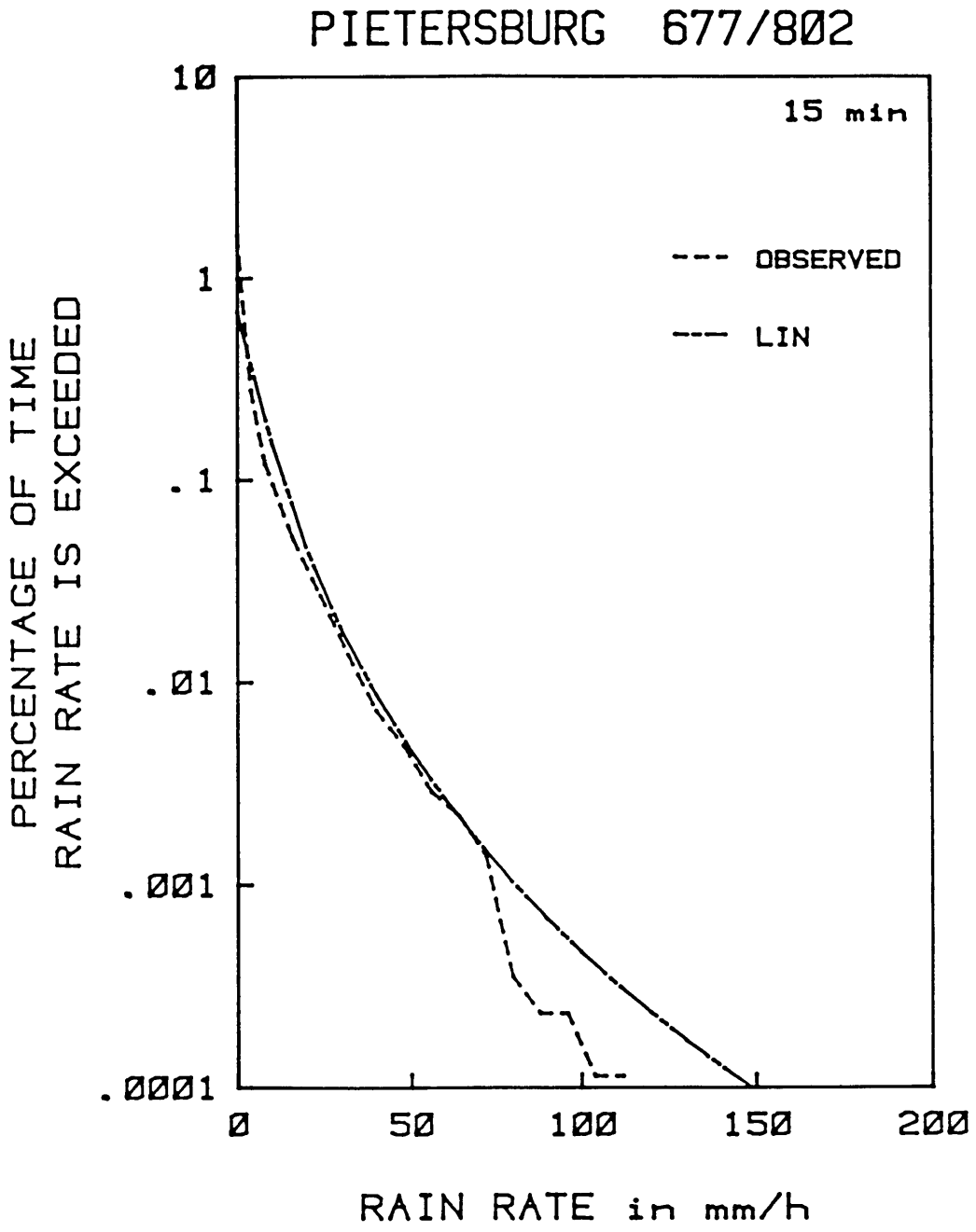

Fig. 18 Rain-rate distributions of 15-min integration time as observed and as calculated by Lin's method, for Pietersburg.

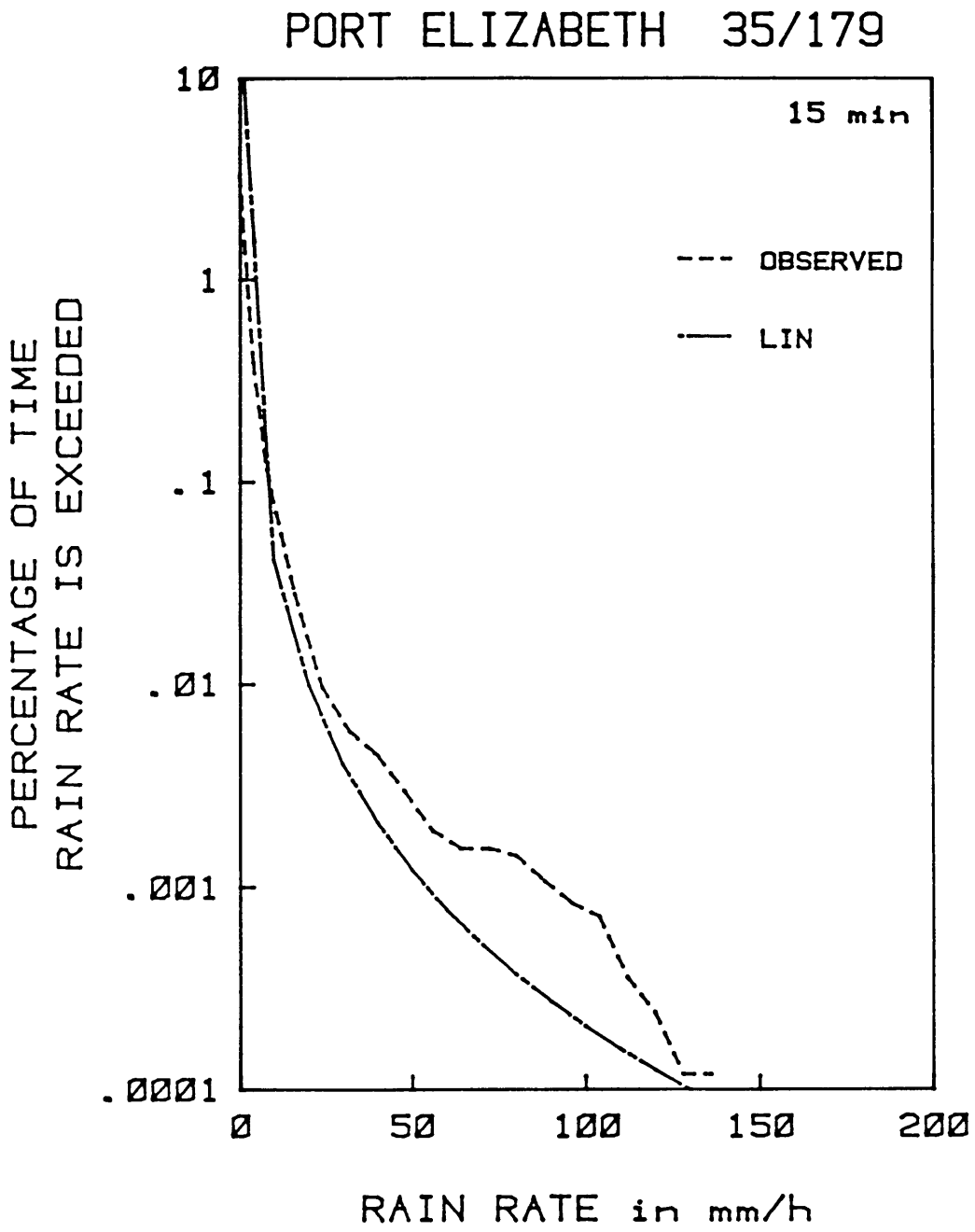

Fig. 19 Rain-rate distributions of 15-min integration time as observed and as calculated by Lin's method, for Port Elizabeth.

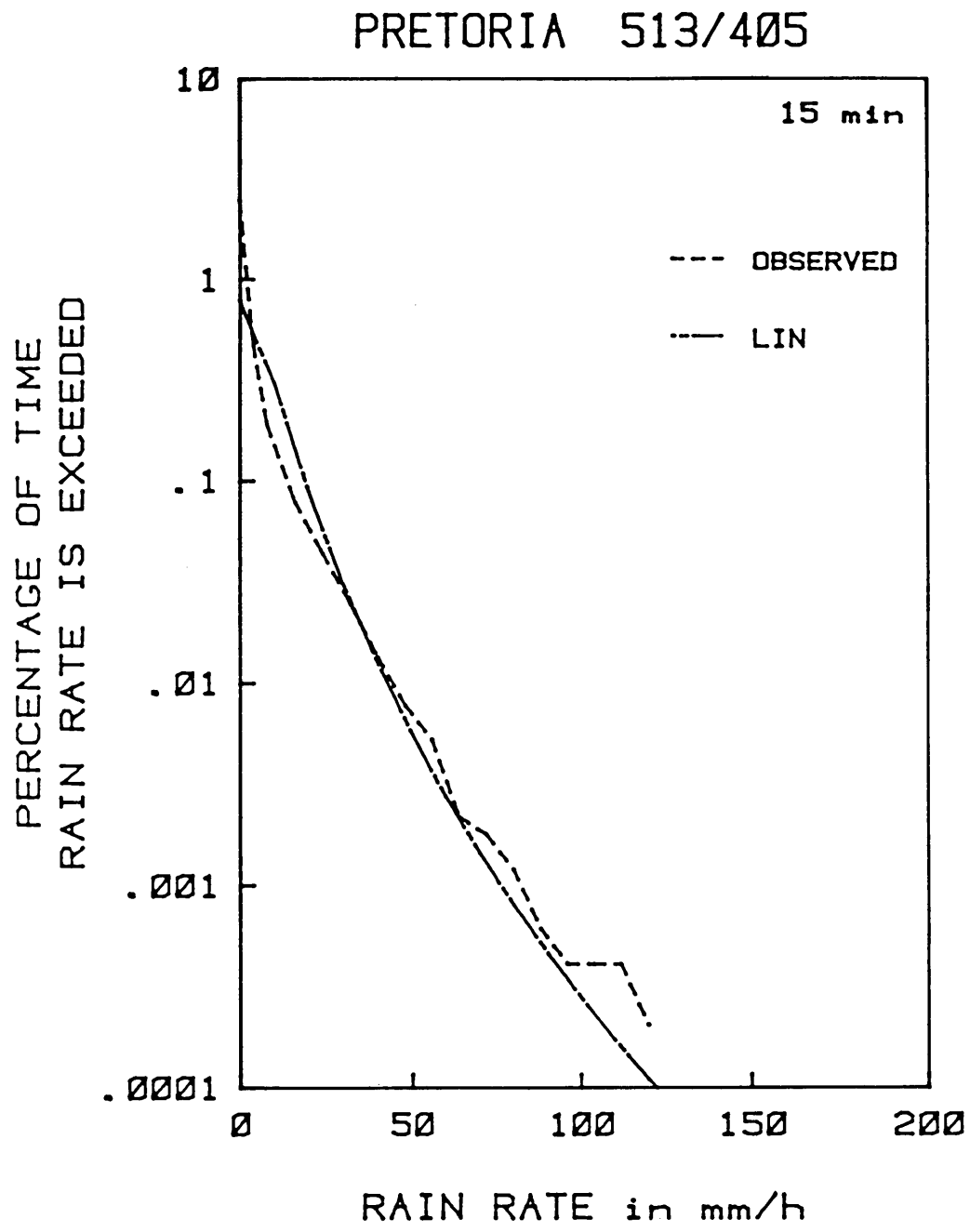

Fig. 20 Rain-rate distributions of 15-min integration time as observed and as calculated by Lin's method, for Pretoria.

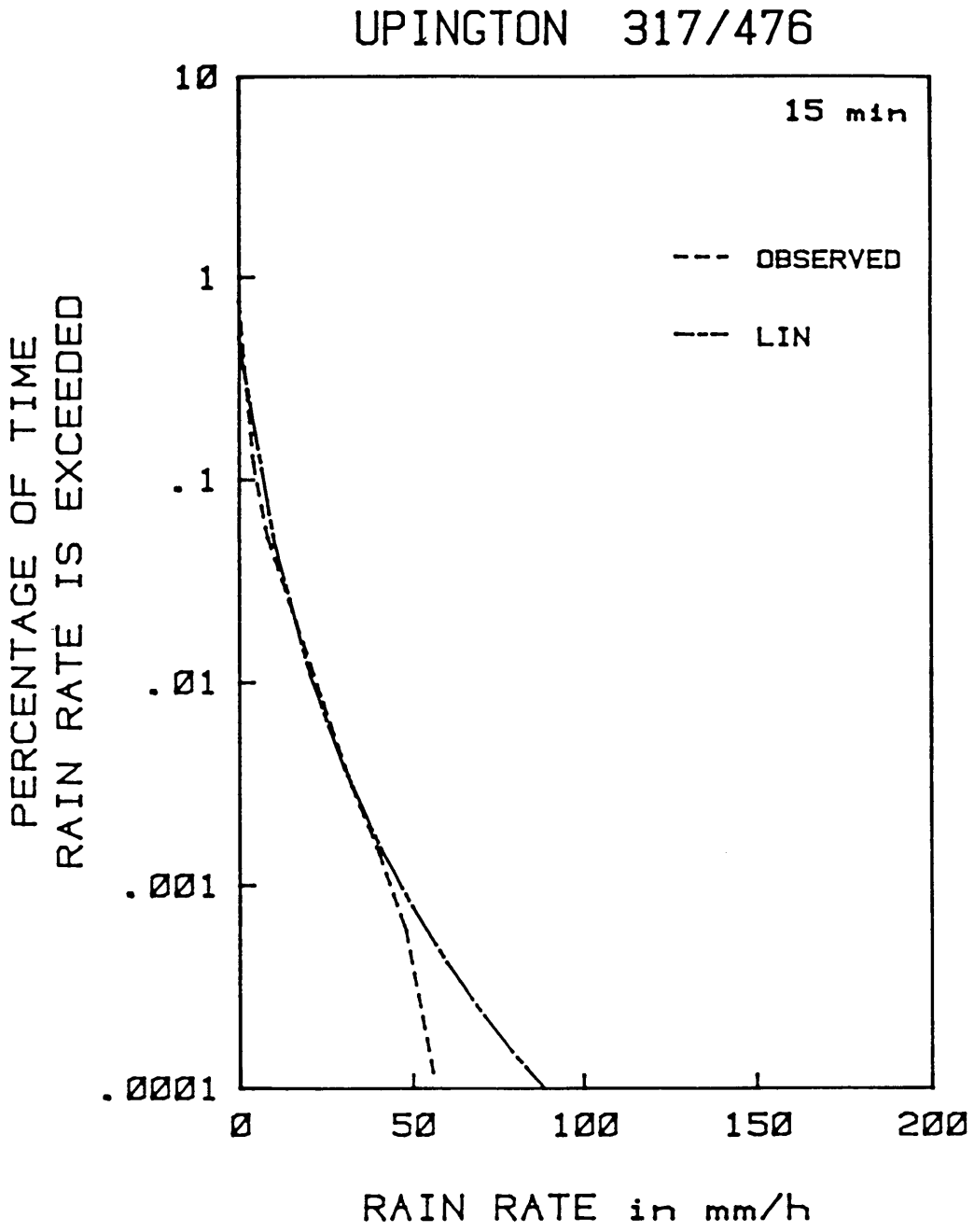

Fig. 21 Rain-rate distributions of 15-min integration time as observed and as calculated by Lin's method, for Upington.

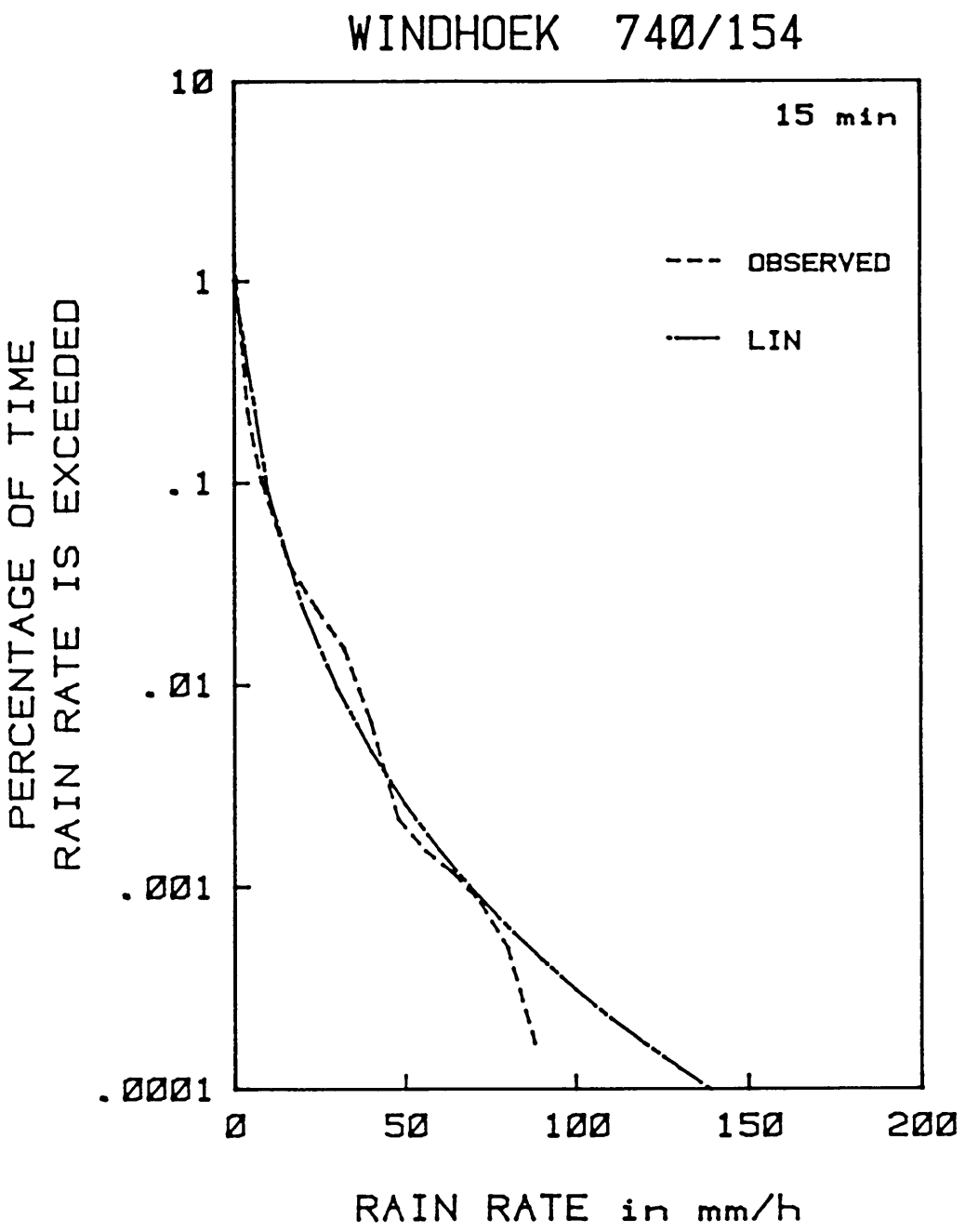

Fig. 22 Rain-rate distributions of 15-min integration time as observed and as calculated by Lin's method, for Windhoek.

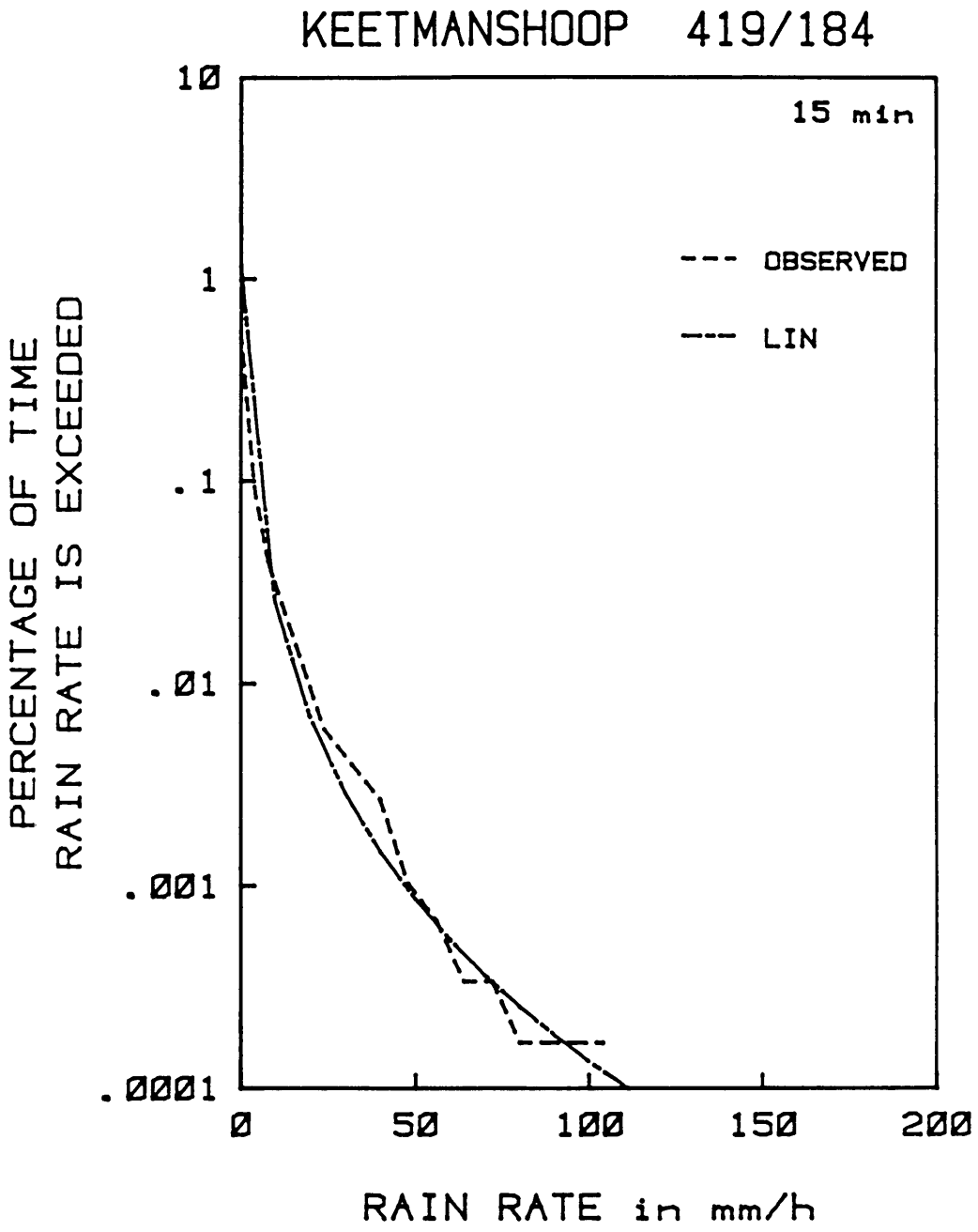

Fig. 23 Calculated 15-min distribution for Keetmanshoop using modified value of α (α=2,25).

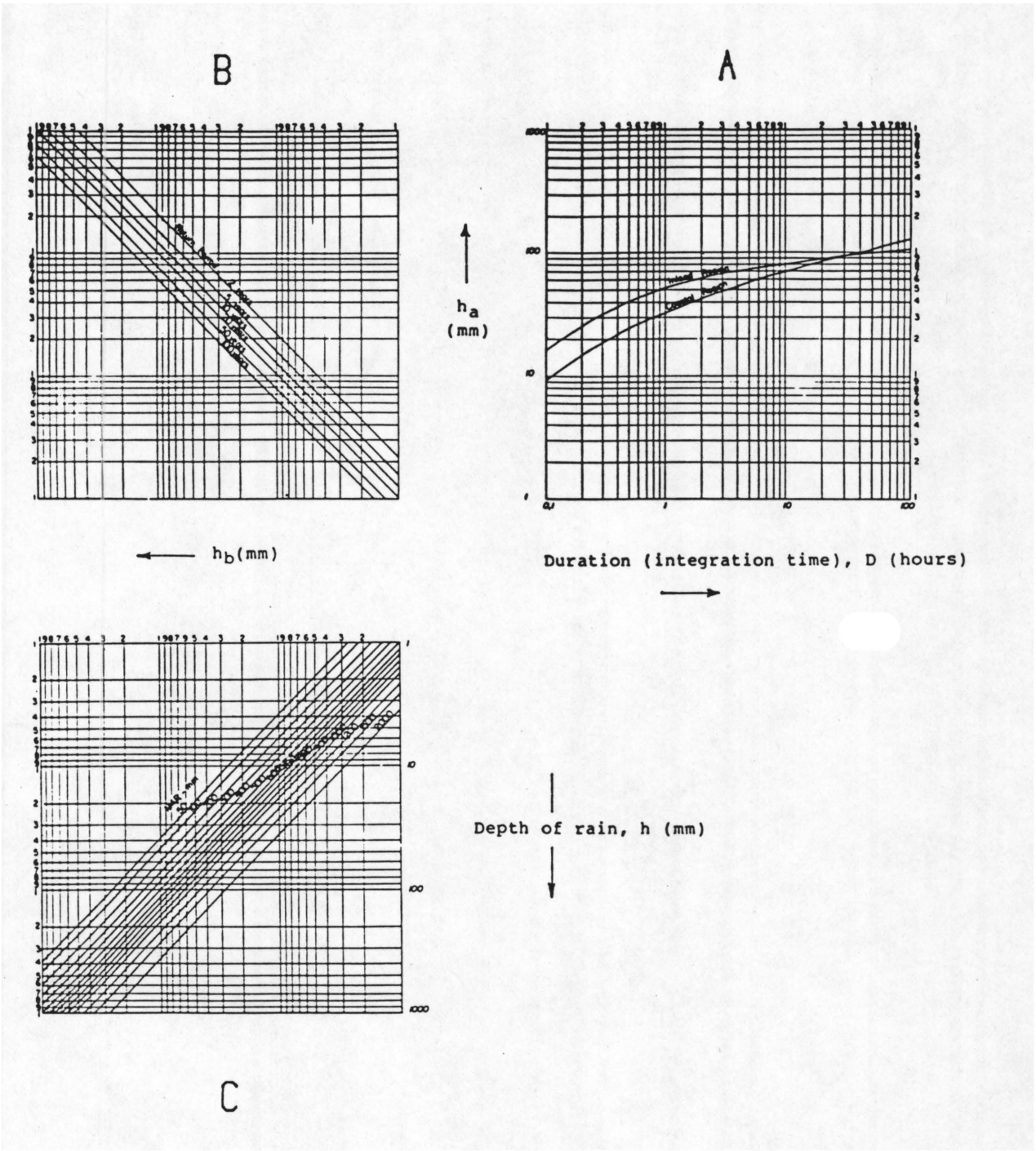

Fig. 24 Midgley & Pitman depth-duration-frequency diagram for point rainfall in Southern Africa. The quantity h in quadrant C is the depth of rain in a D-hour interval to be exceeded with the return period as specified, at a location with mean annual rainfall and climatic region as specified (Courtesy of Midgley and Pitman [1978]).

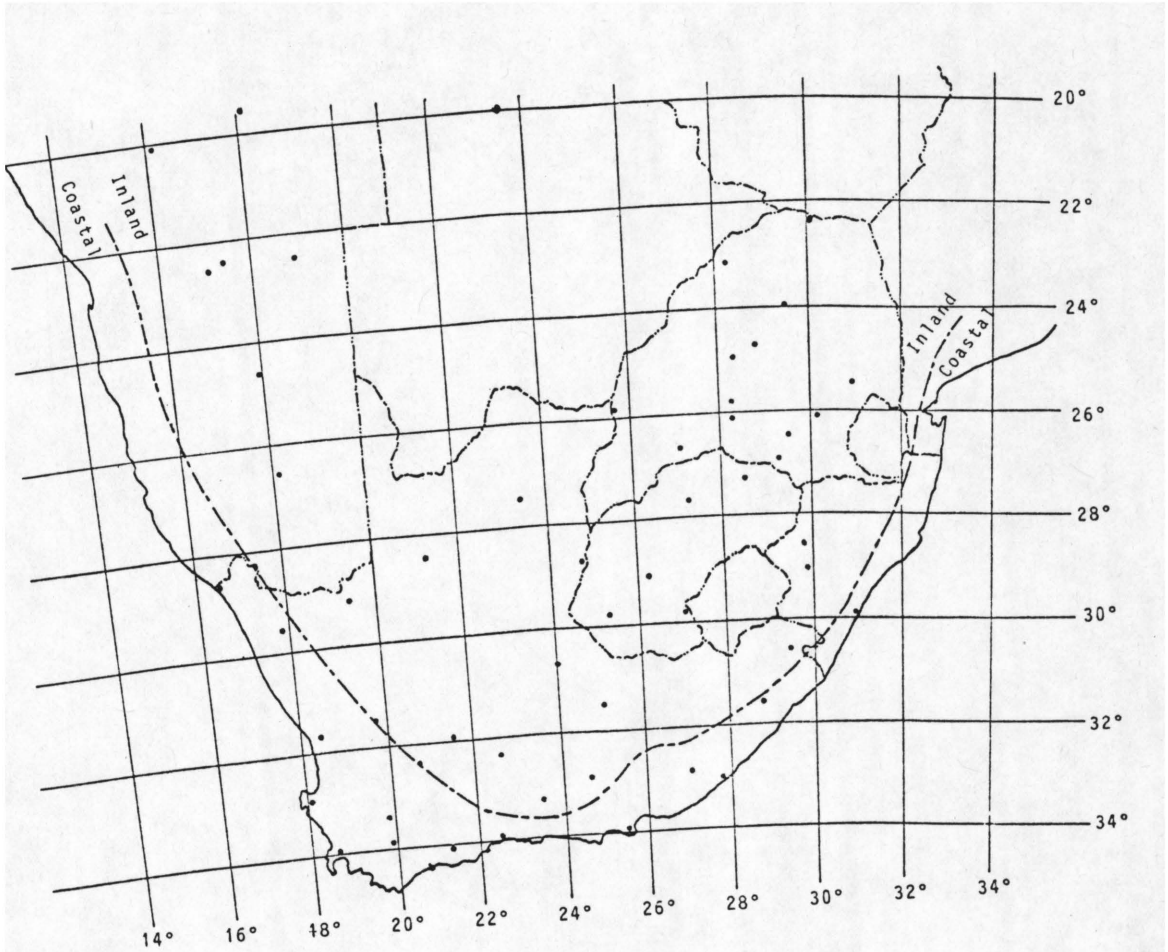

Fig. 25 Map showing location of autographic rainfall stations used in DDF diagram of Midgley and Pitman [1978]. Also shown is a delineation of the climatic regions of 'coastal' and 'inland' by Op ten Noort and Stephenson [1982]. Other details of the stations are given in Table 1.

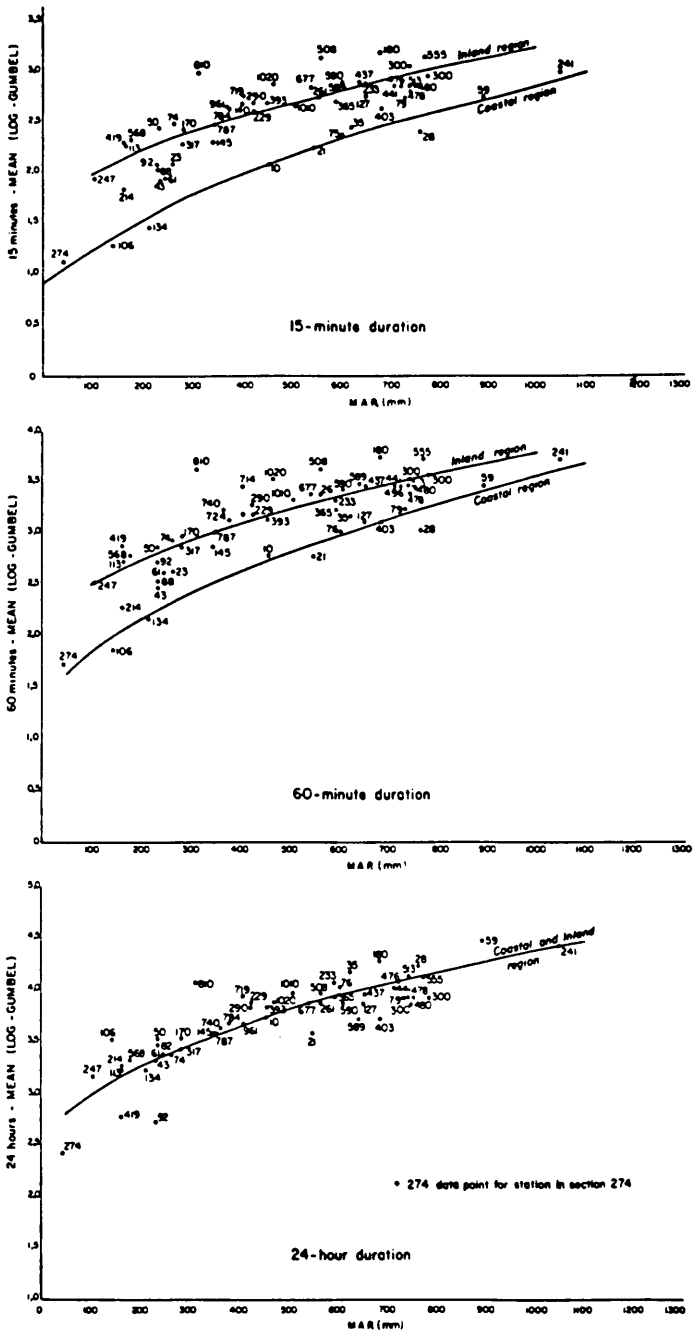

Fig. 26 Relationship between MAR and mean of log-Gumbel distribution, μ. (Courtesy of Midgley and Pitman [1978])

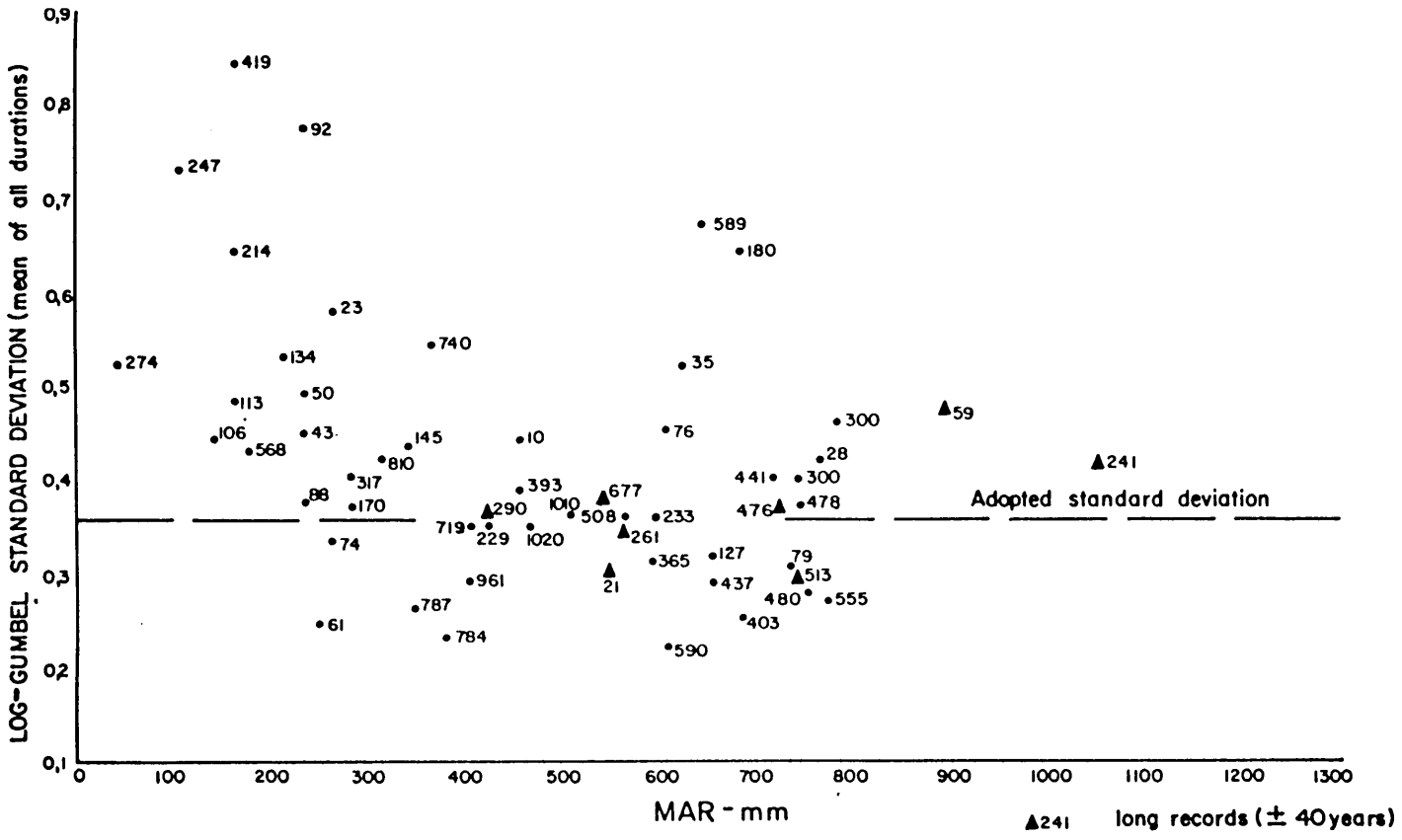

Fig. 27 Relationship between standard deviation and MAR. (Courtesy of Midgley and Pitman [1978])

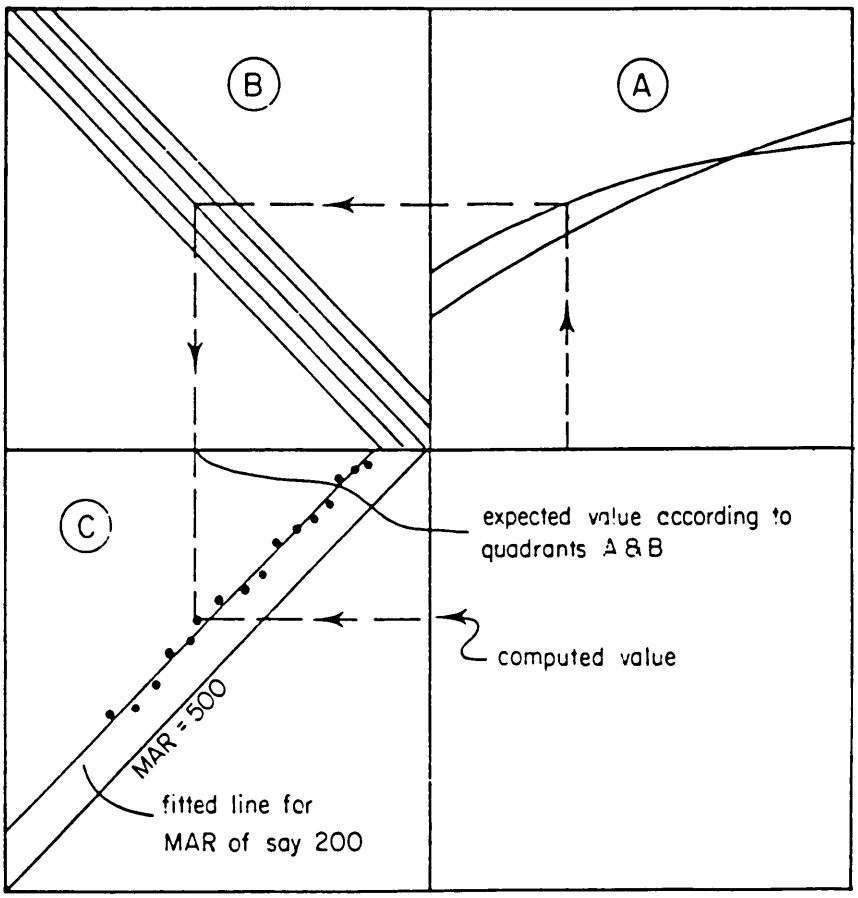

Fig. 28 Method of construction of Midgley-&-Pitman DDF diagram. (Courtesy of Midgley and Pitman [1978])

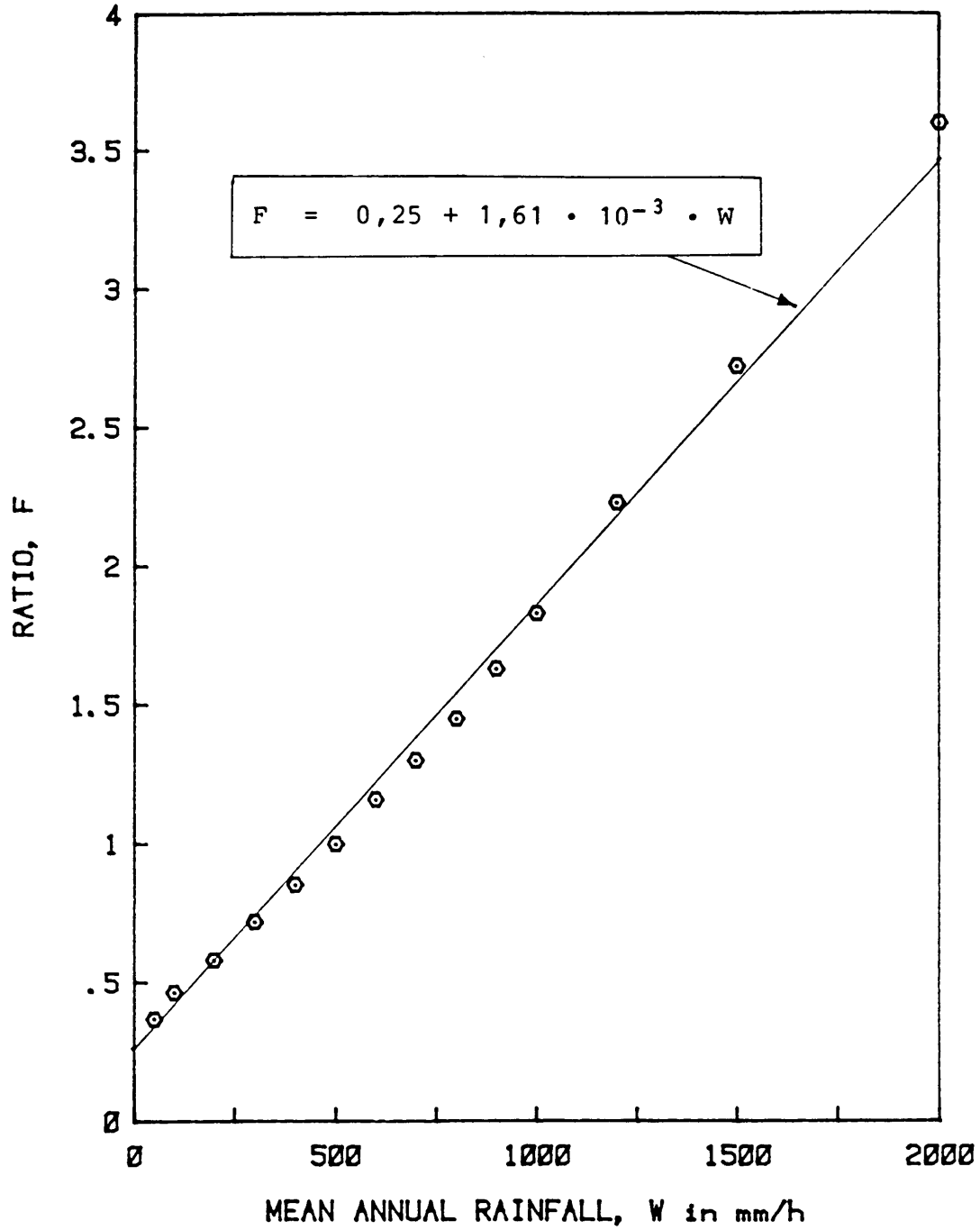

Fig. 29 Straight-line approximation for ratio between rainfall depths of quadrant C.

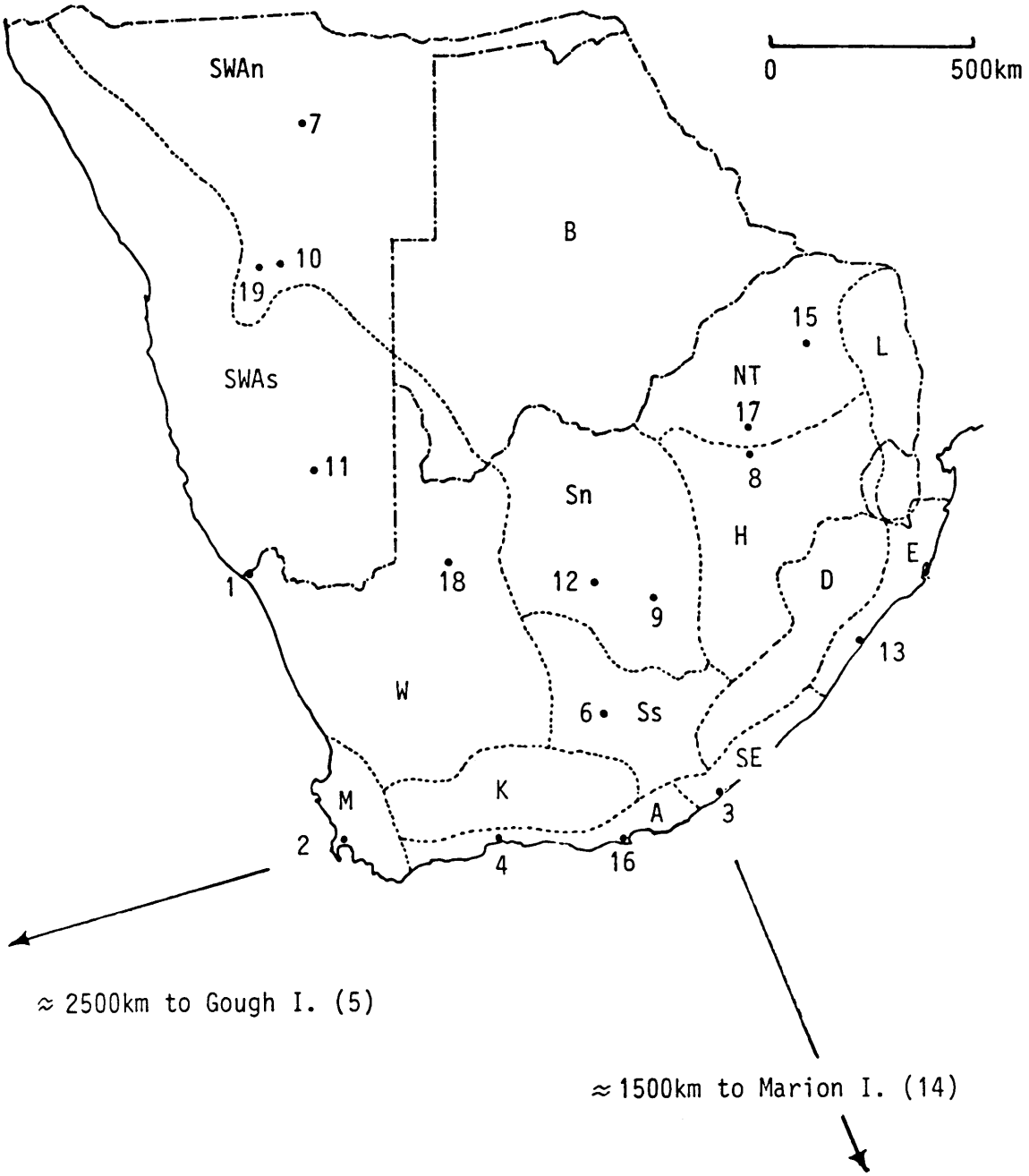

Fig. 30 Map showing location and climatic region of autographic rainfall stations used for evaluation. The numbers refer to Tables 1, 3, 4 and 9. Also given are the climatic regions as defined in Table 8.

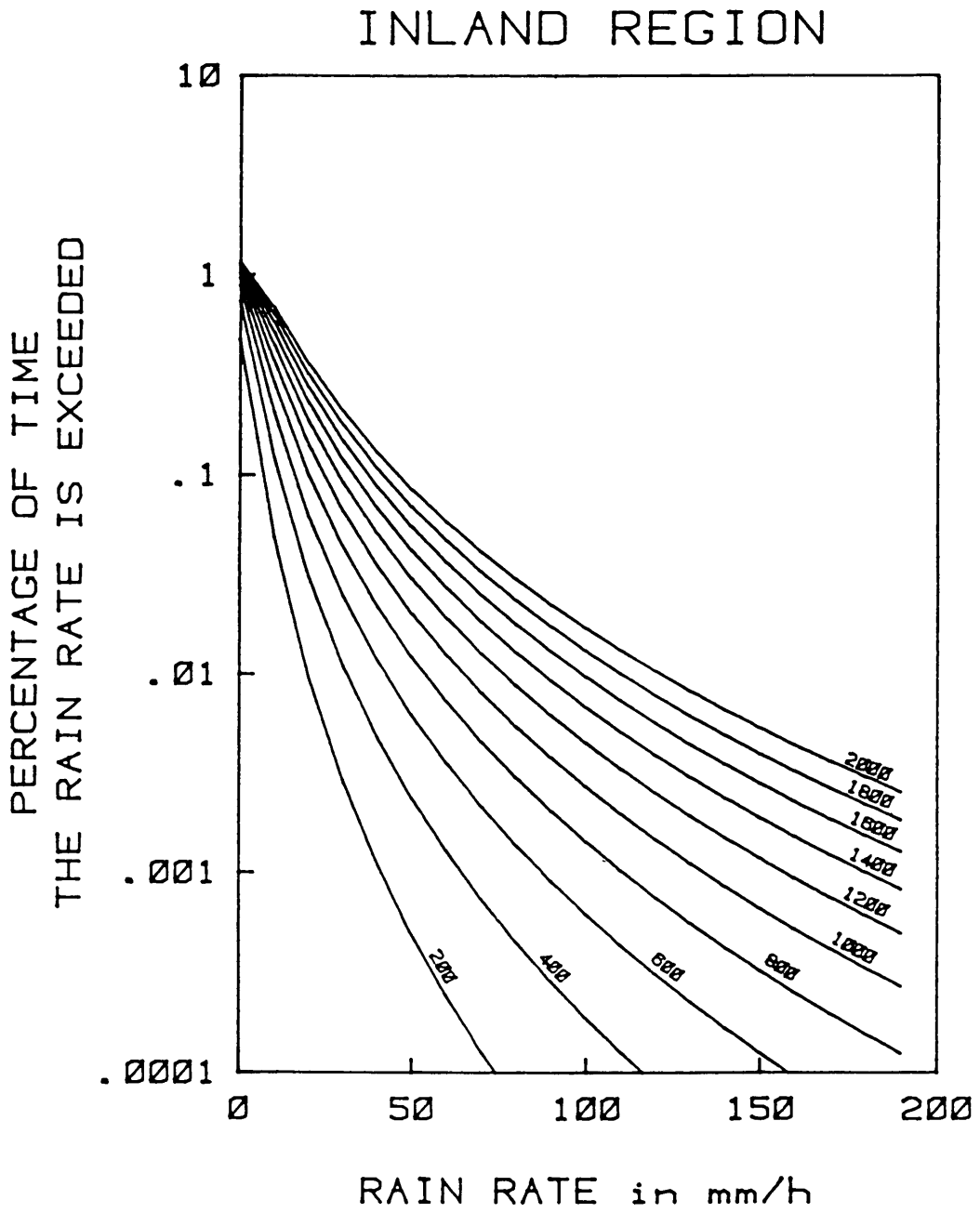

Fig. 31 Five-minute rain rate distributions for the 'inland' region. The variable is MAR (in mm).

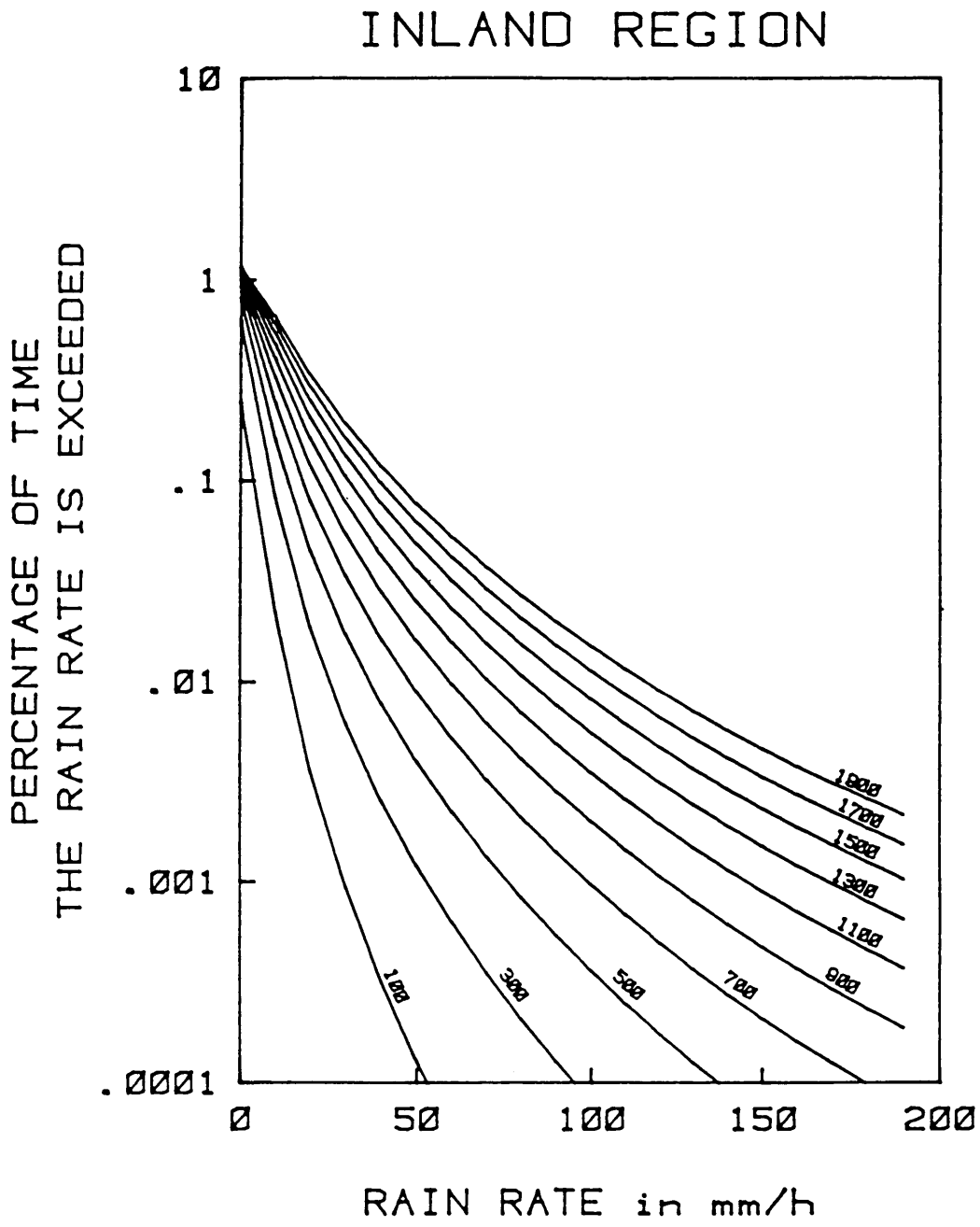

Fig. 32 Five-minute rain-rate distributions for the 'inland' region. The variable is MAR, with values intermediate to those of Fig. 31.

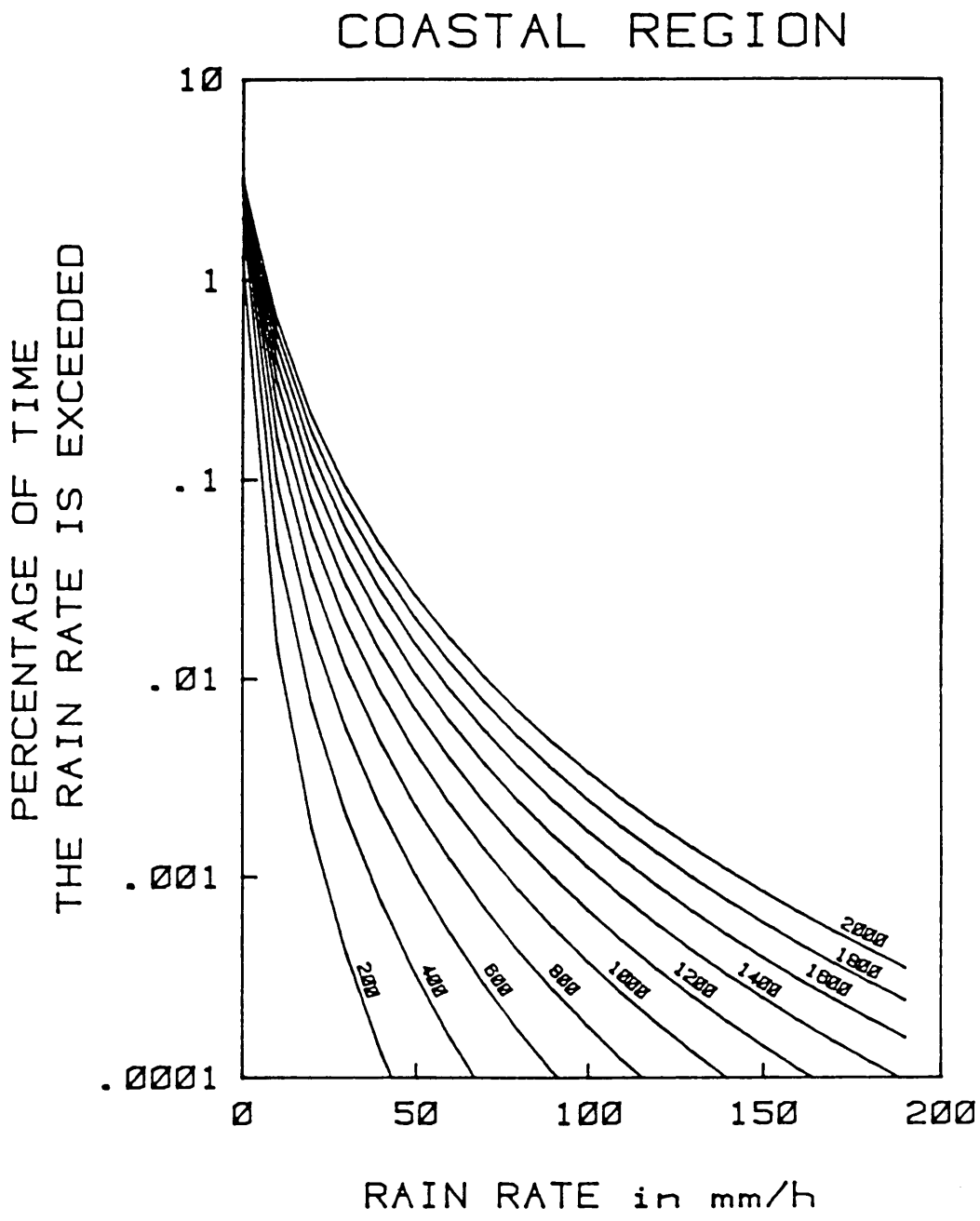

Fig. 33 Five-minute rain-rate distributions for the 'coastal' region. The variable is MAR (in mm).

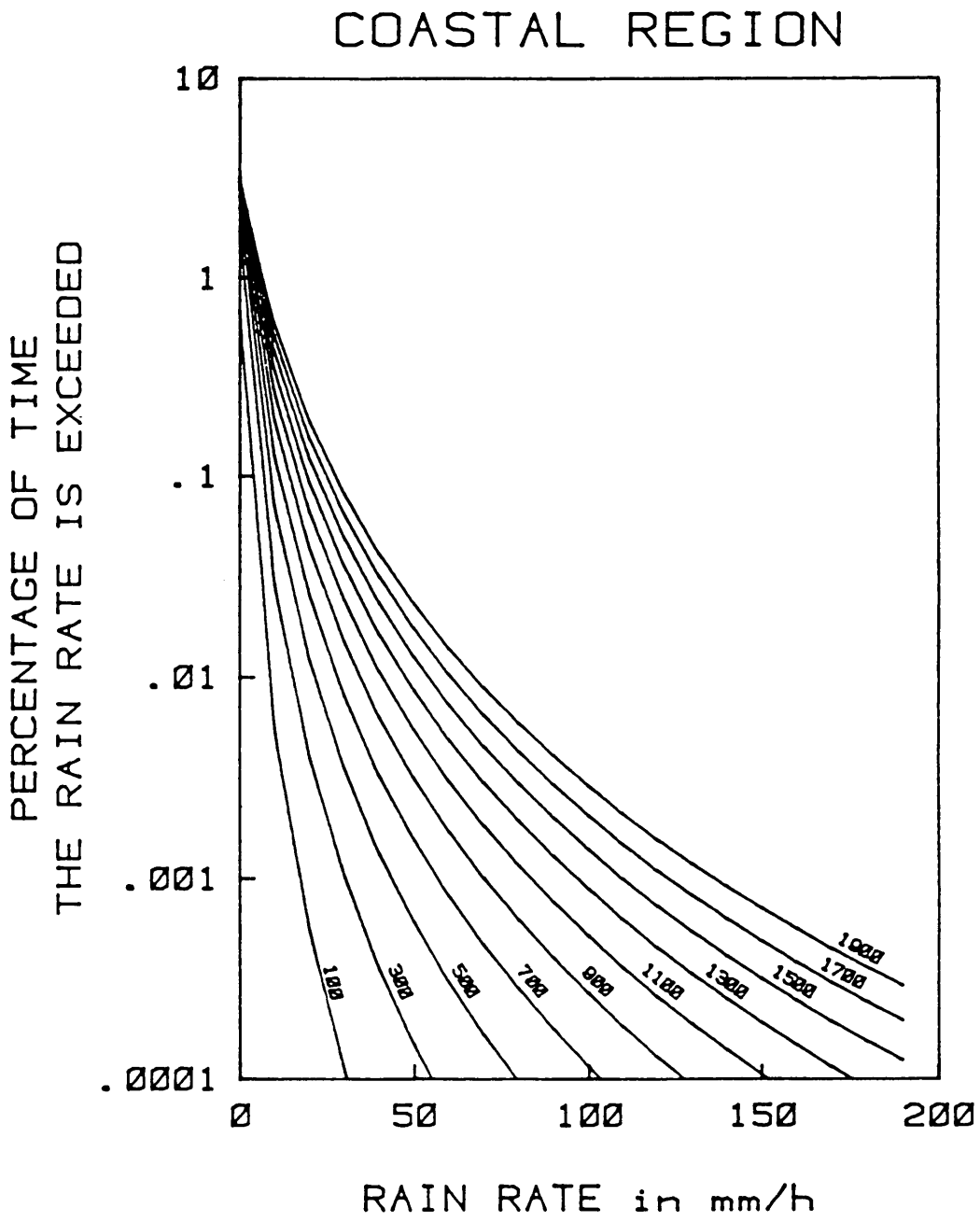

Fig. 34 Five-minute rain-rate distributions for the 'coastal' region. The variable is MAR, with values intermediate to those of Fig. 33.

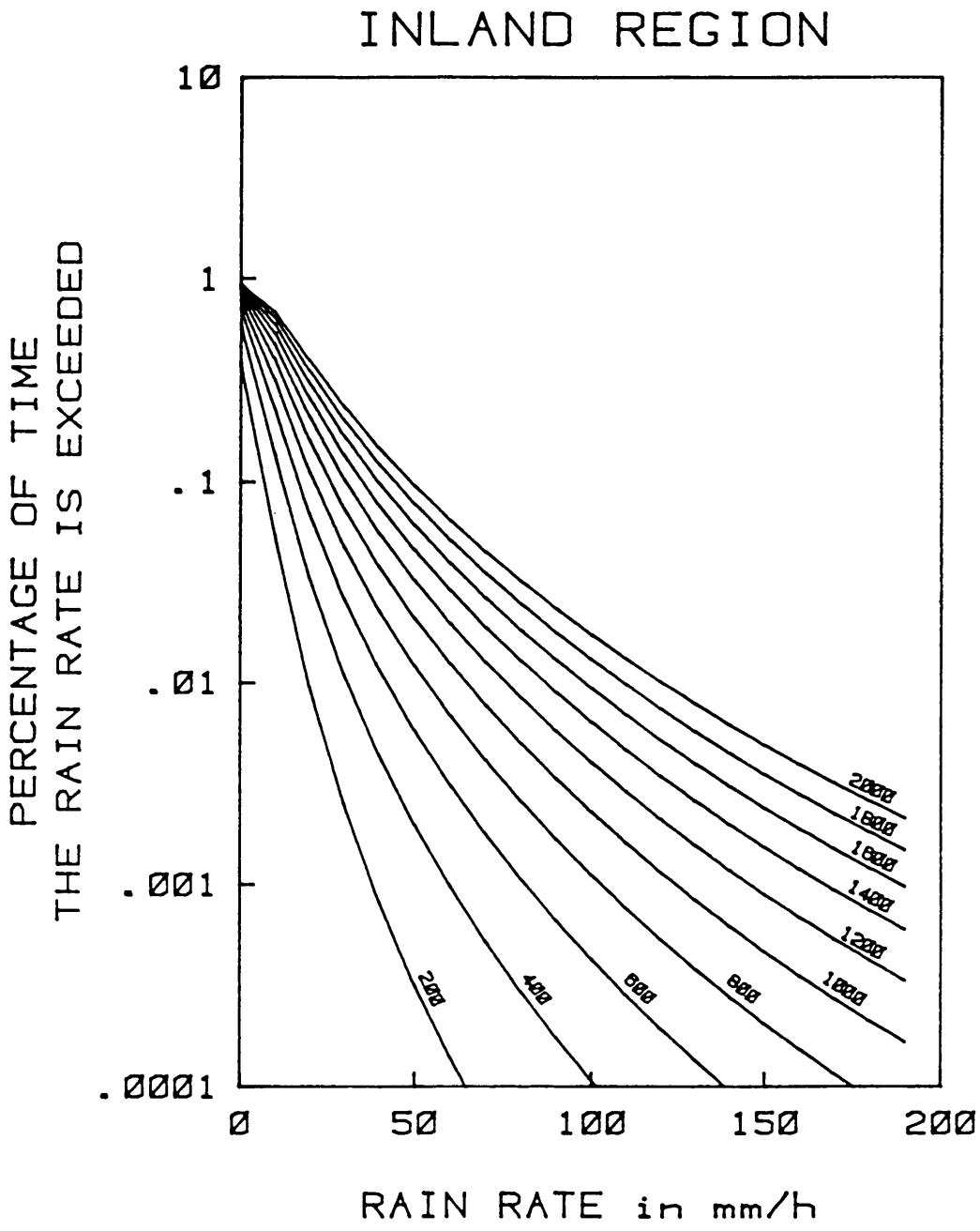

Fig. 35 Fifteen-minute rain-rate distributions for the 'inland' region. The variable is MAR (in mm).

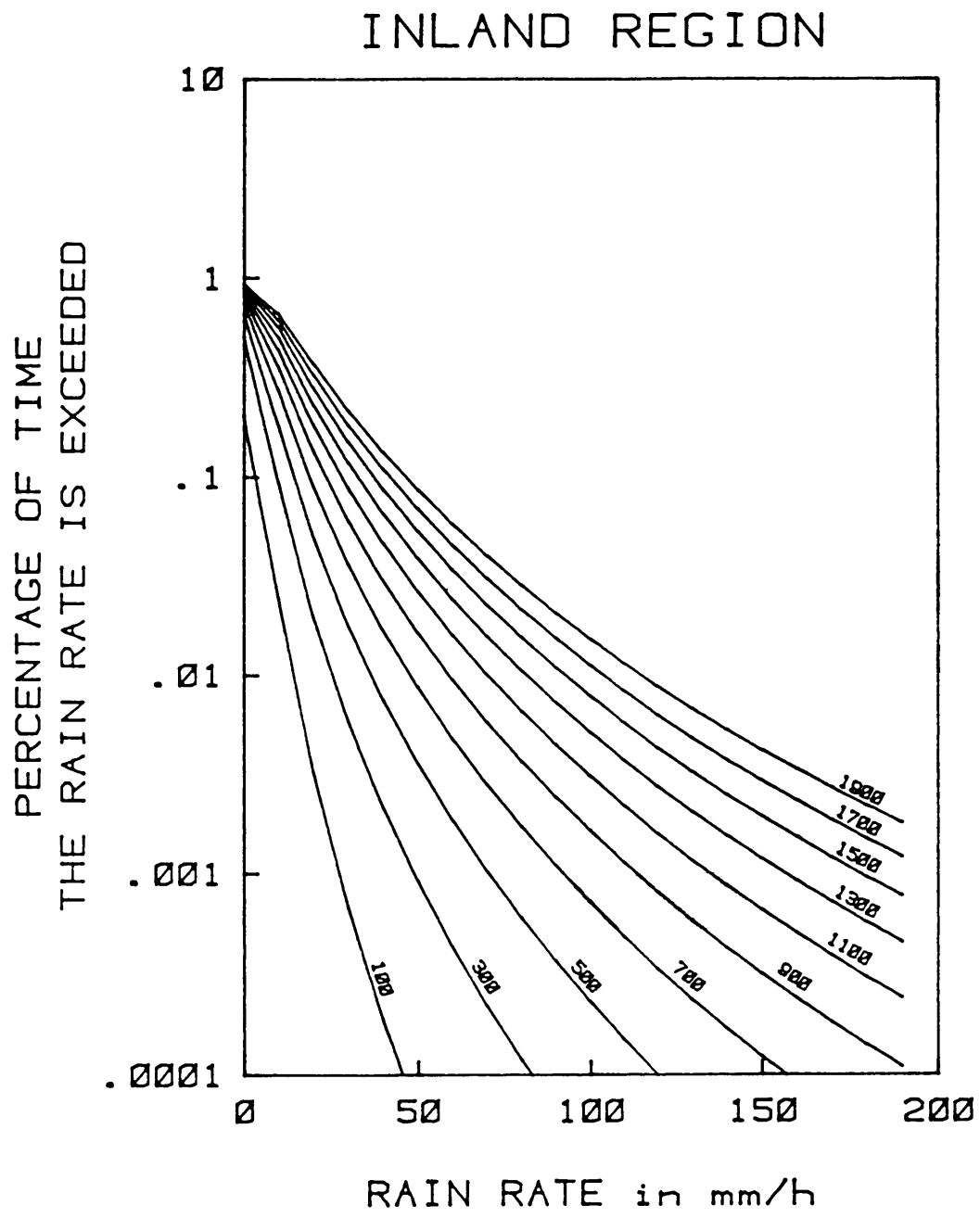

Fig. 36 Fifteen-minute rain-rate distributions for the 'inland' region. The variable is MAR, with values intermediate to those of Fig. 35.

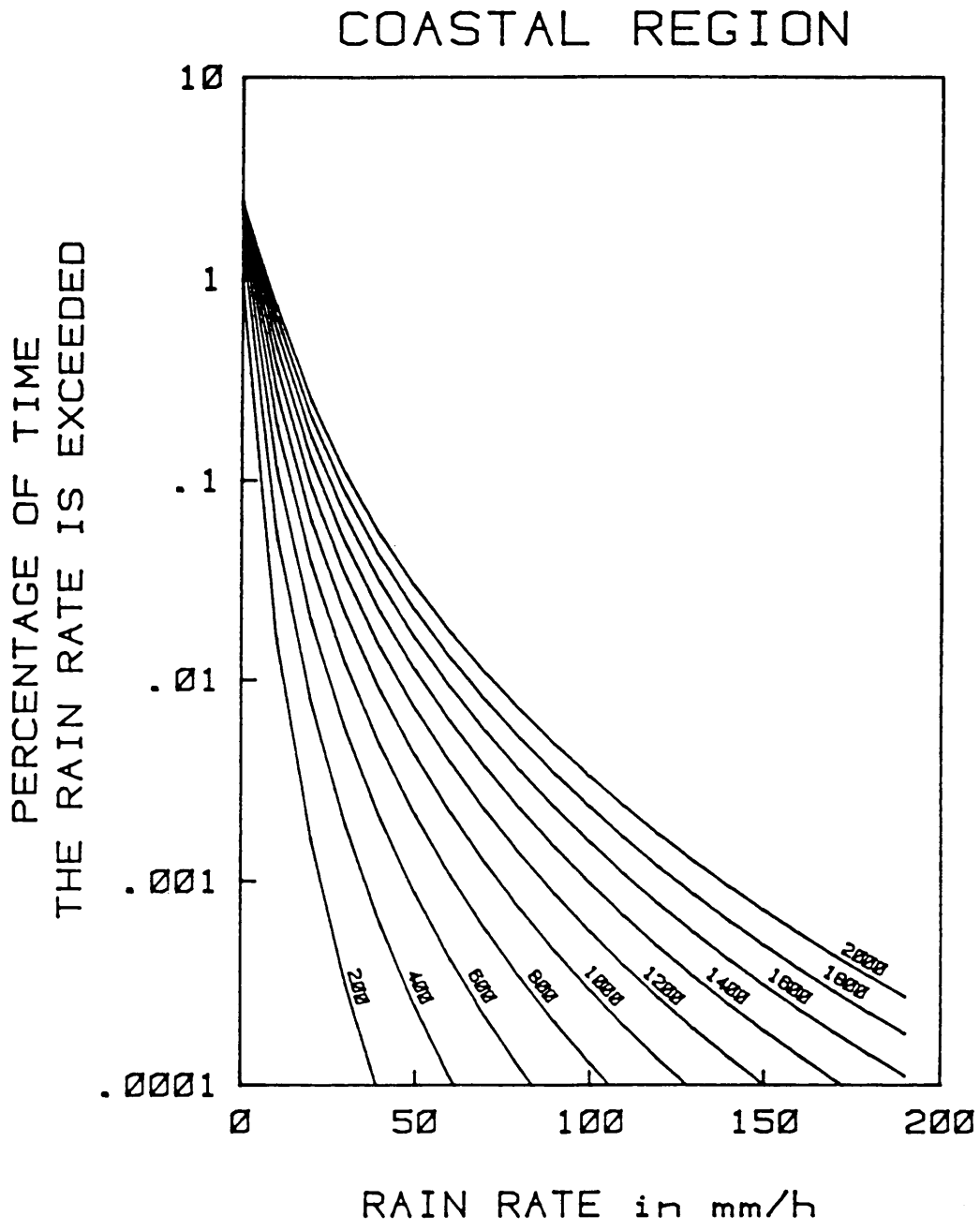

Fig. 37 Fifteen-minute rain-rate distributions for the 'coastal' region. The variable is MAR (in mm).

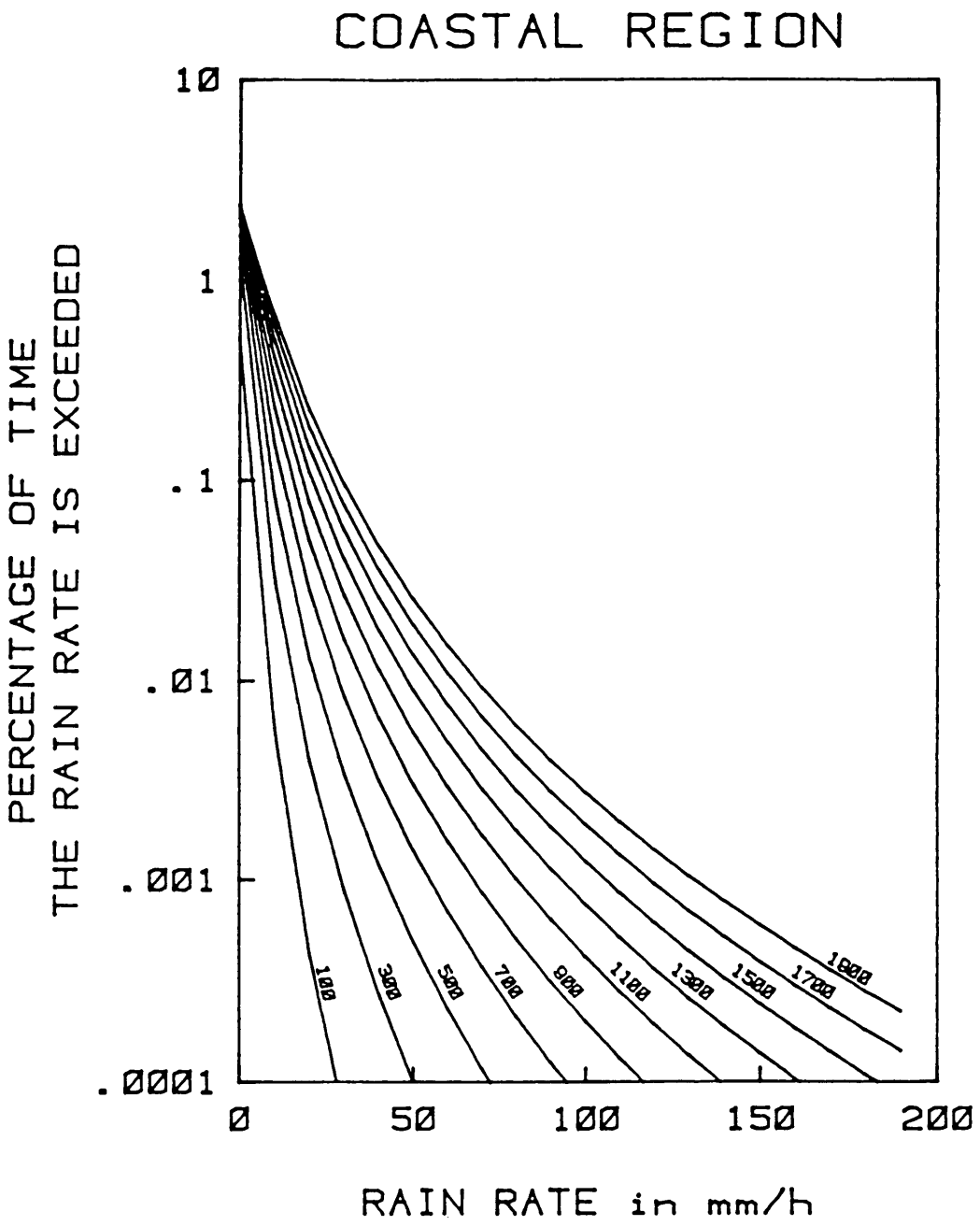

Fig. 38 Fifteen-minute rain-rate distributions for the 'coastal' region. The variable is MAR, with values intermediate to those of Fig. 37.

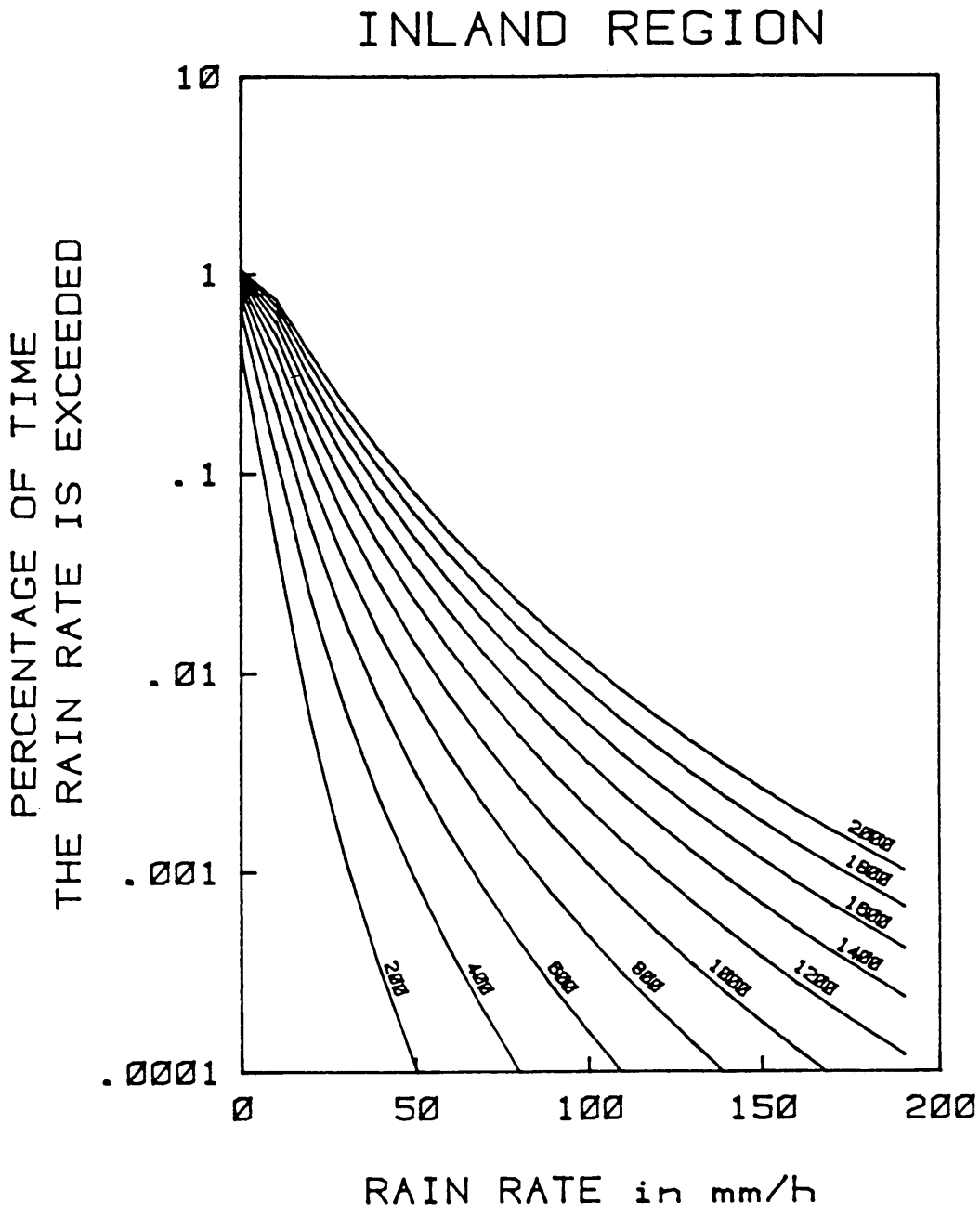

Fig. 39 Thirty-minute rain-rate distributions for the 'inland' region. The variable is MAR (in mm).

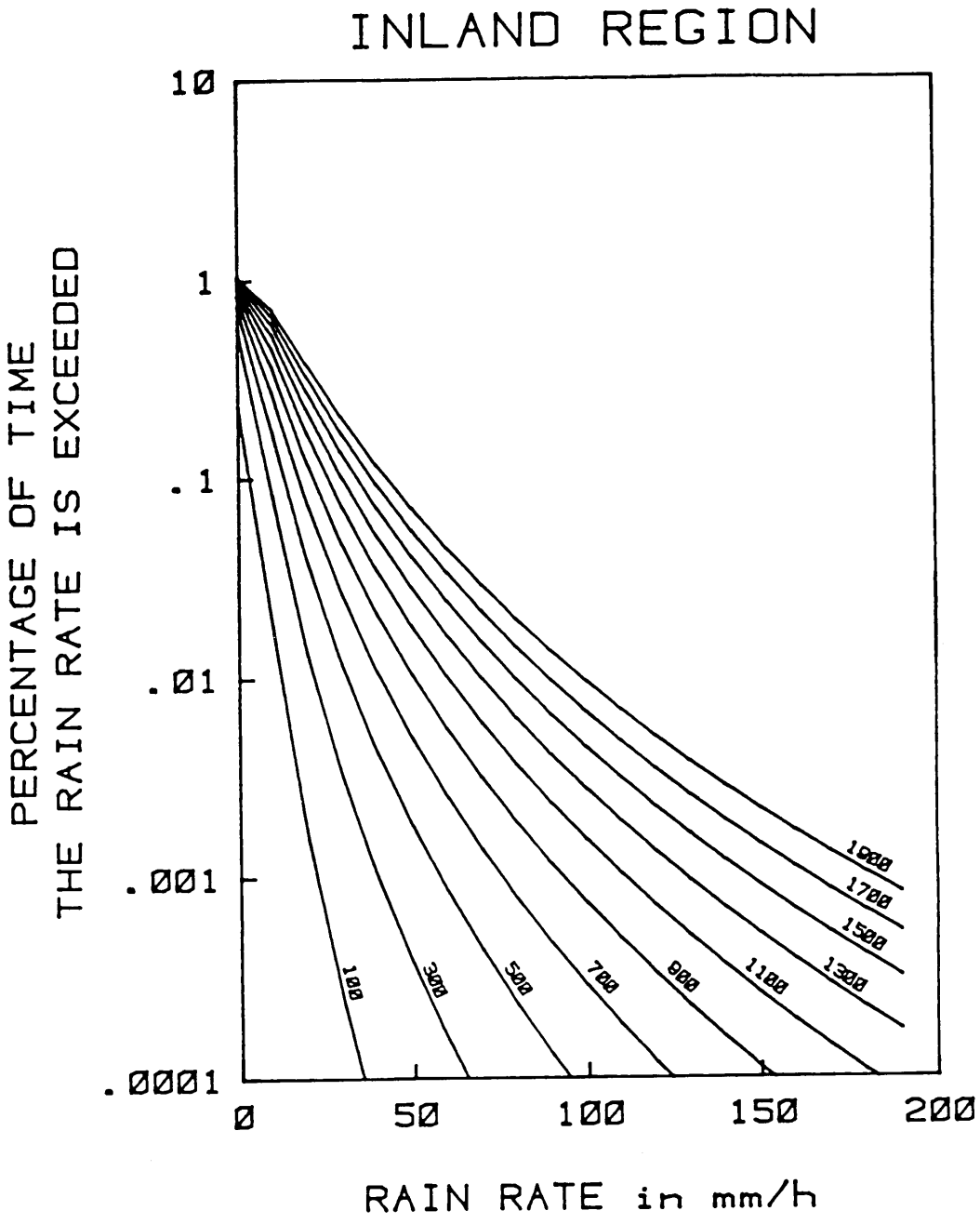

Fig. 40 Thirty-minute rain-rate distributions for the 'inland' region. The variable is MAR, with values intermediate to those of Fig. 39.

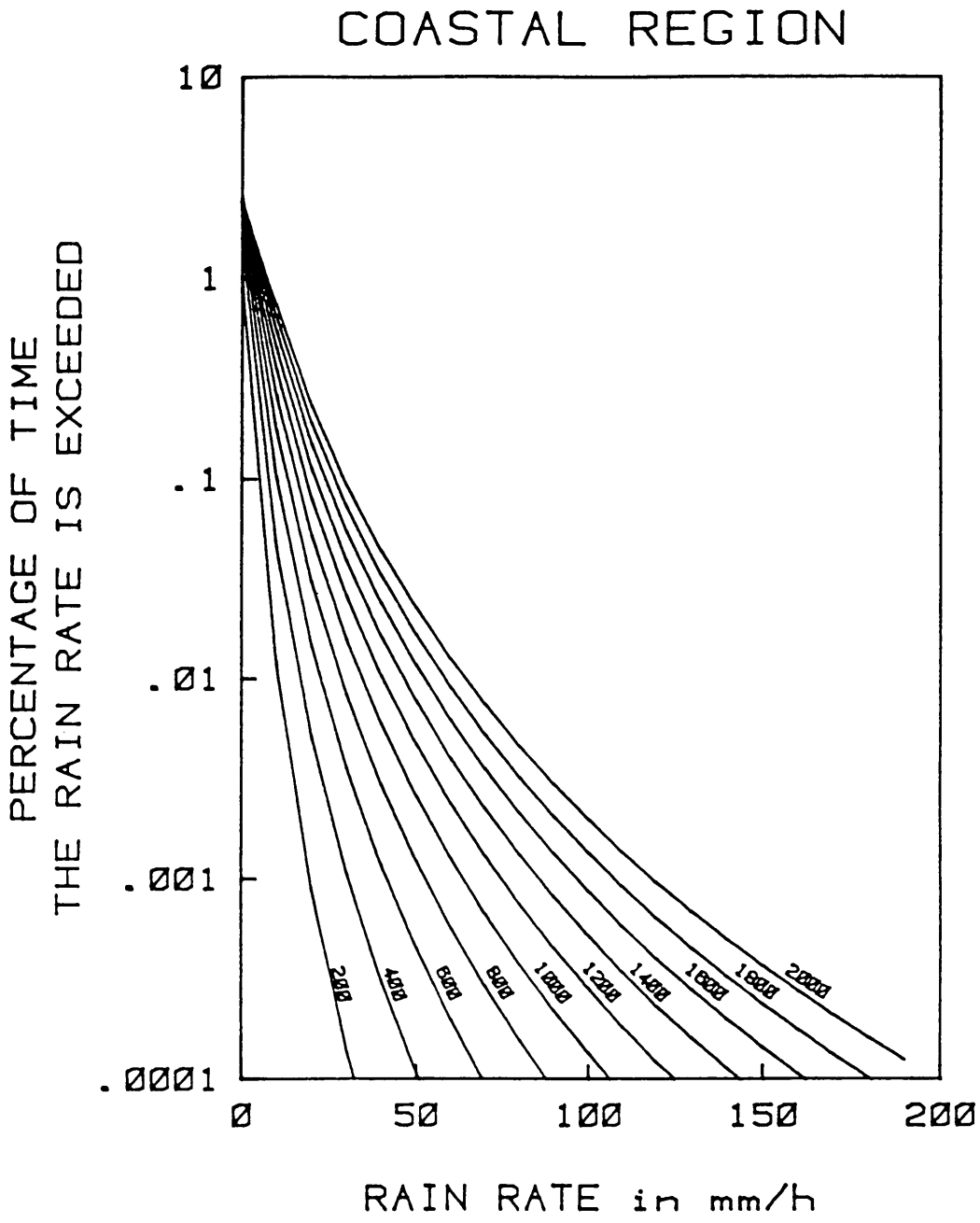

Fig. 41 Thirty-minute rain-rate distributions for the 'coastal' region. The variable is MAR (in mm).

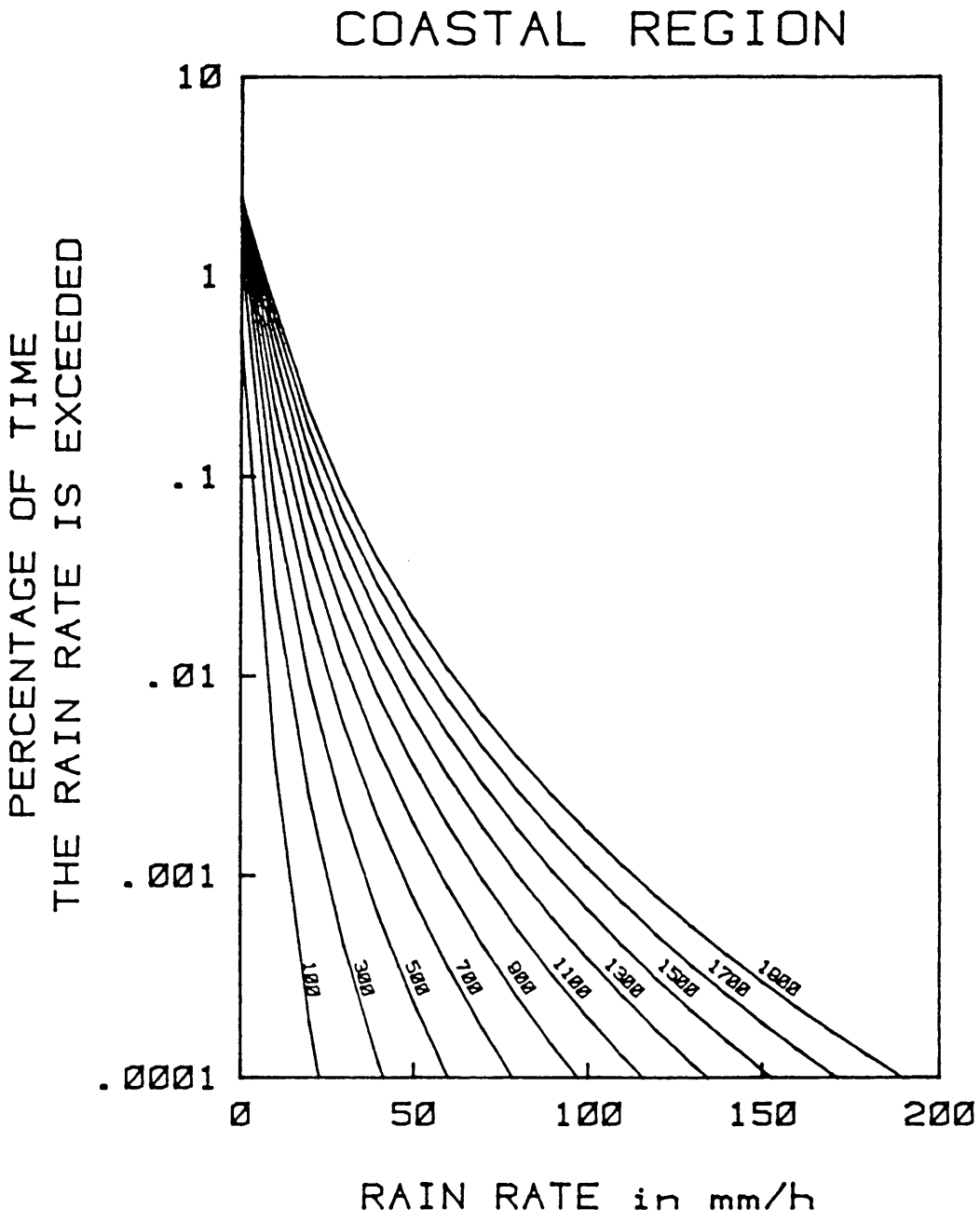

Fig. 42 Thirty-minute rain-rate distributions for the 'coastal' region. The variable is MAR, with values intermediate to those of Fig. 41.

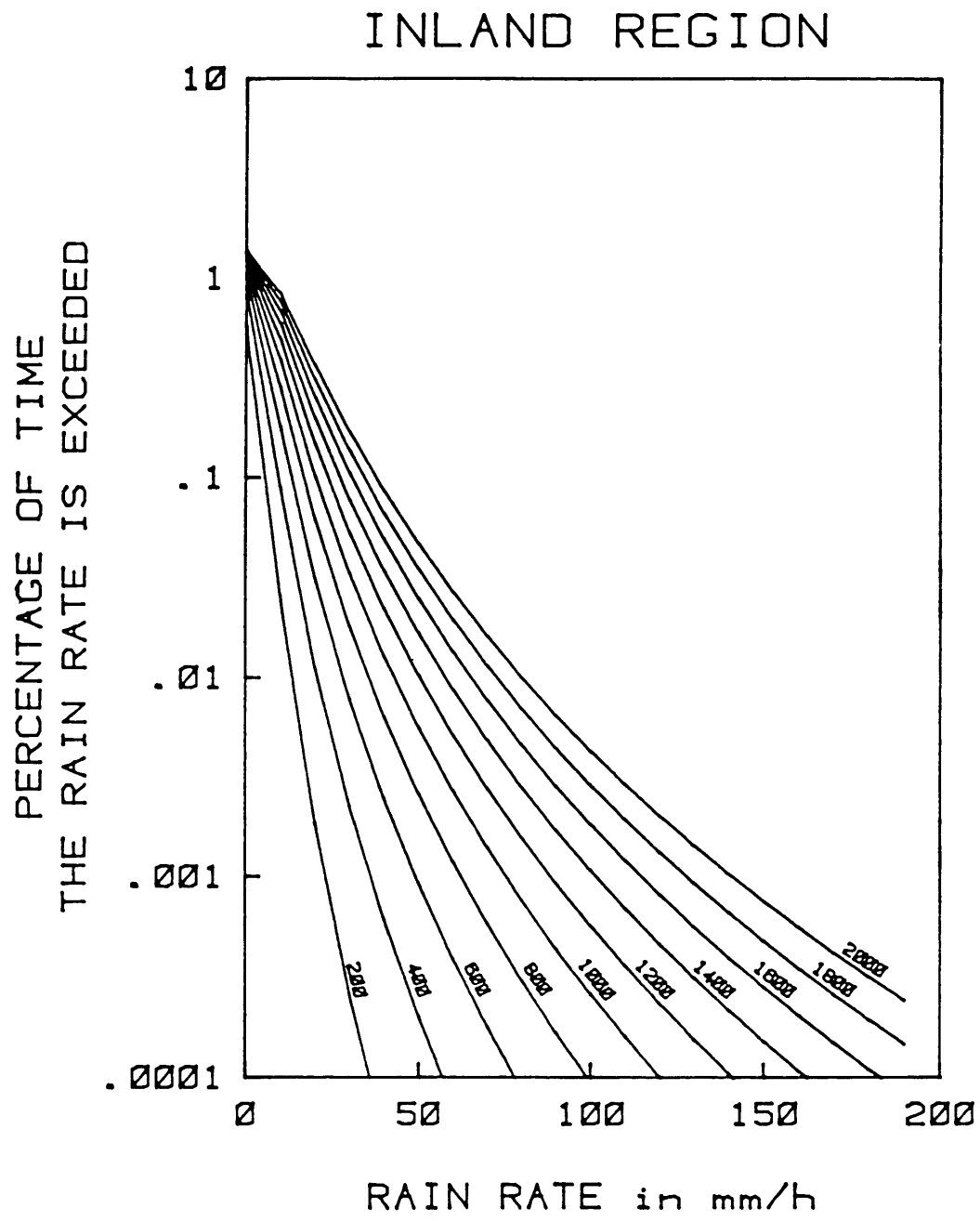

Fig. 43 Sixty-minute rain-rate distributions for the 'inland' region. The variable is MAR (in mm).

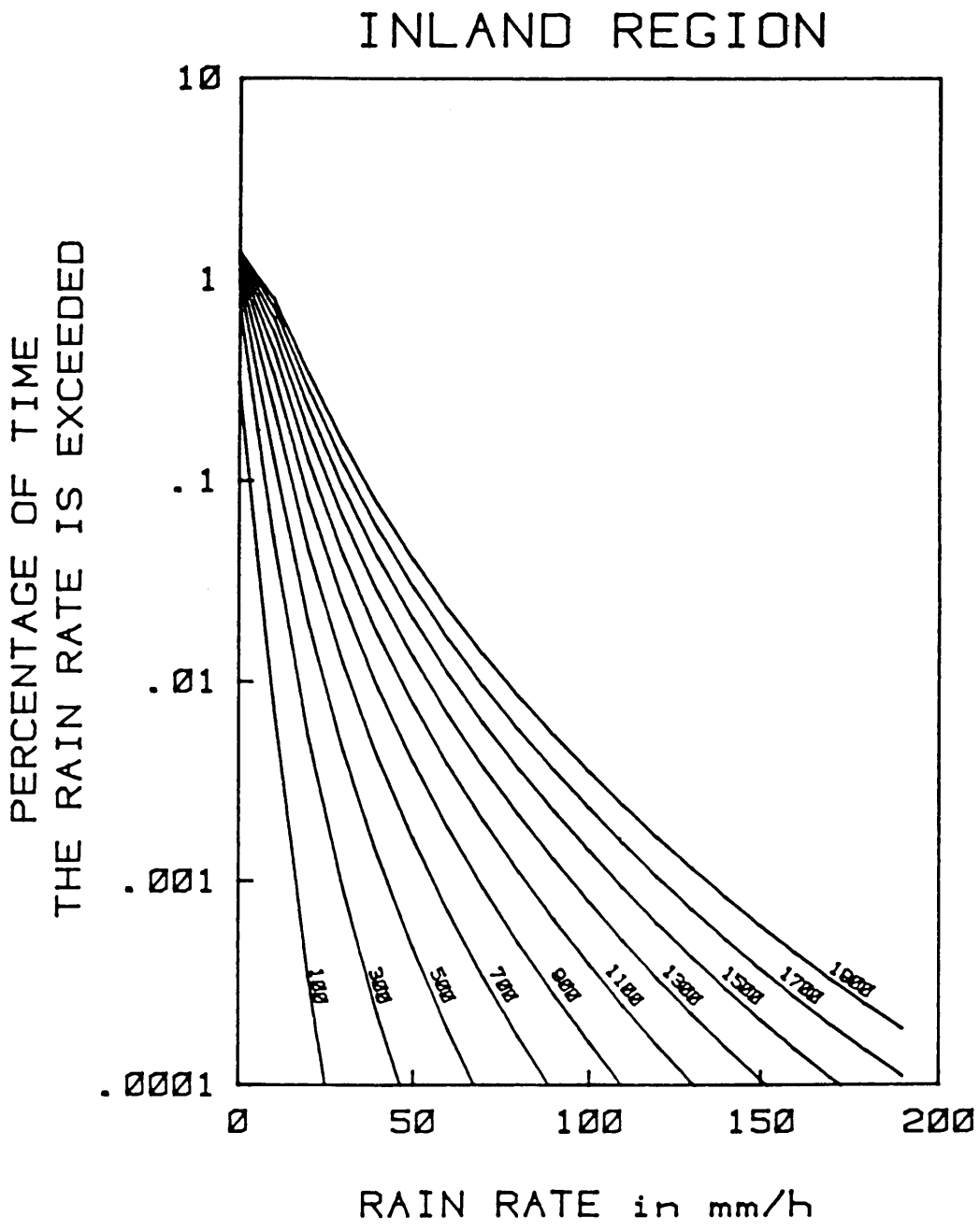

Fig. 44 Sixty-minute rain-rate distributions for the 'inland' region. The variable is MAR, with values intermediate to those of Fig. 43.

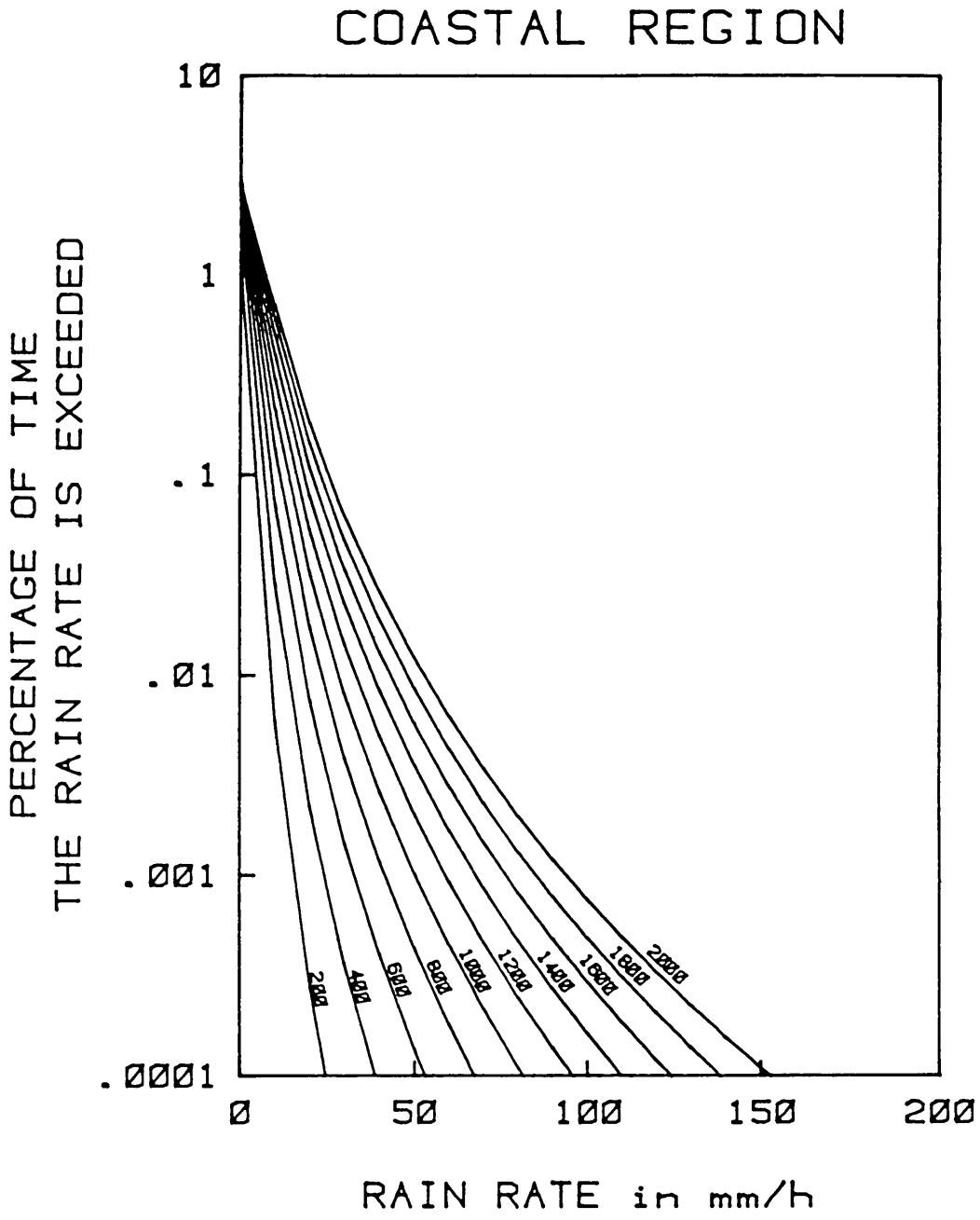

Fig. 45 Sixty-minute rain-rate distributions for the 'coastal' region. The variable is MAR (in mm).

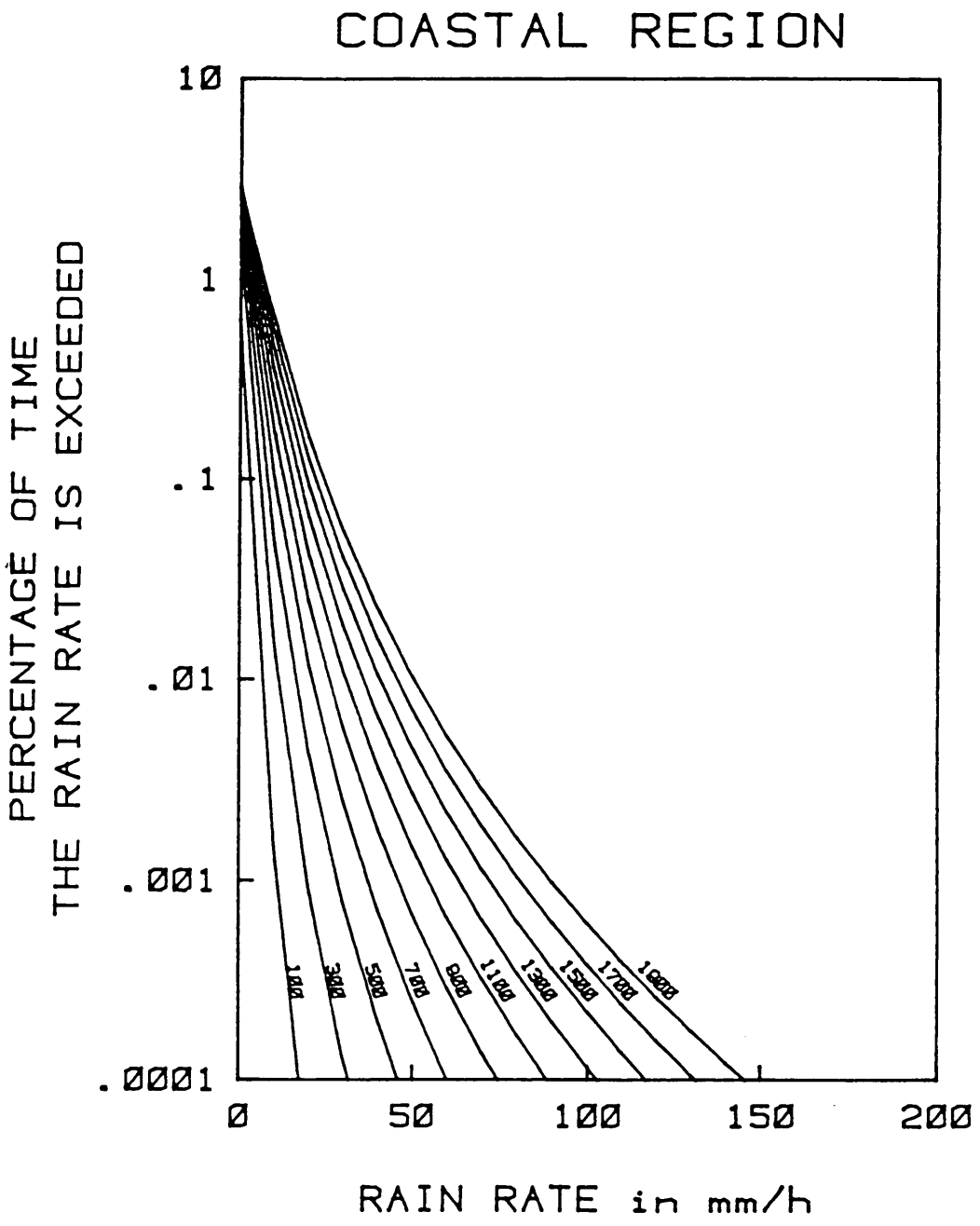

Fig. 46 Sixty-minute rain-rate distributions for the 'coastal' region. The variable is MAR, with values intermediate to those of Fig. 45.

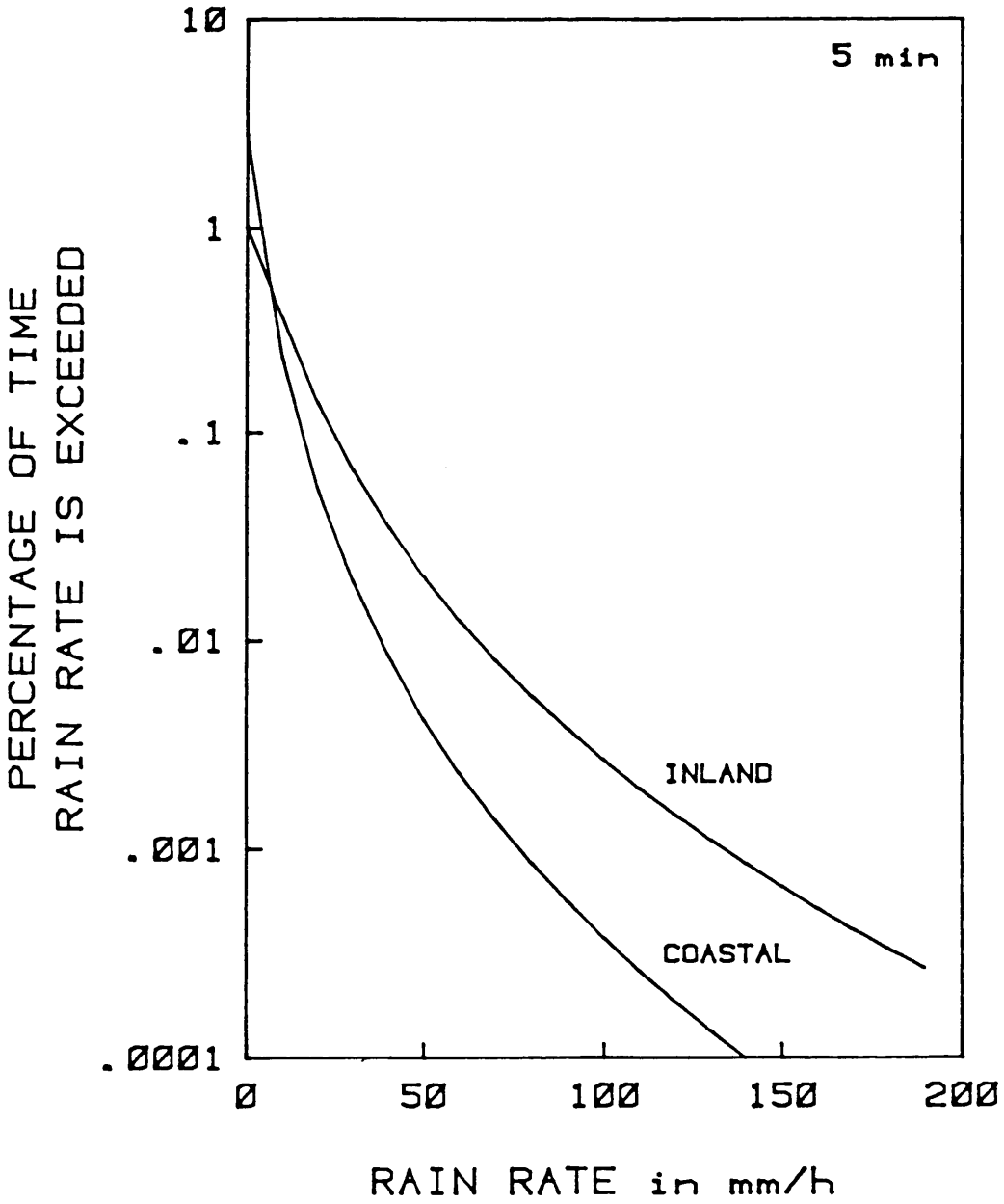

Fig. 47 Rain-rate distributions for the two climatic regions of the model. Integration time = 5 min., MAR = 1000 mm.

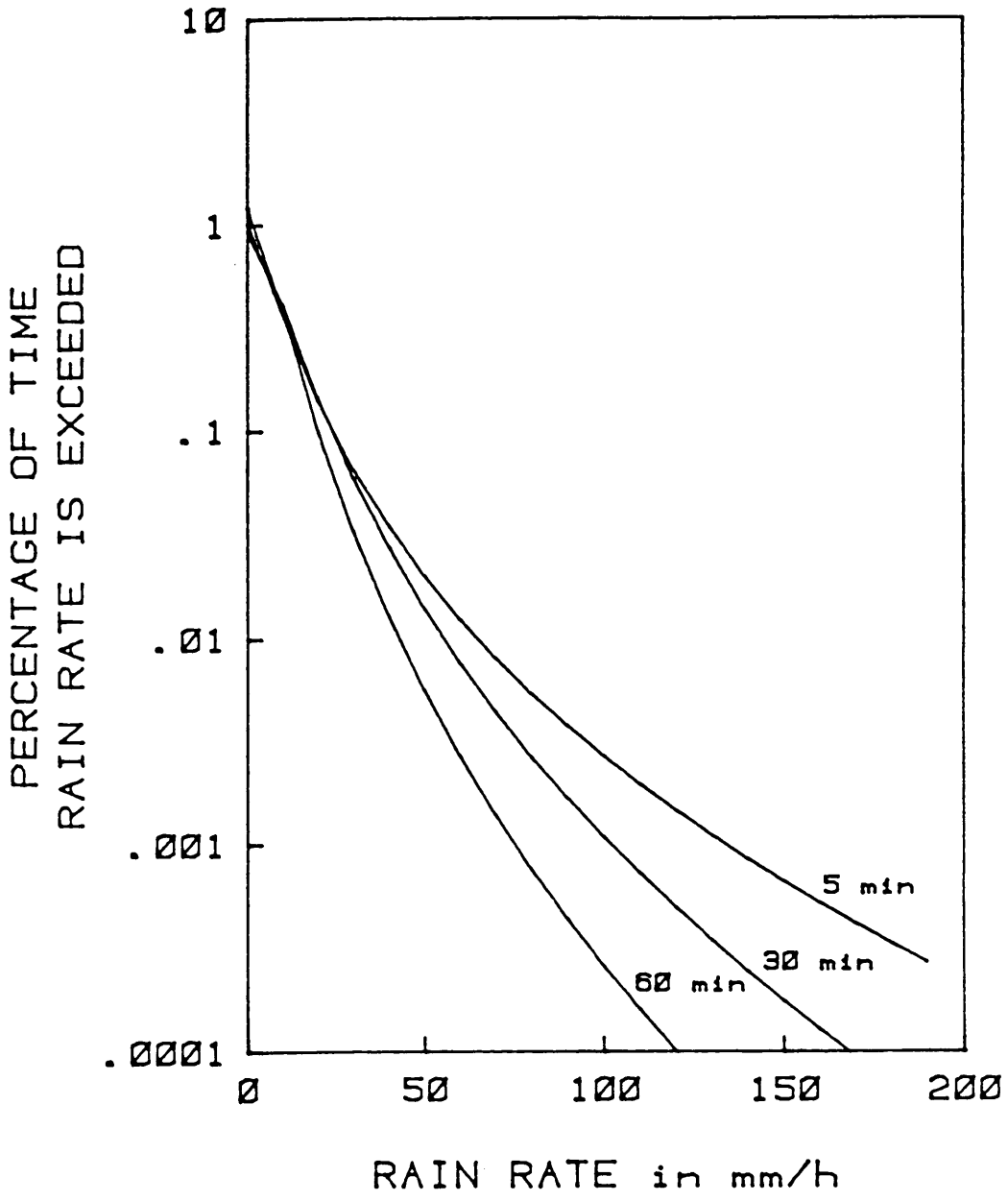

Fig. 48 Rain rate distributions showing the effect of varying the integration time. Region: 'inland', MAR = 1000 mm.

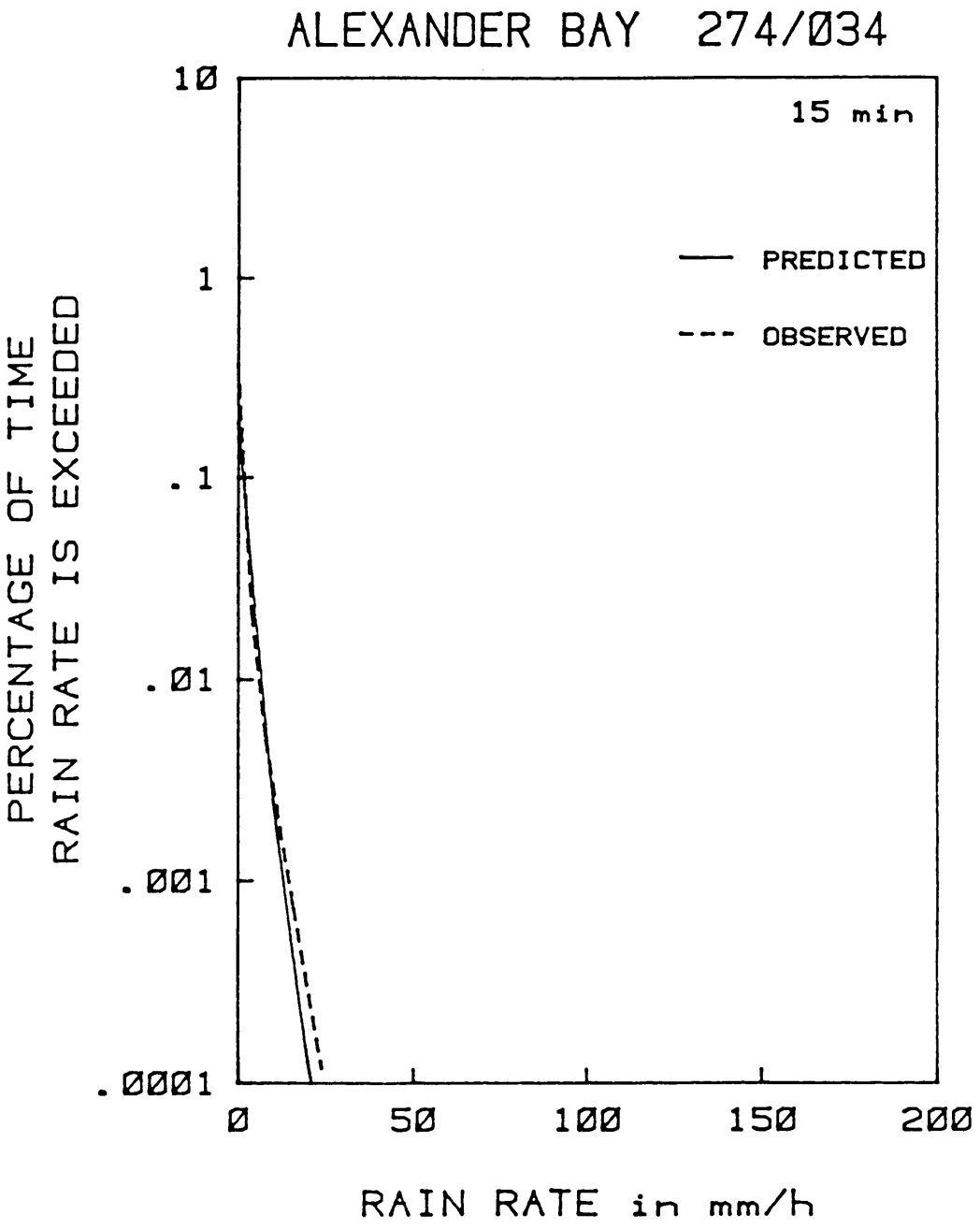

Fig. 49 Observed and predicted 15-min rain-rate distributions for Alexander Bay. MAR=44mm; region: 'coastal'.

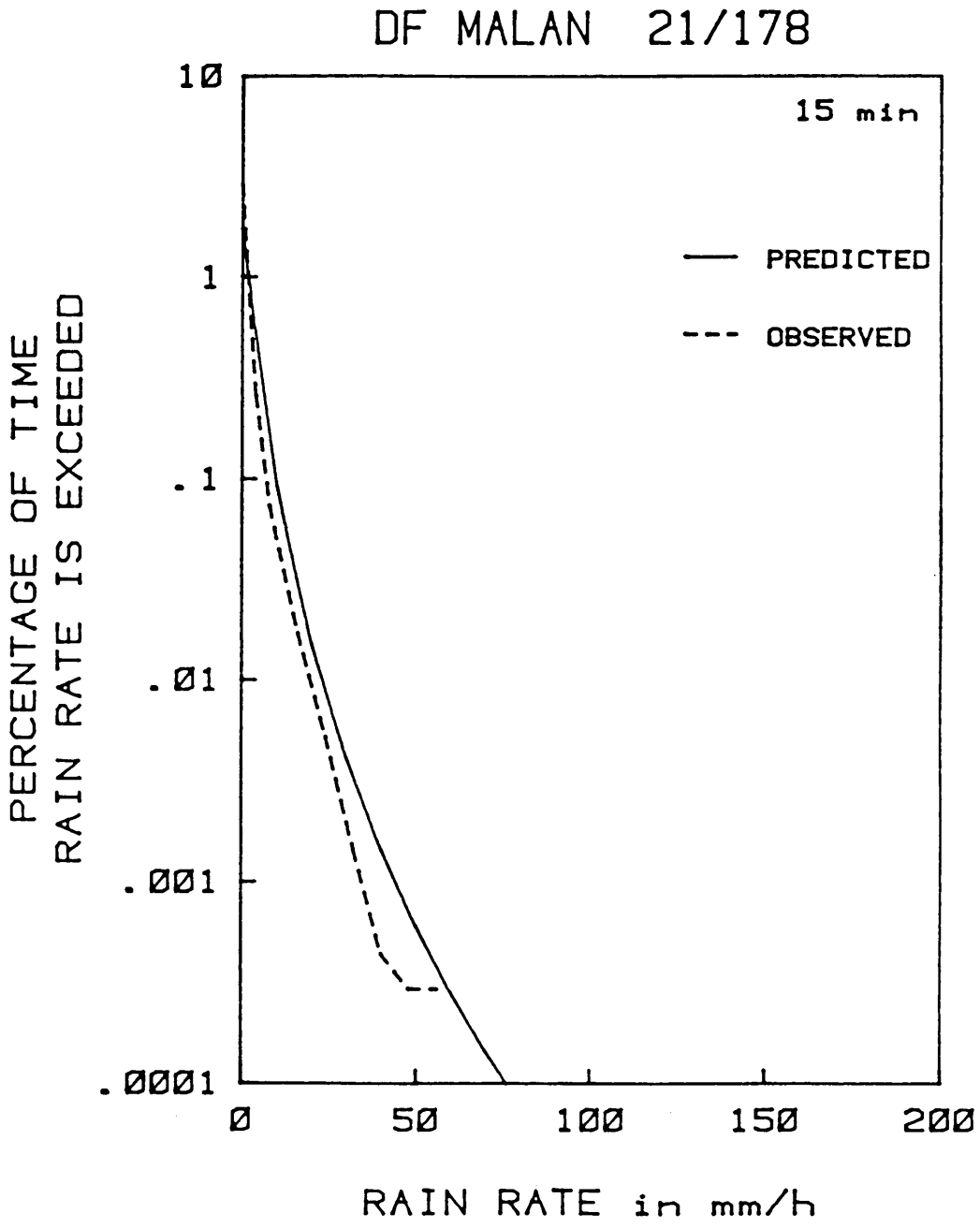

Fig. 50 Observed and predicted 15-min rain-rate distributions for DF Malan. MAR=533mm; region: 'coastal'.

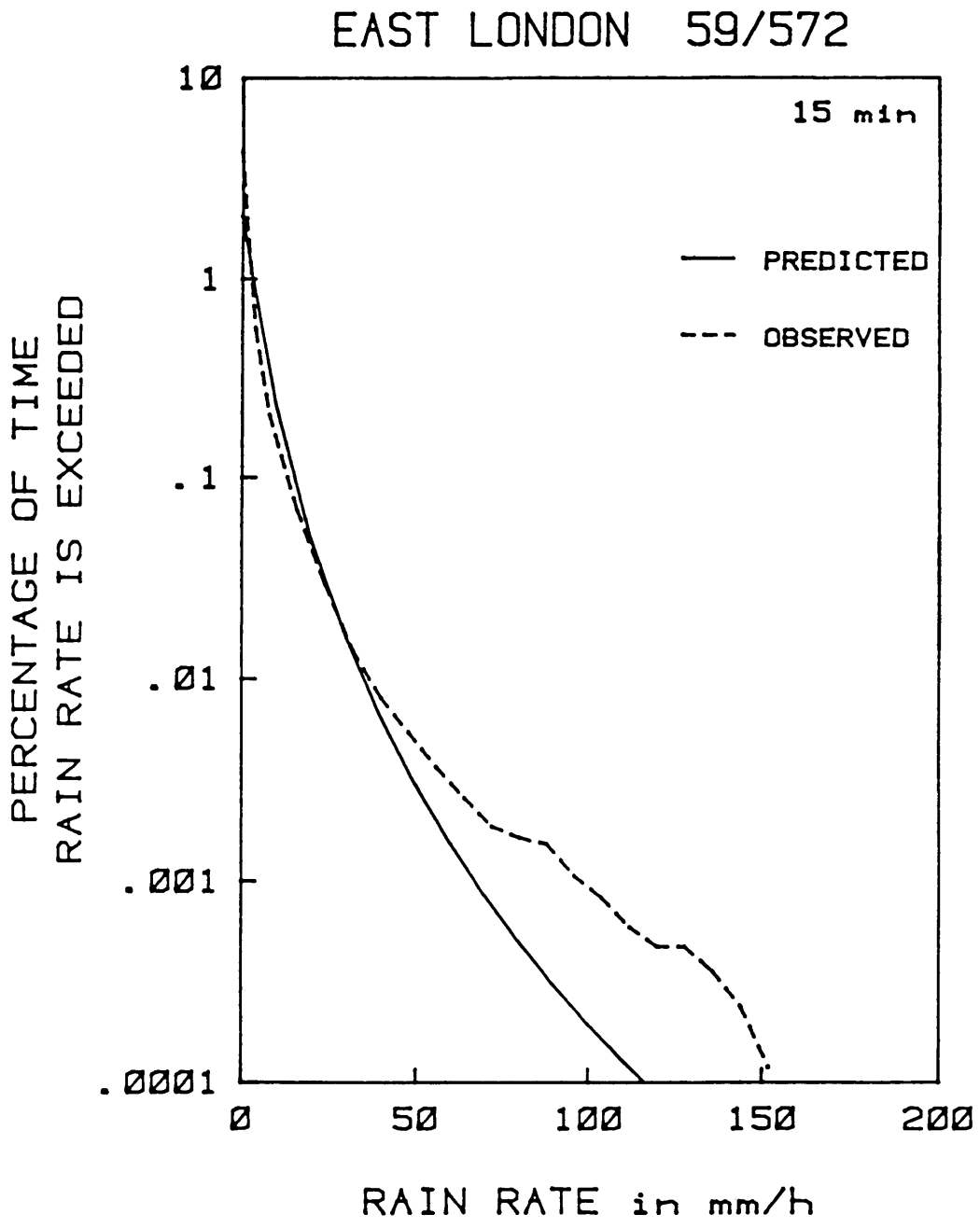

Fig. 51 Observed and predicted 15-min rain-rate distributions for East London. MAR=896mm; region: 'coastal'.

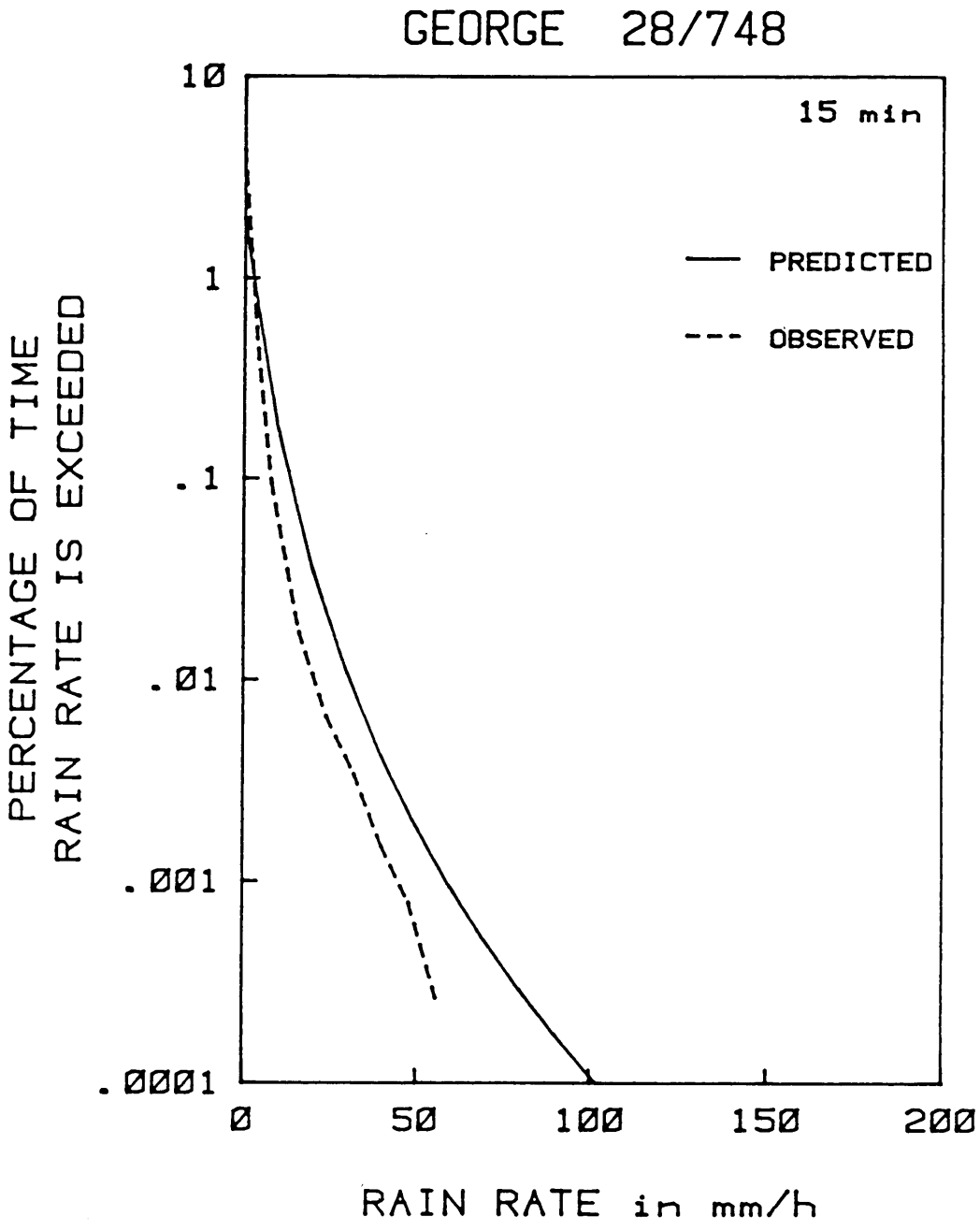

Fig. 52 Observed and predicted 15-min rain-rate distributions for George. MAR=767mm; region: 'coastal'.

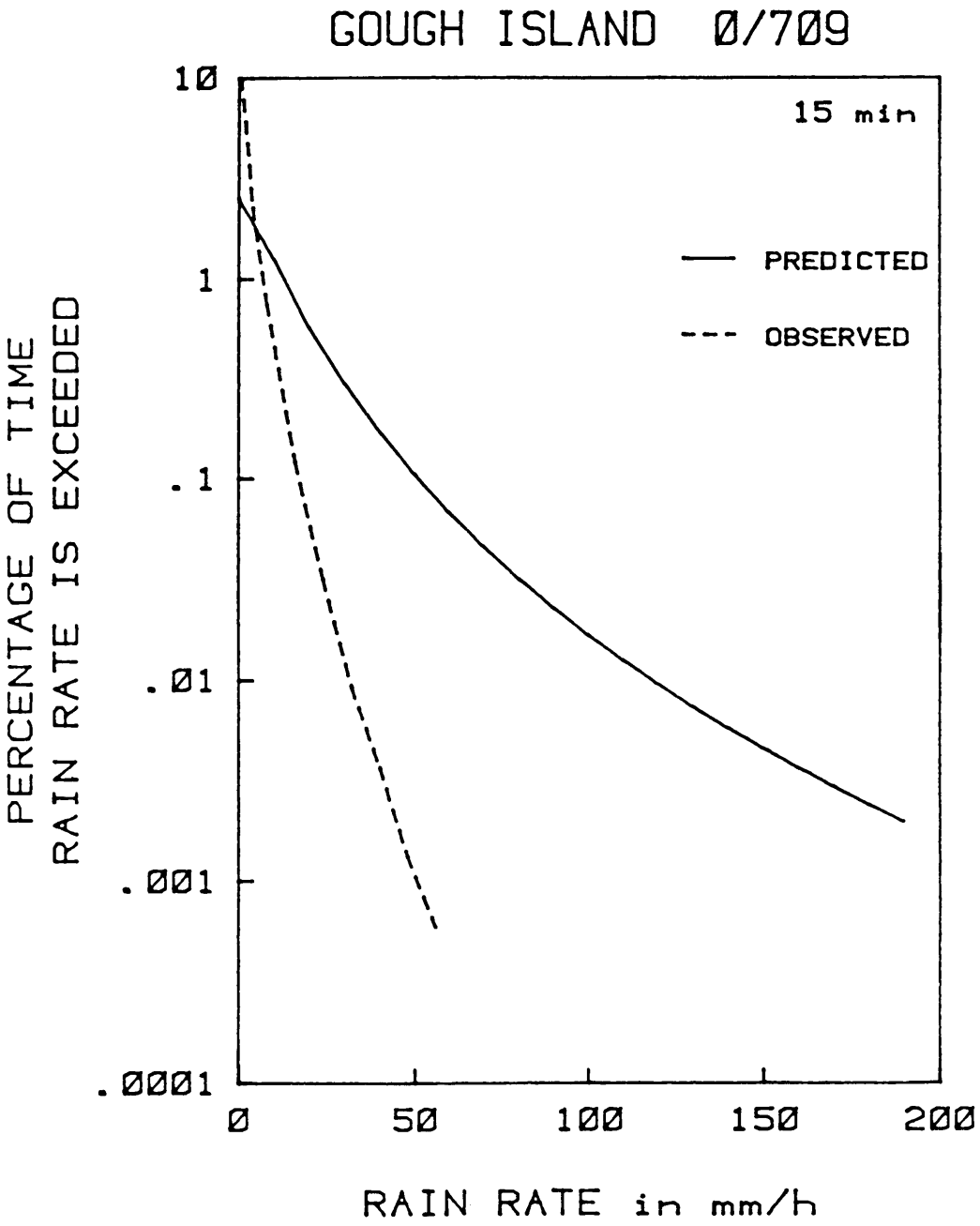

Fig. 53 Observed and predicted 15-min rain-rate distributions for Gough Island. MAR=3397mm; region: 'coastal'.

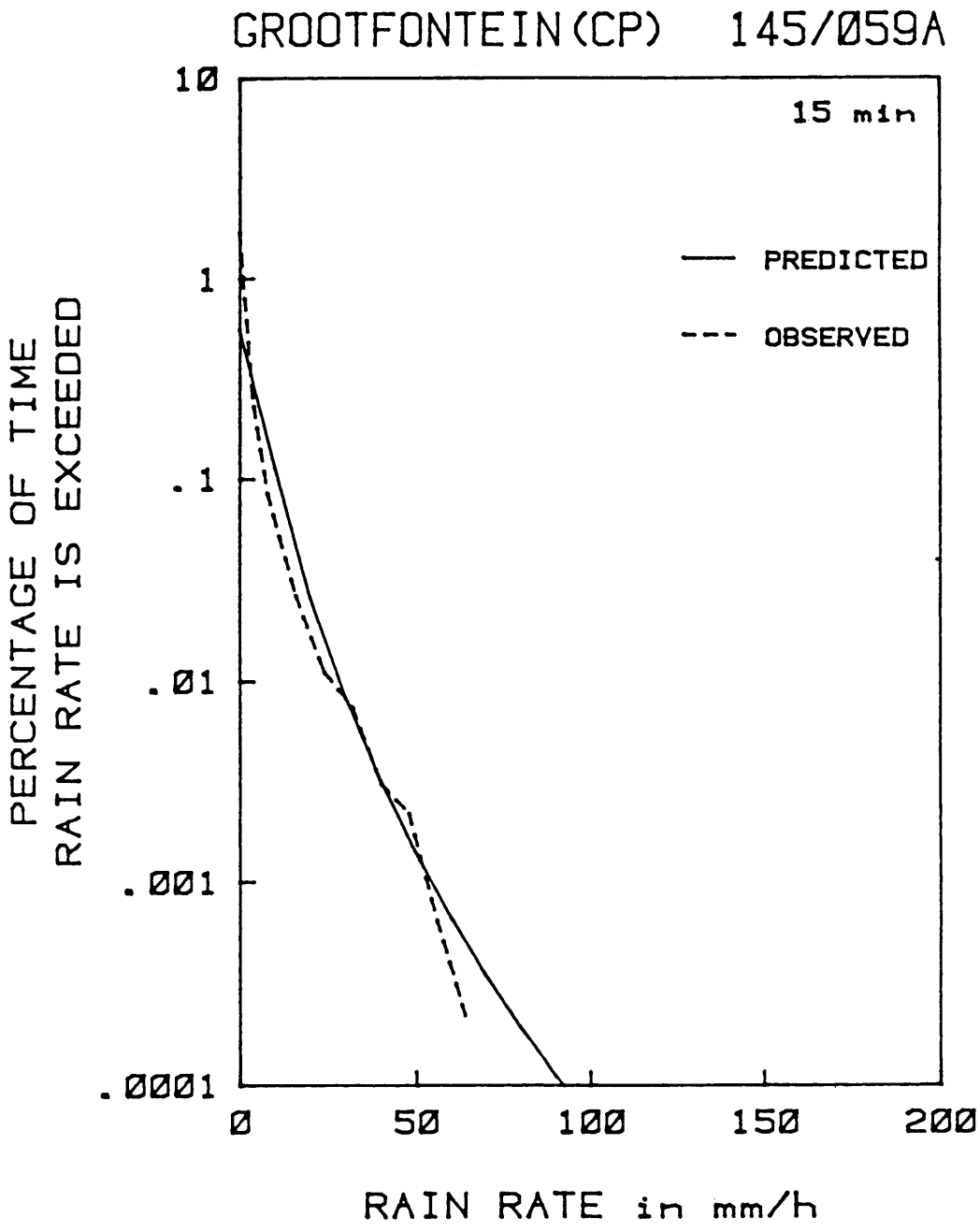

Fig. 54 Observed and predicted 15-min rain-rate distributions for Grootfontein (CP).
MAR=350mm; Region: 'inland'.

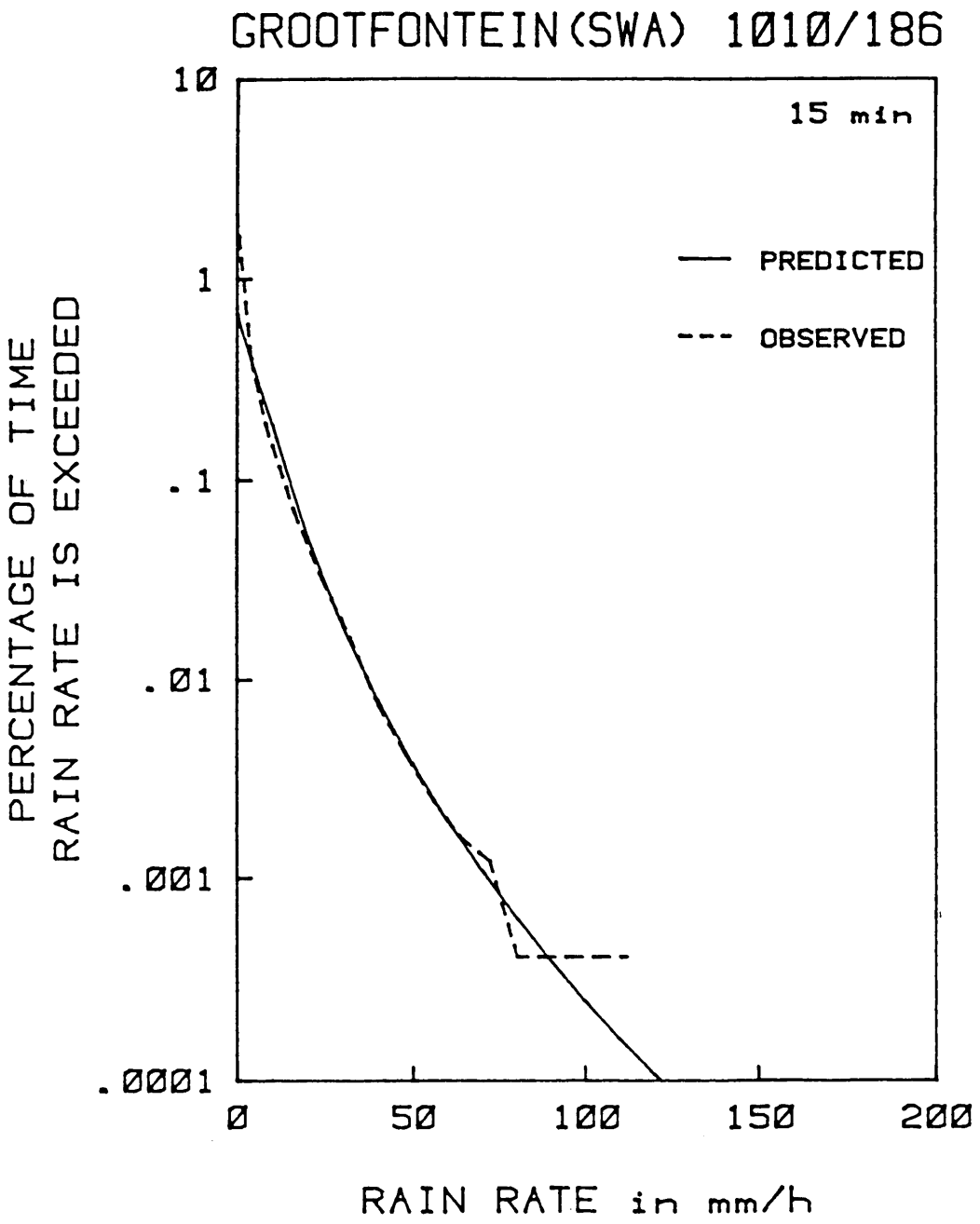

Fig. 55 Observed and predicted 15-min rain-rate distributions for Grootfontein (SWA). MAR=510mm; region: 'inland'.

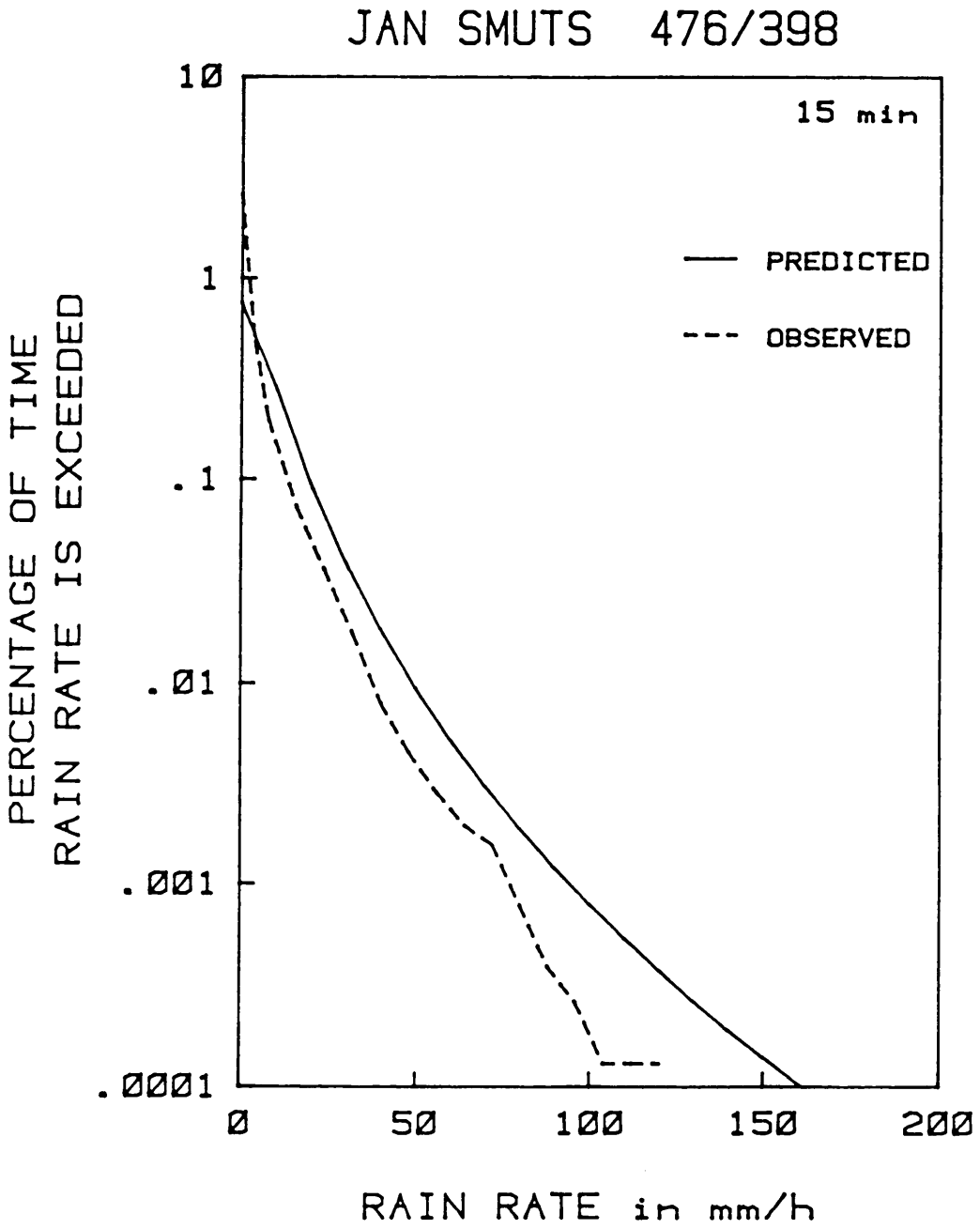

Fig. 56 Observed and predicted 15-min rain-rate distributions for Jan Smuts.
MAR=723mm; region: 'inland'.

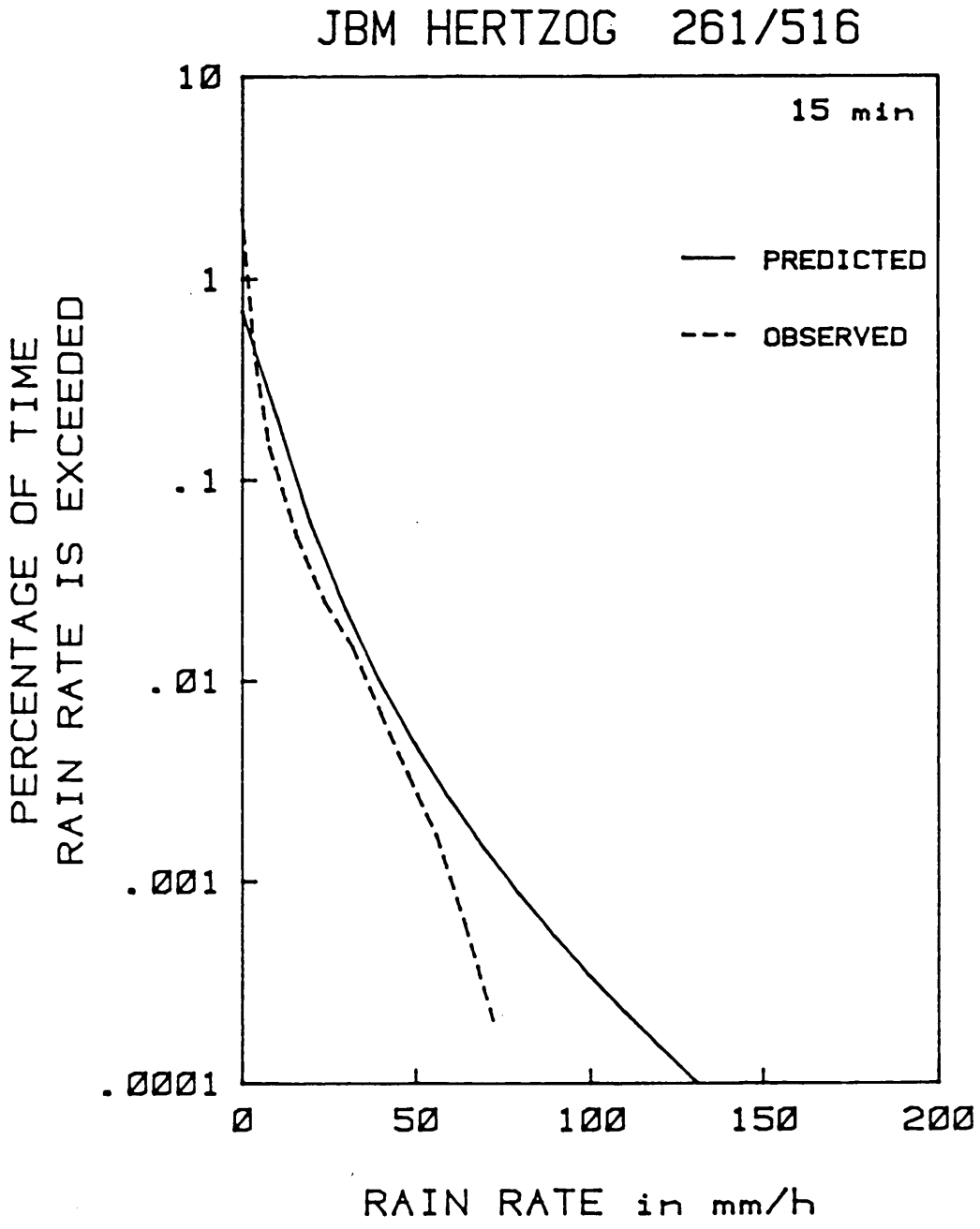

Fig. 57 Observed and predicted 15-min rain-rate distributions for JBM Hertzog.
MAR=561mm; region: 'inland'.

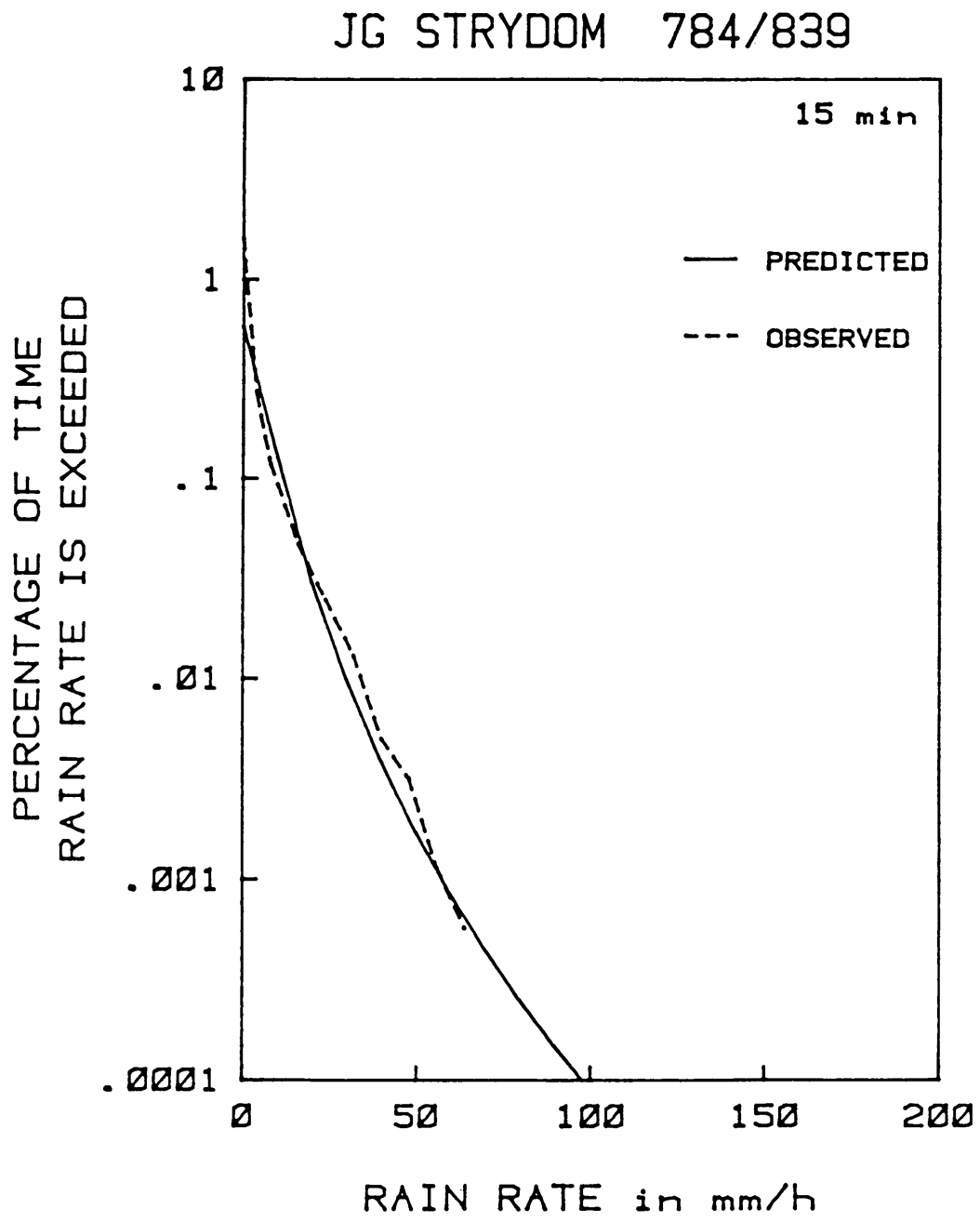

Fig. 58 Observed and predicted 15-min rain-rate distributions for JG Strydom.
MAR=380mm; region: 'inland'.

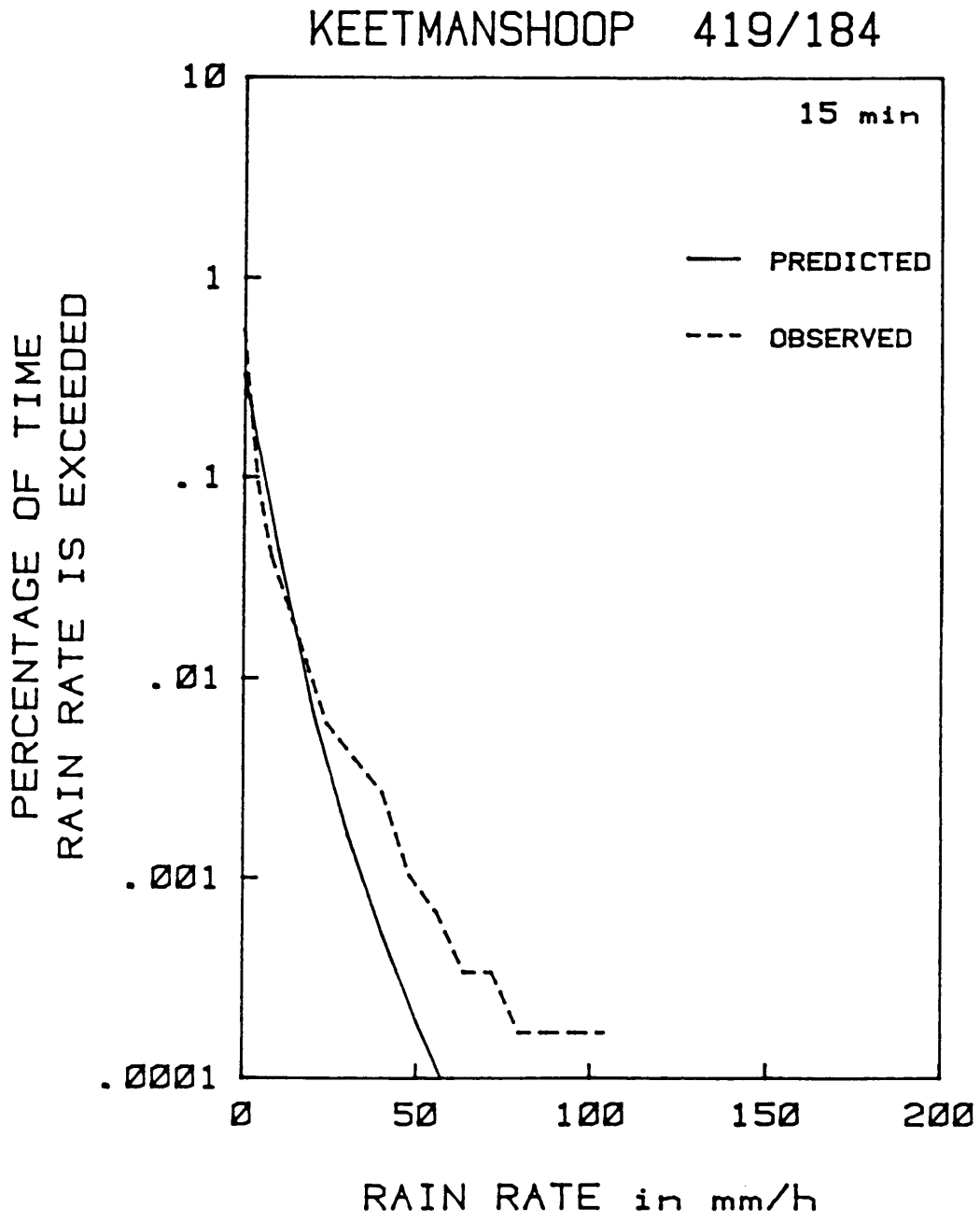

Fig. 59 Observed and predicted 15-min rain-rate distributions for Keetmanshoop.
MAR=163mm; region: 'inland'.

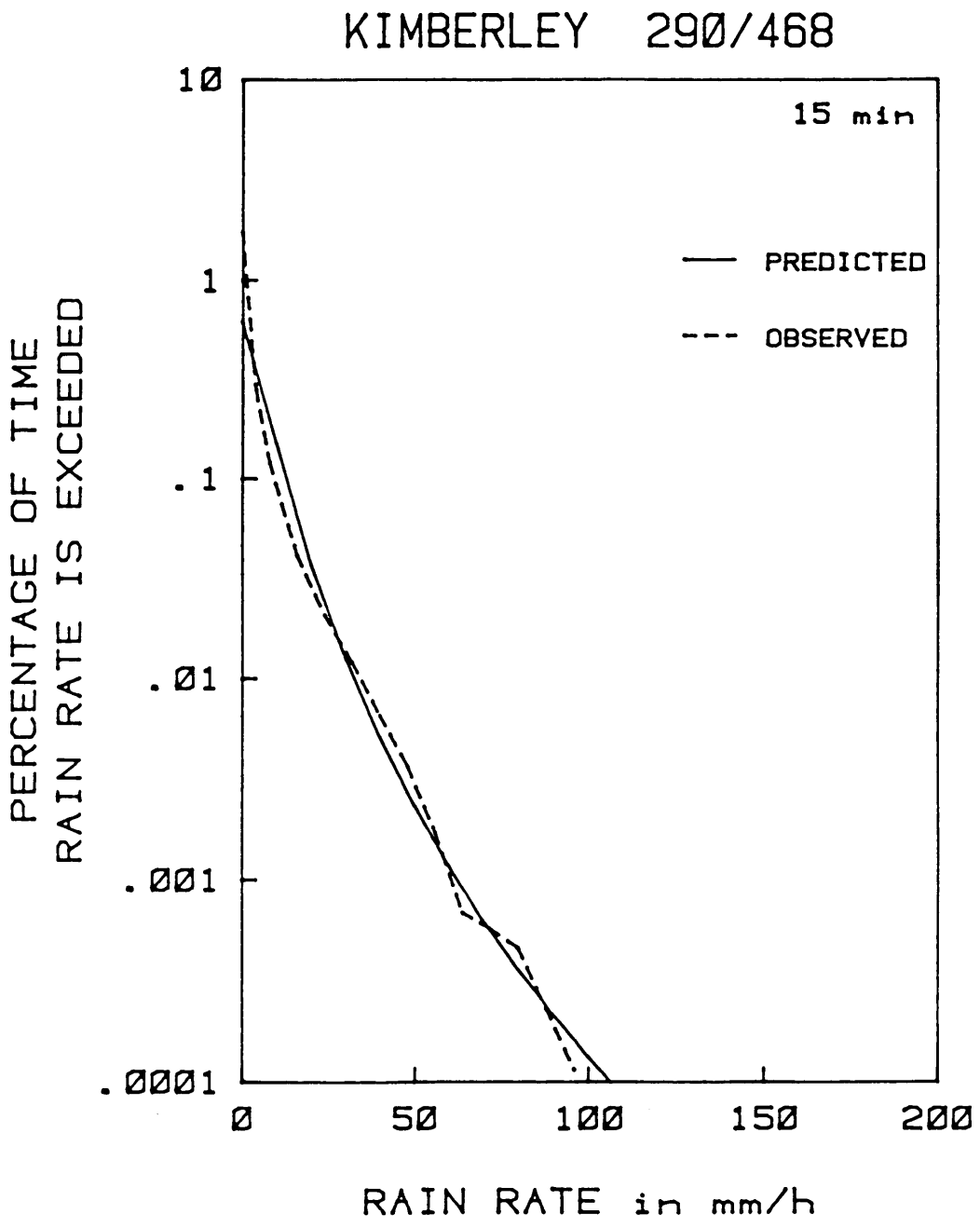

Fig. 60 Observed and predicted 15-min rain-rate distributions for Kimberley. MAR=426mm; region: 'inland'.

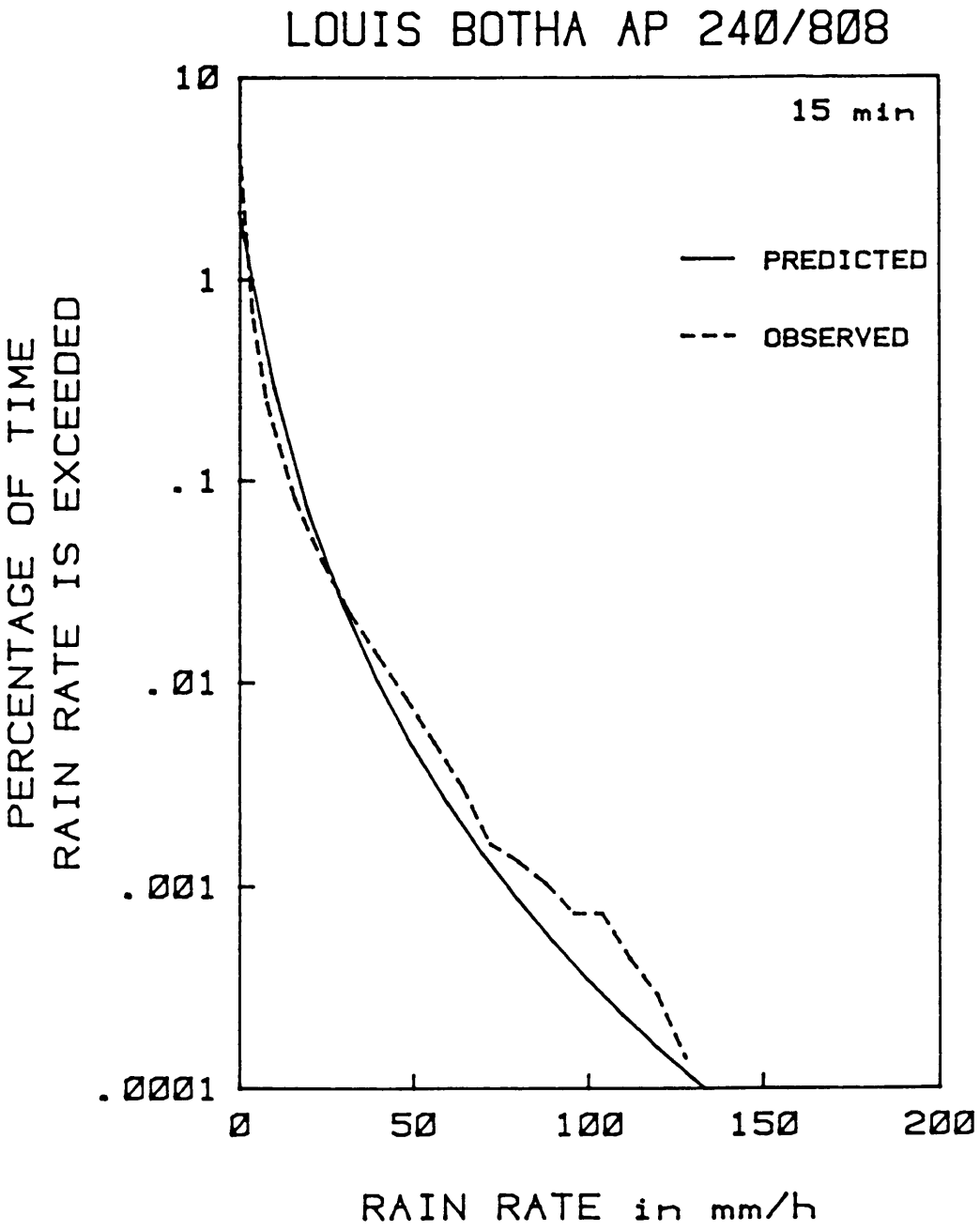

Fig. 61 Observed and predicted 15-min rain-rate distributions for Louis Botha.
MAR=1050mm; region: 'coastal'.

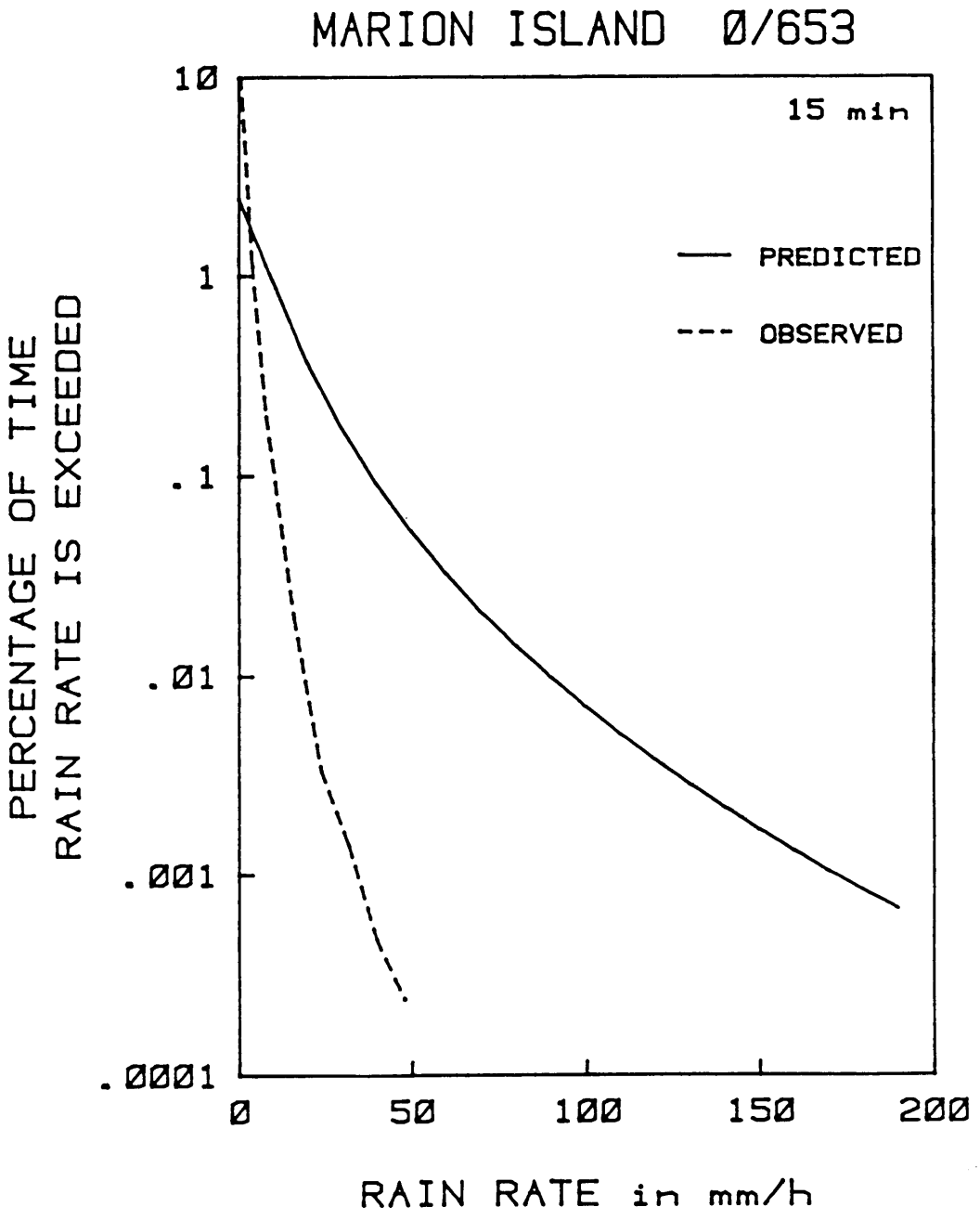

Fig. 62 Observed and predicted 15-min rain-rate distributions for Marion Island.
MAR=2534mm; Region: 'coastal'.

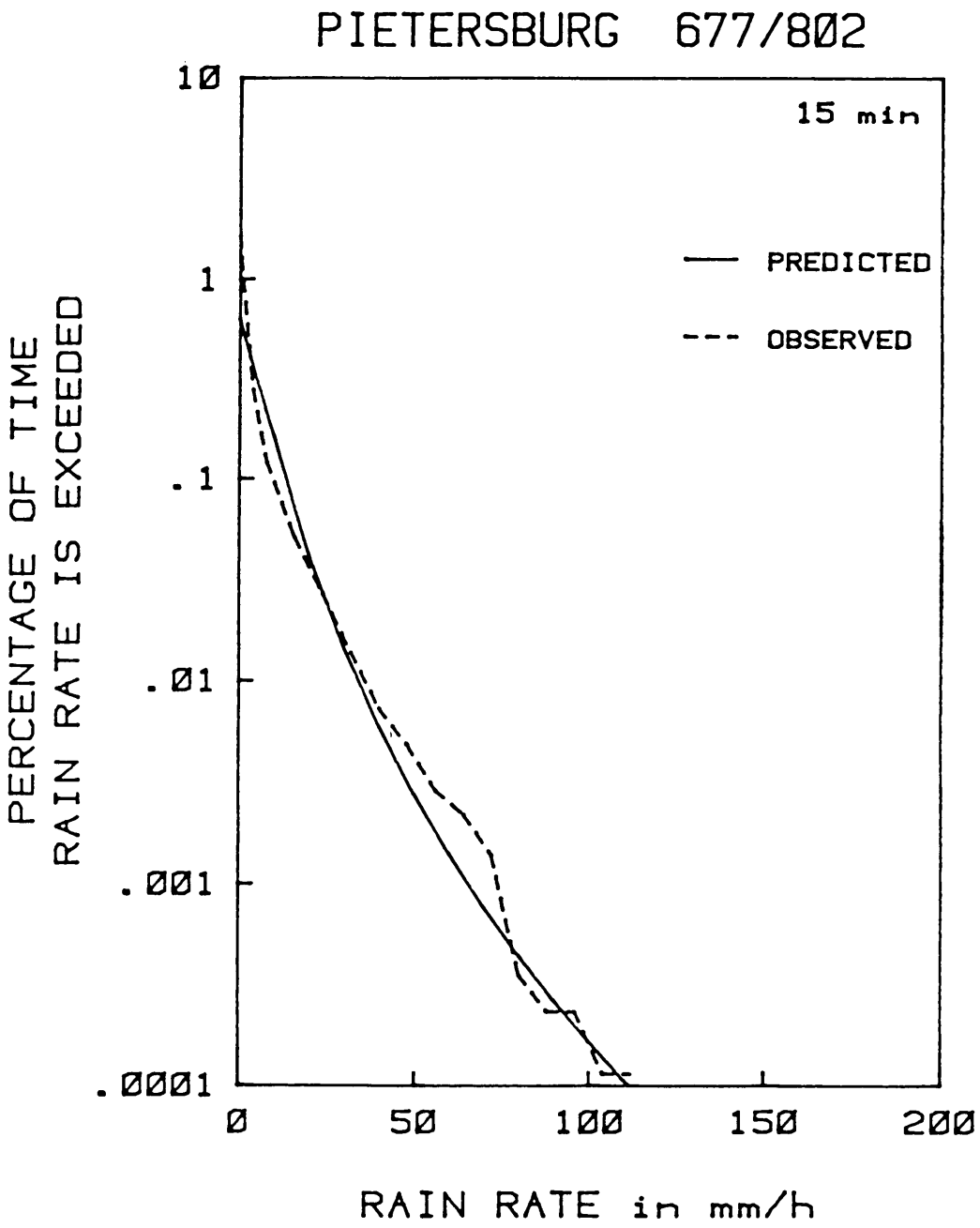

Fig. 63 Observed and predicted 15-min rain-rate distributions for Pietersburg
MAR=454mm; Region: 'inland'.

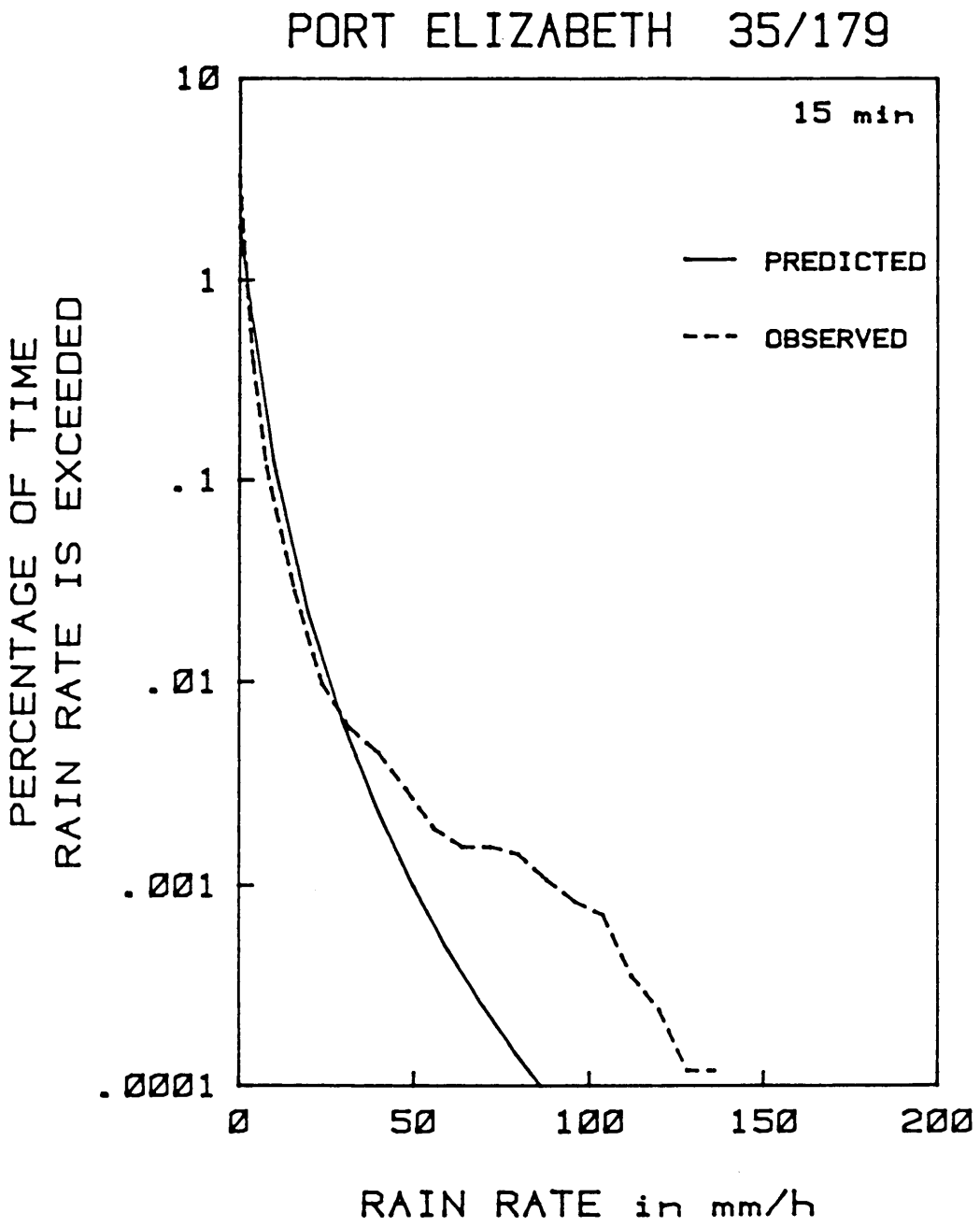

Fig. 64 Observed and predicted 15-min rain-rate distributions for Port Elizabeth.
MAR=626mm; Region: 'coastal'.

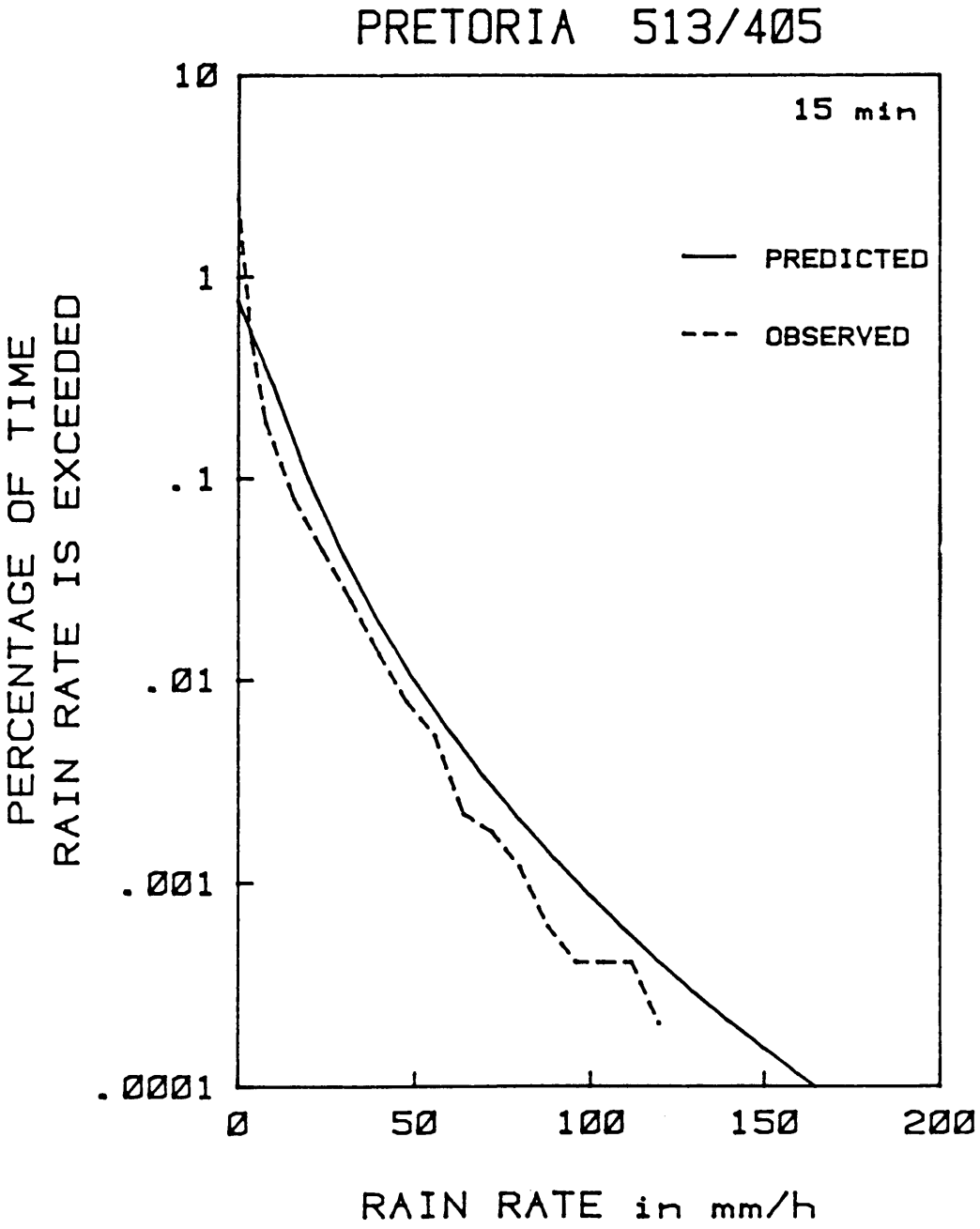

Fig. 65 Observed and predicted 15-min rain-rate distributions for Pretoria (Lynnwood).
MAR=742mm; Region: 'inland'.

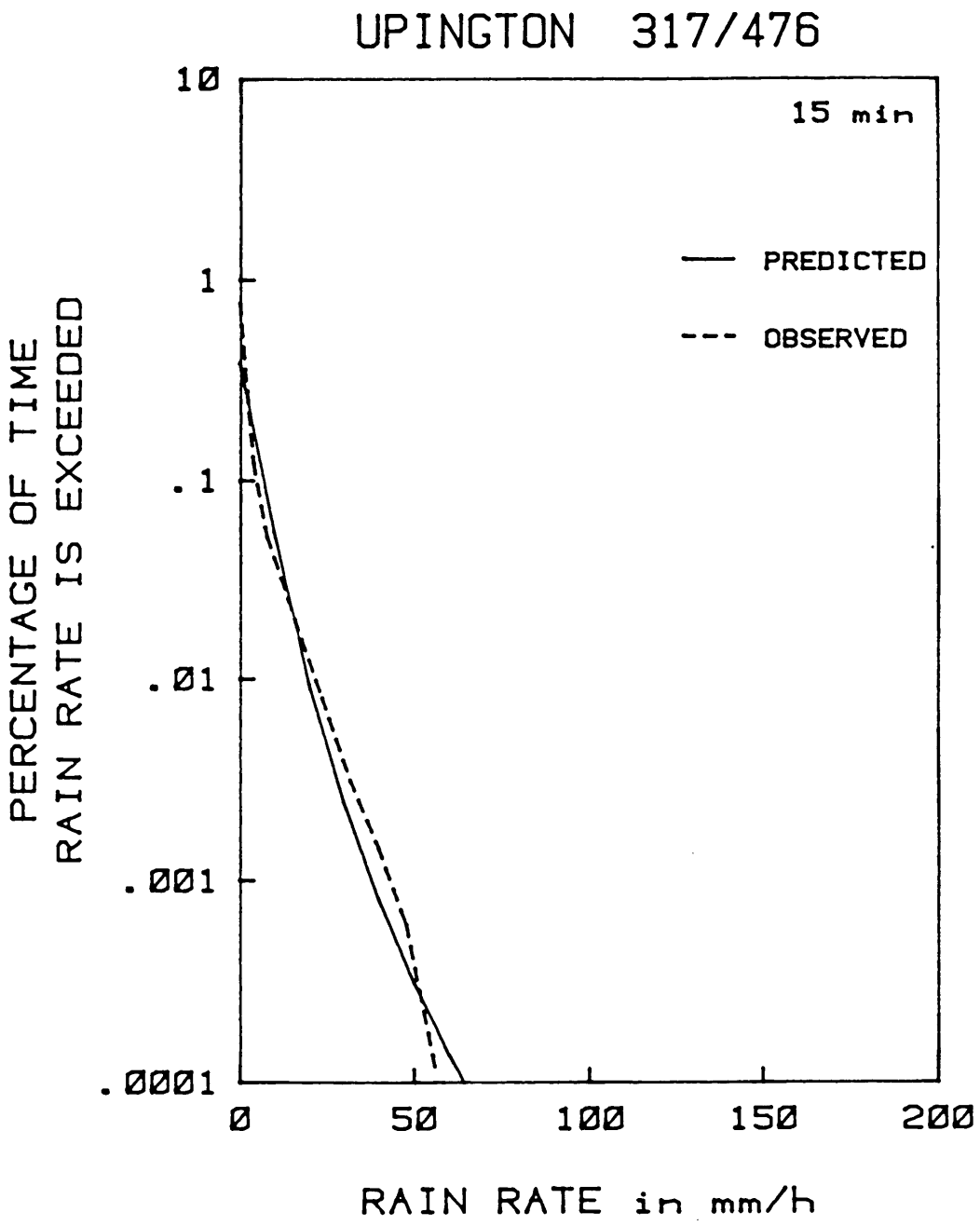

Fig. 66 Observed and predicted 15-min rain-rate distributions for Upington.
MAR=199mm; Region: 'inland'.

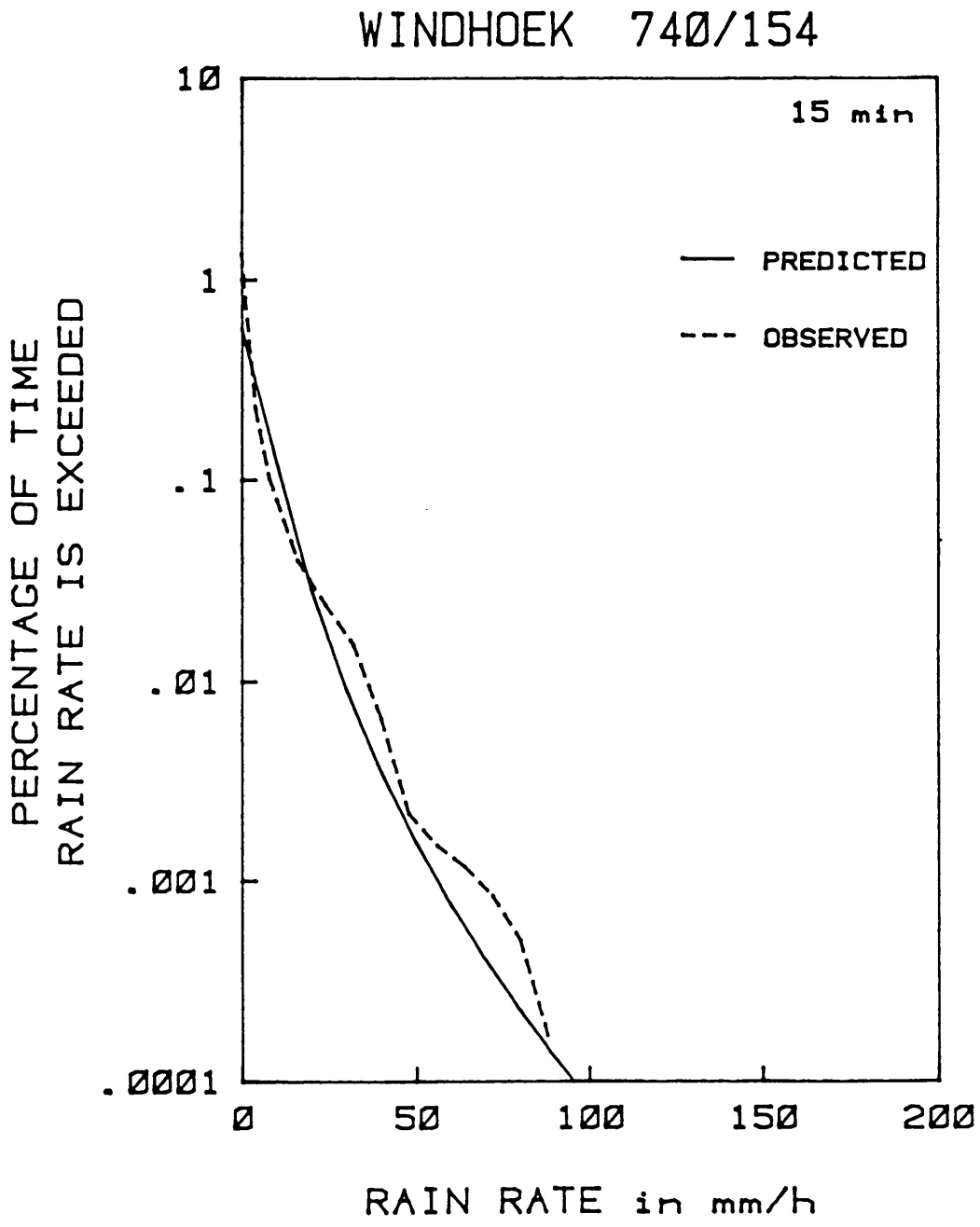

Fig. 67 Observed and predicted 15-min rain-rate distributions for Windhoek.
MAR=367mm; Region: 'inland'.

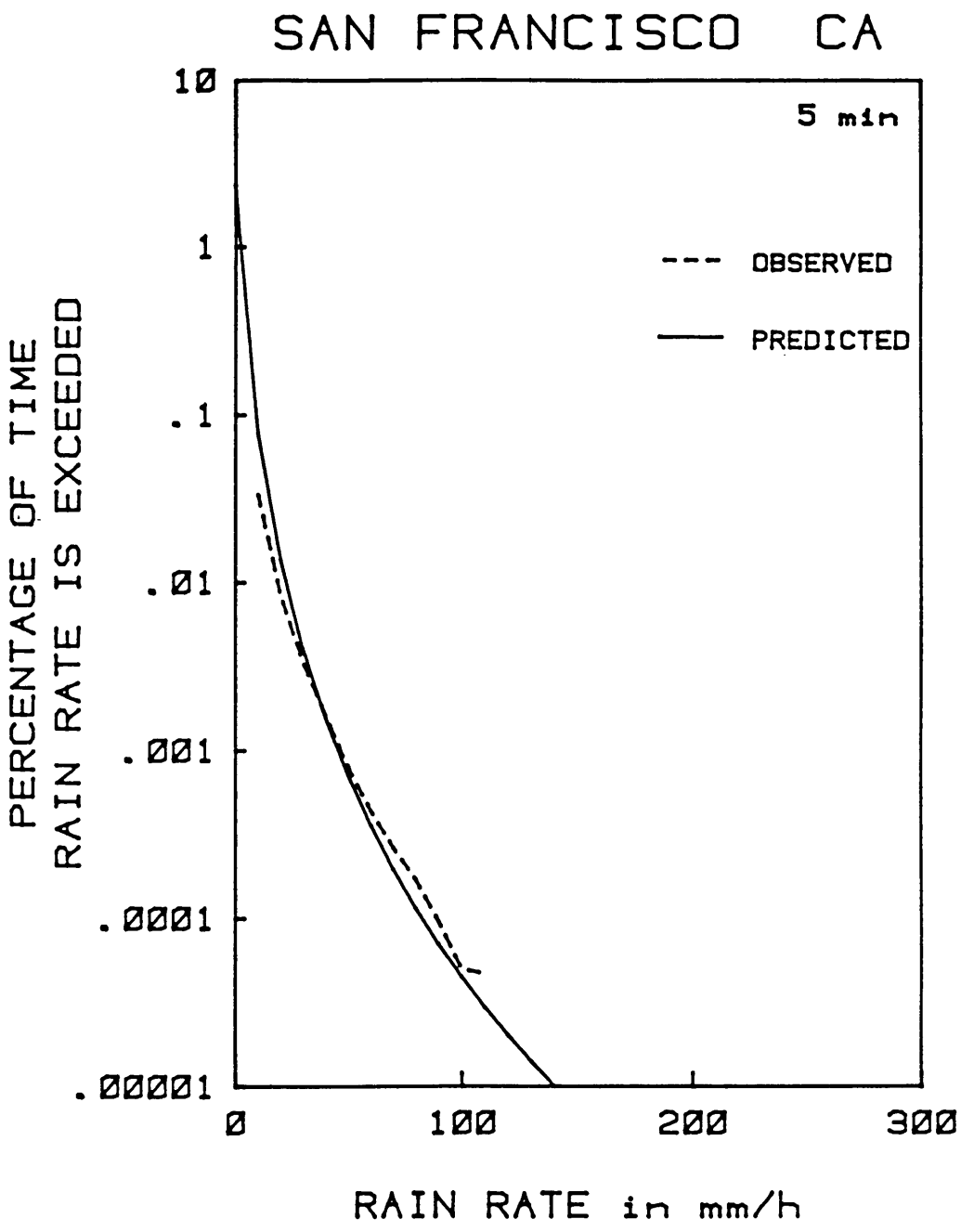

Fig. 68 Observed and predicted 5-min rain-rate distributions for San Francisco, California. MAR=529mm; region: 'coastal'.

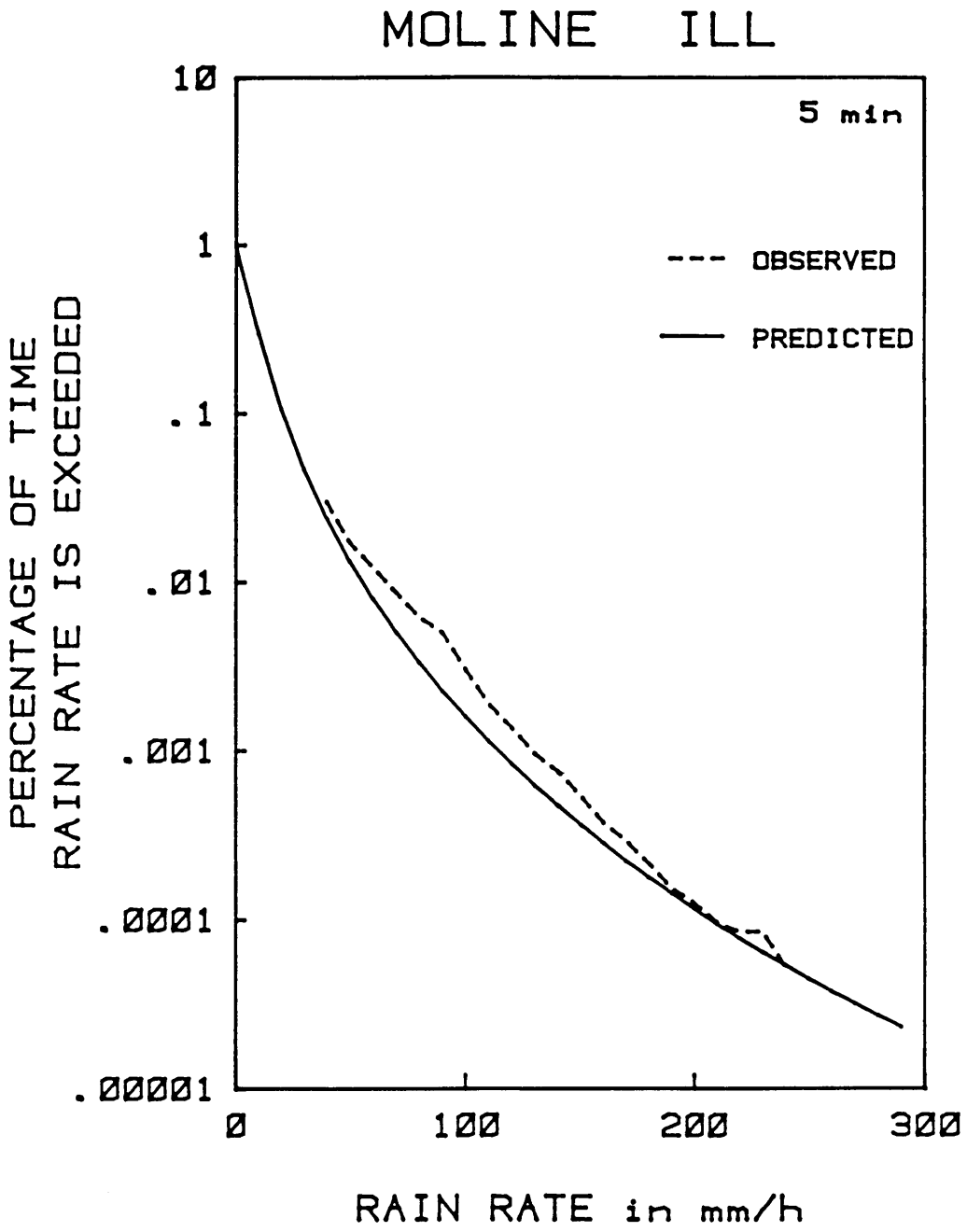

Fig. 69 Observed and predicted 5-min rain-rate distributions for Moline, Illinois.
MAR=833mm; region: 'inland'.

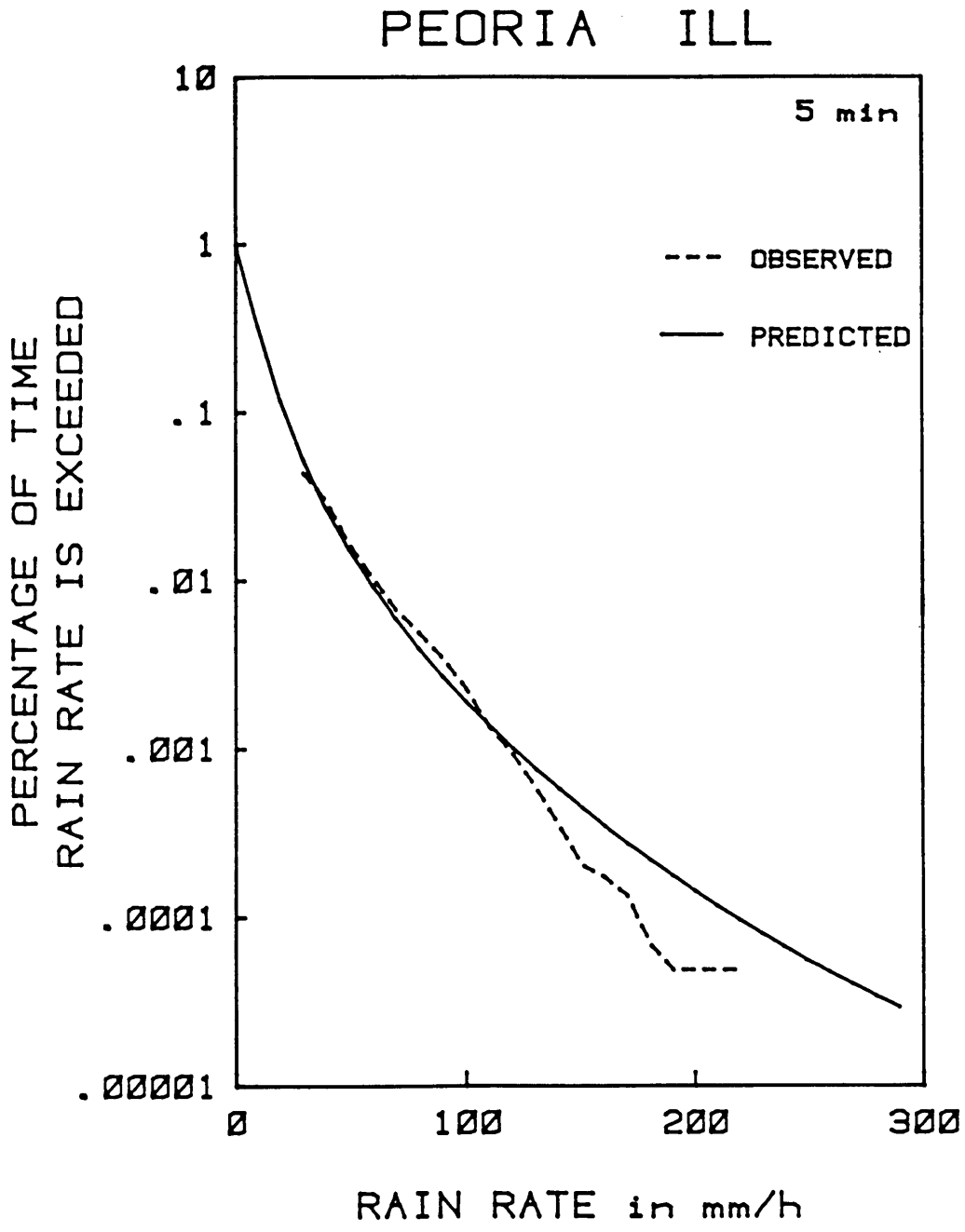

Fig. 70 Observed and predicted 5-min rain-rate distributions for Peoria, Illinois.
MAR=885mm; region: 'inland'.

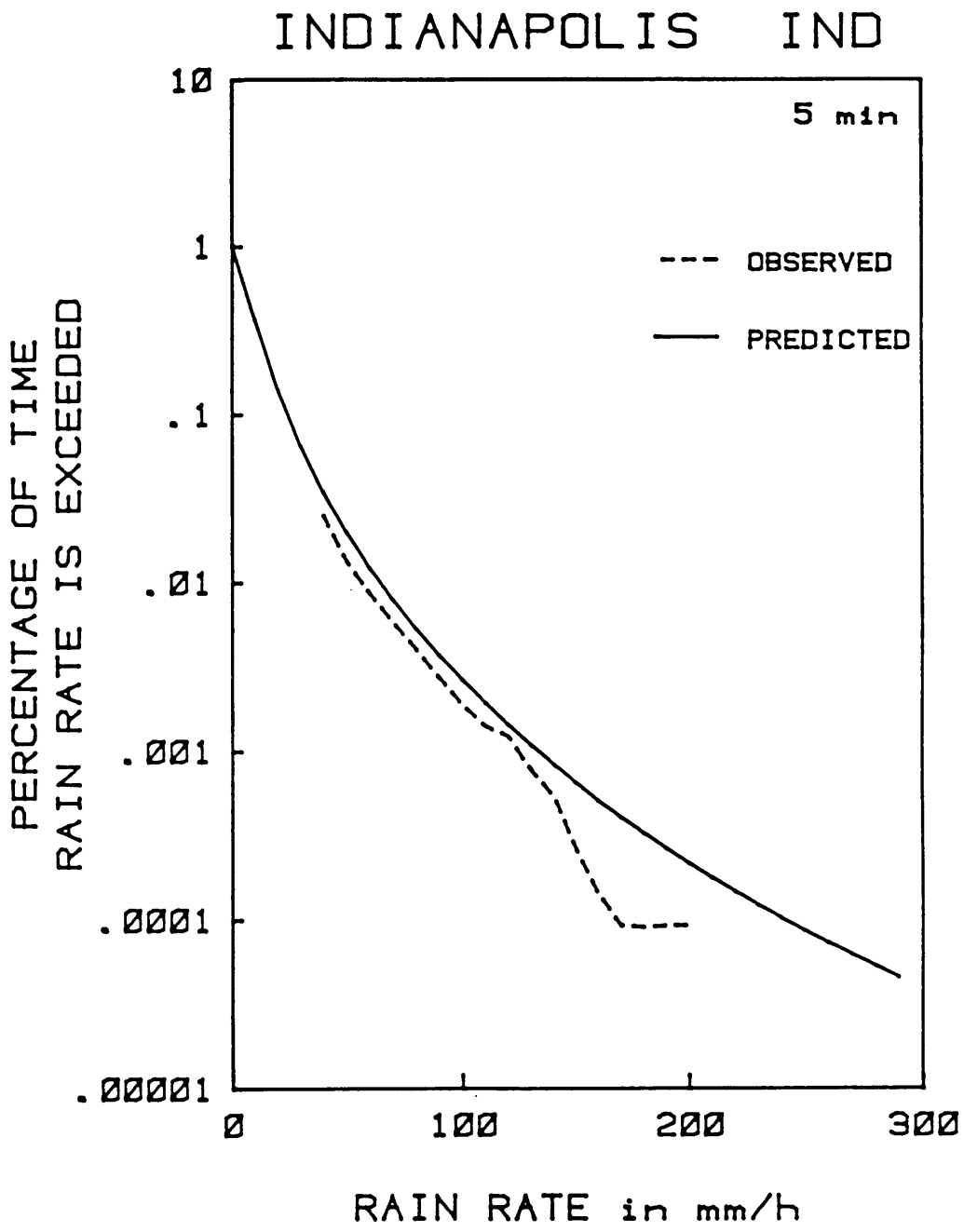

Fig. 71 Observed and predicted 5-min rain-rate distributions for Indianapolis, Indiana. MAR=996mm; region: 'inland'.

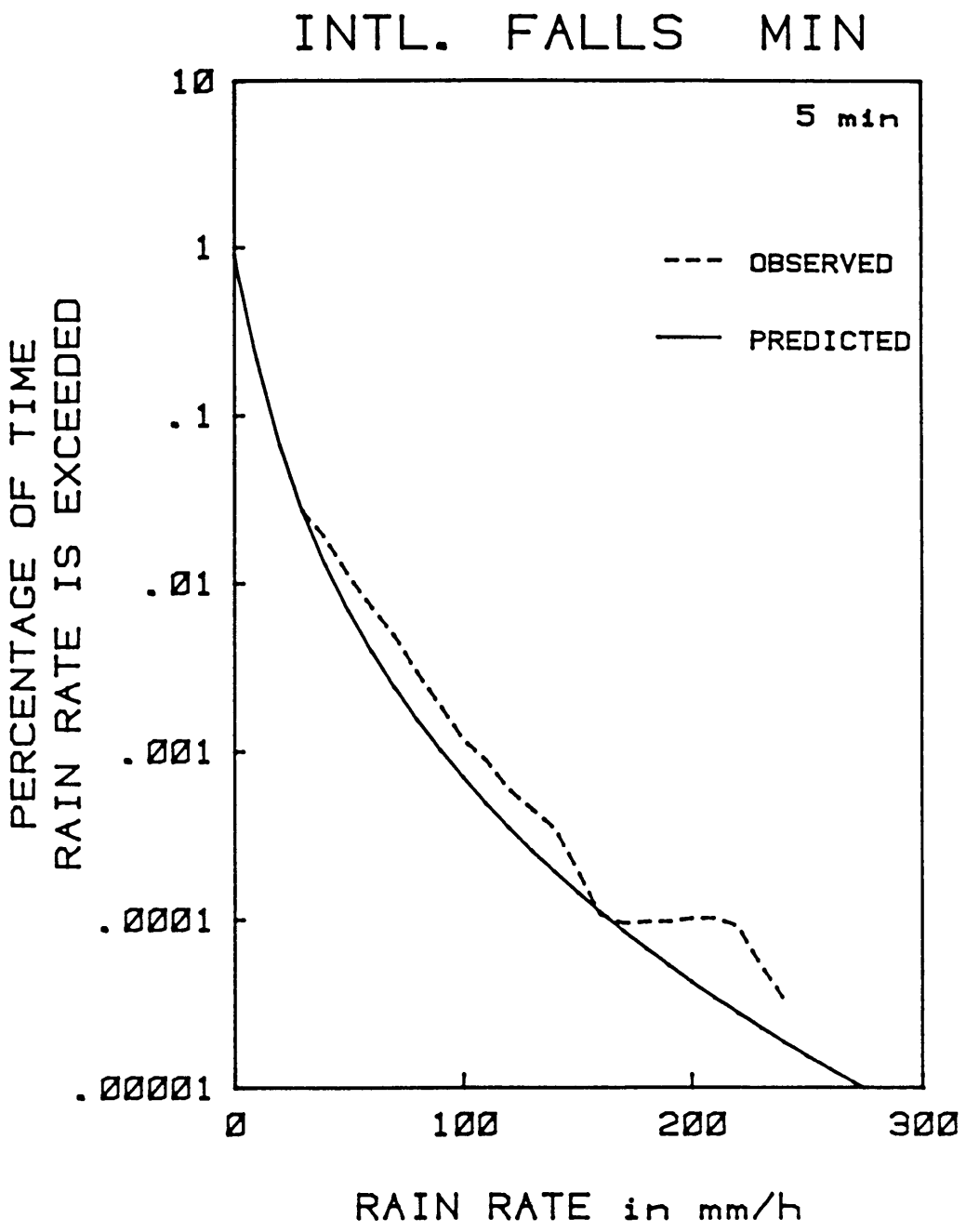

Fig. 72 Observed and predicted 5-min rain-rate distributions for International Falls, Minnesota. MAR=627mm; region: 'inland'.

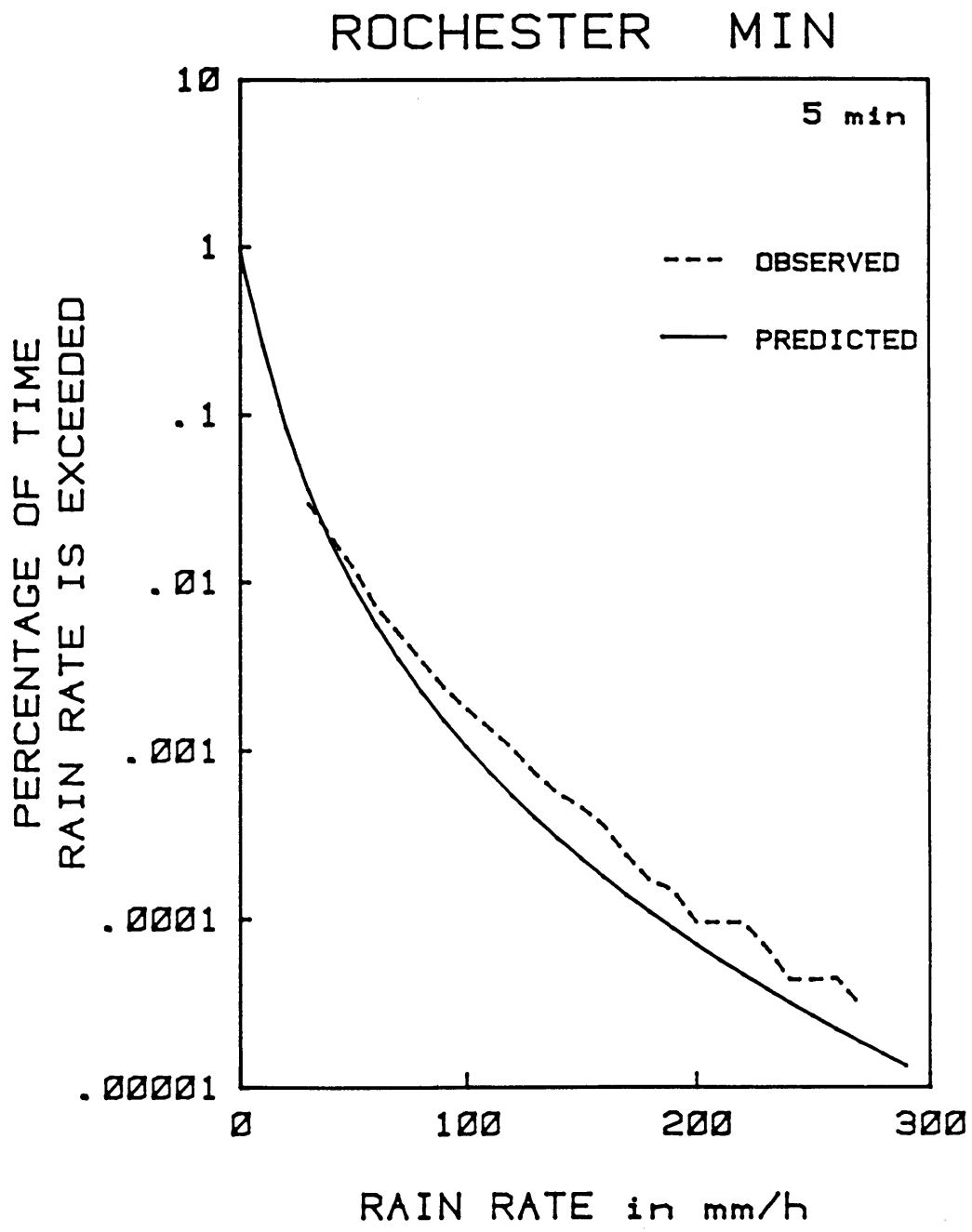

Fig. 73 Observed and predicted 5-min rain-rate distributions for Rochester, Minnesota. MAR=723mm; region: 'inland'.

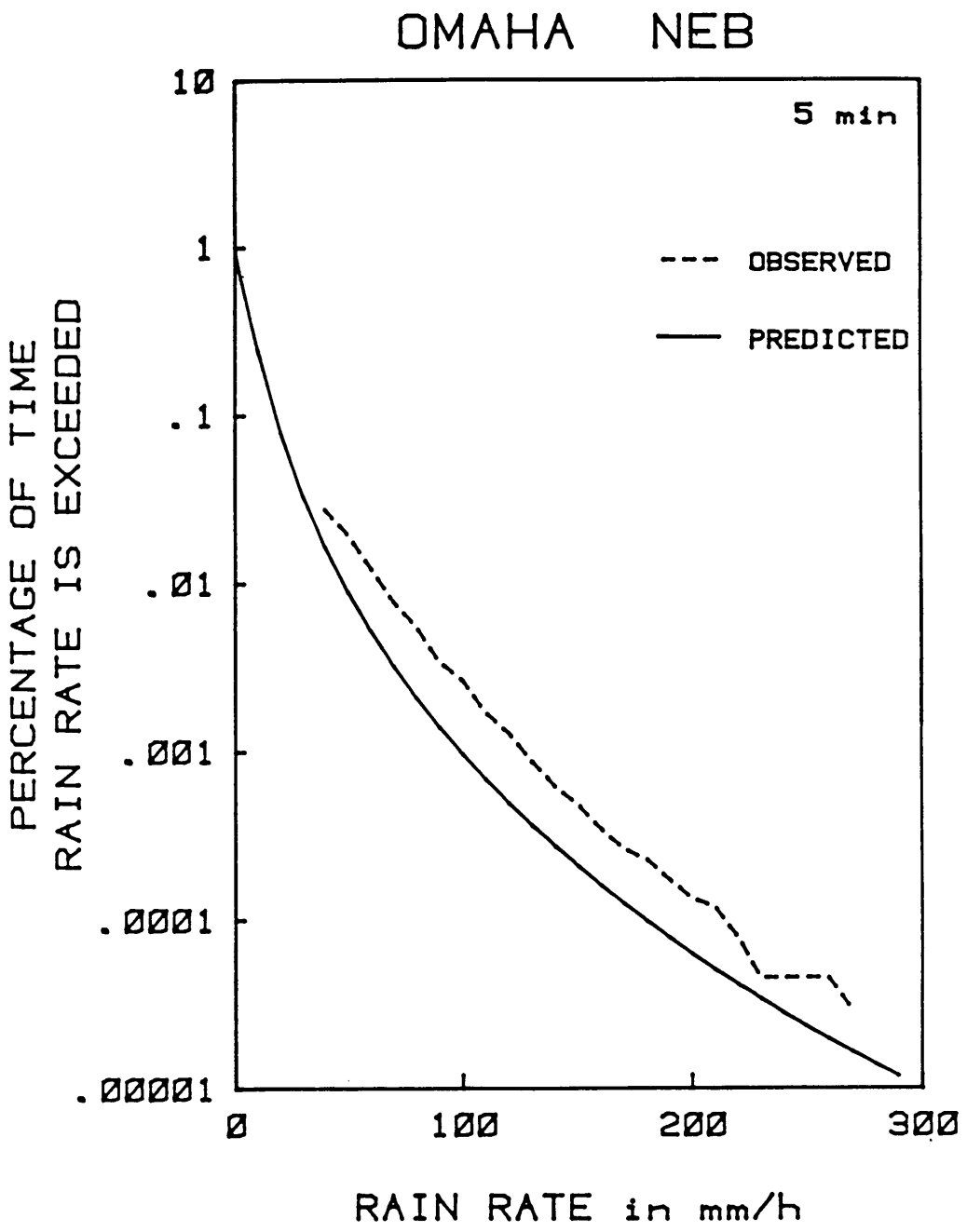

Fig. 74 Observed and predicted 5-min rain-rate distributions for Omaha, Nebraska.
MAR=700mm; region: 'inland'.

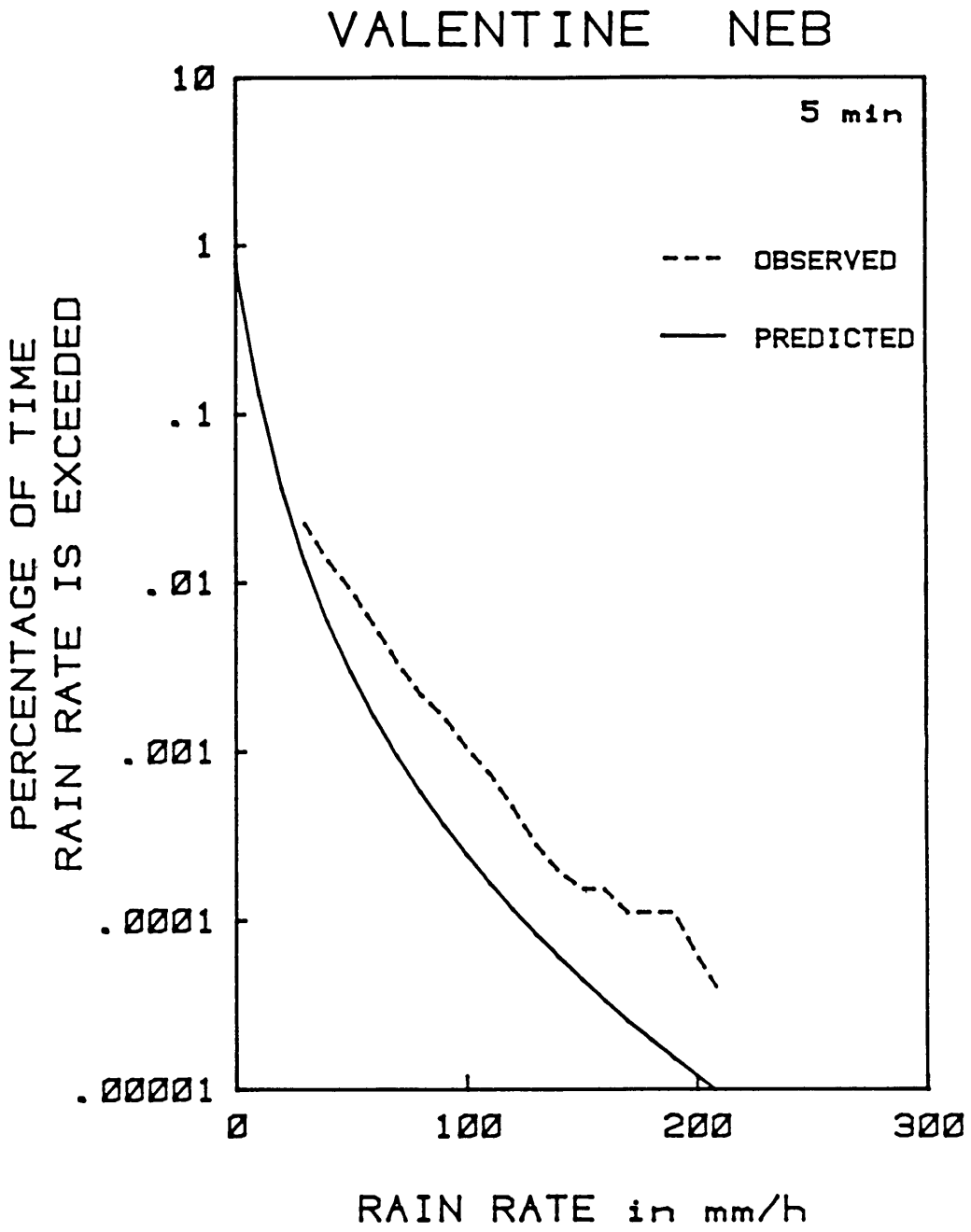

Fig. 75 Observed and predicted 5-min rain-rate distributions for Valentine, Nebraska.
MAR=439mm; region: 'inland'.

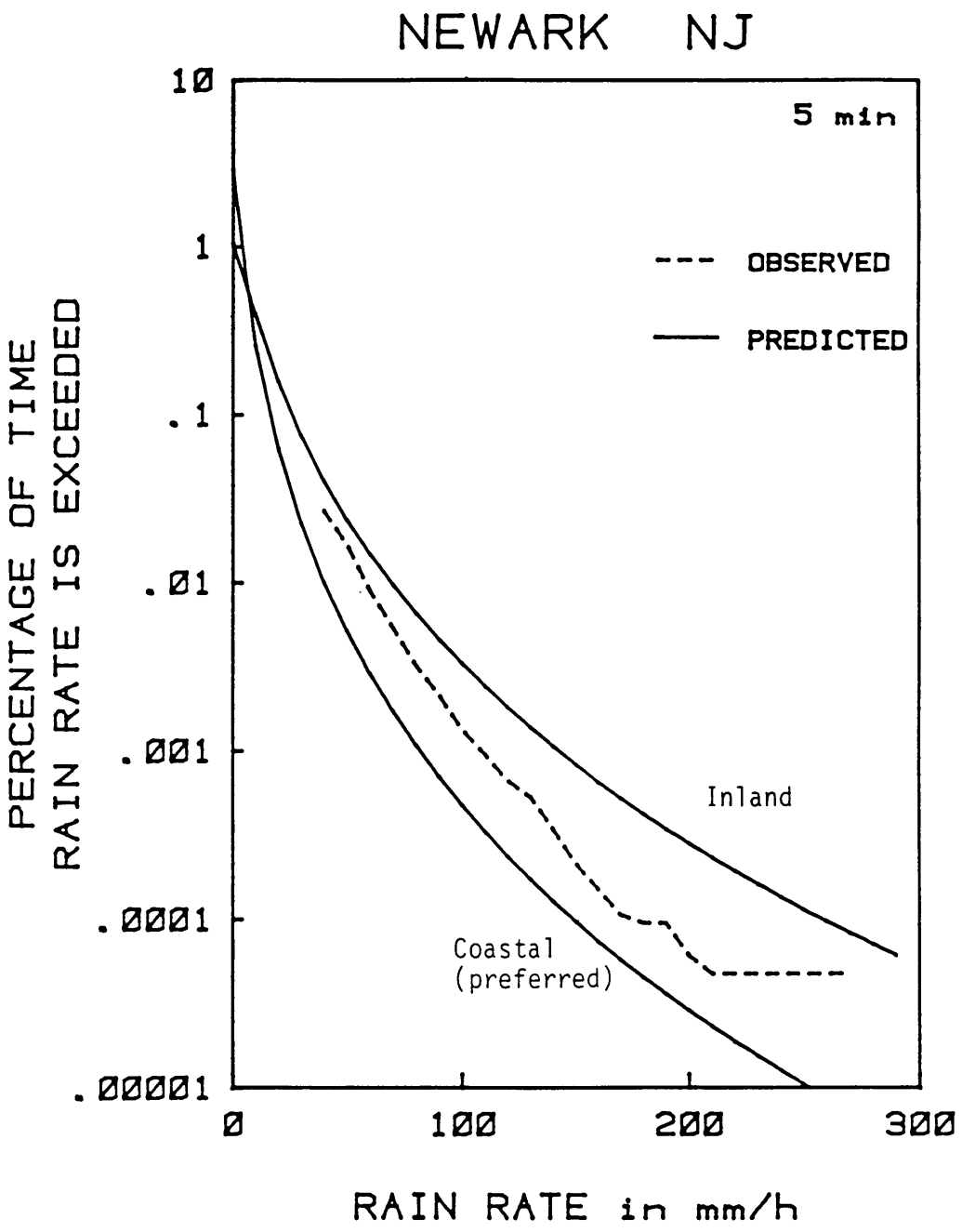

Fig. 76 Observed and predicted 5-min rain-rate distributions for Newark, New Jersey.
MAR=1076mm; region: 'coastal'.

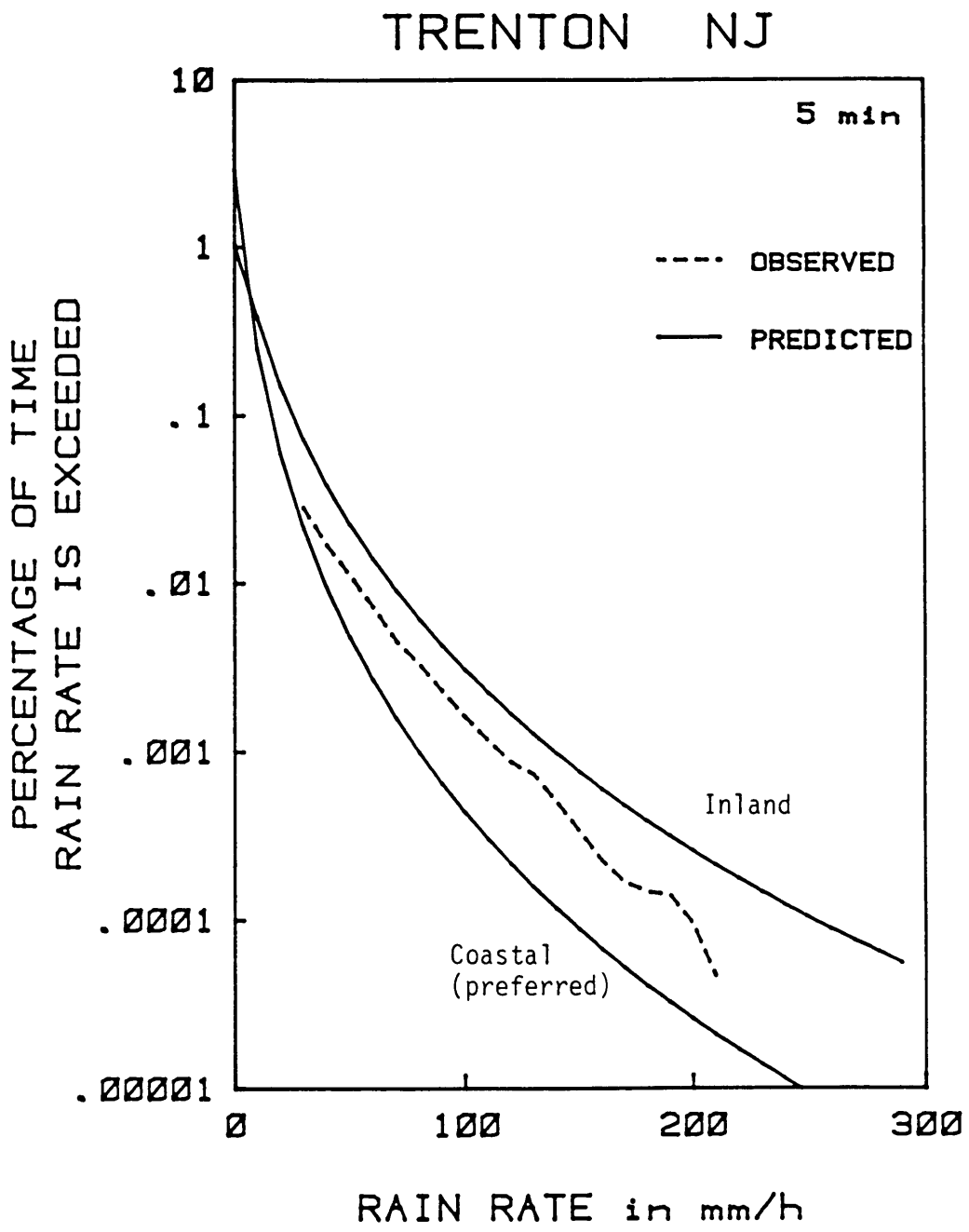

Fig. 77 Observed and predicted 5-min rain-rate distributions for Trenton, New Jersey.
MAR=1049mm; region: 'coastal'.

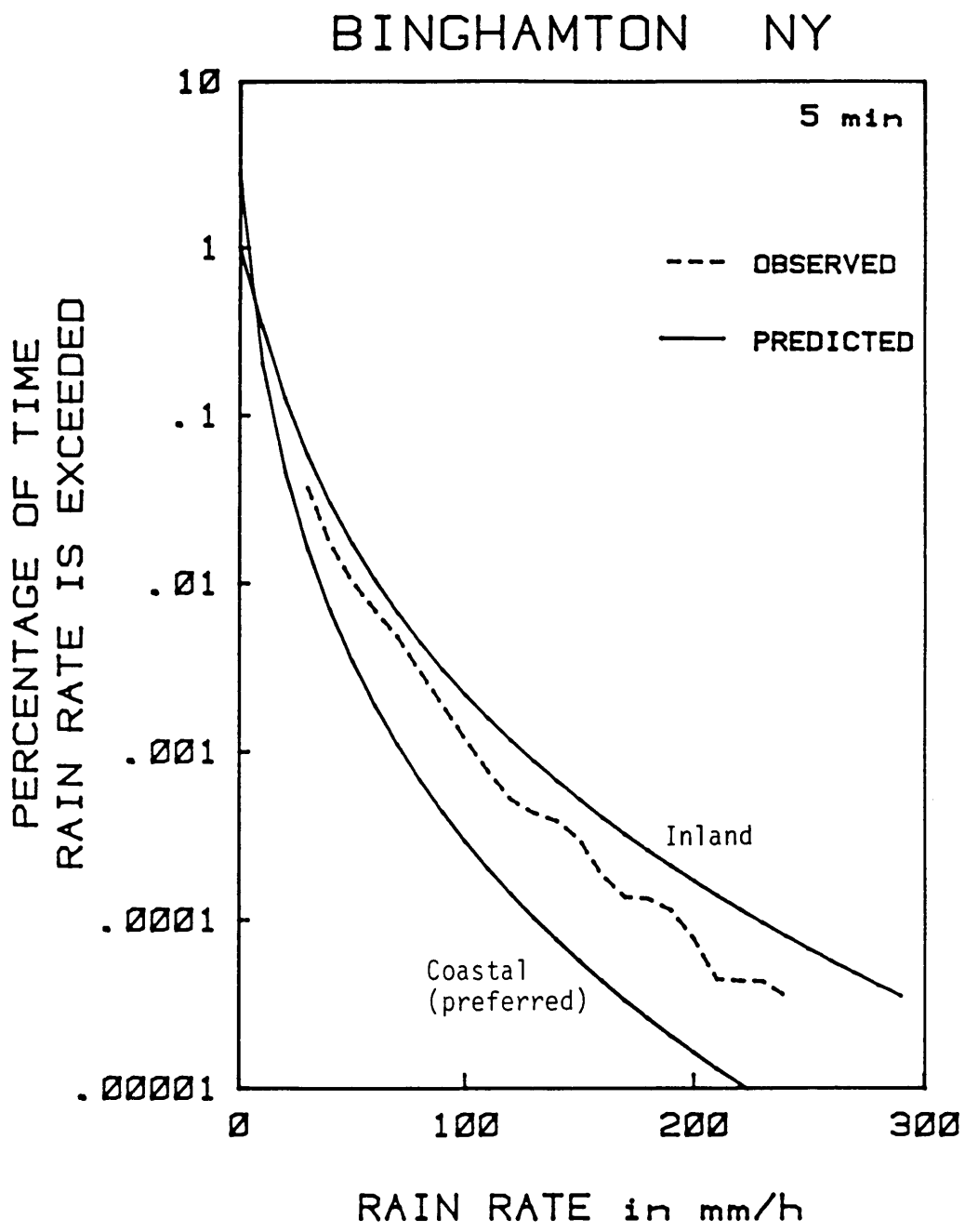

Fig. 78 Observed and predicted 5-min rain-rate distributions for Binghamton, New York. MAR=931mm; region: 'coastal'.

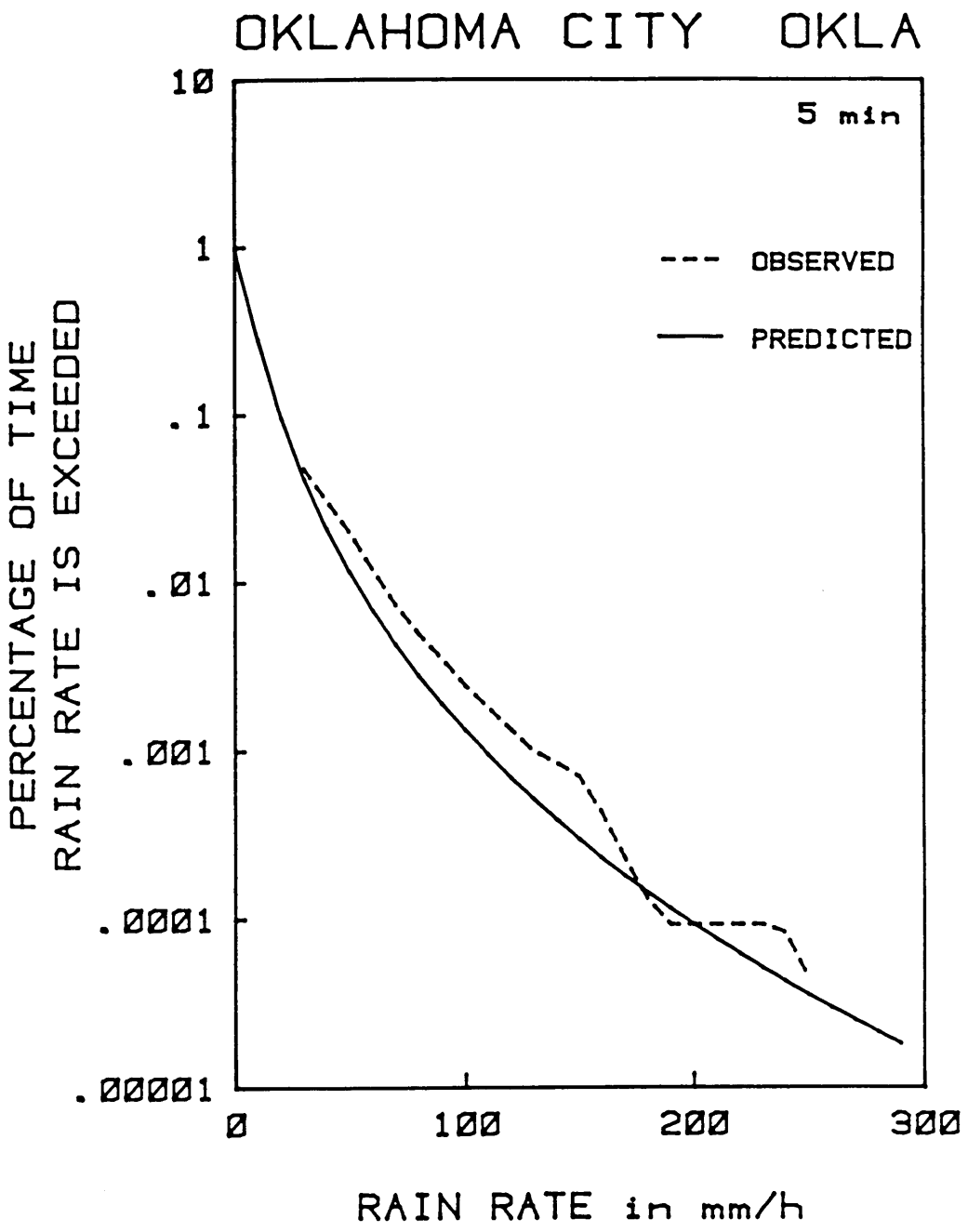

Fig. 79 Observed and predicted 5-min rain-rate distributions for Oklahoma City, Oklahoma. MAR=783mm; region: 'inland'.

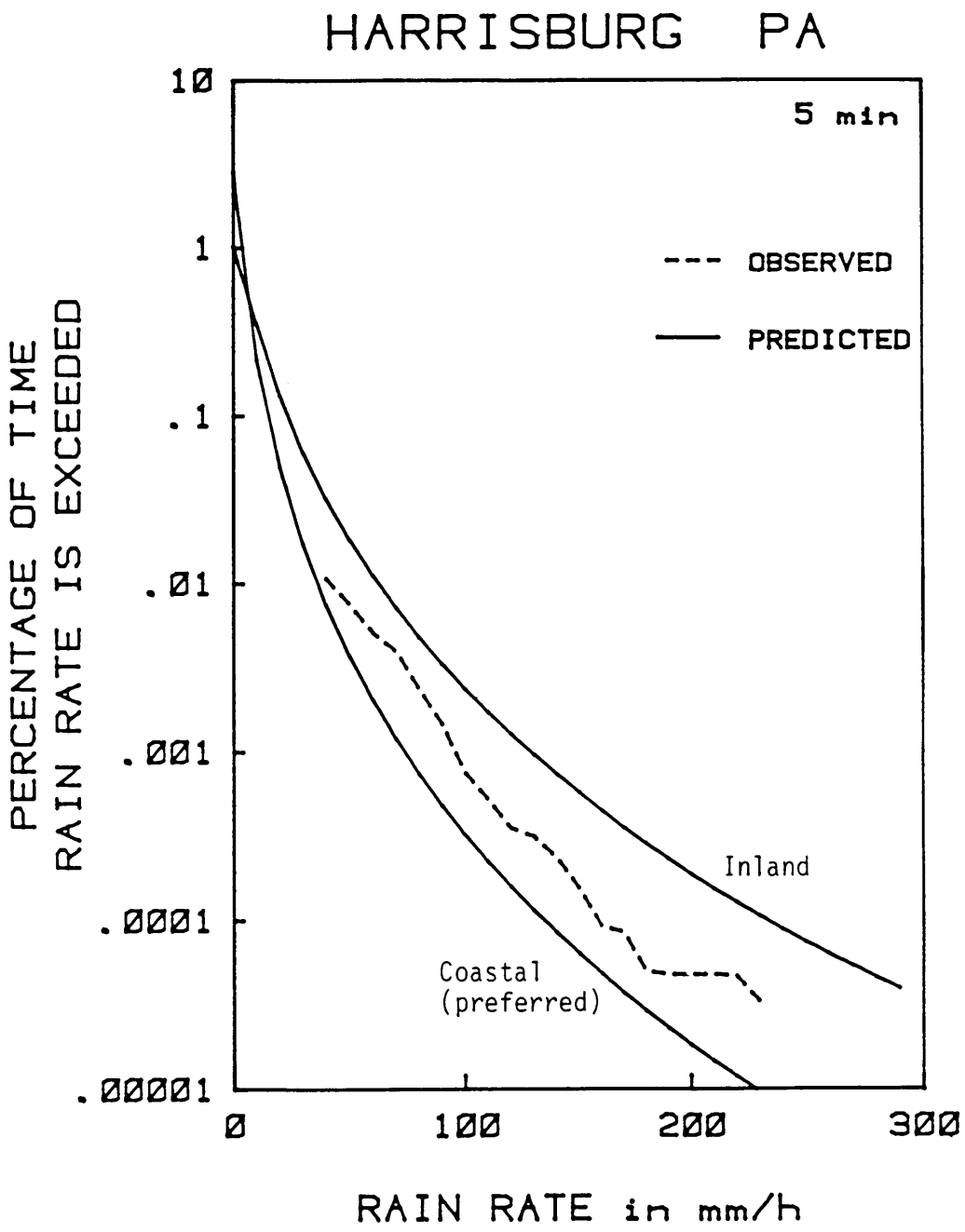

Fig. 80 Observed and predicted 5-min rain-rate distributions for Harrisburg, Pennsylvania. MAR=957mm; region: 'coastal'.

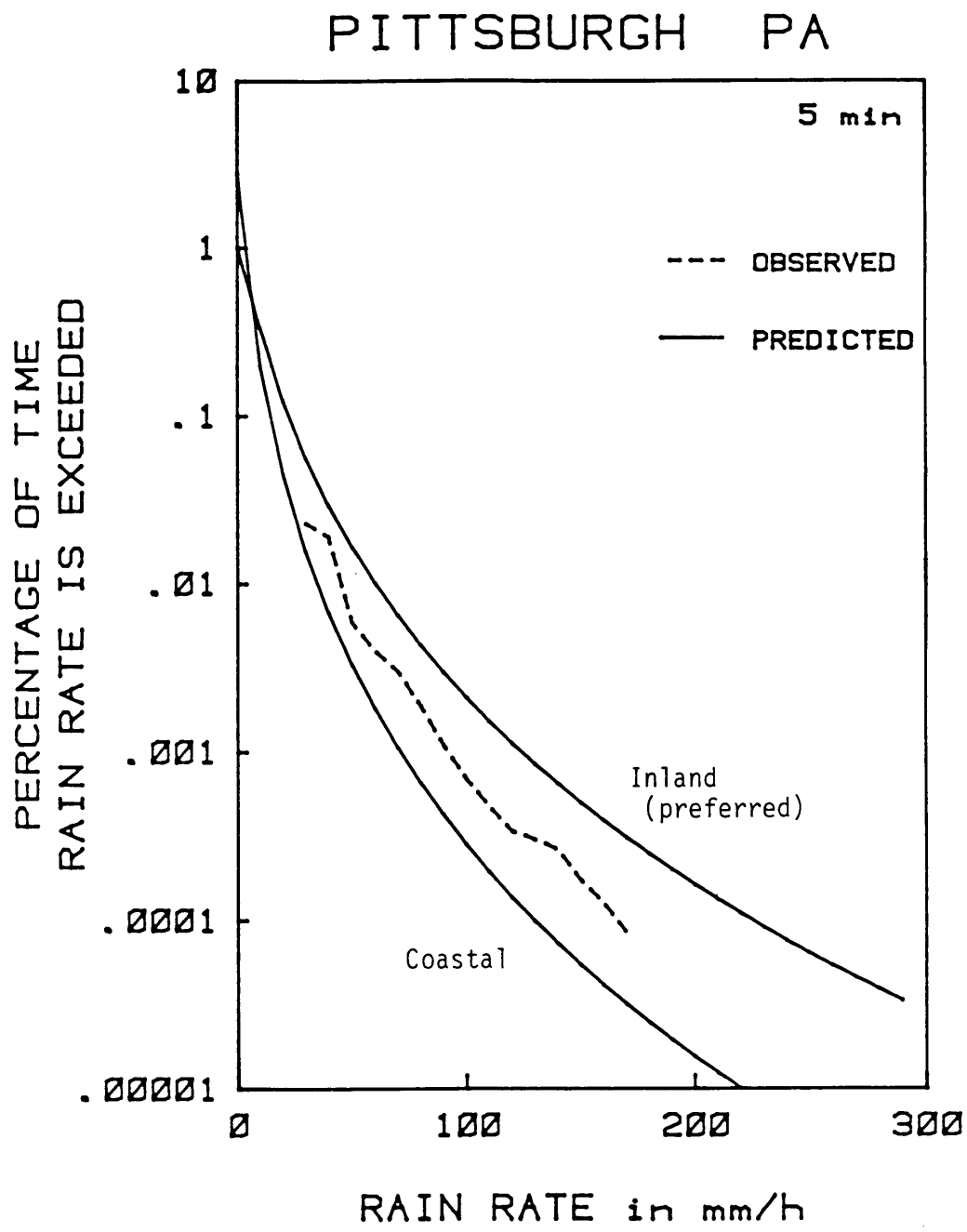

Fig. 81 Observed and predicted 5-min rain-rate distributions for Pittsburgh, Pennsylvania. MAR=918mm; region: 'inland'.

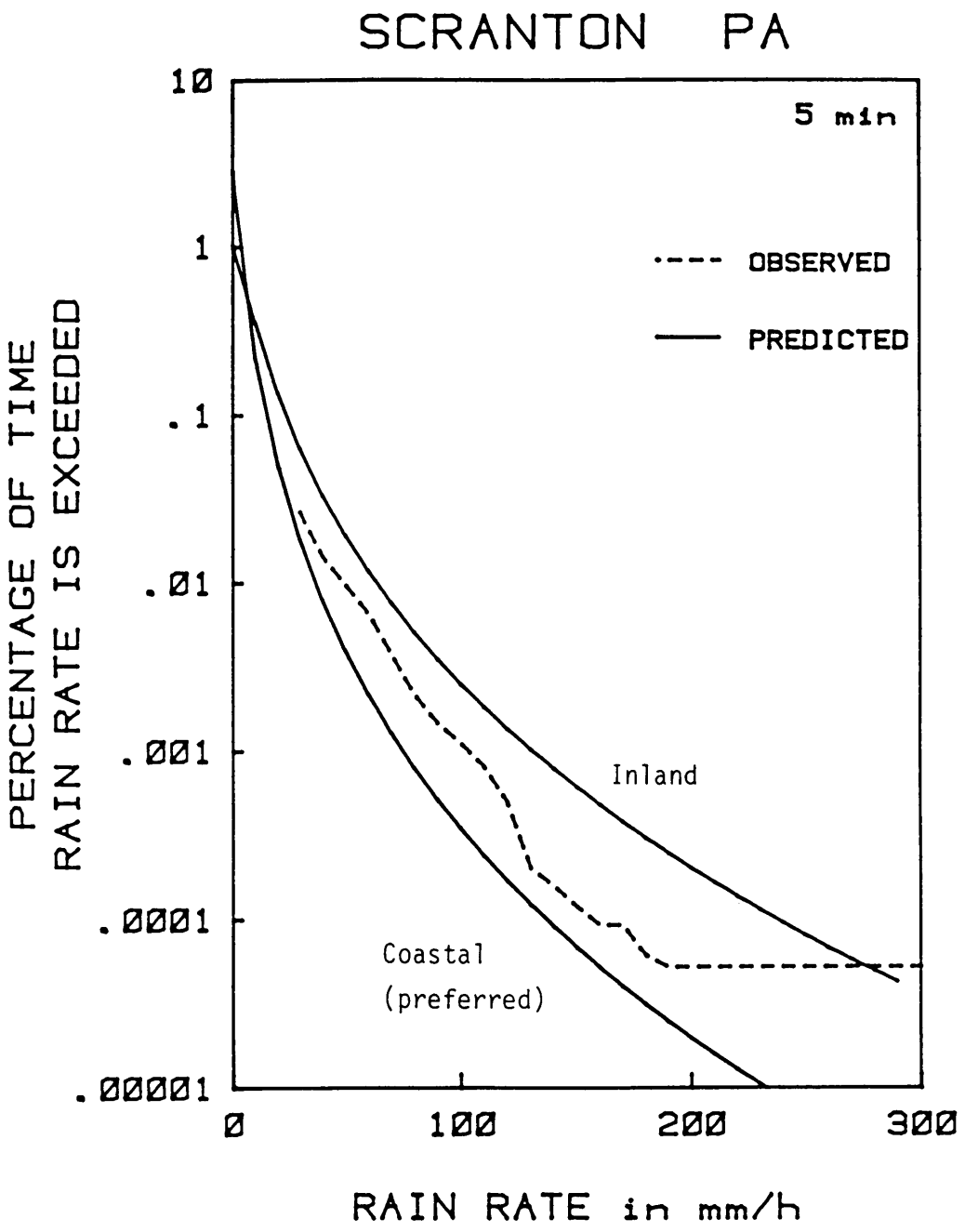

Fig. 82 Observed and predicted 5-min rain-rate distributions for Scranton, Pennsylvania. MAR=977mm; region: 'coastal'.

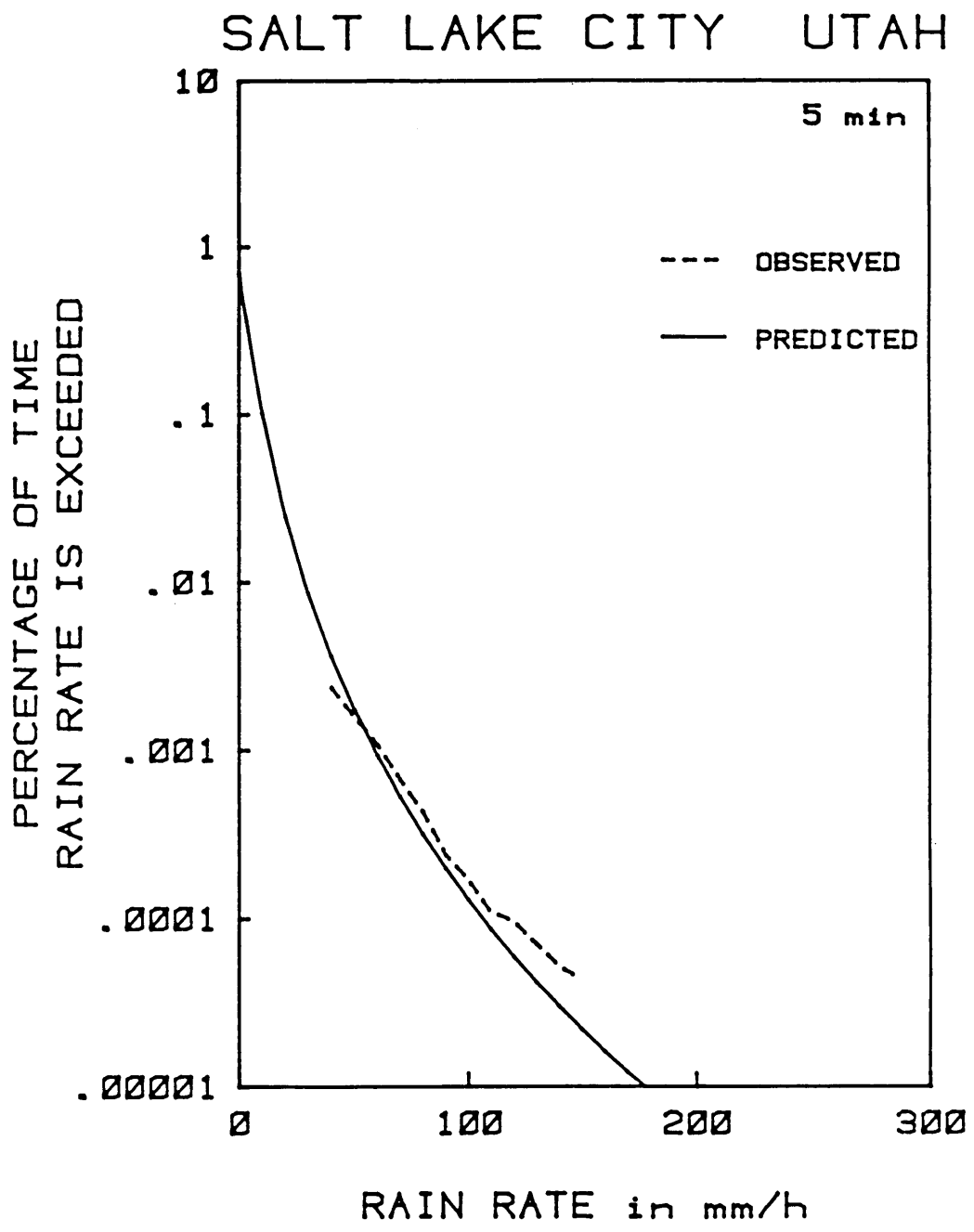

Fig. 83 Observed and predicted 5-min rain-rate distributions for Salt Lake City, Utah. MAR=353mm; region: 'inland'.

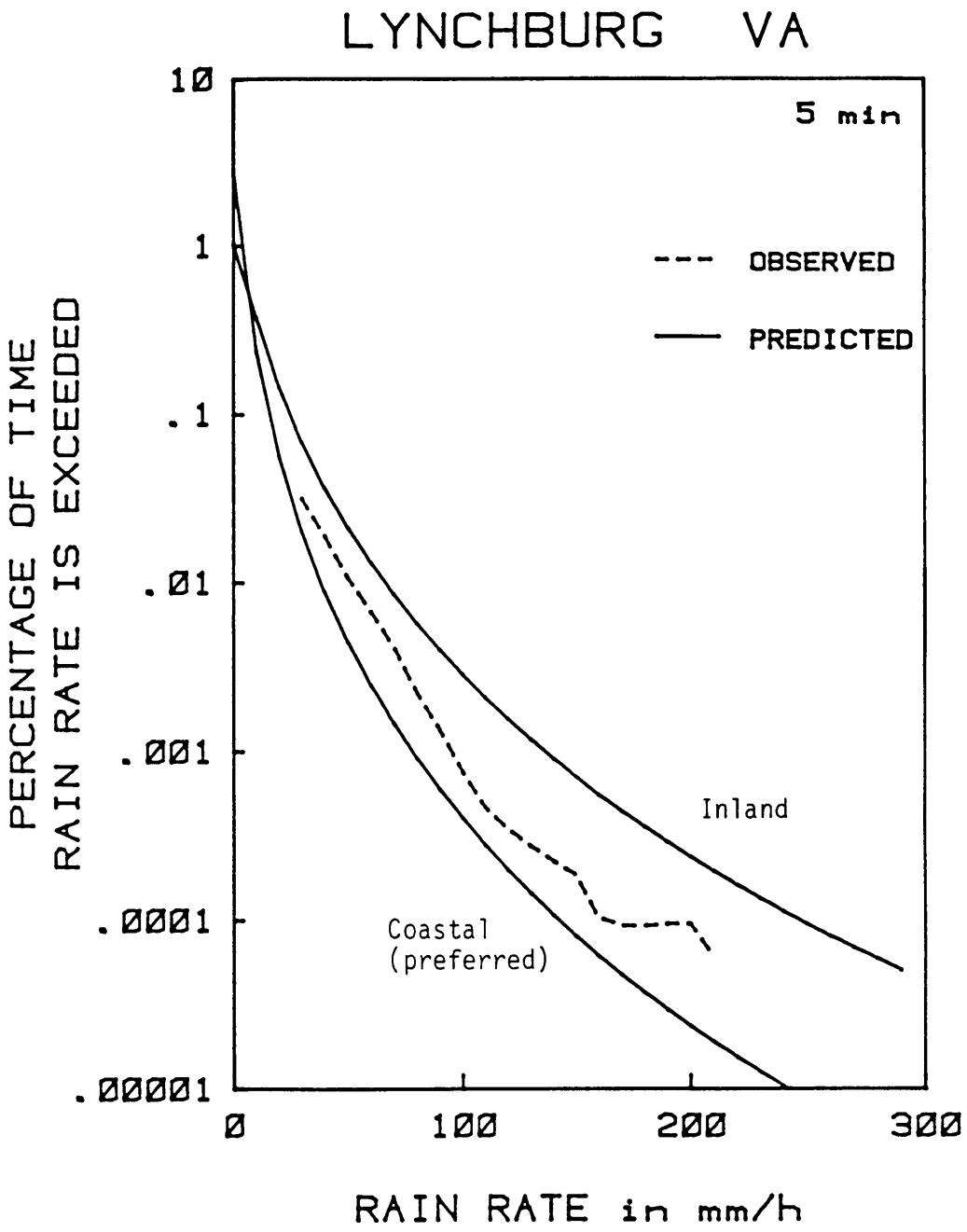

Fig. 84 Observed and predicted 5-min rain-rate distributions for Lynchburg, Virginia.
MAR=1023mm; region: 'coastal'.

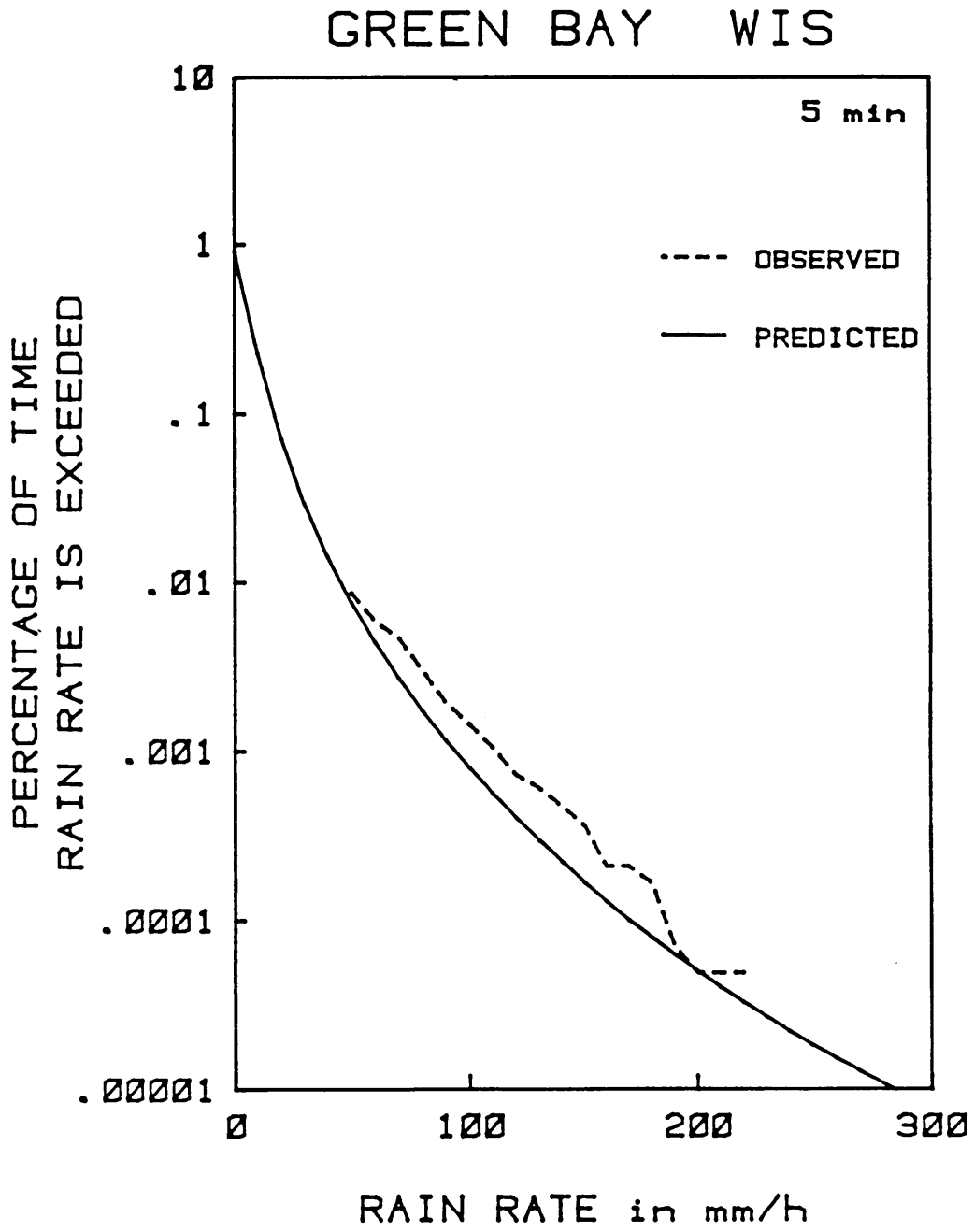

Fig. 85 Observed and predicted 5-min rain-rate distributions for Green Bay, Wisconsin. MAR=656mm; region: 'inland'.

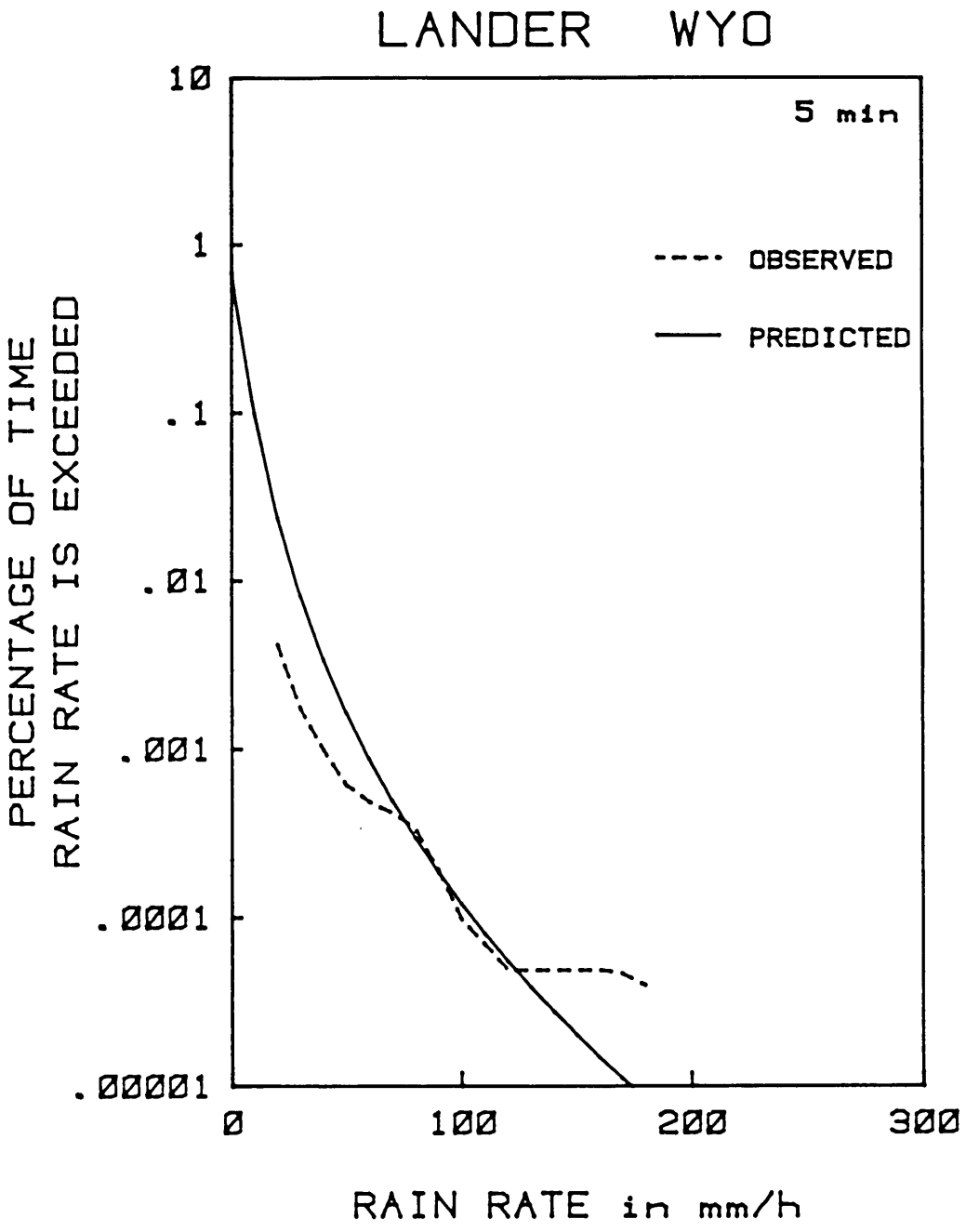

Fig. 86 Observed and predicted 5-min rain-rate distributions for Lander, Wyoming.
MAR=344mm; region: 'inland'.

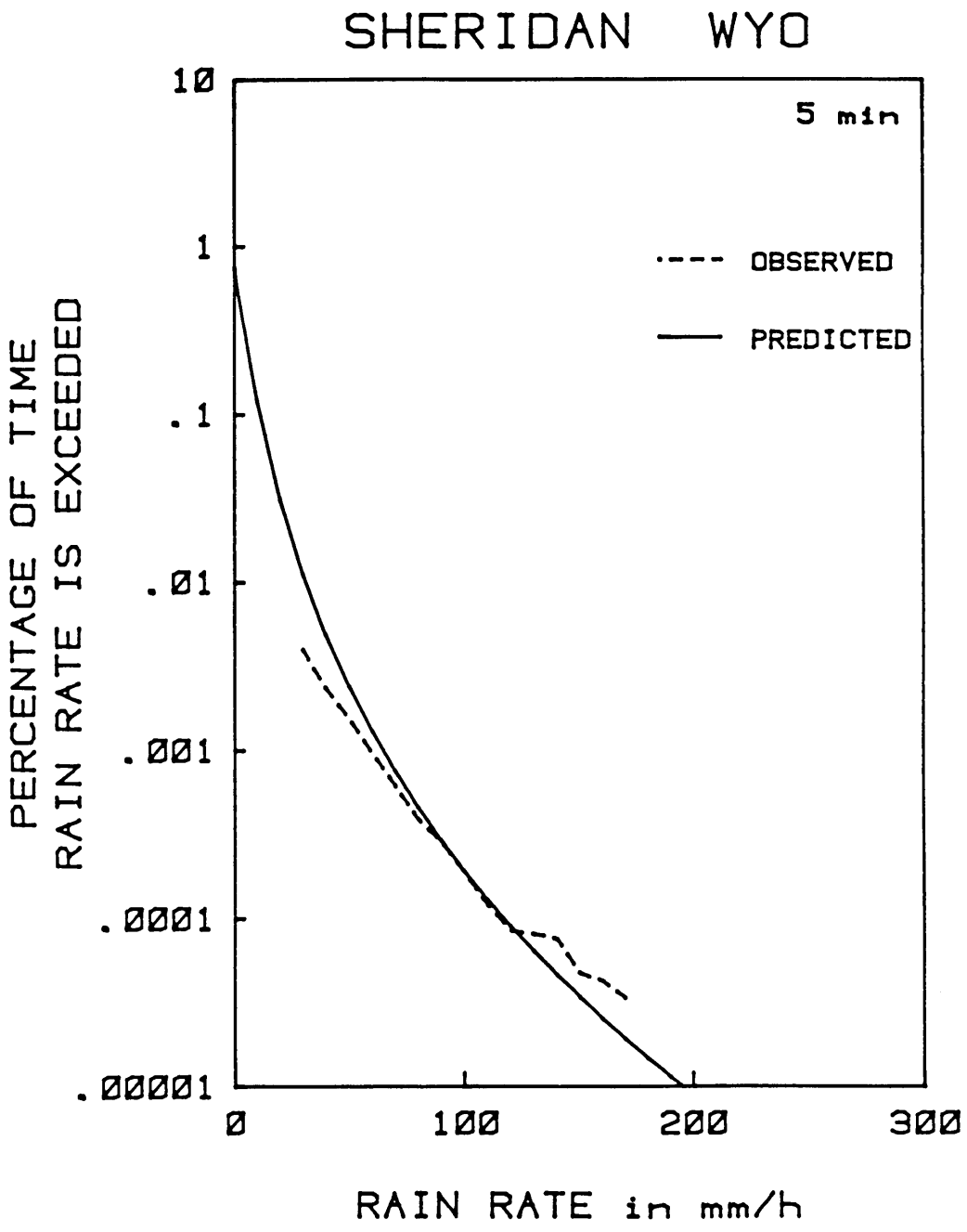

Fig. 87 Observed and predicted 5-min rain-rate distributions for Sheridan, Wyoming.
MAR=404mm; region: 'inland'.

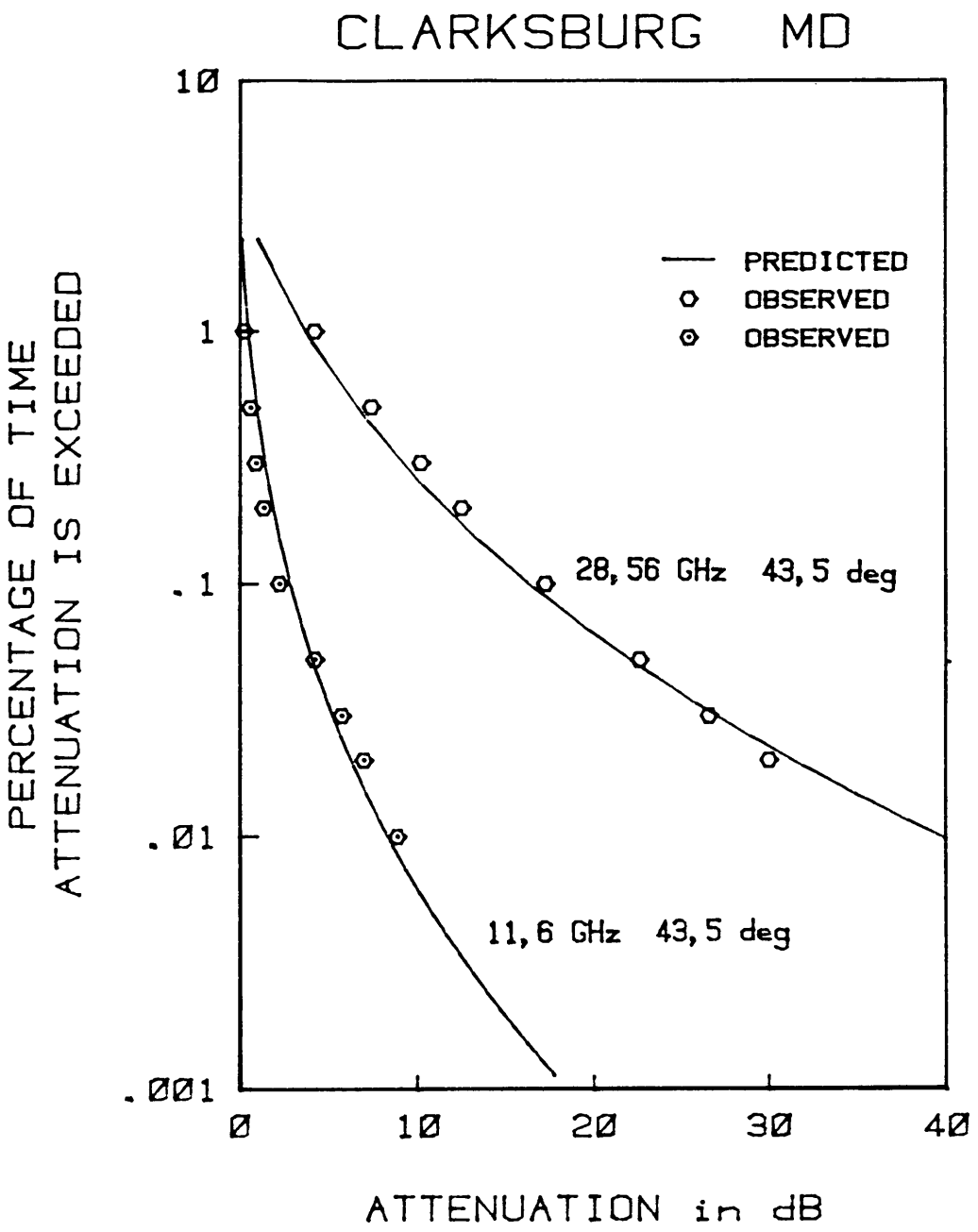

Fig. 88 Predicted and observed distributions for Clarksburg, Maryland. Elevation angle and frequency as shown. Other input parameters: MAR=1036mm; region=coastal; altitude=50m. The observed distribution at 28,56 GHz was obtained by measurement of COMSTAR D-3 during 18 August 1978 to 1 Sept 1980. The 11,6-GHz distribution was obtained by radiometer during the same period [Kumar, 1982].

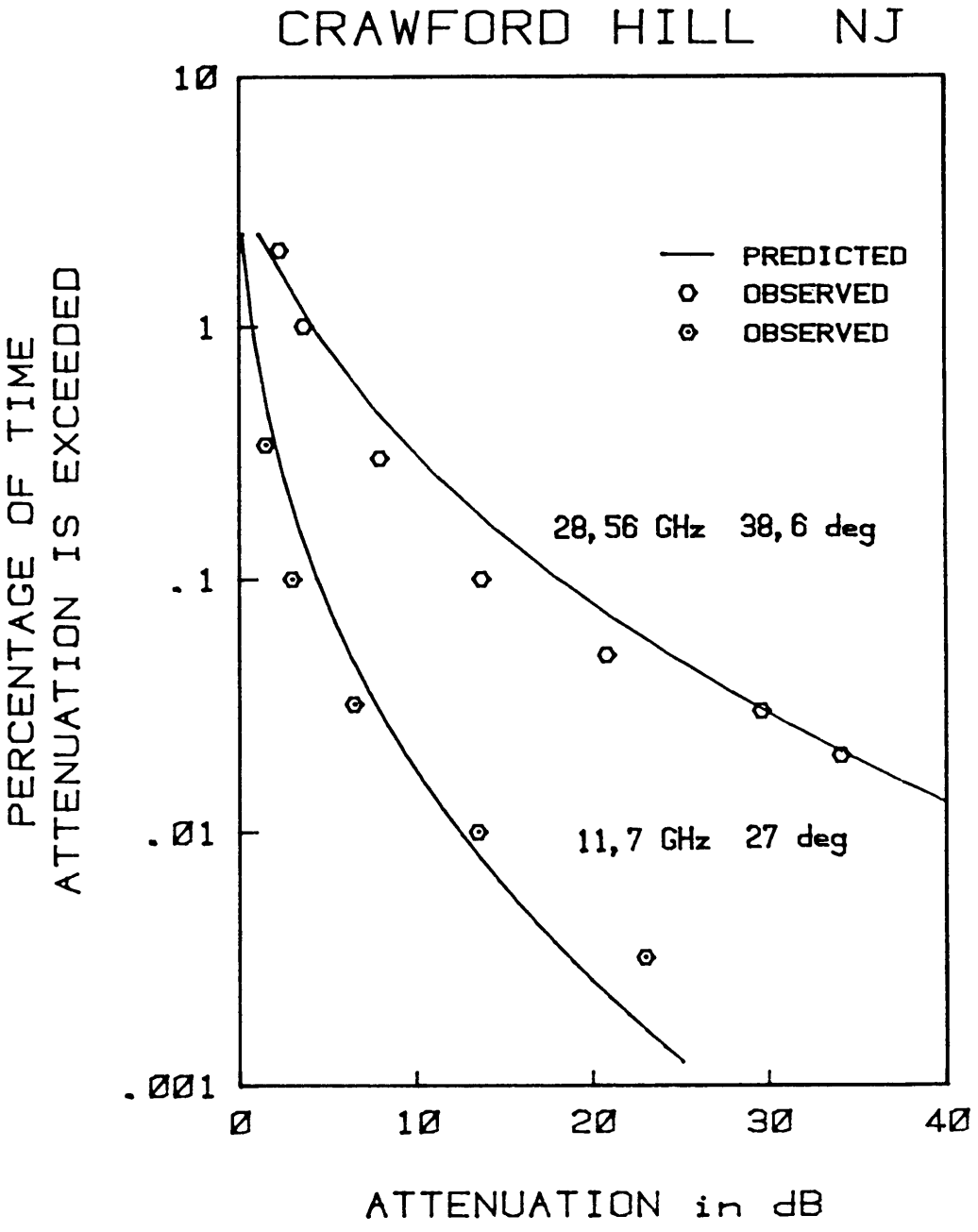

Fig. 89 Predicted and observed distributions for Crawford Hill, New Jersey. Elevation angle and frequency as shown. Other input parameters: MAR=1062mm; region=coastal; altitude=120m. The observed distribution was obtained with COMSTAR B during 19 May 1977 to 18 May 1978. The 11,7 GHz distribution was obtained by measurement with CTS for the period 7 June 1976 to 6 June 1978 [Arnold et al., 1981].

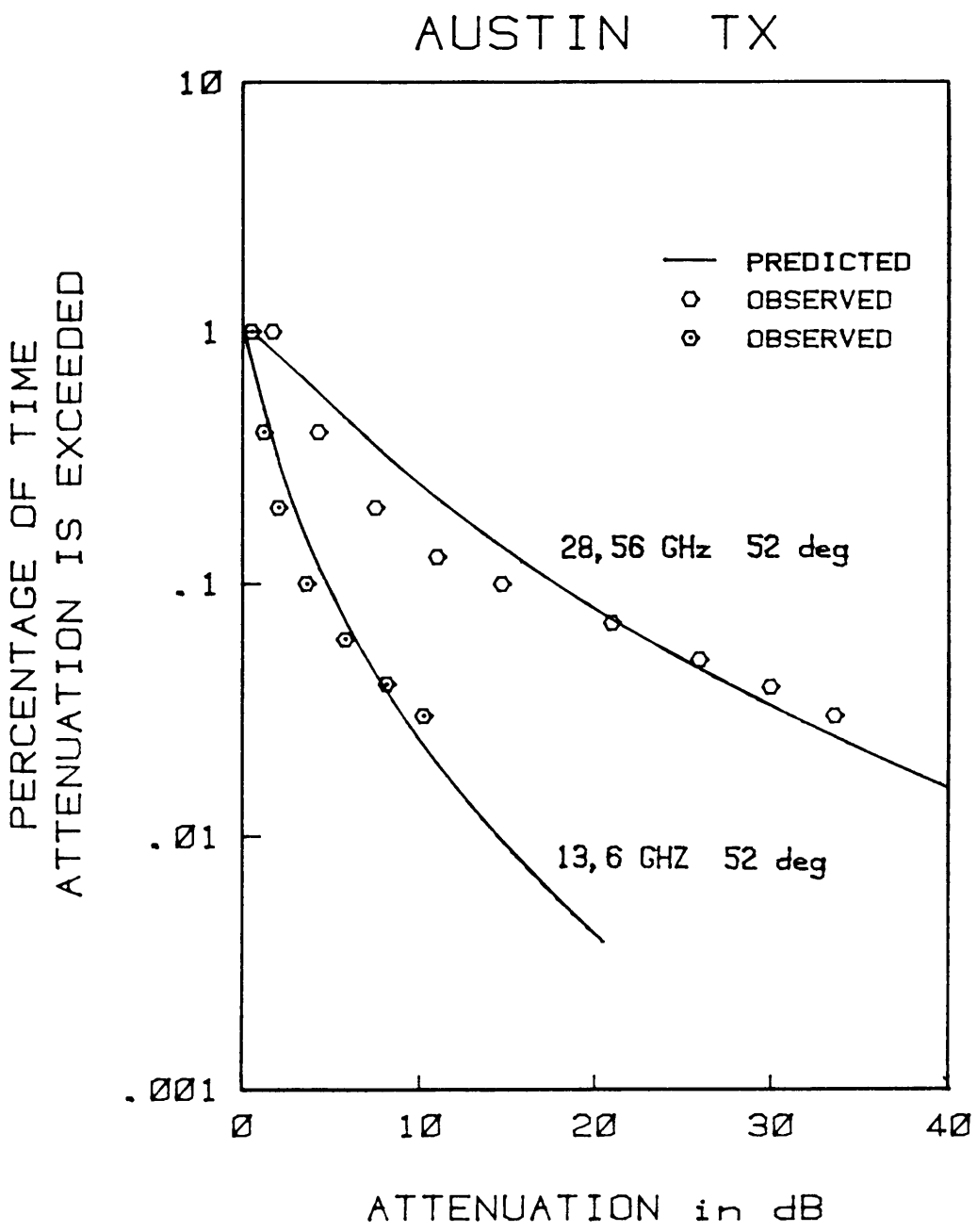

Fig. 90 Predicted and observed distributions for Austin, Texas. Elevation angle and frequency as shown. Other input parameters: MAR=827mm; region=inland; altitude=246m. The observed distribution at 28,56 GHz was obtained with COMSTAR D-3 during October 1978 to August 1980. The 13,6 GHz distribution was obtained by radiometer during the same period [Vogel, 1982].

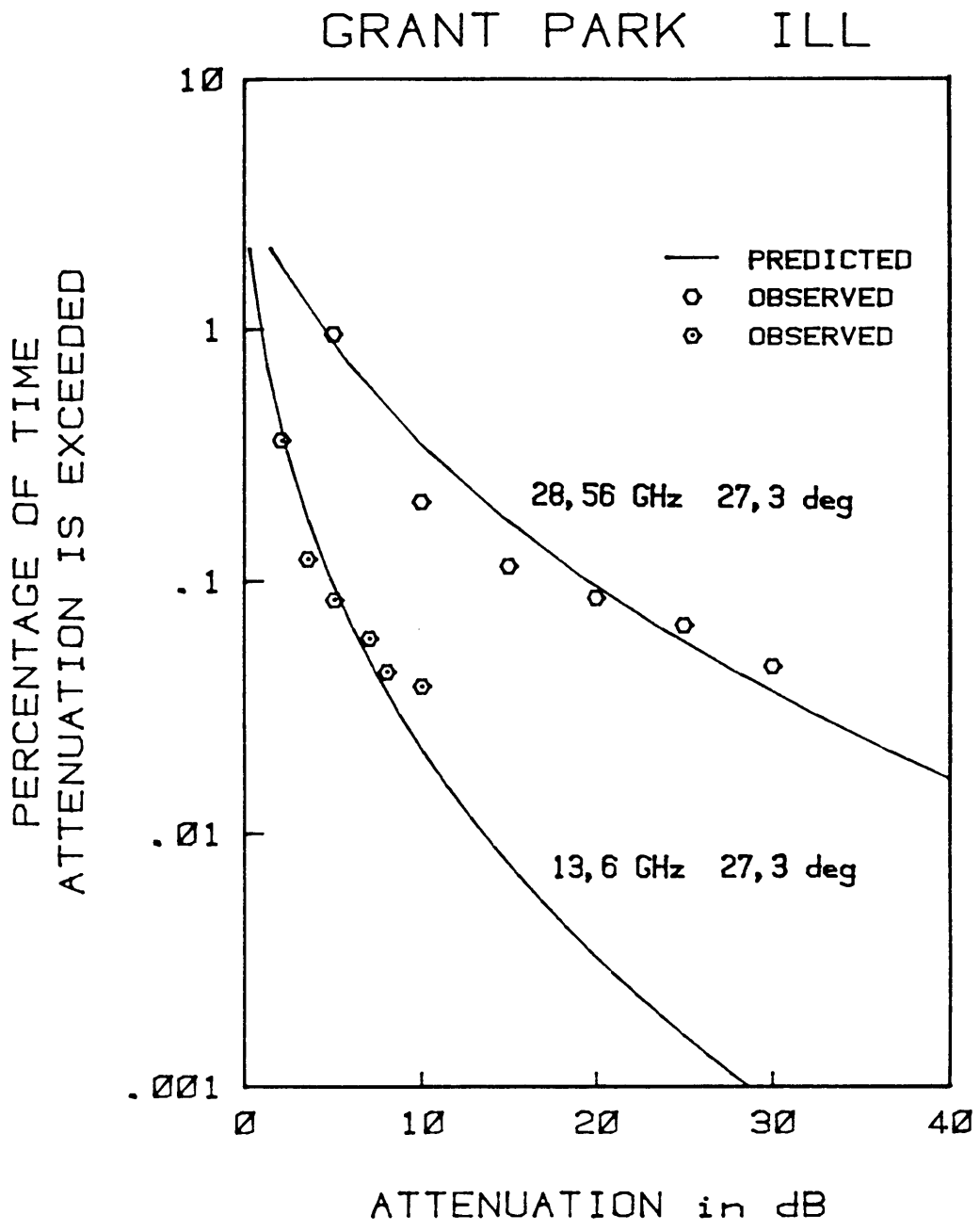

Fig. 91 Predicted and observed distributions for Grant Park, Illinois. Elevation angle and frequency as shown. Other input parameters: MAR=842mm; region=coastal; altitude=200m. The observed distribution at 28,56 GHz was obtained with a COMSTAR beacon during July 1976 to June 1977. The 13,6 GHz distribution was obtained by radiometer during the same period [Lin, 1979].

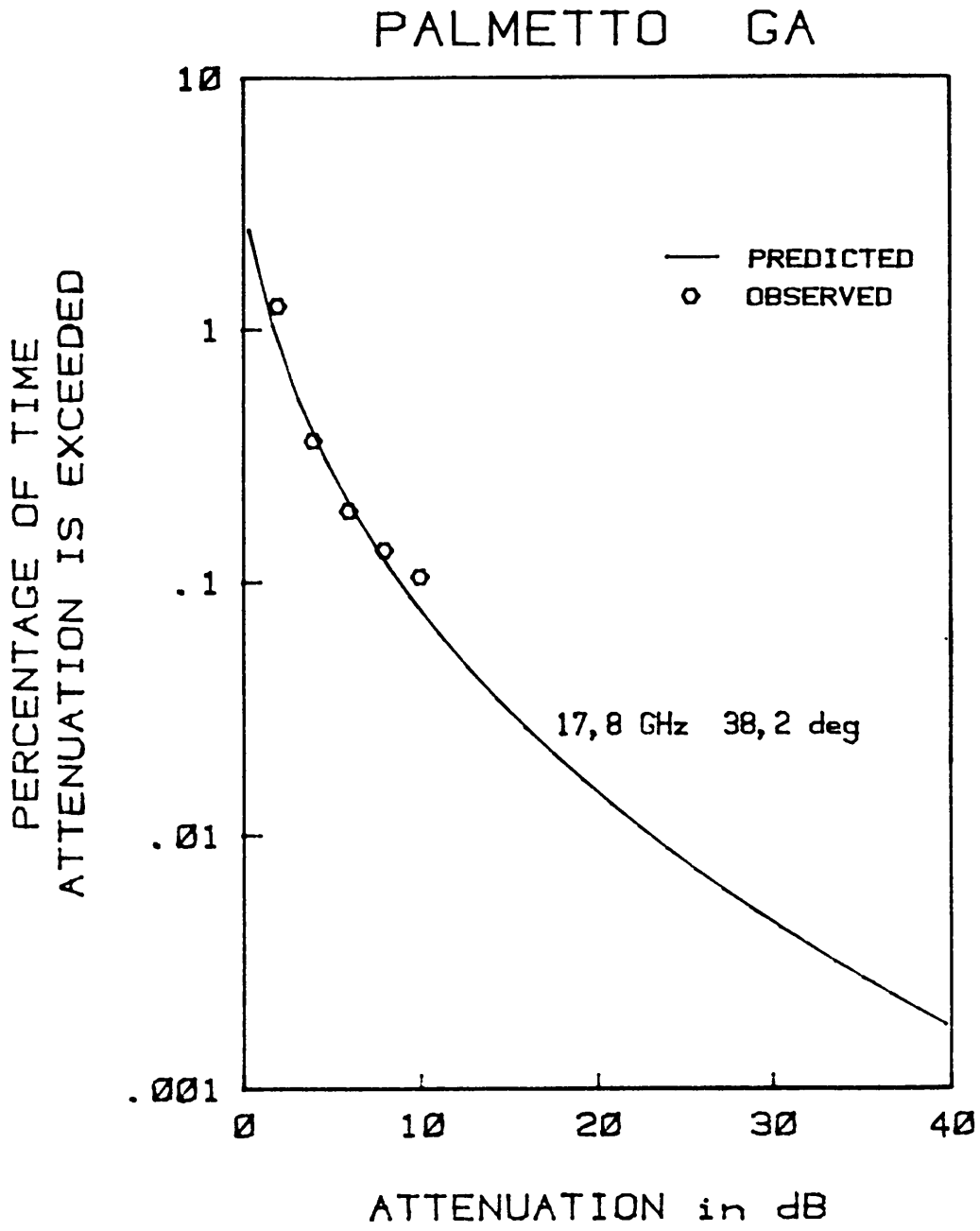

Fig. 92 Predicted and observed distributions at 17,8 GHz for Palmetto, Georgia. Elevation angle as shown. Other input parameters: MAR= 1197mm; region=coastal; altitude=290m. The observed distribution was obtained by radiometer during June 1973 to June 1975 [Lin et al., 1980].

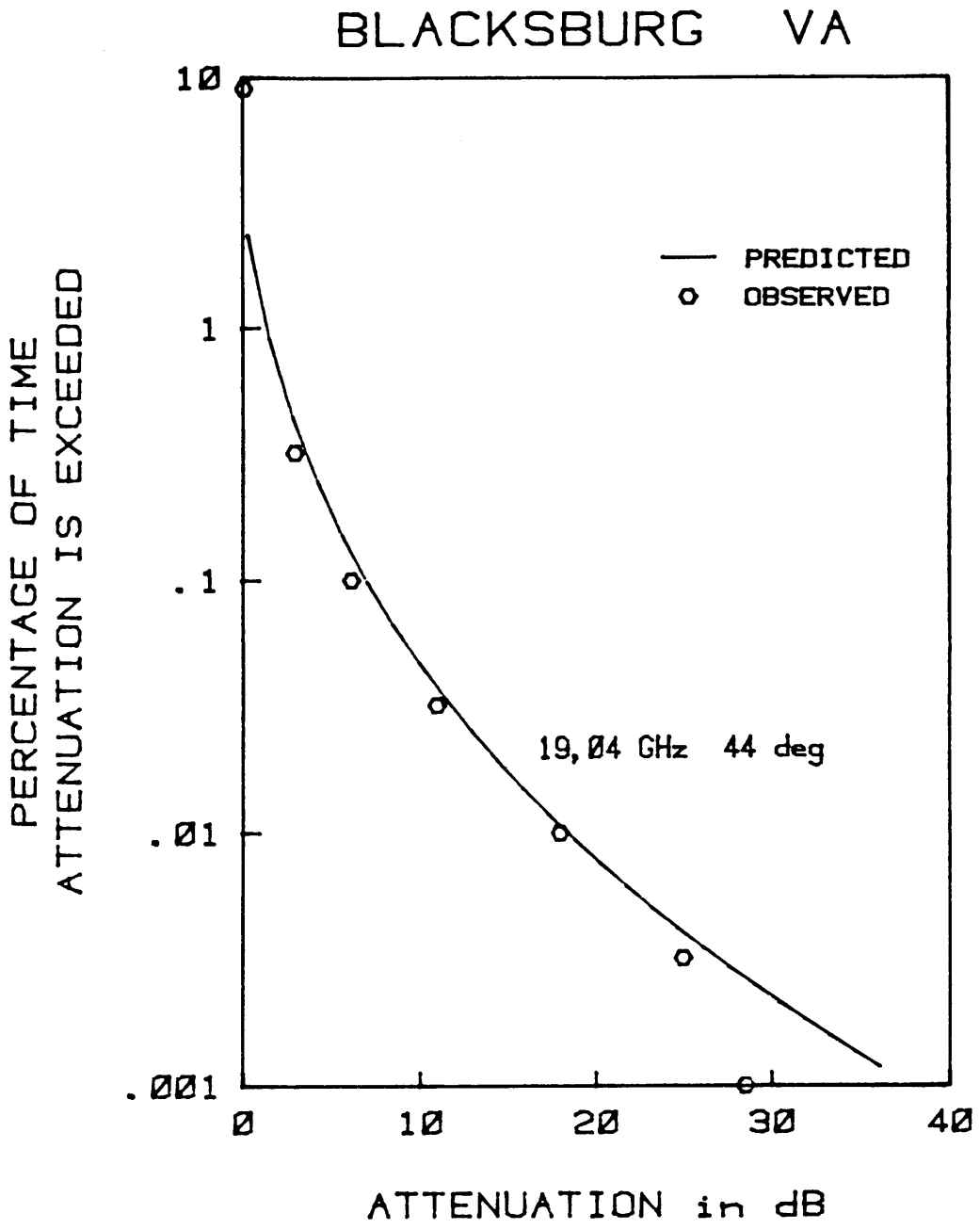

Fig. 93 Predicted and observed distributions at 19,04 GHz for Blacksburg, Virginia. Elevation angle as shown. Other input parameters: MAR=1047mm; region=coastal; altitude=615m. The observed distribution was obtained with COMSTAR during June 1977 to August 1980 [Andrews et al., 1982].

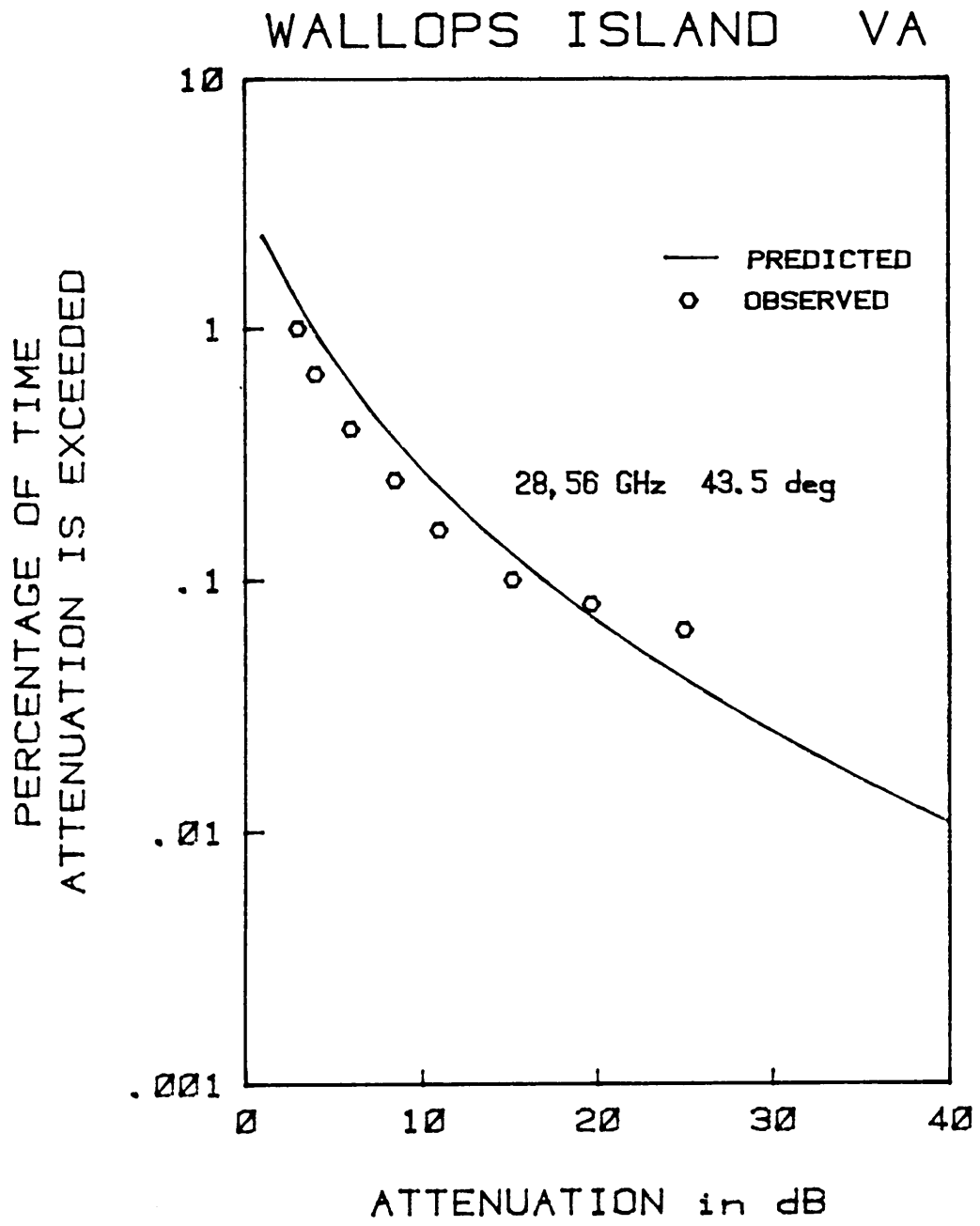

Fig. 94 Predicted and observed distributions at 28,56 GHz for Wallops Island, Virginia. Elevation angle as shown. Other input parameters: MAR=1088mm; region=coastal; altitude= 20m. The observed distribution was obtained with COMSTAR D-2 and D-3 during 1 April 1977 to 31 August 1980 [Goldhirsh, 1982].

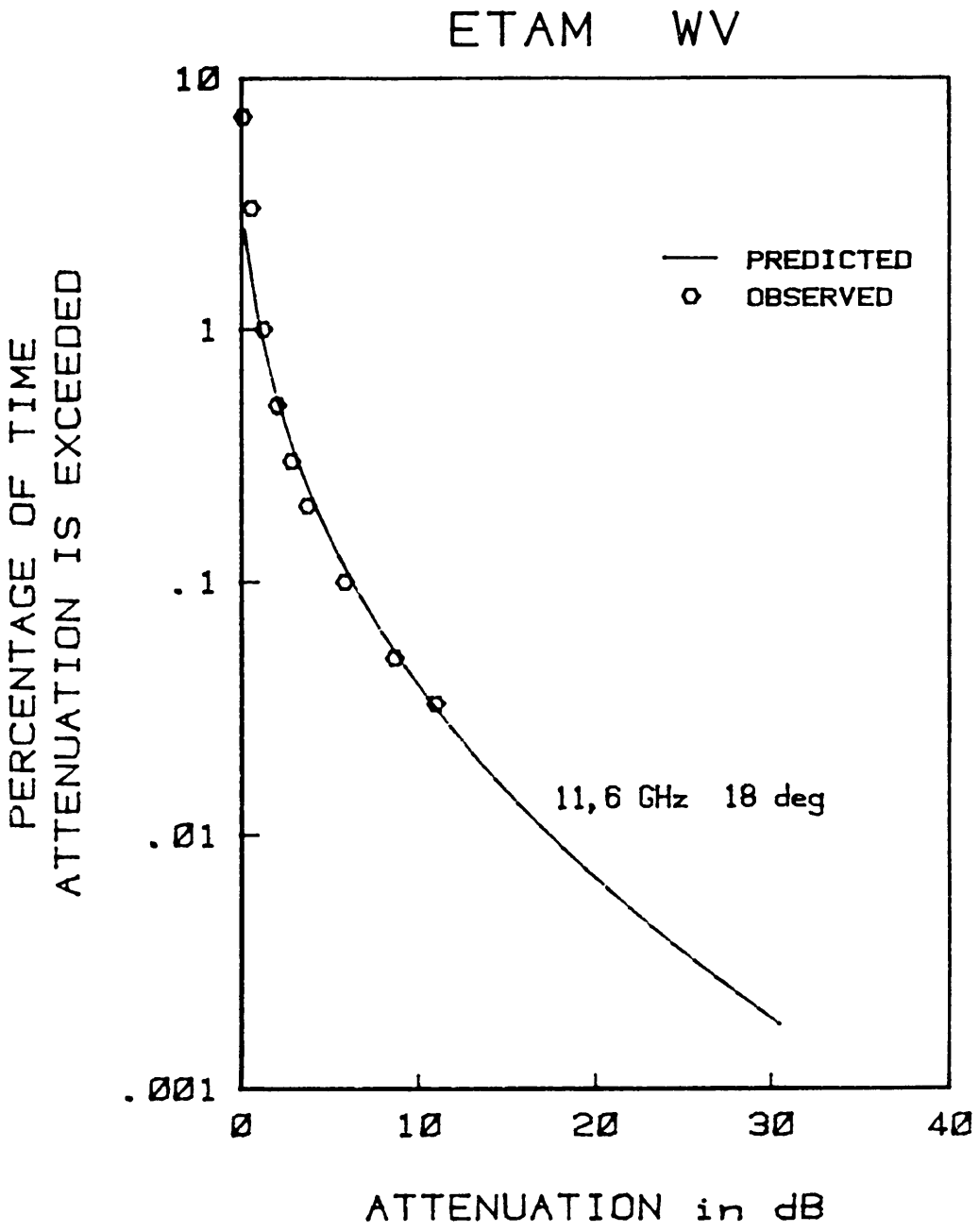

Fig. 95 Predicted and observed distributions at 11,6 GHz for Etam, West Virginia. Elevation angle as shown. Other input parameters: MAR=1201mm; region=coastal; altitude=584m. The observed distribution was obtained by radiometer during 25 October 1977 to October 1978 [Rogers, 1981].

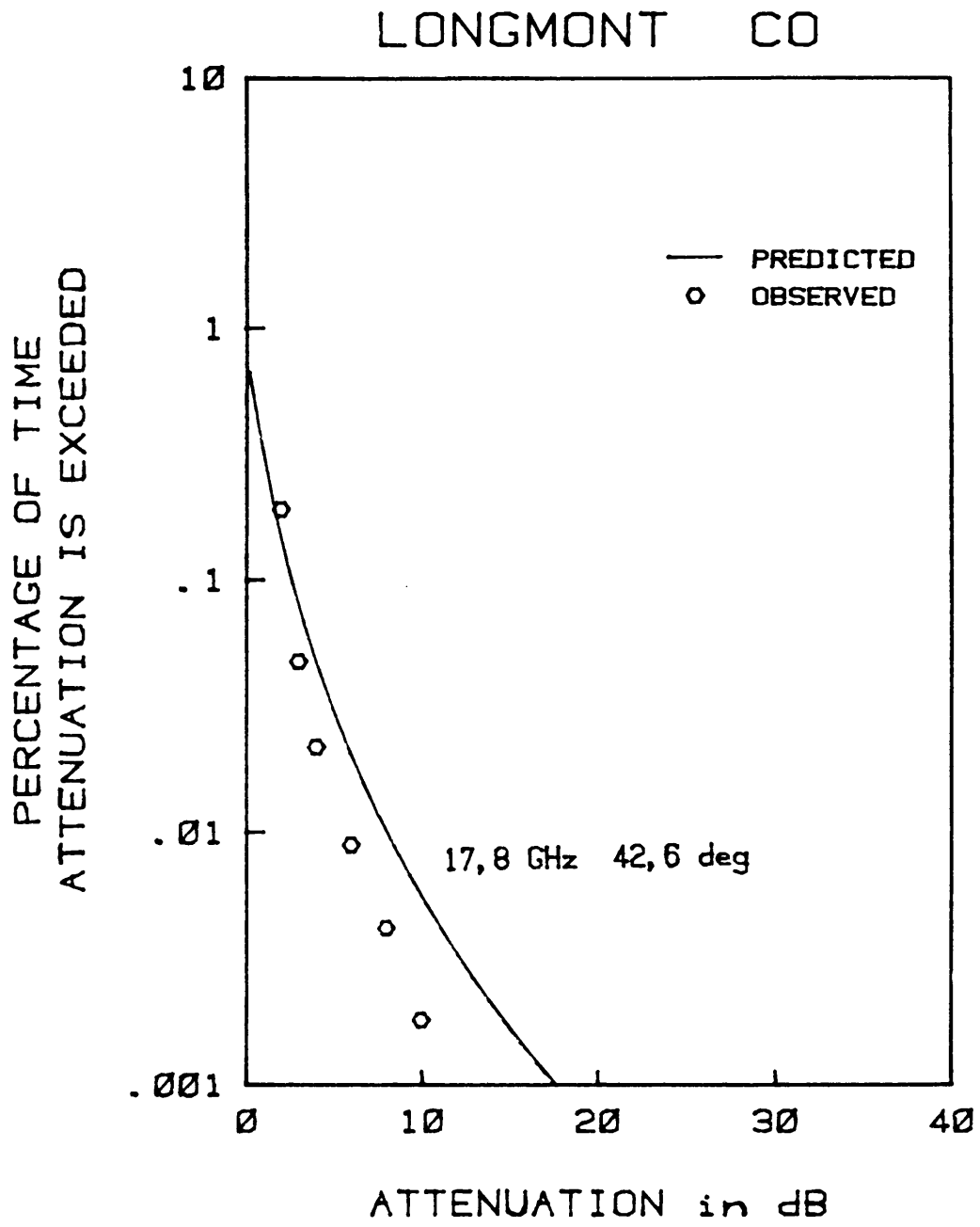

Fig. 96 Predicted and observed distributions at 17,8 GHz for Longmont, Colorado. Elevation angle as shown. Other input parameters: MAR=376mm; region=inland; altitude=1900m. The observed distribution was obtained by radiometer during June 1973 to July 1975 [Lin et al., 1980].

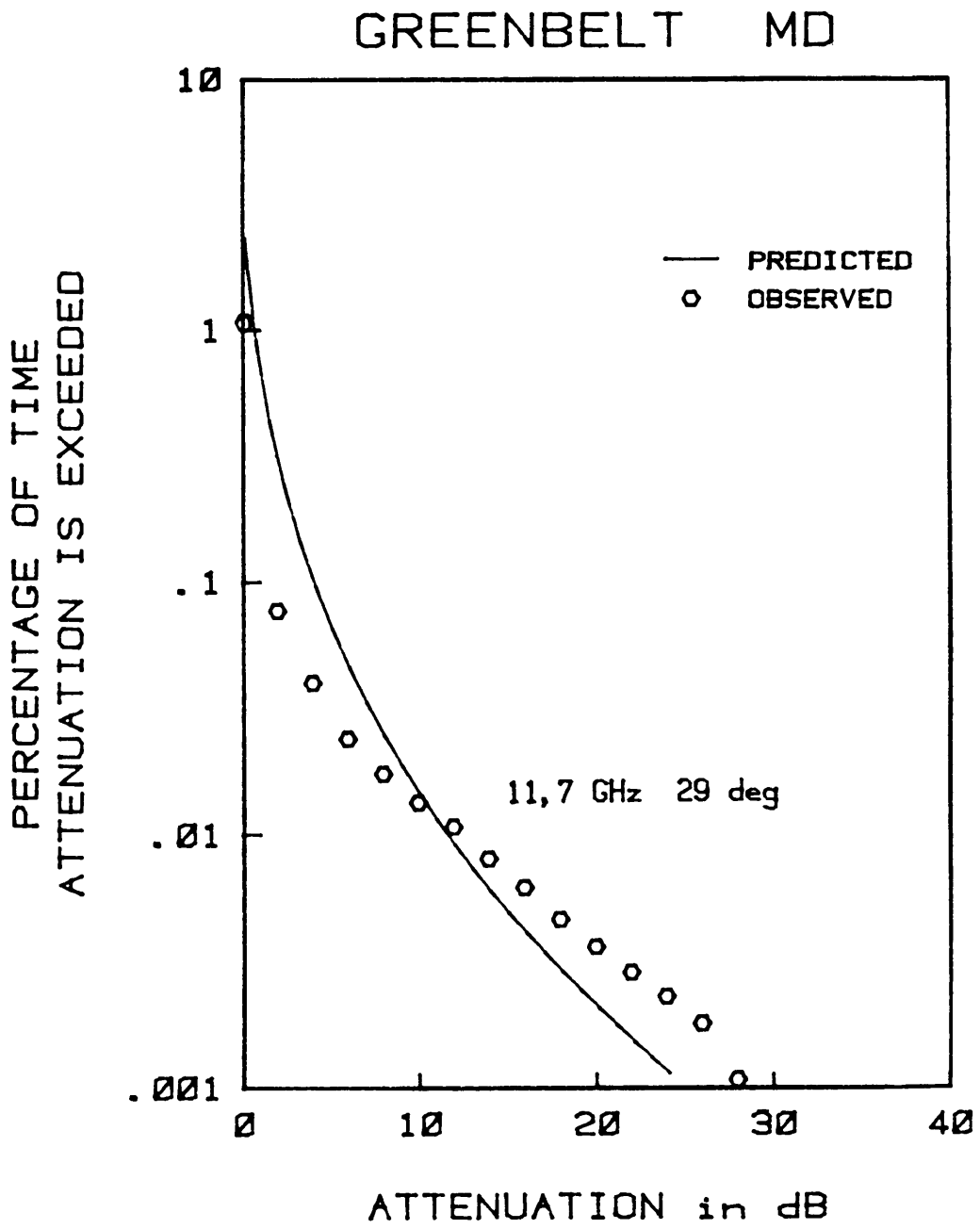

Fig. 97 Predicted and observed distributions at 11,7 GHz for Greenbelt, Maryland. Elevation angle as shown. Other input parameters: MAR=1036mm; region=coastal; altitude=50m. The observed distribution was obtained with CTS during July 1976 to June 1979 [Ippolito, 1981].

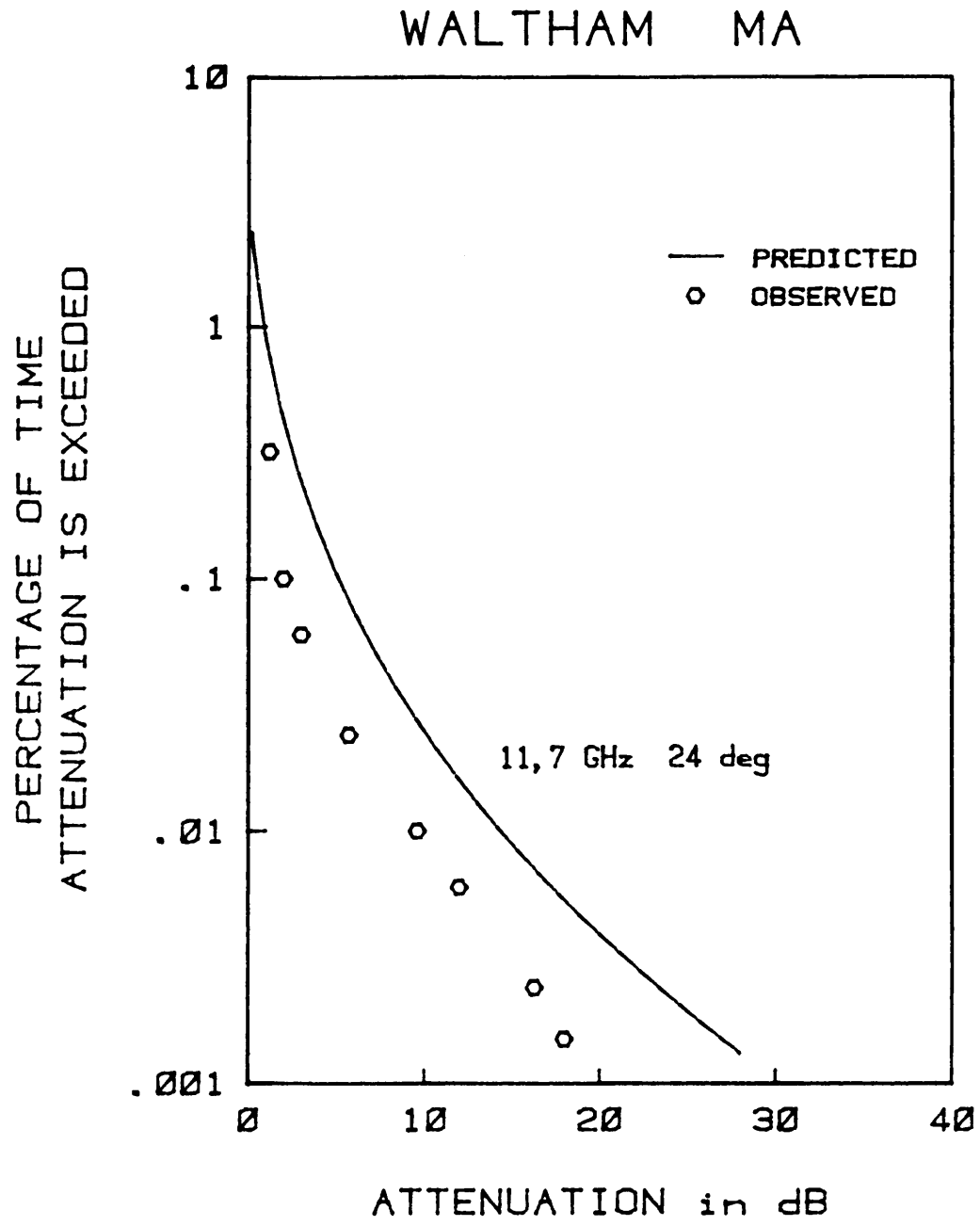

Fig. 98 Predicted and observed distributions at 11,7 GHz for Waltham, Massachusetts. Elevation angle as shown. Other input parameters: MAR=1086mm; region=coastal; altitude=30m. The observed distribution was obtained with CTS during 1 June 1977 to 31 May 1979 [Nackoney and Davidson, 1982].

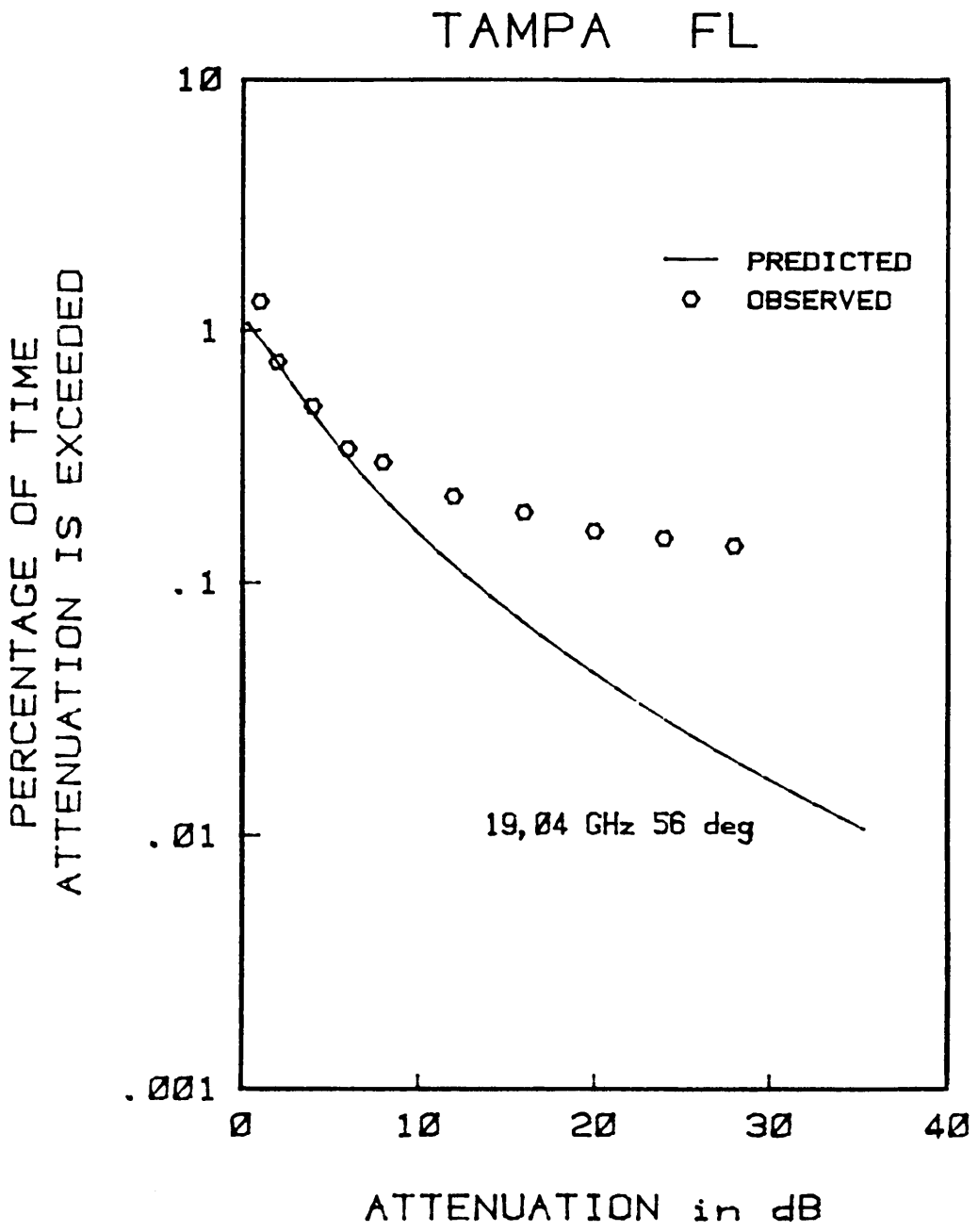

Fig. 99 Predicted and observed distributions at 19,04 GHz for Tampa, Florida. Elevation angle as shown. Other input parameters: MAR=1310mm; region=inland; altitude=60m. The observed distribution was obtained with COMSTAR D-2,-3 and -4 during April 1978 to September 1981 [Tang and Davidson, 1982].

APPENDIX B : TABLES

Table 1 : Details of Southern African rainfall stations with observed 15-min distributions

No*	Location	Weather Bureau Station No	Latitude deg	Latitude min	Longitude deg	Longitude min	Mean annual rainfall MAR (mm)	Elevation (m)	Period of the observed distribution	Climate
1	Alexander Bay	274/034	28	34	16	32	44	21	1952-1975 (24a)	Coastal
2	DF Malan (Cape Town)	21/178	35	58	18	36	533	44	1957-1975 (19a)	"
3	East London	59/572	33	02	27	50	896	125	1951-1975 (25a)	"
4	George	28/748	35	58	22	25	767	221	1950-1964 (15a)	"
5	Gough Island	0/709	40	19	09	54	3397	5	1956-1975 (20a)	"
6	Grootfontein (CP)**	145/059A	31	29	25	02	350	1270	1963-1975 (13a)	Inland
7	Grootfontein (SWA)**	1010/186	19	36	18	07	510	1405	1969-1975 (7a)	"
8	Jan Smuts (Johannesburg)	476/398	26	08	28	14	723	1694	1954-1975 (22a)	"
9	JBM Hertzog (Bloemfontein)	261/516	29	06	26	18	561	1351	1962-1975 (14a)	"
10	JG Strydom (Windhoek, SWA)	784/839	22	29	17	28	380	1700	1966-1975 (10a)	"
11	Keetmanshoop (SWA)	419/182	26	34	18	07	163	1066	1959-1975 (17a)	"
12	Kimberley	290/468	28	48	24	46	426	1198	1951-1975 (25a)	"
13	Louis Botha (Durban)	240/808	29	58	30	57	1050	8	1957-1975 (19a)	Coastal
14	Marion Island	0/653	46	53	37	52	2534	22	1951-1975 (25a)	"
15	Pietersburg	677/802	23	52	29	27	454	1230	1951-1975 (25a)	Inland
16	Port Elizabeth	35/179	33	59	25	36	626	60	1951-1975 (25a)	Coastal
17	Pretoria	513/405	25	45	28	14	742	1372	1951-1965 (15a)	Inland
18	Upington	317/476	28	26	21	16	199	814	1952-1975 (24a)	"
19	Windhoek (SWA)	740/154	22	34	17	06	367	1715	1959-1975 (17a)	"

* Number as on map of Fig. 30

** Abbreviations : CP : Cape Province
SWA : South West Africa.

Table 2 : Annual maximum rainfall depths of 15-min duration for Port Elizabeth

Year	Rainfall depth, H(j)(mm)
1947	10,2
1948	7,4
1949	13,0
1950	9,6
1951	26,7
1952	7,4
1953	6,4
1954	25,1
1955	10,8
1956	18,5
1957	13,2
1958	10,2
1959	23,5
1960	7,2
1961	13,9
1962	13,4
1963	16,0
1964	13,0
1965	6,5
1966	6,5
1967	8,0
1968	34,7
1969	4,5
1970	13,6
1971	10,7
1972	7,1
1973	7,9
1974	20,2
1975	5,3
1976	15,6
1977	12,1
1978	14,2
1979	7,2
1980	8,7
1981	20,0
1982	8,1
1983	6,0

Table 3 : Values of log-Gumbel and lognormal parameters from the application of Lin's method to Southern African locations

No*	Location	α	U	P_0 (%)	R_m (mm/h)	S_R (nepers)	Period of annual-maximum series
1	Alexander Bay	2,13	2,23	1,09	0,16	1,45	1952-1983(32a)
2	D F Malan	3,99	3,45	1,36	3,27	0,79	1938-1983(46a)
3	East London	2,42	3,90	17,56	0,17	1,58	1940-1983(44a)
4	George	3,65	3,38	3,86	1,45	0,95	1949-1963(15a)
5	Gough Island	4,11	3,57	22,40	1,10	0,95	1956-1980(25a)
6	Grootfontein (CP)**	2,25	3,51	7,20	0,15	1,60	1961-1980(20a)
7	Grootfontein (SWA)**	2,53	3,86	3,51	0,66	1,35	1969-1979(11a)
8	Jan Smuts	3,38	4,07	1,28	4,21	0,93	1938-1983(46a)
9	JBM Hertzog	3,09	3,91	1,48	2,55	1,03	1938-1983(46a)
10	JG Strydom	3,76	3,86	0,441	7,44	0,75	1967-1983(17a)
11	Keetmanshoop	1,87	3,35	5,14	0,06	1,88	1956-1983(28a)
12	Kimberley	3,14	3,89	0,85	3,61	0,96	1938-1983(46a)
13	Louis Botha	2,79	4,17	5,15	1,04	1,27	1938-1983(46a)
14	Marion Island	3,23	3,16	106,90	0,11	1,32	1951-1980(30a)
15	Pietersburg	3,12	4,07	0,68	4,86	0,94	1938-1983(46a)
16	Port Elizabeth	2,34	3,56	23,33	0,08	1,67	1947-1983(37a)
17	Pretoria	4,04	4,09	0,79	8,12	0,74	1938-1983(46a)
18	Upington	2,93	3,50	0,50	2,81	0,97	1952-1983(32a)
19	Windhoek(SWA)	2,76	3,88	1,02	2,23	1,11	1956-1983(28a)

* Number as on map of Fig. 30

** Abbreviations : CP : Cape Province
SWA : South West Africa.

Table 4 : Results from the application of Lin's method to Southern African locations

No*	Location	Greatest overall deviation in probability (rain rate in brackets)	Probability deviation at 0 mm/h	Greatest deviation in region above 2 mm/h and above 0,001% (rain rate in (brackets)	Probability deviation at 0,003%
1	Alexander Bay	+3,1(20)	+3,0	+3,1(20)	0
2	D.F. Malan (Cape Town)	+2,5(40)	-2,1	+2,4(10)	+1,6
3	East London	+4,1(0)	+4,1	+3,4(15)	+1,8
4	George	-1,8(45)	-1,1	-1,7(35)	-1,4
5	Gough Island	-2,4(20)	+1,5	-2,4(20)	-1,9
6	Grootfontein (CP)**	+4,2(0)	+4,2	+3,4(5)	-1,7
7	Grootfontein (SWA)**	-2,4(30)	+1,7	-2,4(30)	-1,4
8	Jan Smuts (Johannesburg)	+2,7(105)	-2,1	+1,6(10)	+1,3
9	JBM Hertzog (Bloemfontein)	+4,3(70)	-1,5	+1,6(60)	0
10	JG Strydom (Windhoek, SWA)	-3,6(0)	-3,6	+1,7(10)	-1,1
11	Keetmanshoop (SWA)	+10,2(0)	+10,2	+8,0(2)	-1,8
12	Kimberley	+2,2(95)	-2,1	+1,4(60)	-1,2
13	Louis Botha (Durban)	+2,6(130)	+2,4	+1,9(5)	0
14	Marion Island	+7,4(0)	+7,4	+3,2(5)	-1,3
15	Pietersburg	+3,5(105)	-2,4	+1,7(10)	+1,2
16	Port Elizabeth	+7,1(0)	+7,1	+3,6(5)	-1,8
17	Pretoria	-3,1(0)	-3,1	+2,1(10)	-1,3
18	Upington	+4,5(60)	-1,5	+1,5(10)	0
19	Windhoek (SWA)	+2,8(80)	-1,3	-1,8(30)	+1,2

* Number as on map of Fig. 30

** Abbreviations : CP : Cape Province
SWA : South West Africa.

Table 5 : Details of Southern African rainfall stations with annual maxima available *

(Annual maxima are for 15, 30, 45, 60 and 1440 minutes)

Station number	Station name	Lat S deg	Lat S min	Long E deg	Long E min	MAR mm	Period of record
10/456	Riversdale	34	06	21	16	457,4	1960-1971
21/178	D F Malan	33	58	18	36	550,0	1938-1976
23/710	Robertson	33	50	19	54	266,2	1958-1970
28/833	George	33	58	22	28	766,5	1949-1963
35/179	Port Elizabeth	33	59	25	36	625,9	1947-1976
43/566	Matroosberg	33	26	19	49	237,8	1938-1953
50/887	Willowmore	33	17	23	30	236,8	1961-1968
59/572	East London	33	02	27	50	896,1	1940-1976
61/298	Langebaanweg	32	58	18	10	250,0	1973-1976
74/298	Jansenville	32	58	24	40	267,3	1956-1970
76/134	Somerset East	32	44	25	35	606,4	1961-1970
79/81	Dohne	32	51	27	03	736,7	1965-1971
88/293	Sutherland	32	23	20	40	238,1	1960-1970
92/141	Beaufort West	32	21	22	35	230,3	1940-1970
106/850	Vredendal	31	40	18	29	140,1	1958-1970
113/25	Fraserburg	31	55	21	31	168,7	1958-1970
127/485	Umtata	31	35	28	47	652,6	1957-1969
134/478	Calvinia	31	28	19	46	213,8	1957-1970
145/59	Grootfontein	31	29	25	02	349,9	1961-1976
170/98	De Aar	30	38	24	04	287,4	1958-1970
180/722	Kokstad	30	32	29	25	680,7	1959-1970
214/636	O Kiep	29	36	17	52	161,0	1956-1970
229/556	Fauresmith	29	46	25	19	429,2	1957-1970
233/44	Wepener	29	44	27	02	599,7	1956-1969
241/50	Louis Botha	29	50	31	02	1050,0	1938-1976
247/668	Pofadder	29	08	19	23	104,6	1956-1970

(continued on next page)

* Courtesy of Midgley and Pitman [1978].

Table 5 : Details of Southern African rainfall stations with annual maxima available (continued)

Station number	Station name	Lat S deg	min	Long E deg	min	MAR mm	Period of record
261/516	Bloemfontein	29	06	26	18	560,9	1938-1976
274/034	Alexander Bay	28	34	16	32	44,2	1952-1976
290/68	Kimberley	28	47	24	45	426,3	1938-1976
300/483	Ladysmith	28	33	29	47	780,4	1949-1954
300/690	Estcourt	29	00	29	53	749,3	1959-1966
317/476	Upington	28	26	21	16	199,0	1951-1976
356/398	Kroonstad	27	38	27	14	594,3	1961-1970
393/778	Kuruman	27	28	23	26	456,0	1957-1970
403/886	Frankfort	27	16	28	30	688,7	1961-1970
419/184	Keetmanshoop	26	34	18	07	163,0	1956-1971
487/134	Potchefstroom	26	41	27	05	652,4	1951-1976
441/446	Standerton	26	56	29	15	718,3	1960-1970
476/398	Jan Smuts	26	08	28	14	722,9	1938-1976
478/867	Bethal	26	27	29	29	747,6	1963-1971
480/184	Carolina	26	04	30	07	757,7	1961-1971
508/261	Mafeking	25	51	25	39	561,2	1958-1965
513/405	Pretoria	25	45	28	14	742,1	1938-1976
555/837	Nelspruit	25	27	30	58	776,7	1961-1971
568/817	Mariental	24	37	17	57	180,0	1960-1971
589/594	Towoomba	24	54	28	20	641,2	1947-1972
590/550	Crecy	24	40	28	49	610,0	1956-1965
677/802	Pietersburg	23	52	29	27	454,0	1938-1976
719/370	Marnitz	23	10	28	13	408,1	1958-1972
740/154	Windhoek	22	34	17	06	367,3	1956-1976
784/839	J.G. Strydom	22	29	17	28	380,0	1967-1976
787/838	Gobabis	22	28	18	58	350,0	1960-1971
810/80	Messina	22	20	30	03	312,2	1956-1965
961/247	Outjo	20	07	16	09	409,4	1960-1969
1010/186	Grootfontein	19	36	18	07	510,0	1969-1976
1020/749	Maun	19	59	23	25	468,6	1952-1963

Table 6 : Variation of log-Gumbel standard deviation with integration time*

No.	Location	Station number	Log-Gumbel std. dev. at various integration times			
			15 min	60 min	1440 min	Average
2	D.F. Malan (Cape Town)	21/178	0,294	0,345	0,270	0,303
3	East London	59/572	0,486	0,485	0,468	0,479
8	Jan Smuts (Johannesburg)	476/398	0,338	0,410	0,370	0,372
9	JBM Hertzog (Bloemfontein)	261/516	0,366	0,358	0,328	0,351
12	Kimberley	290/468	0,365	0,445	0,280	0,363
13	Louis Botha (Durban)	240/808A	0,413	0,436	0,410	0,420
15	Pietersburg	677/802	0,385	0,380	0,385	0,383
17	Pretoria	513/405	0,286	0,325	0,292	0,301
Average			0,366	0,394	0,350	0,371

* Courtesy of Midgley and Pitman [1978]

Table 7 : Frequency of occurrence of 15-min depths at Port Elizabeth for 1951 to 1975

Month	No. of Years	0,1-1,0 (mm)	1,1-2,0 (mm)	2,1-4,0 (mm)	4,1-6,0 (mm)	6,1-8,0 (mm)	8,1-10,0 (mm)	10,1-12,0 (mm)	12,1-14,0 (mm)	14,1-16,0 (mm)	16,1-18,0 (mm)	18,1-20,0 (mm)	20,1-22,0 (mm)	22,1-24,0 (mm)	24,1-26,0 (mm)	26,1-28,0 (mm)	28,1-30,0 (mm)	30,1-32,0 (mm)	32,1-34,0 (mm)	34,1-36,0 (mm)
January	25	1823	114	45	21	3		1	1	1										
February	25	1769	121	37	17		2	2	1											
March	25	2411	208	64	8															
April	25	2176	156	75	14	9	1	2												
May	25	2340	318	88	15	4	2	1	2											
June	25	2161	245	79	13	4														
July	25	1953	194	51	6	2	1													
August	25	2595	290	95	22	4	1	3												
September	24	2514	249	83	13	3	1	2	2	2			3	2	1	3	1	1		1
October	25	2347	185	53	11	2	1		1			1								
November	25	1473	155	46	9	1	2	1	1											
December	25	1323	135	38	9	1	1	1	1											

Table 8 : Southern African climate zones*

Zone	Region : Type of climate and Köppen classification in brackets
W	Namaqualand and Northwestern Cape Province; Desert Climate; (BW).
M	Southwestern Cape Winter rainfall area; Mediterranean Climate; (Cs).
K	Karoo (great and little); Mainly Desert Climate; (BW and BSk).
A	Southern Cape Coastal Belt; Rain during all seasons; (Cf).
SE	Southern Coastal Belt; Warm temperate with Summer rainfall Max.; (Cfw).
E	Eastern Coastal Belt and Zululand; Subtropical with Summer rains; (Cfw and Cfa).
D	Drakensberg escarpment (interior Natal and Kaffraria); Warm temperate with Summer rainfall; (Cwb).
L	Lowveld (Eastern Transvaal); Hot Steppe (Savanna) with Summer rainfall; (BShw).
NT	Northern Transvaal; Hot Steppe with Summer rainfall; (BShw mainly).
H	Highveld (Southern Transvaal, Eastern Orange Free State and Lesotho; Warm temperate with Summer rainfall; (Cwb).
Sn	Northern Steppe (Northern Cape Province and Western Orange Free State); Steppe, Summer and Autumn rainfall; (BS(kh)w).
Ss	Southern Steppe (Northeastern Cape Province); Cold Steppe with Autumn rainfall maximum; (BSkw').
SWAn	Northern interior of South West Africa; Hot Steppe; Summer rainfall; (BShw).
SWAs	Southern part of South West Africa; and Namib; Hot Desert; Rainfall in Summer and Autumn; (BWhw).
B	Botswana: Hot Steppe; Summer rainfall; (BShw).

* See map of Fig.30

Table 9 : Results of 15-min distributions from model for Southern African locations

No*	Location	Greatest overall deviation in probability (rain rate in brackets)	Probability deviation at 0 mm/h	Greatest deviation in region above 2 mm/h and above 0,001% (rain rate in (brackets)	Probability deviation at 0,003%
1	Alexander Bay	-2,3 (20)	-1,9	-1,3 (15)	0
2	D.F. Malan (Cape Town)	+2,9 (45)	-1,7	+2,4 (35)	+2,0
3	East London	-5,2 (115)	-2,1	-2,2 (65)	-1,9
4	George	+5,2 (55)	-2,2	+3,0 (45)	+2,6
5	Gough Island	+139,0 (55)	-6,0	+108,0 (50)	+52,0
6	Grootfontein (CP)**	-3,0 (0)	-3,0	+1,6 (10)	0
7	Grootfontein (SWA)**	-3,1 (0)	-3,1	+1,2 (10)	0
8	Jan Smuts (Johannesburg)	+5,0 (105)	-3,4	+2,2 (55)	+2,2
9	JBM Hertzog (Bloemfontein)	+6,4 (70)	-3,2	+2,3 (60)	+1,6
10	JG Strydom (Windhoek, SWA)	-2,8 (0)	-2,8	-1,5 (45)	-1,4
11	Keetmanshoop (SWA)	-5,0 (45)	-1,7	-5,0 (45)	-4,4
12	Kimberley	-2,8 (0)	-2,8	+1,5 (15)	-1,3
13	Louis Botha (Durban)	-2,3 (105)	-2,1	-1,5 (60)	-1,5
14	Marion Island	222,0 (45)	-5,8	+127,0 (30)	+92,0
15	Pietersburg	-2,5 (0)	-2,5	-2,0 (65)	-1,5
16	Port Elizabeth	-10,0 (80)	-1,8	-2,7 (50)	-2,4
17	Pretoria	+2,5 (90)	-3,2	+2,0 (70)	+1,6
18	Upington	-2,0 (0)	-2,0	-1,7 (40)	-1,5
19	Windhoek (SWA)	-2,4 (0)	-2,4	-1,9 (30)	-1,3

* Number as on map of Fig. 30

** Abbreviations : CP : Cape Province
SWA : South West Africa.

Table 10 : Details of North American locations with observed 5-min distributions

Location	Mean annual rain-fall, W (mm)	Approx. distance from nearest coast (km)	Köppen climatic region*
San Francisco, CA	529	10	Csb
Moline, ILL	833	1350	Dfa
Peoria, ILL	885	1250	Dfa
Indianapolis, IND	996	970	Cfa
Internat. Falls, MIN	627	1900	Dfb
Rochester, MIN	723	1600	Dfa
Omaha, NEB	700	2100	Dfa
Valentine, NEB	439	1800	Dfa
Newark, NJ	1076	20	Cfa
Trenton, NJ	1049	50	Cfa
Binghamton, NY	931	250	Dfb
Oklahoma City, OKLA	783	1500	Cfa
Harrisburg, PA	957	200	Cfa
Pittsburgh, PA	918	450	Cfa
Scranton, PA	977	170	Cfa
Salt Lake City, Utah	353	950	Csa
Lynchburg, VA	1023	280	Cfa
Green Bay, WIS	656	1300	Dfb
Lander, WYO	344	1250	Dfb
Sheridan, WYO	404	1300	BSw

* From Climatic Atlas of the United States, S.S. Visher, Harvard Univ. Press, 1954, 403 pp, p 368

Table 11 : Results of 5-minute distributions from model for North American locations

Location	Climate region	Greatest overall deviation in probability (rain rate in brackets)	Greatest deviation down to 0,0001% (rain rate in brackets)	Greatest deviation down to 0,001% (rain rate in brackets)	Probability deviation at 0,003%	Probability deviation at 0,0001%
San Francisco, CA	Coastal	+2,3(10)	+2,3(10)	+2,3(10)	+1,2	-1,4
Moline, ILL	Inland	-2,2(80)	-2,2(80)	-2,2(80)	-1,9	0
Peoria, ILL	"	+2,5(170)	-2,5(170)	-1,2(90)	-1,3	+2,5
Indianapolis, IND	"	+4,3(170)	+4,3(170)	+1,5(50)	+1,3	+4,3
Internat. Falls, MIN	"	-3,2(220)	-2,0(70)	-2,0(70)	-1,9	0
Rochester, MIN	"	-2,1(220)	-2,1(160)	-1,8(110)	-1,6	-1,4
Omaha, NEB	"	-2,6(100)	-2,6(100)	-2,6(100)	-2,5	-2,3
Valentine, NEB	"	-7,1(190)	-7,1(190)	-4,2(100)	-3,5	-6,6
Newark, NJ	Coastal	-4,7(250)	-3,4(50)	-2,9(80)	-3,0	-2,1
Trenton, NJ	"	-4,7(130)	-4,7(130)	-3,8(120)	-3,4	-3,8
Binghamton, NY	"	-5,5(190)	-5,5(190)	-4,6(70)	-4,3	-5,4
Oklahoma City, OKLA	Inland	-2,3(150)	-2,3(150)	-1,9(120)	-1,8	+1,3
Harrisburg, PA	Coastal	-3,8(220)	-3,5(70)	-3,2(70)	-3,2	-2,0
Pittsburgh, PA	Inland	+3,5(170)	+3,4(160)	+2,1(70)	+2,1	+3,4
Scranton, PA	Coastal	-5,2(230)	-3,4(110)	-4,0(110)	-2,8	-1,6
Salt Lake City, Utah	Inland	-1,9(150)	-1,6(120)	+1,5(40)	-	-1,6
Lynchburg, VA	Coastal	-4,1(200)	-2,8(70)	-2,9(70)	-2,6	-1,8
Green Bay, WIS	Inland	-2,1(150)	-2,1(150)	-1,8(110)	-1,7	-1,4
Lander, WYO	"	+5,7(20)	+5,7(20)	+4,3(30)	+5,2	+1,2
Sheridan, WYO	"	+2,8(30)	+2,8(30)	+3,0(30)	+2,8	+1,0

Table 12 : Comparison of results in region above 2 mm/h and above 0,001%

Method	Locations with deviation of 4 and below	Locations with deviation of 3 and below	Locations with deviation of 2 and below
Lin's method in S. Africa	18(95%)	13(68%)	9(47%)
Model in S. Africa*	16(94%)	16(94%)	10(59%)
Model in N. America	17(85%)	14(70%)	7(35%)

* Excluding islands.

Table 13 : Comparison of results at a fixed probability of 0,003%

Method	Locations with deviation of 4 and below	Locations with deviation of 3 and below	Locations with deviation of 2 and below
Lin's method in S. Africa	19(100%)	19(100%)	19(100%)
Model in S. Africa*	16(94%)	16(94%)	13(76%)
Model in N. America	18(90%)	14(70%)	8(40%)

* Excluding islands

Table 14 : Details of North American locations with observed rain-attenuation distributions

Location	Mean annual rainfall, W (mm)	Climatic region used in rain-rate model	Ground elevation (m)	Approx. distance from coast (km)
Longmont, Colorado	376 (Denver)	Inland	1900	1440
Tampa, Florida	1310 (Tampa)	Inland	60	40
Palmetto, Georgia	1197 (Atlanta)	Coastal	290	380
Grant Park, Illinois	842 (Chicago Midway)	Coastal	200	1280*
Clarksburg, Maryland	1036 (Washington National)	Coastal	50	200
Greenbelt, Maryland	1036 (Washington National)	Coastal	50	180
Waltham, Massachusetts	1086 (Boston)	Coastal	30	30
Crawford Hill, New Jersey	1062 (Trenton/Atlantic City av)	Coastal	120	40
Austin, Texas	827 (Austin)	Inland	246	250**
Blacksburg, Virginia	1047 (Roanoke)	Coastal	615	400
Wallops Island, Virginia	1088 (Washington Natl./Norfolk av)	Coastal	20	10
Etam, West Virginia	1201 [Rogers, 1981]***	Coastal	584	390

* 40 km from Lake Michigan

** From Mexican Gulf

*** Figure taken from reference shown.

APPENDIX C : THE MIDGLEY-AND-PITMAN DEPTH-DURATION-FREQUENCY DIAGRAM FOR POINT RAINFALL IN SOUTHERN AFRICA

(a) Brief description

Midgley and Pitman [1978] published a report giving a depth-duration-frequency (DDF) diagram for Southern Africa (shown in Fig. 24), for use by hydrological engineers. The multi-axis diagram relates the probability (or return period) of exceeding a rainfall amount (depth of rain) in a specified collecting interval (the duration), to the mean annual rainfall (MAR) and climatic region of the location. Mean annual rainfall ranges from 50 to 2000 mm and two climatic regions, i.e. 'inland' and 'coastal', are indicated. It is stated that the 'inland' region is associated with areas where convective thunderstorm rain predominates and the 'coastal' region with areas where widespread frontal rain predominates. The collecting interval (called 'storm duration' in the Midgley-and-Pitman report, but referred to as rain-gauge integration time in this thesis) ranges from 6 minutes to 100 hours. The diagram had been devised by modelling the annual maxima of rainfall depth of various durations of 56 widely spread autographic rainfall stations in Southern Africa on mean annual rainfall, climatic region and integration time.

The rain-rate model that this thesis concerns itself with utilizes the analytical relationships in the diagram to obtain expressions for the extreme-value parameters α and U, to be applied in Lin's extreme-value method. The relationships of the DDF diagram were derived by modelling the annual maximum rainfall depths on the log-Gumbel

extreme-value distribution. The reader is referred to the theory of the latter in Appendix D. In this appendix the analytical relationships and method of construction of the diagram are given in detail.

(b) Analytical relationships

The diagram had been devised using the following steps:

Step 1

The series of annual maximum rainfall depths, $H_1(j)$ (in mm), for each of 15-, 30-, 45-, 60- and 1440-minute integration times (clock-time durations or averaging periods) were abstracted from the autographic rainfall data of each of 56 Southern African rainfall stations, listed in Table 5 and shown on the map of Fig. 25. The data amounted to about 1000 stations years or an average of about 17 years of data per station per integration time. The 56 stations are representative of the majority of the main climatic regions of the subcontinent, as is illustrated by the climatic regions of the map of Fig. 30. Their values of mean annual rainfall range from 44 to 1050 mm/a.

Step 2

Gumbel and log-Gumbel distributions as given by Eq. D1 of Appendix D were fitted to the series of annual maxima, $H_1(j)$, of the eight stations with the longest records (± 40a). In the case of the Gumbel distribution Eq. D1 becomes

$$P(h) = P(H_1 \geq h) = 1 - e^{-e^{-y}} \qquad (C1)$$

where h is the variate rainfall depth in mm, H_1 is the annual maximum rainfall depth exceeding the variate and y is the reduced variate, which from Eq. D3 (Appendix D) is given by

$$y = \alpha(h - U) \qquad (C2)$$

The asymptotic forms of the scale and location parameters α and U were obtained by the method of moments, i.e. using Eq. D6, D9, D10, D13 and D14 of Appendix D. Asymptotic forms were probably used for ease of computation, but it is to be noted that they will result in small errors. In these equations X(j) is given by

$$X(j) = H(j) \qquad (C3)$$

and x by

$$x = h$$

In the case of the log-Gumbel distribution the distribution function is also given by Eq. C1, but y becomes

$$y = \alpha\{\ln(h) - U\} \qquad (C4)$$

and X(j) becomes

$$X(j) = \ln\{H(j)\} \qquad (C5)$$

Gumbel and log-Gumbel distributions were obtained for all of the integration times, i.e. 15, 30, 45, 60 and 1440 minutes. The eight stations represented both inland and coastal climatic regions, with a range of mean annual rainfalls from 44 to 1050 mm.

Step 3

A chi-square goodness-of-fit test was done on each of the Gumbel and log-Gumbel distributions. The Gumbel distribution was rejected 9 times out of 40, while the log-Gumbel distribution produced only one rejection out of 40, which is within the acceptability limit of 5% as laid down in the chi-square test.

Step 4

On the basis of the general acceptability of the log-Gumbel distribution, this distribution was fitted to the annual-maximum series of the remaining 48 stations as well, for integration times of 15, 60 and 1440 minutes.

Step 5

The log-Gumbel means for the 56 stations (indicated by μ for brevity) and for each of the above three integration times, were then plotted against mean annual rainfall, as shown in Fig. 26. Smooth curve approximations were made by least-squares regression, which clearly shows a rise in the log-Gumbel mean with an increase in MAR. Also, a clear distinction was borne out between 'coastal' and 'inland' stations at the lower integration times. According to Midgley and Pitman this behaviour is attributed to a high incidence of thunderstorm activity in the interior, which gives rise to high intensities over short periods. The absence of a distinction between 'coastal' and 'inland' stations at the 1440-minute (24h) level is due to frontal rains in coastal regions being able to match the production from prolonged thunderstorm activity.

Step 6

The following generalised equations, i.e. equations applying to arbitrary locations on the subcontinent, were derived for the log-Gumbel mean μ from the curves of Fig. 26:

15-min integration time:

'coastal' region: $\mu = 0{,}0742\ W^{\frac{1}{2}} + 0{,}4902$ (C6)

'inland' region: $\mu = 0{,}0570\ W^{\frac{1}{2}} + 1{,}3995$ (C7)

60-min integration time:

'coastal' region: $\mu = 0{,}0786\ W^{\frac{1}{2}} + 1{,}0647$ (C8)

'inland' region: $\mu = 0{,}0598\ W^{\frac{1}{2}} + 1{,}9020$ (C9)

1440-min integration time:

Both regions: $\mu = 0{,}0640\ W^{\frac{1}{2}} + 2{,}3559$ (C10)

where W is the mean annual rainfall (in mm).

Step 7

An analysis similar to that of the log-Gumbel mean was attempted for the log-Gumbel standard deviation (indicated by σ, for brevity). A plot of the average standard deviation of the three integration times for every station against MAR revealed no clear trend, as can be seen from Fig. 27. This was attributed by the authors to sampling error. The majority of stations had records of the order of 10 years, which is regarded as inadequate for establishing the standard deviation with a reasonable degree of confidence.

An investigation into the standard deviation of the eight stations with the longest records revealed a much smaller spread with MAR. Also, there was no trend apparent with increasing integration time, as can be seen

from Table 6. This prompted the authors to adopt a generalized blanket value, invariant with integration time, MAR and climatic region. The value was chosen to be approximately equal to the average value of the standard deviations of the eight stations. It is given by

$$\sigma = 0,359$$

It is noted that at this point, i.e. with σ and μ defined, it is possible to describe the behaviour of the annual maximum rainfall depth, H_1, at any location by a generalized log-Gumbel distribution, given by

$$P(h) = P(H_1 \geq h) = 1 - e^{-e^{-y'}} = \frac{1}{Q(h)} \qquad (C11)$$

where

$$y' = \alpha'[\ln(h) - U'] \qquad (C12)$$

and where the prime sign is used to distinguish the distribution of H_1 from other distributions discussed in this thesis.

In the above expressions h is the variate rainfall depth, the amount likely to be exceeded by an annual maximum, H_1. The value of α' is invariant and is given by Eq. D13 of Appendix D as

$$\alpha' = \frac{\pi}{\sqrt{6}\sigma}$$

$$= \frac{\pi}{\sqrt{6} \cdot 0,359}$$

$$= 3,5726 \qquad (C13)$$

where the above-mentioned value of σ is used.

The value of U' is given by Eq. D14 of Appendix D as

$$U' = \mu - \frac{\gamma}{\alpha'}$$

$$= \mu - \frac{0,57721}{3,5725}$$

$$= \mu - 0,16157 \qquad (C14)$$

where γ is Euler's Constant given by $\gamma = 0,57721$

The value of μ is obtained from one of Eqs. C6 to C10, depending on the required integration time and the climatic region of the location in question, and utilizing the appropriate value of MAR.

Using the procedure given above, distributions may be obtained at 15-, 60- and 1440-minute integration

time. However, as there is an interest in other integration times as well, a procedure for interpolating and extrapolating is required. (For the purpose of rain-attenuation prediction the main requirement, of course, is an integration time of 5 minutes).

Step 8

For the purpose of interpolating and extrapolating to other integration times an equation of the following form was adopted in the DDF diagram:

$$h = \frac{r_0 \cdot D}{(1+BD)^n} \qquad (C15)$$

where h is the rainfall amount likely to be exceeded at a specified return period and D is the integration time. The constants r_0, B and n are associated with a particular climatic region, MAR and return period. The authors give no reason for choosing this particular form of equation. It has however been noted that a relationship of the same form has been established for annual maximum rain rates in the United Kingdom [NERC, 1975] and that that has been employed for the purpose of developing rain-rate climatologies for rain-attenuation prediction [Watson et al., 1981, p 44 and Watson et al., 1982, p 24][1].

---

1. The UK relationship is given as $r = r_0/(1 + BD)^n$ where r is the rain rate exceeded. As r is defined as $r = h/D$, the two expressions are equivalent.

(c) Method of construction of quadrants

The diagram was constructed on the basis of the assumption that the D-minute variate of the log-Gumbel distribution, which is a function of MAR and climatic region of the location, can be approximately equivalently represented by a set of graphical relationships. The relationships are given in the form of the three quadrants of Fig. 24. They were constructed as follows:

Quadrant A

Firstly, the integration-time relationship of the annual maximum rainfall depth likely to be exceeded at a return period of 20 years and an MAR of 500 mm was incorporated into quadrant A. It is a special case of the relationship of Eq. C15 in the previous section, where the values of r_0, B and n are now chosen to satisfy simultaneously the relationship of Eq. C15 and the distribution of Eq. C11 with Q(h) set to 20a, as well as Eqs. C6 to C10 with MAR = 500 mm, and with α' set at the value of Eq. C13. This is done as follows:

From Eq. C11

$$y' = \ln\left[\ln\left\{\frac{Q(h)}{Q(h)-1}\right\}\right] \qquad (C16)$$

which for Q(h) = 20 years becomes

$$y' = -\ln\{\ln(\frac{20}{20-1})\}$$

$$= 2,9702 \qquad (C17)$$

From Eq. C12, for 20 years

$$\ln(h) = \frac{y'}{\alpha'} + U'$$

$$= \frac{2,9702}{\alpha'} + U'$$

Therefore

$$h = e^{\{\frac{2,9702}{\alpha'} + U'\}}$$

Substituting for α' from Eq. C13, h becomes

$$h = e^{\{\frac{2,9702}{3,5726} + U'\}}$$

$$= e^{(0,8314 + U')} \qquad (C18)$$

But U', from Eq. C14, is given by

$$U' = \mu - 0,16157 \qquad (C19)$$

Considering a 15-minute integration time and the 'inland' region, then μ, from Eq. C7, is given by

$$\mu_{15} = 0,0570\ W^{\frac{1}{2}} + 1,3995$$

With a mean annual rainfall W of 500 mm

$$\mu_{15} = 0,0570 \times 500^{\frac{1}{2}} + 1,3995$$
$$= 2,674$$

Substituting this value into Eq. C19

$$U' = 2,674 - 0,16157$$
$$= 2,5124$$

Eq. C18 for 15 minutes and the 'inland' region then becomes

$$h_{15} = e^{(0,8314 + 2,5124)}$$

$$= e^{3,344}$$

$$= 28,3 \text{ mm} \qquad \text{(C20)}$$

This then is the 15-minute value for an 'inland' location with 500 mm/a, likely to be exceeded once in 20 years. As can be seen, the value agrees with that at 15 minutes on the 'inland' curve of quadrant A of Fig. 24.

Following the same procedure, but using the expressions of Eqs. C9 and C10, values of h for integration times of 60 and 1440 minutes, respectively, and for the 'inland' region, may be obtained. The following three equations may then be set up for the 'inland' region, using Eq. C15 with the appropriate integration times (in hours):

$$h_{15} = \frac{0,25r_0}{(1+0,25B)^n} = 28,3 \qquad \text{(C21)}$$

$$h_{60} = \frac{r_0}{(1+B)^n} = 51,1 \qquad \text{(C22)}$$

$$h_{1440} = \frac{24r_0}{(1+24B)^n} = 88,8 \qquad (C23)$$

Simultaneously solving Eqs. C21 to C23 then renders the values of r_0, B and n for the 'inland' region. A similar procedure is followed to obtain the values for the 'coastal' region.

The relationship of quadrant A is therefore given by

$$h_a = \frac{r_0 \cdot D}{(1+BD)^n} \qquad (C24)$$

where h_a is the annual maximum exceeded at a return period of 20 years and a MAR of 500 mm, and where r_0, B and n are given by the following table:

	'Inland' region	'Coastal' region
r_0	217,8	122,8
B	4,164	4,779
n	0,8832	0,7372

Quadrant B

In this quadrant, shown in Fig. 24, a log-Gumbel distribution is used to transform h_a, the 20-year, 500-mm/a value to h_b, the $Q(h_b)$-year, 500-mm/a value. From Eq. D2, Appendix D, and using a notation to distinguish the distribution in this quadrant from other distributions, we have

$$Q(h_b) = \frac{1}{1 - e^{-e^{-y''}}} = \frac{1}{P(h_b)} \qquad (C27)$$

where

$$y'' = \alpha''\{\ln(h_b) - U''\}$$

$$= 3{,}5726\ \{\ln(h_b) - U''\} \qquad (C28)$$

where h_b is the D-minute annual maximum rainfall exceeded with return period $Q(h_b)$ and MAR = 500 mm, and which is represented on the horizontal axis of quadrant B. The extreme-value parameter α'' was chosen to be equal to α', with value as in Eq. C13.

The straight lines on the log-log scale of quadrant B represent fixed ratios between h_a and h_b for any return period. This can be seen by rewriting Eq. C28 to

give

$$h_b = e^{\left\{\frac{y''}{35726} + U''\right\}} \qquad (C29)$$

At a return period of 20 years, where per definition $h_b = h_a$, we have

$$(h_b)_{20} = h_a = e^{\left\{\frac{y''_{20}}{3,5726} + U''\right\}} \qquad (C30)$$

where y''_{20} is the 20-year value of y", which from Eq. C27 is given by

$$y'' = -\ln\left[\ln\left\{\frac{Q(h_b)}{Q(h_b)-1}\right\}\right] \qquad (C31)$$

Therefore

$$y''_{20} = -\ln\left[\ln\left\{\frac{20}{20-1}\right\}\right]$$

$$= 2,9702$$

Eq. C30 may therefore be rewritten to give

$$(h_b)_{20} = h_a = e^{\left\{\frac{2,9702}{3,5726} + U''\right\}} \qquad (C32)$$

The ratio h_b/h_a from Eqs. C29 and C32 is

$$\frac{h_b}{h_a} = e^{\left\{\frac{y''-2,9702}{3,5726}\right\}} \qquad (C33)$$

The ratio is therefore only determined by the value of y", which in turn is determined by the return period, according to Eq. C31. A constant return period therefore gives a constant ratio.

Quadrant C

In quadrant C the Q(h_b)-year, 500-mm/a maximum rainfall depth exceeded h_b is transformed to the Q-year, W-mm/a value h by the straight lines on the log-log scale. The straight lines on the quadrant's log-log scale were obtained in the following way: A range of MARs between 50 and 1000 mm was selected. For a particular region, integration time and MAR, values of h were calculated at return periods of 2, 5, 10, 20, 50 and 100 years, using Eqs. C12, C13, C14 and C6 to C10. The process was repeated for integration times of 15, 60 and 1440 minutes. The values generated were plotted on the vertical scale of quadrant C against the rainfall depths as expected from quadrants A and B (on the horizontal

scale of quadrant C). A best-fit line was then drawn through all the points representing the particular MAR (see Fig. 28). The process was repeated for all the selected values of MAR. It is to be noted that the 500-mm line naturally forms the centre line in quadrant C, as that was chosen as the reference value of MAR when the values of r_0, B and n as per quadrant A were obtained. Provision was made for mean annual rainfalls of up to 2000 mm by extrapolation on the basis of extreme rainfall depth exceeded being proportional to MAR. The lines of quadrant C aid in the interpolation for various integration times as they effectively map those points for integration times other than 15, 60 and 1440 minutes. The lines represent a fixed ratio between h and h_b at a fixed level of MAR. By plotting these ratios as a function of MAR as in Fig. 29 it was found that

$$h = h_b F \tag{C34}$$

where F is given approximately by

$$F = 0,25 + 1,61 \cdot 10^{-3} \cdot W \tag{C35}$$

where W is the mean annual rainfall (in mm).

That straight lines could, in quadrant C, be fitted to the data with negligible fitting error (according to Midgley and Pitman) is proof that the graphical presentation of quadrants A, B and C gives a quantity h which is very nearly equivalent to the variate of a log-Gumbel distribution of the form of Eq. C11 with reduced variate

given by Eq. C12 and α' and U' given by Eqs. C13 and C14. This is an aspect to be exploited in Chapter 5 of the thesis.

APPENDIX D : THE GUMBEL AND LOG-GUMBEL DISTRIBUTIONS

The cumulative probability distribution of a series of annual maxima $X_1(j)$ may, according to Gumbel [1954], after Lin [1976 and 1978], be approximated by

$$P(x) = P(X_1 \geq x) = 1 - e^{-e^{-y}} \qquad (D1)$$

where $P(X_1 \geq x)$ is the probability (expressed as the fraction of years) that the variate x will be exceeded by an annual maximum X_1. The frequency (or return period) Q(x) (in years) is therefore

$$Q(x) = Q(X_1 \geq x) = \frac{1}{P(x)} = \frac{1}{1 - e^{-e^{-y}}} \qquad (D2)$$

In the above expressions y is called the reduced variate and is given by

$$y = \alpha(x - U) \qquad (D3)$$

The parameter α is a parameter of scale (or dispersion) and U is a parameter of position or location (the mode).

The distribution of Eq. D1 is sometimes called the Gumbel distribution. When x, and therefore X_1, assume a

logarithmic form, it becomes what is sometimes called the log-Gumbel distribution.

The parameter α is defined by

$$\alpha = \frac{\sigma_z}{\sigma_x} \tag{D4}$$

and the parameter U by

$$U = \overline{X}_1 - \frac{\overline{z}}{\alpha} \tag{D5}$$

where

$$\overline{X}_1 = \frac{1}{M} \sum_{j=1}^{M} X_1(j) \tag{D6}$$

with $\overline{X}_1$ being the sample mean of the series of annual maxima, $X_1(j)$, of M years; j = 1, 2, 3 ...M. In the case of x being of a logarithmic form it is sometimes called the log-Gumbel mean.

$$\overline{z} = \frac{1}{M} \sum_{j=1}^{M} z(j) \tag{D7}$$

with z(j) being

$$z(j) = -\ln\left[-\ln\left\{\frac{j}{M+1}\right\}\right] \qquad (D8)$$

Furthermore

$$\sigma_x = \sqrt{\overline{X_1^2} - \overline{X}_1^2} \qquad (D9)$$

which is the sample standard deviation of $X_1(j)$, called the log-Gumbel standard deviation when $X_1(j)$ is logarithmic, and where

$$\overline{X_1^2} = \frac{1}{M}\sum_{j=1}^{M}[X_1(j)]^2 \qquad (D10)$$

Also

$$\sigma_z = \sqrt{\overline{z^2} - \overline{z}^2} \qquad (D11)$$

where

$$\overline{z^2} = \frac{1}{M} \sum_{j=1}^{M} [z(j)]^2 \qquad (D12)$$

Furthermore, the asymptotic values of α and U, i.e. when the number of years become infinitely large, are given by

$$\alpha = \frac{\pi}{\sqrt{6}\sigma_x} \qquad (D13)$$

$$U = \overline{X}_1 - \frac{\gamma}{\alpha} \qquad (D14)$$

where γ = 0,57721 (Euler's Constant)

APPENDIX E : SPECIMEN CALCULATION OF MODEL CUMULATIVE RAIN-RATE PROBABILITY

Question:

Using the rain-rate model expressions, calculate the probability of exceeding a rain rate of 50 mm/h at an integration time of 5 minutes for a location in the 'coastal' region with a mean annual rainfall of 1000 mm.

Answer:

From Eq. 5.5, Section 5.2, with MAR = 1000 mm

$$F = 0,25 + 1,61 \cdot 10^{-3} \cdot 1000$$

$$= 1,86 \qquad (E1)$$

Substituting for F and D in Eq. 5.37, with D = 0,0833h (5 minutes)

$$U = \ln\left[\frac{122,8}{(1 + 4,779 \cdot 0,0833)^{0,7372}} \cdot 1,86\right] - 0,8314$$

$$= 4,3526 \qquad (E2)$$

The number of 5-minute intervals per year, from Eq. 3.8 (Section 3.1) is

$$N = \frac{8760}{0,0833} = 105124 \qquad (E3)$$

The value of α from Eq. 5.21 is

$$\alpha = 3,5726 \qquad (E4)$$

By substitution of N, U, α and W in Eqs. 3.5 to 3.7 we have

$$S_R = \frac{P_0 \cdot 105124}{3,5726} \cdot \phi \left[\Phi^{-1} \left[1 - \frac{1}{P_0 \cdot 105124} \right] \right] \qquad (E5)$$

$$R_m = \exp\left[4,3526 - S_R \cdot \Phi^{-1} \left[1 - \frac{1}{P_0 \cdot 105124} \right] \right] \qquad (E6)$$

$$1000 = R_m \cdot e^{\frac{S_R^2}{2}} \cdot P_0 \cdot 8760 \qquad (E7)$$

Eqs. E5 to E7 may be solved by computer to give

$$P_0 = 0,02829 \qquad (E8)$$

$$S_R = 1,02372 \text{ nepers} \tag{E9}$$

$$R_m = 2,38973 \text{ mm/h} \tag{E10}$$

The cumulative distribution of rain rate is given by Eq. 3.4 (Section 3.1) as

$$P(R>r) \simeq P_0 \cdot \frac{1}{2} \operatorname{erfc} \left[\frac{\ln(r) - \ln(R_m)}{\sqrt{2}\, S_R} \right]$$

This, when substituting for P_0, S_R and R_m from Eqs. E8 to E10 becomes

$$P(R>r) = 0,02829 \cdot \frac{1}{2} \operatorname{erfc} \left[\frac{\ln(r) - \ln (2,38973)}{\sqrt{2} \cdot 1,02372} \right] \tag{E11}$$

The probability at a rain rate of 50 mm/h then becomes

$$P(R>50) = 0,02829 \cdot \frac{1}{2} \operatorname{erfc} \left[\frac{\ln(50) - \ln(2,38973)}{\sqrt{2} \cdot 1,02372} \right]$$

$$= 0,02829 \cdot \frac{1}{2} \operatorname{erfc} [2,10038] \tag{E12}$$

From the theory of the error function [Schwartz, 1970] we have

$$\frac{1}{2}\,\mathrm{erfc}(\chi) = \frac{1}{2}\left[1 - \mathrm{erf}(\chi)\right] \tag{E13}$$

and

$$\mathrm{erf}(\chi) = \frac{2}{\sqrt{\pi}} \int_0^{\chi} e^{-\upsilon^2} d\upsilon \tag{E14}$$

From Eq. E12 it is clear that

$$\chi = 2{,}10038 \tag{E15}$$

Therefore, from Eqs. E14 and E15

$$\mathrm{erf}(2{,}10038) = \frac{2}{\sqrt{\pi}} \int_0^{2{,}10038} e^{-\upsilon^2} d\upsilon \tag{E16}$$

From Jahnke et al. [1960] (Table 7, p. 31)

$$\mathrm{erf}(2{,}10038) = 0{,}997026 \tag{E17}$$

From Eqs. E17 and E13

$$\frac{1}{2}\ \text{erfc}\ (2{,}10038) = \frac{1}{2}\ (1 - 0{,}997026)$$

$$= \frac{1}{2}\ (0{,}002974)$$

$$= 0{,}001487$$

Eq. E12 then becomes

$$P(R>50) = 0{,}02829 \cdot 0{,}001487$$

$$= 0{,}00421\%$$

giving the probability of exceeding 50 mm/h. This value corresponds to the point at 50 mm/h on the 1000-mm curve of Fig. 33, which gives a family of curves from the model.

APPENDIX F : SPECIMEN CALCULATION TO TEST FOR VALIDITY OF α AND U

Question

What depth of rain over 15 minutes is to be exceeded once in a hundred years at a 'coastal' location with a mean annual rainfall of 1000 mm?

Answer

From Eq. 5.37, Section 5.2 for a 'coastal' location

$$U = \ln \left[\left\{ \frac{122,8}{(1 + 4,779D)^{0,7372}} \right\} \cdot F \right] - 0,8314 \qquad (F1)$$

From Eq. 5.5

$$F = 0,25 + 1,61 \cdot 10^{-3} \cdot 1000$$

$$= 1,86 \qquad (F2)$$

Then, with D = 0,25h (15 minutes)

$$U = \ln \left[\frac{122,8}{(1 + 4,779 \cdot (0,25)^{0,7372}} \cdot 1,86 \right] - 0,8314$$

$$= 4,0202 \qquad \text{(F3)}$$

It can be seen from Eq. 5.21 that $\alpha = 3,5726$. Substituting this value and the above value of U in Eq. 3.3 gives

$$y = 3,5726 \left[\ln(r) - 4,0202 \right] \qquad \text{(F4)}$$

From Eq. 3.2, with $Q(R_1 > r) = 100a$

$$y = \ln \left[\ln \frac{100}{100 - 1} \right]$$

$$= 4,6 \qquad \text{(F5)}$$

Eq. F4 therefore becomes

$$4,6 = 3,5726 \left[\ln(r) - 4,0202 \right]$$

Therefore

$$\ln(r) = \frac{4,6}{3,5726} + 4,0202$$

$$= 5,3078$$

and

$$r = 201,9 \text{ mm/h}$$

This then is the rainfall rate over 15 minutes exceeded once in a hundred years. However, the rainfall depth is required, which is given by Eq. 5.11 as

$$h = rD$$

$$= 201,9 \cdot 0,25$$

$$= 50,5 \text{ mm.}$$

If the DDF diagram of Fig. 24 is used to obtain the depth exceeded it is proceeded as follows:

Quadrant A is entered at 0,25 h and from the 'coastal' curve it is projected horizontally until the 100-year line of quadrant B is met. It is then projected vertically down to the 1000-mm line of quadrant C and then horizontally to find the depth exceeded on the vertical axis. In doing so a value h which is almost exactly 50 mm is obtained. That confirms the validity of the expressions for α and U, obtained in Chapter 5.

APPENDIX G : COMPARISON OF CCIR RAIN-RATE DISTRIBUTIONS WITH OBSERVED DISTRIBUTIONS

In Fig. 3 the standard rain-rate distribution curves are given for CCIR [1982a] regions C, D, E, K and N, which cover the Southern African subcontinent. Also shown are observed distributions for two locations, both well within region E. Curve 'a' is the observed distribution over 24 years for Alexander Bay, which is location No. 1 on the map of Fig. 30. Curve 'b' is the observed distribution over 14 years for JBM Hertzog Airport (Bloemfontein) which is location No. 9 on the map. The observed curves are based on an integration time of 15 minutes, while the CCIR curves are of the order of one minute. According to Watson et al. [1981, p 10-14] the conversion factor between probabilities of different integration times, at a fixed level of rain rate, is fairly invariant with location. On that basis the ratio in 1-minute probabilities for the two locations at, say, the 10 mm/h level, should be approximately the same as the ratio in 15-minute probabilities. The 15-minute ratio can be seen from the graph to be about two orders of magnitude, suggesting the same then for the 1-minute probabilities. This difference of two orders of magnitude within region E by far exceeds the differences offered between regions C, D, E and K. It is also clear that no single CCIR curve could represent the 1-minute distributions of both locations. The CCIR regional designation therefore does not adequately provide for the variation within regions on the Southern African subcontinent.

APPENDIX H : LIST OF SYMBOLS

a	A constant in the expression for specific attenuation, aR^b.
A_T	Total path attenuation in dB.
b	A constant in the expression for specific attenuation, aR^b.
B	A constant used in an expression to relate annual maximum rainfall rates of various integration times, which are likely to be exceeded.
C_R	Quotient of equiprobable 60-minute rain rate upon 5-minute rain rate.
D	Rain-gauge integration time in hours (called duration in the Midgley and Pitman report).
DDF diagram:	The Midgley-and-Pitman depth-duration-frequency diagram.
erfc[~]	The complementary error function.
F	An empirical factor relating the annual maximum rainfall depth exceeded h (in mm) to the intermediate rainfall depth h_b, in quadrant C of the DDF diagram.
G	Altitude of the earth station above mean sea level in km.
h	The annual maximum rainfall depth exceeded, or variate, in quadrant C of the DDF diagram.
H	The variable rainfall depth (in mm) over a specified integration time or duration, related to variable rain rate R by H = RD.
H_1	The annual maximum rainfall depth (in mm) exceeding the variate h and related to the annual maximum rain rate R_1 (in mm/h) by $H_1 = R_1D$
$H_1(j)$	The series of annual maximum rainfall depths for years 1,2,...,j,...M

h_a An intermediate value of rainfall depth (in mm) likely to be exceeded by an annual maximum and used in quadrants A and B of the DDF diagram. In value, equal to the actual rainfall depth h exceeded by an annual maximum at a return period of 20 years and a mean annual rainfall of 500 mm.

h_b An intermediate value of extreme rainfall depth (in mm) likely to be exceeded, and used in quadrants B and C of the DDF diagram. The value represents the actual rainfall h to be exceeded every $Q(h_b)$ years at a location with 500 mm/a.

$(h_b)_{20}$ The value of h_b at a return period of 20 years, also equal to h_a.

h_R The rain height in km.

L Length of radio path in km.

$\overline{L}(R)$ Characteristic path length in Lin's attenuation model.

$\ln[\sim]$ The natural logarithm.

M The number of years of the annual series of maxima.

MAR Abreviation for mean annual rainfall of a location W (in mm).

n A constant used in an expression to relate annual maximum rainfall rates of various integration times, which are likely to be exceeded.

N The number of rain-gauge integration-time intervals per year.

P(h) Identical to $P(H_1 \geq h)$

$P(h_b)$ The probability that an amount of rainfall h_b will be exceeded by an annual maximum; h_b being a 500-mm/a value, represented on the horizontal axis of quadrant B of the DDF diagram.

$P(H_1 \geq h)$ The probability that the variate rainfall depth h will be exceeded by an annual maximum H_1.

$P(r)$	Identical to $P(R>r)$.
$P(R>r)$	The cumulative probability that the variate rain rate r will be exceeded.
$P(R_1>r)$	The cumulative probability that the annual maximum rain rate R_1 will exceed a rain rate r, expressed as a fraction of years.
P_0	The probability that rain will fall at the location in question, equal to $P(R>0)$
$P(x)$	Identical to $P(X_1>x)$.
$P(X_1>x)$	The cumulative probability that the annual maximum X_1 will exceed the variate x, expressed as a fraction of years.
$P(h)$	In the theory of the DDF diagram, the log-Gumbel distribution of the annual maximum rainfall depth H_1 - the variate being h (in mm/h).
Q	The return period in general, but also the return period of the variate h of quadrant C in the DDF diagram.
$Q(h)$	The reciprocal of $P(h)$, expressed as the return period (in years).
$Q(h_b)$	The reciprocal of $P(h_b)$, expressed as the return period (in years).
$Q(r)$	The reciprocal of $P(r)$, expressed as the return period (in years).
$Q(R_1>r)$	Identical to $Q(r)$.
$Q(x)$	The reciprocal of $P(x)$, expressed as the return period (in years).
$Q(X_1>x)$	Identical to $Q(x)$
r	The rain rate variate (in mm/h) in the log-Gumbel and lognormal distribution functions, but also the variate of the cumulative parent distribution of rain-rate, in general.
r_0	A constant used in an expression to relate annual maximum rainfall rates of various integration times, likely to be exceeded.

R	The variable rain rate (in mm/h).
R_1	The annual maximum rain rate (in mm/h).
$R_1(j)$	The series of annual maximum rain rates, in mm/h.
R_m	The median value of rain rate R during the raining time (in mm/h).
S_R	The standard deviation of ln(R) (in nepers).
U	In the log-Gumbel distribution function, a parameter of location (position), also called 'the mode', and also the mode of the rain-rate model.
U'	A parameter of location such as U, but specifically pertaining to the distribution of rainfall depth P(h), in the DDF diagram.
U''	A parameter of location such as U, but specifically pertaining to the distribution of the rainfall depth, $P(h_b)$, of quadrant B of the DDF diagram.
W	The mean annual rainfall (in mm).
x	The variate, in general, in the Gumbel or log-Gumbel distribution function.
X_1	The annual maximum in general.
$X_1(j)$	A series of annual maxima, in general.
$\overline{X}_1$	The average of $X_1(j)$.
y	In the log-Gumbel distribution function, the reduced variate, in general, and also the reduced variate of the rain-rate model.
y'	A reduced variate such as y, but specifically pertaining to the distribution of rainfall depth P(h) in the DDF diagram.
y''	A reduced variate such as y, but specifically pertaining to the distribution of rainfall depth $P(h_b)$ in the DDF diagram.
α	In the variate of the Gumbel or log-Gumbel distribution function, a parameter of dispersion, and also the dispersion parameter of the rain-rate model.

α'	A dispersion parameter such as α, but pertaining to the distribution of rainfall depth P(h) in the DDF diagram.
α''	A dispersion parameter such as α, but pertaining to the distribution of rainfall depth $P(h_b)$ in the DDF diagram.
θ	Elevation angle of the earth-station antenna.
$\phi[\sim]$	The normal probability density function.
$\Phi^{-1}[\sim]$	The inverse normal probability function.
σ_z	Defined by Equation D11, Appendix D.
σ_x	Defined by Equation D9, Appendix D.
$\bar{z}$	Defined by Equation D7, Appendix D.
σ	The log-Gumbel standard deviation, as used in the DDF diagram.
γ	Euler's Constant, equal to 0,57721.
μ	The log-Gumbel mean, as used in the DDF diagram.